BIODEGRADABLE MICROPARTICLE FOR STEM CELL DELIVERY AND DIFFERENTIATION

Anita Sukmawati

Thesis submitted to The University of Nottingham

for the degree of Doctor of Philosophy

April 2013

ABSTRACT

The formation of three-dimensional (3D) models for tissue engineering purpose provides a more conducive environment to enable complex biological interactions and processes between cells, biomaterials and bioactive molecules. Microparticles (MP) can be used as supporting matrix for 3D construct in cells and a carrier to deliver bioactive agents for cell development and differentiation, particularly for bone tissue engineering. Poly(glycerol adipate) (PGA) is a potential polymer for tissue engineering purposes as it is biodegradable and has biocompatibility with several cells. The aim of this study is to modify PGA polymer for MP with well-defined properties for drug encapsulation and release, promote cell-MP interaction and evaluate the osteogenic differentiation with MP incorporation in mouse embryonic stem (mES) and osteoblast cells. The PGA polymer has been modified by substituting 40% pendant hydroxyl groups onto the polymer backbone with stearoyl (C_{18}) groups to increase encapsulation efficiency of drug within MP. Further modification was tethering one carboxyl terminus in PGA polymer with maleimide-poly(ethylene glycol) (MIHA-PEG-NH_2) linker for ligand attachment on the surface of MP. Collagen, as a ligand, was modified by attaching iminothiolane to give a functional thiol group for interaction with maleimide group on the surface of 40%C_{18}-PGA-PEG-MIHA MP. The microparticles were prepared using an emulsification method. Dexamethasone phosphate (DXMP) and simvastatin (SIM) were encapsulated within the MP. The MP-cell aggregate formation was evaluated as well as cell metabolism activity. The effect

of polymer modification on drug release from MP was evaluated in the cells by analyzing osteogenic differentiation in cells. The MP prepared from modified PGA polymer exhibited high encapsulation efficiency of SIM in MP. By adjusting the formulation parameters, the release of SIM from MP could be extended to 21 days. The collagen attachment on the surface of 40%C_{18}-PGA-PEG-MIHA MP promoted cell metabolic activity and produced more extensive markers related to osteogenic differentiation.

ACKNOWLEDGMENTS

I would like to thanks my supervisors Dr. Lee Buttery and Dr. Martin Garnett for their invaluable support with all aspects throughout this work and Dr. Weng Chan for his kind guidance in chemistry part of this project. Their encouragement during practical work and written thesis contributed to the success of my PhD study.

I also deeply appreciate for the help I received from my colleagues in Tissue Engineering Group (Dr. Glen Kirkham, Laura, Adam), Drug Delivery D-16 Lab (Yasmin, Delyan, Zeeshan and Ali), Chemistry C-22 CBS building (Shaun, Amer), who were keen to provide help and advice whenever I needed. Thanks also to technicians: Sue Dodson who gave cell culture training, Paul Cooling who provided training and generous help in HPLC work, Teresa Marshall and Christine Grainger-Boultby for all technical help during practical work.

I would also thanks to Islamic Development Bank for giving opportunity and sponsorship for me to study in The University of Nottingham, and Universitas Muhammadiyah Surakarta (UMS), Indonesia, for giving temporary-leave permission whilst I studied in UK. I extend my thanks also for all friends in IDB students-UK association, particularly at The University of Nottingham, for our friendship and giving me opportunity to contribute in our society for a better future.

And finally, my thanks go to my parents for their blessing and encouragement to continue my study and letting me fly away from home to achieve the goal. I love you and I am nothing without you.

DECLARATION

I declare that this thesis is the result of my own work which has been mainly undertaken during my period of registration for the degree of Doctor of Philosophy at The University of Nottingham.

PUBLISHED ABSTRACT AND POSTER

Published Abstract:

Sukmawati, A., Chan, W.C, Garnett, M.C, Buttery, L., *Biodegradable microparticles for cell aggregation and proliferation.* Journal of Tissue Engineering and Regenerative Medicine, 2012. **6**: p. 371-372.

Poster:

A. Sukmawati, W.C. Chan, M.C. Garnett, L. Buttery, *Synthesis and characterization modified poly(glycerol-adipate) microparticles for three-dimensional tissue engineering purpose*, presented at Colloids and Nanomedicine 2012, Amsterdam 2012.

TABLE OF CONTENTS

LIST OF FIGURES

LIST OF TABLES

LIST OF EQUATIONS

LIST OF ABBREVIATIONS

^{1}H-NMR	:	Proton nuclear magnetic resonance
2D	:	Two-dimensional
3D	:	Three-dimensional
40%C_{18}-PGA	:	40% stearoyl substituted poly(glycerol adipate)
40%C18-PGA-PEG-MIHA	:	40% stearoyl substituted PGA coupled with MIHA-PEG-NH_2
ALP	:	Alkaline Phosphatase
Alpha MEM	:	Alpha Modified Eagles Medium
ASC	:	Adult Stem Cell
bFGF	:	Basic Fibroblast Growth Factor
BMP	:	Bone Morphogenetic Protein
BMP-2	:	Bone Morphogenetic Protein-2
BMSC	:	Bone Marrow Stromal Stem Cell
BSA	:	Bovine Serum Albumin
CA	:	Coacervating Agent
CEE	:	Columnar Epiblast Epithelium
CF	:	Continous Flow
DCC	:	*N,N*-dicyclohexylcarbodiimide
DCM	:	Dichloromethane
Diamine PEG	:	Diamine poly(ethylene glycol)
DMEM	:	Dulbecco's Modified Eagle Medium (DMEM)
DNTB	:	5-5'-dithiobis-2-nitrobenzoic acid
DXM	:	Dexamethasone
DXMP	:	Dexamethasone 21-disodium phosphate
EB	:	Embryoid bodies
ECM	:	Extracellular Matrix
ESC	:	Embryonic Stem Cell
FBS	:	Fetal Bovine Serum

FITC	:	Fluorescein-5-isothiocyanate
FTIR	:	Fourier Transform Infrared
HBSS	:	Hanks Balanced Salt Sodium
HCl	:	Hydrochloric acid
HEPA	:	High Effiency Particulate Air
HPLC	:	High Performance Liquid Chromatography
HPMC	:	Hydroxypropil methylcellulose
HRP-DAB	:	Horseradish peroxide-Diamino-benzidine
HSC	:	Hematopoeitic Stem Cell
IGF	:	Insulin-like Growth Factor
iPS	:	Induced Pluripotent Stem cell
$KMnO_4$	:	Potassium permanganat
LIF	:	Leukemia Inhibitory Factor
MeOH	:	Methanol
mES	:	mouse Embryonic Stem cell
MIHA	:	*N*-maleimidohexanoic acid
MIHA-PEG-NH_2	:	Maleimide-poly(ethylene glycol)
MP	:	Microparticle
MSC	:	Mesenchymal Stem Cell
NaCl	:	Sodium chloride
NGF-β	:	Nerve Growth Factor Beta
NHS	:	*N*-hydroxysuccinimide
O/W	:	Oil in water
PBS	:	Phosphate Buffer Saline
PDGF	:	Platelet Derived Growth Factor
PEG	:	Poly(ethylene glycol)
PFA	:	Paraformaldehyde
PGA	:	Poly (glycerol adipate)
PLGA	:	Poly (lactic-co-glycolic acid)
PLLA	:	Poly (L-lactide)
pNPP	:	p-nitrophenyl phosphate

PVA	:	Poly (vinyl alcohol)
RGD	:	Arginine- Glycine-Aspartic acid
SCM	:	Standard Culture Medium
SD	:	Standard Deviation
SEM	:	Standard Error of Mean
SIM	:	Simvastatin
SNL	:	STO Neo-Leukemic
SS	:	Sample and Separate
SSEA	:	Stage Specific Embryonic Antigen
TGF	:	Transforming Growth Factor
THF	:	Tetrahydrofuran
TLC	:	Thin Layer Chromatography
TRA	:	Tumor Rejection Agent
VEGF	:	Vascular Endothelial Growth Factor
W/O	:	Water in oil
W/O/W	:	Water in oil in water

CHAPTER 1

1. INTRODUCTION

1.1. Tissue Engineering

1.1.1. Background

Tissue engineering arose out of the demands by surgeons in regenerating functionally active tissues to replace those lost due to trauma, congenital malformations or various diseases. The term tissue engineering relates to the use of living cells for replacement, repair and regeneration of various tissues and organs and also be used to describe approaches for tissue replacement by creating tissue outside the body and then implanting it in the body [1]. Current methods for tissue replacement are mainly the use of autografts, allografts or metallic devices. However, these methods are associated with several limitations including donor site morbidity, shortages in supply, poor integration with target and potential induction of immunological reactions. These limitations highlight the need for development of therapies based on tissue engineering principles [2].

Tissue engineering in the area of cell technology has to meet a number of challenges including the source of cell, the use of technology and the manipulation of cell function. Other issues include how to design and engineer tissue constructs with/without delivery vehicles and developing the technology to make these

constructs available to clinicians. The last issue relates to the integration of cells into the living system where the engineering of immune acceptance is the most critical issue. The success in tissue engineering will only be accomplished if these issues could be addressed [3].

The initial issue for engineering a tissue or organ substitute is a source of the cells to be employed. The cells need to be available in sufficient quantity and guaranteed to be free of pathogens and contamination. The source of the cells could be autologous, allogenic, or xenogenic and each of these sources has both advantages and disadvantages as indicated in Table 1.1.

Table 1.1. Cell Source for Tissue or Organ Substitution[3]

Type	Source	Condition
Autologous	Patient's own cells	Acceptable by immune system, but does not lend itself to off-the-shelf availability.
Allogenic	Cell from other human sources	May require arrangement for immune acceptance and be able to lend itself for off-the-shelf availability.
Xenogenic	Cell from different species	Requires arrangement for immune acceptance and must also deal with animal virus transmission.

Once a particular cell type has been selected, the next issue is the manipulation of functional characteristics of the cell to accomplish the desired behaviour. This could be achieved by controlling a cell microenvironment including its matrix, the mechanical stresses to which it is exposed, or its biochemical environment. Alternatively, the cell could be genetically reprogrammed which may include the modification of matrix synthesis, inhibition of immune response, diminishing of

thrombogenicity, expression of specific biologically active molecules, and the controlling of cell proliferation [3].

The next challenge in tissue or organ substitution is to develop into a well-organized three-dimensional (3D) architecture with mimicking functional characteristics of the specific tissue. A delivery vehicle for the cells also has a role in tissue or organ substitution therefore several approaches have been used to engineer a tissue-like substitute. Cells can be seeded on a polymeric scaffold to allow them to produce their own matrix. Alternatively, a layer of cells can produce their own matrix to become a sheet of tissue [3]. Once a cell product has been manufactured, it can be delivered to the clinician using particular conditions such as at room temperature or cryopreserved [3].

Integration of an engineered tissue into the living system is the final challenge to mimicking the nature. Various animal models have been established to the study of different diseases. Regrettably, these models are somewhat unproven in their capacity to evaluate the success of the tissue engineering concept. This is also found in human clinical trials. Immune response also has an important role in the success of any tissue engineering approach. Therefore, it would be desirable to have periodic assessment for a tissue substitute viability and functionality as well as a post-implantation strategy for the patient [3].

1.1.2. Three Dimensional (3D) cell culture

Most research in cell culture has been established on 2-dimensional (2D) surfaces. In 2D culture, cells are grown in micro-well plates, tissue culture flasks and petri dishes which provide convenience and high cell viability in 2D culture [4]. The conventional 2D cell culture systems are sufficient to improve the understanding of basic cell biology but the system is insufficient to describe three-dimensional (3D) complexities in living tissue. *In vivo*, cells are supported by a complex 3D extracellular matrix (ECM) which allows cells to communicate *via* direct contact and through the secretion of a plethora of cytokines and trophic factors. In contrast, flattened morphology in 2D culture system forces cells to adopt unnatural characteristics and require an adaptation to survive due to the lack of specific ECM environment [4, 5]. Therefore, 2D cultures fail to represent the complex and dynamic environment of the body [4].

In pharmaceutical development, mimicking the behaviour of cells *in vivo* is the essential step for improving accuracy of prediction. It can be achieved by creating a cell microenvironment that can support cell growth, organization, and differentiation [4, 5]. There are several methods to engineer and model 3D interactions *in vitro,* including natural aggregation using stirred or rotary cell culture, physically encouraging cell to cell interaction, hanging drop culture, or growth with 3D matrices [6].

Aggregation of cellular spheres can be done by constant rotation of regular culture dishes, or use of a spinner flask or in a conical tube within a roller drum. The critical

factors for these methods are the size of dishes, flasks, or tubes for cell culture and the speed of the rotation [7]. The size of the dishes, flasks, or tubes will affect the diffusion of nutrient. Effective nutrient delivery and waste removal from cell culture could be achieved by increasing speed of rotation. However, higher speed will create turbulent flow and higher shear stress that can induce cell necrosis in the periphery of the 3D cell constructs. Therefore, this issue should be addressed to develop reproducible 3D engineered constructs [8]. It was reported that spheroid formation by agitation for porcine hepatocytes gave a simple and reproducible result. Hepatocyte culture in spheroids exhibited higher metabolic activity compared to those in monolayer cultures [9].

Three-dimensional (3D) formation of cells could also be achieved by encouraging aggregation. The principle of this method is manipulation of cell surface chemistry. Surface of the cell can be functionalized with biotin *via* a covalent hydrazine bond. Addition of avidin into suspension of biotinylated cells rapidly cross-links cells into aggregates as avidin and biotin have a high binding affinity [6]. The other method to induce multicellular 3D formation is hanging drop method. In this method, cells in suspension have been hung as a drop from the lid of a petri dish. Gravity assures the cells collect at the bottom of the drop and to assemble as 3D multicellular aggregates [10, 11]. The hanging drop method is compatible with various cell types and has been used in tissue engineering to form tissue-like cancer models, for gene-function analysis, and in the design of functional microlivers, microhearts and microcartilage [10]. The advantage of the hanging drop method is the number of the cells in 3D aggregate could be controlled by adjusting the number of cells in the initial

suspension. However, the liquid volume of a drop should be less than 50 microliter in order to maintain the surface tension of a hanging drop on the lid. Furthermore, changing the medium during cultivation is also not possible on hanging drop [11].

Providing 3D cell constructs can also be achieved by seeding the cells on matrices. The matrices, also known as scaffolds, are engineered to promote the standard 2D cell culture system to a 3D platform and act as a temporary substrate for supporting and guiding tissue formation in various *in vitro* and *in vivo* settings [2, 12]. Scaffolds could also be implanted directly *in vivo* to guide the function of regeneration in a defective tissue or organ. Designing a scaffold could be possible through understanding the cell-ECM interaction in native tissue. Therefore, the main theme of designing matrices or scaffolds for tissue engineering is to understand the correlation between matrices or scaffold properties and biological function [2, 12, 13].

1.1.3. Tissue Engineering Scaffold

The main components of engineered tissue for developing biological substitutes of tissues or organs are cells, scaffolds and signals for stimulating cell growth. A scaffold has a function as a matrix for cells to attach and support subsequent tissue development including deposition of extracellular matrix (ECM) [2, 14]. The ECM is a solid matrix in normal tissues which is an important component of all organs to provide structural scaffolding and contextual information. When cells are placed in contact with a suitable matrix, the cells start to multiply, proliferate, differentiate, secrete factors like ECM molecules and remodel their environment [2, 13].

The finest scaffold for an engineered tissue should be able to act as ECM of the target tissue. However, it is difficult to precisely mimicking the dynamic nature of ECM in native tissue. Therefore, a basic concept of scaffold in tissue engineering is, at least partially, to mimic the architectural, biological and mechanical features of tissue's ECM as shown in Table 1.2 [14].

Table 1.2. Comparison between Extracellular Matrix (ECM) in Native Tissue and Scaffold [14]

	Function of ECM	Function of Scaffold
1.	Support the cells to stay live.	Support exogenous cells to attach, grow, migrate and differentiate *in vitro* and *in vivo.*
2.	Support the mechanical properties of the tissues.	Gives the required shape and mechanical stability to the tissue defect as well as rigidity and stiffness to the engineered tissue.
3.	Delivers bioactive signals for cells to respond to their microenvironment.	Facilitates the cells to proliferate and differentiate by active interaction with the cells.
4.	Provide a reservoir of growth factors and activates their effects.	Provide a delivery vehicle and reservoir for exogenous growth factors.
5.	Gives a flexible physical environment to allow remodelling of tissue.	Gives an empty space volume for vascularization and formation of new tissue during remodelling.

The material for a scaffold should meet several criteria including [15, 16]:

1. It should be biocompatible and biodegradable to support the formation of a new tissue with no inflammation involved.
2. It should retain an adequate structure composition and be responsible for an appropriate 3D architecture of the tissue renewal.

3. It should be tailored to supply the particular cell types with nutrition and others biological needs for cell proliferation.
4. It should interact with cells, support cell adhesion and promote ECM deposition [17].

Initial interaction between cell and scaffold plays an important role in 3D culture. Several factors have determined the initial interaction of scaffold with the cell, such as chemical composition, surface energy, roughness and topography of the top surface layers [15].

Materials for scaffolds can be synthetic or biological, biodegradable or non-bio degradable, depending on the purpose. There are some main types of material used as biomaterial for scaffold including natural polymer, synthetic biodegradable and synthetic non-biodegradable polymer (Table 1.3) [17].

Table 1.3. Type of materials for scaffold and its properties [17]

Materials	Properties	Examples
Natural polymers	– Most of them are biodegradable. – Better interactions with cells to support cells performance.	Protein (silk, collagen, gelatin), polysaccharides (cellulose, amylose, dextran), polynucleotides (DNA, RNA).
Synthetic biodegradable polymers	– Biodegradable. – Could be tailored based on specific purpose (biodegradability, porosity and mechanical characteristics). – Stable for long time storage. – The cost is cheaper compared to natural polymers.	Polylactide, polyglycolide, poly(l-lactide-co-glycolide), polyhydroxyalkanoates.
Synthetic non-biodegradable polymer	– Forms a tight bond with tissue in physiological fluid. Insufficient biocompatibility and biodegradability. – Could be combined with natural polymer to achieve desired properties to meet biological and mechanical properties.	Hydroxyapatite, tricalcium phosphate, silicate and phosphate glasses, glass-ceramics.

Several types of scaffold are available for clinical use including porous scaffold, fibrous scaffold, polymeric-bioceramic composite scaffold, acellular scaffold and microsphere scaffold.

1.1.3.1. Porous Scaffold

Porous scaffolds have a high porosity and interconnected pore network to mimic the ECM construction and allow cells to interact with their environment. Moreover, the porosity also supports cells to adhere and proliferate on the scaffold [17, 18]. The key parameter for initial cell impregnation within scaffold is the pore size of the scaffold as it will subsequently affect cell proliferation, differentiation and tissue formation. The optimal sizes of pores in scaffold have been suggested for regenerating various cell types *in vivo*. The larger pore volume of fibrous scaffold made from poly(ethylene terephthalate) lead to larger size of cells aggregate [12].

Transport of bioactive material and nutrient to cells within the scaffold is also affected by the pore size of scaffold. Cells seeded in scaffold often exhibit hypoxia which induces cell death as a result of insufficient diffusion of nutrient within the 3D structure [12, 19]. The bone formation using bone morphogenetic protein was more rapid in scaffold with large pore diameter (350 μm) compared to bone formation in small pore diameter (90-120 μm). It showed that different pore size could affect the onset time of vascularization and differentiation of the cell [12].

The size of pores within the scaffold could be controlled during fabrication. However, it is hard to achieve controlled structure and pore size using conventional method of scaffold fabrication such as solvent casting, particulate leaching, gas foaming, freeze drying, electro spinning and laser sintering. In order to solve this problem, several techniques to produce highly controlled scaffold structure have been introduced, such as solid free-form fabrication (SFF), microfluidic patterning, laminar flow

patterning and projection stereo lithography (PSL) based on computer-aided design (CAD) [19, 20]. These methods could produce narrow variations in structure and pore-size of scaffold. It has been reported that controlled fabrication scaffolds produced significantly higher glycosaminoglycan (GAG) compare to those fabricated by conventional methods. That concludes that controlled method of scaffold fabrication gave promising in reproducible formation of functional engineered tissue [12, 19].

1.1.3.2. Fibrous Scaffold

Fibrous scaffolds have high surface-area to volume ratio which gives excellent property to enhance cell attachment, proliferation, migration and differentiation [17, 21]. Fibrous structure can be considered as a potential tissue engineering scaffold as it adopts the structure of natural ECM. The structure of fibrous scaffold plays an important role in cell behaviour as well as in the maturation process for tissue regeneration. In order to act as ECM, the diameter of fibres should be in a nanometer scale. It has been found that collagen type I, which is the base attachment structure for cells in many tissues, has a nano-fibrous structure [22-24]. There are three common techniques available for nano fibrous fabrication: electrospinning, self-assembly, and phase separation.

Fabrication using electrospinning technique is a most widely used for tissue engineering application due to simplicity and ability to produce nano-fibres from various materials [17, 24] In this technique, an electric field draws a polymer solution from an orifice and brings it to a collector to produce a polymer fibre with a certain diameter. The diameter of fibre can be controlled by varying the concentration of the

polymer solution. The higher concentration of polymer solution produces larger diameter of fibre [24].

The second technique for fibrous scaffold fabrication is a self-assembly technique. This technique is applied to produce supramolecular architectures by putting together molecules which spontaneously form a large assembly. The structure is well-ordered with stable arrangement through a non-covalent interaction such as hydrogen bonds, Van der Waals interaction, electrostatic interaction and hydrophobic interaction. Biomolecules such as peptides and proteins have been produced using this technique and showed capability to support cell growth. Peptide-based self-assembling structures can be assembled in the presence of cells and allow encapsulation of cells within the structure. In addition, the problem of stimulating cell growth into a preformed scaffold can be avoided [17, 24, 25]. The formation of a fibrous scaffold using self-assembly usually produces a smaller fibre diameter compared to those produced by electrospinning. However, it has not been demonstrated with this technique how to control pore size and pore structure which are important for cell incorporation, migration and proliferation [24].

The last technique that has been used for fabrication of fibrous scaffold is phase separation. The principle of this method is thermally induced phase separation to produce a nanofibrous scaffold. During the process, polymer is dissolved in a solvent, and then by controlling the temperature of polymer solution, it separates into two phases, a polymer-rich phase and a polymer-lean phase. Afterwards, the solvent in the polymer-lean phase is removed by extraction, evaporation or sublimation to produce a porous polymeric scaffold. In contrast, when the temperature is lowed

enough to freeze the solvent in the polymer-rich phase, it forms frozen solvent and a concentrated polymer phase. The pores would be formed later after removal of the frozen solvent. Different pore morphologies and structures can be produced by varying the polymer concentration, solvent and temperature to induce phase separation [24, 26].

1.1.3.3. Polymeric-bioceramic composite scaffold

Ceramics and their composites are attractive as scaffold material since they meet the requirement for the mechanical and physiological necessities of the host tissue, particularly for bone tissue engineering [17, 27, 28]. A ceramic scaffold could be used as a delivery vehicle for drug, however the release pattern of drug from ceramic scaffold is difficult to control [28]. Ceramics in tissue engineering, can be categorized into three classes [17]:

1) Non absorbable (inert), for examples alumina, zirconia, silicone nitrides and carbons.
2) Bioactive or surface reactive (semi inert), for examples glass ceramics and dense hydroxyapatite.
3) Biodegradable or resorb-able (non-inert), for example aluminium calcium phosphate, coralline, and tricalcium phosphate.

The main purpose of materials for bone tissue engineering is to fill bone defects. Thus, these materials should be able to maintain appropriate mechanical strength, be osteoconductive and biodegradable to provide a space for the formation of the new bone. Materials such as hydroxyapatite and tricalcium phosphate have been used for this purpose since they have similarity to chemical and structural properties of bone

mineral. However, the clinical application for these materials is limited due to their stiffness and brittleness. To overcome this problem, these materials have been combined with polymer into a composite to give materials with improved mechanical properties. The addition of polymer to the materials can alter the biodegradation rate of the scaffold [17, 29] and also control release drug from scaffold [28]. The inorganic components in natural bones such as calcium phosphate, hydroxyapatite and tricalcium phosphate can be combined into a composites with several materials like poly (l-lactide-co-glycolide), poly(l-lactic-acid), chitosan, collagen, and gelatin [17, 28] .

1.1.3.4. Acellular Scaffold

As an alternative to a biodegradable scaffold, the use of matrix from a biological source is a favourable option. This concept has been used in acellular tissue matrices. Acellular matrices are the matrices produced by excluding cellular components from tissue by mechanical or chemical manipulation to produce collagen-rich matrices. They can be used alone or seeded with cells. The degradation rate for these matrices is slow and generally replaced by ECM of transplanted cells [17, 30-32]. The advantages of using acellular scaffold are they retain suitable anatomical structure after the decellularisation process, maintain original ECM architecture and encourage cell adhesion, reduce immunological response and facilitate the development of similar biomechanical properties [17, 30].

Preparation of acellular matrices can be achieved by several methods including repetitive freezing/thawing, high pressure treatment, enzymatic and chemical processes [30, 33]. However, repetitive freeze/thawing and the high pressure

method could deposit undesired cells detritus. Consequently, this method would result in an acellular scaffold with potential immunogenic issues. The immunogenic problem could be avoided by enzymatic process, but it would disrupt and digest part of the ECM. Sandmann *et al* [33] demonstrated a chemical process using the detergent sodium dodecyl sulphate to decellullarize ovine meniscus. The processed menisci produced cell-free scaffolds and did not alter collagen fibre arrangement within the scaffold [33]. A combination of enzymatic and chemical process has been demonstrated to yield acellular scaffold. Collaboration between hyper-hypotonic washes, enzymatic digestion and detergent treatment was used to produce acellular scaffolds from porcine cardiac tissue. The acellularized porcine cardiac extracellular matrix presented a fibre myocardial architecture and the myocytes seeded in the scaffold expressed typical functional cardiac markers such as α-actinin, troponin I and connexin 43 [34].

1.1.3.5. Microsphere Scaffold

Drug delivery method based on microsphere could be applied in tissue engineering for encapsulation of bioactive signal or living cells within the microsphere. Microspheres also can be tailored as carriers to modulate spatial and time-specific release profile. Moreover, microspheres can be used as matrices to encourage cell attachment and proliferation [16, 17, 35]. Generally, a polymer is used as a matrix to encapsulate the drugs or bioactive agents and then release the drug at a moderately slow rate for a prolonged period of time [17, 36]. Microspheres in tissue engineering system can be injected with a syringe or combined with the scaffold used for implantation. Additionally, it can be used for aggregating cells to form a 3D construct

and then implanting the construct at the later stage, particularly for bone and cartilage tissue engineering [16]. Polymers from synthetic or biologically-derived materials can be used to build a microsphere scaffold for tissue regeneration and replacement.

Synthetic polymers are good candidates for tissue engineering application as their physical and chemical properties can be readily controlled and manipulated for certain purposes. Some of the synthetic polymers available for regenerative medicines and drug delivery are poly(hydroxy acid), poly(lactic acid), poly(glycolic acid), and poly(lactide-co-glycolide). They are biocompatible and approved by US Food and Drug Administration. Moreover, these polymers will degrade gradually into water soluble and nontoxic by-product, and then be eliminated from implant site by the normal metabolic pathways [36].

Regarding biocompatibility, biologically-derived polymers are naturally compatible molecules and produce the required responses in cells, tissues, or organ [36]. These types of polymers can be obtained by enzymatic processes or extraction from plant, animal or algae. Some biologically-derived polymers, such as collagen, fibronectin, fibrin and glycosaminoglycans, are inspired by extracellular matrix. These materials can be useful to guide morphogenesis in tissue development. Silk as a protein-derived biomaterial could be used as well as polysaccharide from plant (cellulose, galactans, alginate), animal (chitin, chitosan, hyaluronic acid) and microbial (dextran, xanthan gum) sources [16].

Physical characteristics of microspheres such as particle size, shape, and porosity take important roles in the release of encapsulated compounds from microspheres. [35, 36]. The size of microspheres can be controlled by passing polymer solution through a nozzle to create a specific size of droplet [35, 37]. Pore size also plays an important role for releasing drugs from microspheres as the presence of pores in the microspheres increase the motion of the active diffusing species such as drug molecules or bioactive agents. Therefore, the high porosity provides a high release of molecules from microspheres [38]. Increase in molecular weight and polymer concentration resulted in a significant decrease of molecule release from microspheres [39].

1.1.4. Injectable Scaffold in Tissue Engineering

The aim in tissue engineering is to obtain functional substitutes for damaged tissue using 3D construct of scaffold, living cells and bioactive molecules. The 3D structure can be pre-formed outside the body and implanted or injected as a mixture of bioactive molecules and scaffold precursors which form a 3D structure *in situ.*

The advantage of using an injectable scaffold for tissue regeneration is to minimize patient discomfort due to surgical intervention, reduce risk of infection, scar formation and the cost of treatment. Additionally, an injectable scaffold would be able to take the shape of the tissue defect and fill it without prior knowledge of size and shape cavity. As a carrier for bioactive molecules, an injectable scaffold could be used as a controlled release device [40, 41]. However, the injectable scaffold system should be able to support a suspended cell population during the solidification

process [41]. After injection, an injectable scaffold will generate a 3D matrix where cells can adhere, proliferate and differentiate. In tissue engineering, an injectable scaffold is a promising system for tissue regeneration particularly for bone and soft tissue regeneration [40].

An injectable system for tissue regeneration should meet criteria for both tissue engineering and drug delivery. Most importantly, the rate of degradation for injectable scaffold materials should ideally match the formation of the new tissues. Moreover, porosity in the scaffold should be enough to support cell growth and diffusion of nutrients as well as transport of waste products from the cells. Bioactive agents should be presented in the scaffold in order to promote cell growth and differentiation. It can be provided by combining scaffold with growth factor or adhesion-specific peptide which can mimic the extracellular matrix to produce suitable signals for cells [41]. Adhesion-specific peptides, like arginine-glycine-aspartic acid (RGD) sequences could be incorporated in the injectable scaffold to promote specific functions of the cells. However, the selection of suitable peptide sequences and optimization of the density and distribution of the peptide sequences are important issues. The injectable scaffold acts as a reservoir e.g. for growth factors that releases the bioactive molecules at target site for a certain length of time. Since most growth factors have short half-lives, the important consideration is how to retain their bioactivity and effectively release them to site of action with optimal dosage, timing and correct order [40].

An injectable scaffold should undergo a mild solidification process close to physiological condition in order to keep cells viable and retain biomolecule activity.

There are several types of solidification for injectable scaffold including chemical polymerization and crosslinking, thermo gelation, ionic crosslinking and self-assembly.

1) Chemical polymerization and crosslinking

Solidification of an injectable scaffold can be achieved *in situ* by using chemical activated polymerization or crosslinking. A monomer or macromer with unsaturated bond or photosensitive functional group will react in the presence of an initiator to form cross links which is activated by temperature or light. The properties of crosslinkable polymers depend on types and concentration of initiators as well as the ratio and density of crosslinking agent. Additionally, the period of reaction, temperature and intensity of visible light also play major roles for thermal and photochemical cross linking. The most common used crosslinkable polymers in tissue engineering are (meth)acryloyl, styryl, coumarin, phenylazide, and fumaryl monomers [40, 41]. An initiator like ammonium persulfate/N,N,N′,N′-tetramethylethylenediamine can be used with oligo(poly(ethylene glycol) fumarate) to produce a hydrogel construct at 37°C [41].

The crosslinkable polymer could be combined with microparticles to give porous injectable composites with an ability to incorporate drugs and growth factors. Common microparticles loaded into injectable scaffolds were made from poly(lactic-co-glycolic acid), poly(propylene fumarate) and gelatin. Gelatin microparticles loaded with growth factor have been used to encapsulate cells within the composite and provide shielding for cells during the crosslinking

process. This microparticle was then incorporated with poly(propylene fumarate). The composite showed the ability to induce proliferation and glycosaminoglycan production in chondrocytes [41].

2) Thermo gelation

Some aqueous polymer solutions can be activated to produce a gel by an alteration in temperature. These kinds of hydrogels do not require a chemical agent to solidify as a gel and the gelation point can be arranged close to normal body temperature. Hence, they can be injected in a liquid form and become solid inside the body. Natural polymers like cellulose derivatives, chitosan and gelatin have been reported for use as injectable scaffolds based on thermo gelation. On the other hand, synthetic polymer like poloxamer (Pluronics®), poly(ethylene glycol), and poly(N-isopropylacrylamide) are most widely use due to their thermal behaviour [40, 41].

3) Ionic crosslinking

Gel formation could be induced by ionic crosslinking. A naturally derived polysaccharide, alginate, in aqueous solution can perform a reversible gel in the presence of di- or trivalent cations, for example Ca^{2+}. Alginate is a biomaterial which consists of 1,4-linked β-D-mannuronic acid (M) and α-L-guluronic acid (G) in varying proportions and sequential arrangement. The ionic inter chain bridges are formed as the cations bind the guluronic acid blocks in alginate chains. As an injectable extracellular matrix analogue, alginate has an advantage from its biocompatibility for *in vitro* cell culture [40, 41] .

The gelation rate in alginate depends on concentration of cation, alginate composition, and gelation temperature. Increasing concentration of cation gives a high gelation rate and alginate with higher G content or longer G segment achieved faster gelation process. However, a higher alginate concentration tends to decrease gelation rate. Mechanical properties and uniformity of hydrogels are influenced by gelation rate. Homogenous structure of the gel with greater mechanical strength can be achieved at a lower gelation rate. Additionally, the desired mechanical strength is achieved with increasing alginate concentration, ionic content, molecular weight and G content in alginate. A lipid vesicle, like liposome, can be used to release calcium based on temperature, to induce rapid formation of alginate hydrogels [40, 41].

4) Self-assembling systems

In a self-assembling system, neither chemical cross linking agents nor initiators are involved. Polymer spheres, often referred to as nano- or microparticle, were mixed with a cells suspension in suitable cell culture medium then injected to the site of defect. Avidin could be added to support crosslinking formation of particles with the cells if biotin ligands are incorporated. The advantage for this self-assembly process is to avoid chemical exposure to the cells which potentially induces cytotoxicity. However, the mechanical strengths of self-assembly systems are often lower than chemically crosslinked systems. Therefore, self-assembled systems are inappropriate for use in load or tension bearing connective tissue [40, 41].

Incorporation of particles as a matrix for injectable scaffold could induce macrophage response. Fortunately, this immune response can be controlled by modifying the surface properties of particles. It has been found that particles coated with hydrophilic polymer chain, such as PEG, could exhibit less immune response and decrease clearance from the blood. The important factors for injectable particles are ratio of particle to cells and the type of injection system used. Ratio of particle to cells is not only important for dosing purpose but also to control the ability for injection in a clinical setting. Moreover, the effect of injection time should be considered. Injectability of the system is also affected by needle gauge. The appropriate needle gauge should be considered to be able to deliver the composite with a reasonable amount of force needed for injection, but which is acceptable for the patient [41].

1.2. Stem Cells

1.2.1. Background

The cell source becomes an important parameter for replacement therapy. Fully differentiated adult cells have limited ability to proliferate and tend to lose their phenotype during *in vitro* expansion. Hence, these limitations make stem cells useful as a potential source of cells for tissue engineering [2]. Stem cells have self-renewal properties, capacity to produce more undifferentiated stem cells and differentiate into one or more functional mature cells. The self-renewal capability of stem cells can be encouraged and retained for certain periods of time, even years, to produce a large number of cells [42, 43]. However, inside the body, stem cells do not divide frequently and remain dormant until they receive signals to start or stop dividing.

Hence, stem cells are usually quite rare and only limited amount being found in particular region of human body. The tight control of self-renewal in stem cells is necessary to control these cells to not divide indeterminately as it will induce over population of the cells and potentially become a cancer [43].

The principle rule of cell therapy is to explore the natural capacity of the human body to rebuild tissues through the regeneration process. Since stem cells have ability to differentiate to various cell lineages, it has the potential for use in tissue engineering and replacement therapy for various tissue such as for heart disease, bone or connective tissue disorders, neural defects, and haematological disorders [42]. The capacity of stem cells to differentiate into other types of cells can be classified into 3 types [42, 43]:

1) Totipotent: The cell has ability to differentiate into all types of cells that contribute to the formation of fertilised egg or zygote
2) Pluripotent: the cell has capacity to differentiate into almost all cell types including germ cells but not the placental tissue. Example for this type is embryonic stem cells.
3) Multipotent: The cell has ability to differentiate into most mature cells and featured tissue. Example for this type is hematopoietic stem cells.

The cells potency state depends on the genetics of the cells. Moreover, the environment of the cell's location also plays an important role. The process of cells to differentiate into a particular characteristic usually involves the formation of intermediate progenitor cells. Progenitor cells, or transit amplifying cells, differentiate into more specific cells than stem cells and have the ability to divide but

with very limited capacity for self-renewal [43]. The isolation of stem cells from different sources may provide adequate number of cells for various diseases as well as enhance application or autologous transplantation [42].

1.2.2. Types of Stem Cells

Based on the source, stem cells can be classified into adult stem cells, embryonic stem cells and induced pluripotent stem cells.

1) Adult stem cells

Adult stem cells (ASC) are undifferentiated cells in tissue with limited self-renewal and differentiation capacity. They are supposed to play important roles in the repair mechanism intrinsic to many tissues and organs [1, 3]. ASC usually differentiated into the cell types of tissue where they originally located, thus ASC are categorized to be multipotent cells [42, 43].

The ASC derived from embryonic germ layers consists of endodermal, mesodermal and ectodermal (Figure 1.1) [42, 44]. The most common of ASC is isolated from bone marrow, a mesoderm derived tissue. Bone marrow consist of 2 types of stem cells: hematopoietic and stromal mesenchymal stem cells [1, 42]. The bone marrow stem cells can be maintained without adding specific growth factors but they need specific growth factors for *in vitro* differentiation into several cell types such as osteoblast, chondrocytes, adipocytes, stromal cells, tendon cells and muscle cells [43].

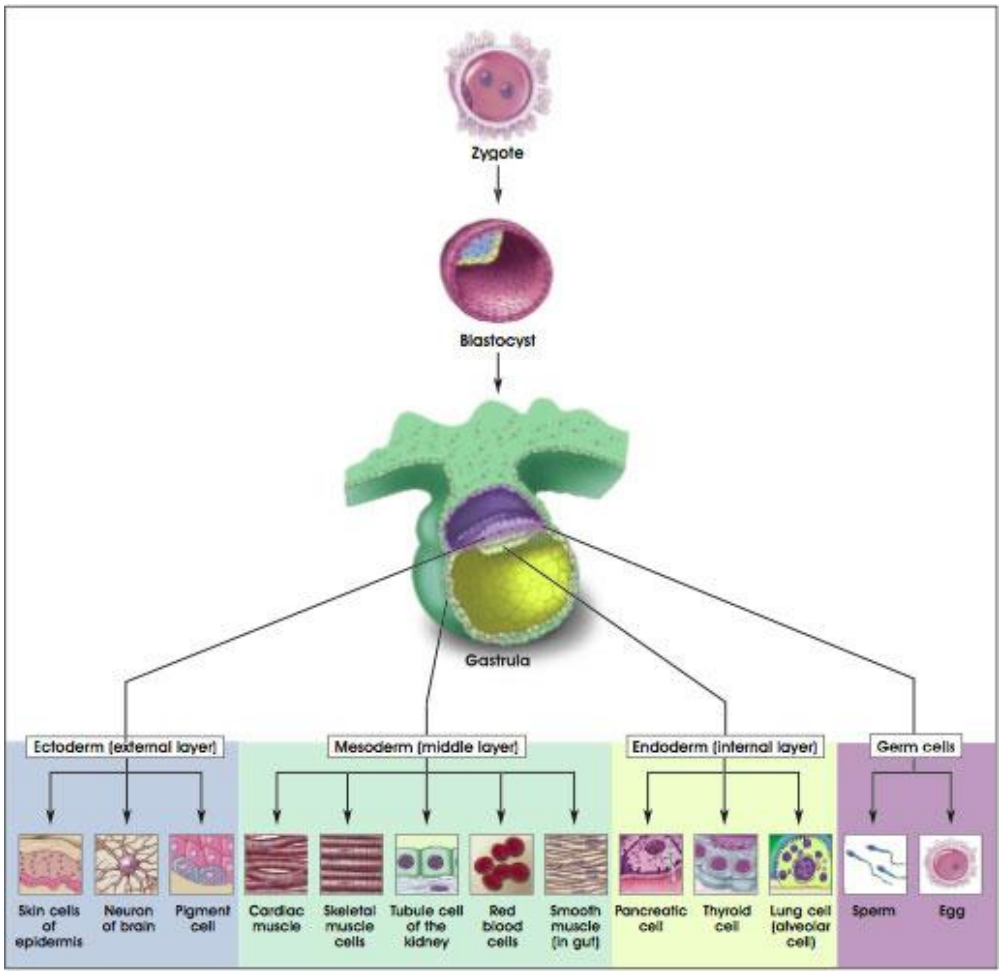

Figure 1.1. Schematic diagram showing the differentiation of human tissues from germ layers. Image is taken from Chandross, K.J. and É. Mezey (2002) without any modification [44].

In addition, several tissues like skin, gut and liver, also contain a population of stem cells to replace or heal cells that are missing due to normal wear or injury as these particular tissues have a high cell attrition rate. Cartilage, brain, heart and teeth also have been shown to contain a population of stem cells but with limited capacity for normal repair. The capacity of ASC to self-renew and differentiate is controlled by tissue-specific environmental factors. This environmental factor, referred as “stem

cell niche" is important to maintain homeostasis of the cells and to limit cells to differentiate, become apoptotic or produce other signalling that would reduce stem cell reserves. The "niche" controls the cells not to become overpopulated in a tissue which would potentially lead to cancer. Therefore, it is important to understand the relationship between stem cells and their niche to utilise cells effectively for therapeutic application [3, 43].

Cells obtained from less-mature sources like umbilical cord blood and foetal tissues also categorized as adult stem cells. Characteristic of stem cells from umbilical cord blood and foetal tissue are similar to hematopoietic stem cells (HSC) and bone marrow stromal stem cells (BMSC) [43]. Umbilical cord blood stem cells contain an original sub population of CD34, CD38 HSC [42]. Accordingly, the characteristics and ability to differentiate into multiple linages, umbilical cord blood stem cells and foetal stem cells are potentially useful for allogenic transplants.

2) Embryonic stem cells

Embryonic stem cells (ESC) are isolated from the inner cell mass of pre-implantation embryo during blastocyst stage [3, 43]. ESCs are usually isolated before day 5 when the entire embryo consists of a few hundreds of cells. In human embryo, manipulation is restricted to 14 days from its creation as this period is a specific stage in embryonic development. ESC have ability to differentiate into all specialized cell types but they unable to form tissue like placenta. For this reason, ESC is categorized as pluripotent, not totipotent [43].

The first lines of ESC were produced from mouse blastocyst in 1981, then from human ESC lines 17 years later. Currently, at least 225 human ESC lines have been produced in different laboratories by isolation of cells on mouse feeder layers of undifferentiated fibroblast [42, 43, 45]. As human ESC are derived from different embryos, they express different gene characteristics [3]. Besides culturing ESC on mouse feeder layer fibroblasts, ESC also can be cultured on human fibroblast derived from tissue like neonatal foreskin. Human ESC was recently cultured on human foetal fibroblast and animal-free product cell media in order to minimize transfer of potential harmful agents like animal pathogens. Co-culture of ESC cells with another type of cell is possible to be achieved on the surface coated with ECM preparation like gelatin or purified ECM protein, laminin [43].

The pluripotency of ESC can be maintained in culture by adding Leukemia-Inhibitory Factor (LIF), however, LIF alone is not sufficient for human ESC. Human ESC cultures require supplementation of basic fibroblast growth factor (bFGF) or the presence of a feeder layer. Both mouse ESC and human ESC express common transcription factors like NANOG, OCT4 and alkaline phosphatase but they slightly vary in expression in stage specific embryonic antigen (SSEA) [43, 45].

ESC will differentiate immediately after removal from the feeder layer and LIF or bFGF. The ES cells are usually maintained in suspension culture to form embryoid bodies, which contain endodermal, mesodermal and ectodermal cell lineage. ESC cells differentiate and proliferate in embryoid bodies as they mimic the process of gastrulation in early development of an embryo. However, not all ES cells have

capability to form embryoid bodies. Some of human ESC showed inability to form this structure [43].

3) Induced pluripotent stem (iPS) cells

Induced pluripotent stem cells (iPSC) are adult cells reprogrammed through retroviral transfection to resemble the pluripotency of embryonic stem cells [3, 46]. The use of viruses to introduce genes of pluripotency may cause mutation by viral insertion into the genome and result in abnormal proliferation. However, recent development of inducing pluripotency under protein-controlled conditions may eliminate the risks [46].

Identification and evaluation of iPSC begin with identifying compact colonies that have a distinct border and well-defined edge as well as large nucleus and scant cytoplasm. Although many colonies appear similar to ESC morphology, only a subset of these has comparable molecular and functional features. Furthermore, fully reprogrammed cells showed pluripotency markers including OCT4, SOX2 and NANOG, reactivate telomerase gene expression, down-regulate THY1 and up-regulate SSEA. Functional characterisation of iPSC can be assessed by *in vitro* differentiation as embryoid bodies or through two-dimensional (2D) differentiation in a culture dish. The current method to evaluate the function of iPSC involves teratoma formation. The potency of iPSC to differentiate *in vivo* is assessed by injecting the cells subcutaneously or intramuscularly to immune-deficient mice. If they formed well-defined tumours containing elements of each of the three germ layers, it can be conclude that the cells are truly pluripotent [47].

Although both iPSC and ESC show pluripotency, they are not identical in differentiation ability. Some mouse iPSC showed lower teratoma formation compared to mouse ESC. In addition, some human iPSC showed lower tendency to differentiate along hematopoietic and neuroephithelial lineage than human ESC. These findings elicit that iPSC has lower differentiation capability than ESC. Moreover, differentiation capacities of iPSC depend on the origin of the cells [47]. Generating patient-specific stem cells through reprogramming is a long-standing goal in field of regenerative medicines. The differences between iPSC and ESC do not diminish potential use of iPSC in medical application. Some research showed the utilisation of iPSC to use for disease modelling, drug screening, gene therapy and tissue engineering [46, 47].

1.2.3. Stem Cells for Bone Regeneration

Bone can be used as a prototype model for tissue regeneration, thus stem cells could be used to engineer functional tissue for implantation or preserve physiological function of bone [48]. Some basic considerations have been used to decide the source of cells for bone regeneration. These include [49]:

1. The source of the cells: from patient's own cells (autologous) or another person cells (allogeneic)
2. The availability and efficiency of cells for isolation
3. The use of primary osteogenic cells or self-renewal stem cell
4. The homogeneity and ability to control osteogenic induction
5. The possibility of automation and control the generation of cells

For bone construct preparation, cells are isolated and expanded *in vitro*. Approximately, 70 million of bone cells are required to form 1 cm^3 new bone. The critical step in expansion process is to maintain a stable expression of osteogenic phenotype and to avoid non-specific tissue development[49].

Source of stem cells for bone regeneration can be divided into two main categories. They are adult stem cells and embryonic stem (ES) cells.

1. Adult stem cells

   Bone marrow contains adult mesenchymal stem cells which have the ability to differentiate into several cells lineage including adipocyte, osteoblast, chondrocyte, cardiac myocyte, skeletal myocyte, neural cell, hepatic cell and renal tubular cell [50-52]. The proportion of mesenchymal stem cell (MSC) in bone marrow is around 0.001% to 0.01% of the total of adult bone marrow [49, 50]. Adult MSC contain positive marker for CD29, CD44, CD105 and CD166 and has ability to be doubling within 2 days [51].

   The use of MSC for bone regeneration is simple. Cells are isolated and expanded *ex vivo*. Then, cells are loaded into an appropriate carrier and transplanted *in vivo* [53]. All MSC can be maintained in undifferentiated state, yet sometimes difficult to maintain cell plasticity *in vitro*. Decrease in cells plasticity is indicated by decrease in proliferation rate and reduced capacity to differentiate into multiple cells lineage. In addition, cells differentiation potency is affected by the cell culture condition [50]. The potency of cells to differentiate can be

maintained by adjusting the appropriate condition *in vitro*, for example using collagen as substrate for cell culture, and using supplements in cell media [49].

Evaluation of differentiation potential in adult stem cells isolated from several tissues can be identified through the expression of surface antigen using flow cytometry, molecular, biochemical and histology assay. The bone marker gene expression related to functional osteogenesis have been used recently to design a mathematical model for bone formation capacity in synovial periosteal stem cell [49].

2. Embryonic stem cells

Embryonic stem (ES) cells have the capacity to continuously self-renew and differentiate into all cell types in the body to be established for replacement therapy [50, 54]. However, culture conditions for ES cells are more complex than adult stem cells. They are cultured in mitotically inactivated feeder layer in media supplemented with basic fibroblast growth factor [49]. The ES cells are characterised by specific surface antigens such as stage-specific embryonic antigen -4 (SSEA-4), tumor rejection agent-1-60 (TRA-1-60), TRA-1-81, alkaline phosphatase, telomerase activity, and expression of transcription factors OCT4, NANOG and SOX2 [49, 54].

Differentiation of ES cells commonly initiated by growing ES cells as aggregates in suspension culture, which are called embryoid bodies (EB). The EB leads to the formation of multi-differentiated structures. The capability for osteogenesis in EB appeared after 4 or 5 days of culture [49, 50]. Nevertheless, this method has limitations as the differentiated cells become heterogeneous. Individual cells

may receive different signals depending on their location in EBs. As a consequence, the several methods have been developed to select the required cells based on specific cell surface markers [50]. Co-culture ES cells with stromal cells can be used to induce differentiation, then followed by immunoselection of mesenchymal stem cell-like population [49]. Differentiation in ES cell could be induced by culturing ES cells in serum and media containing growth factors, for example, the osteoblast lineage can be developed in murine ES cells by culturing in media supplemented with ascorbic 2-phosphate, β-glycero phosphate and dexamethasone [49, 54].

Bone tissue contains 4 types of cells and their composition are varied throughout the body [55] :

1. Osteoblasts, as bone matrix producing cells
2. Osteoclasts, as bone matrix degrading cells
3. Osteocytes, the mature osteoblasts in mineralisation matrix
4. Osteoprogenitor, immature cells which have capability to differentiate into osteoblasts.

Differentiation of osteoblast as a bone-forming cell can be subdivided as in Figure 1.2. The phases are related with sequential expression of the genes involved in biosynthesis, organization and mineralisation of bone cellular matrix. The initial phase for osteoblast differentiation is proliferation which involves genes for proliferation (e.g., c-fos), progress of cells cycle (e.g., cyclins, histons) and biosynthesis of ECM (e.g., collagen type I). The next stage of osteoblast differentiation is maturation which involves genes for maturation and organisation of

bone extracellular matrix, for example alkaline phosphatase. Eventually, after proliferation and differentiation of osteoid, they become mineralized. In this phase, expression of genes related to deposition of hydroxyapatite occurred including osteopontin and osteocalcin [56, 57].

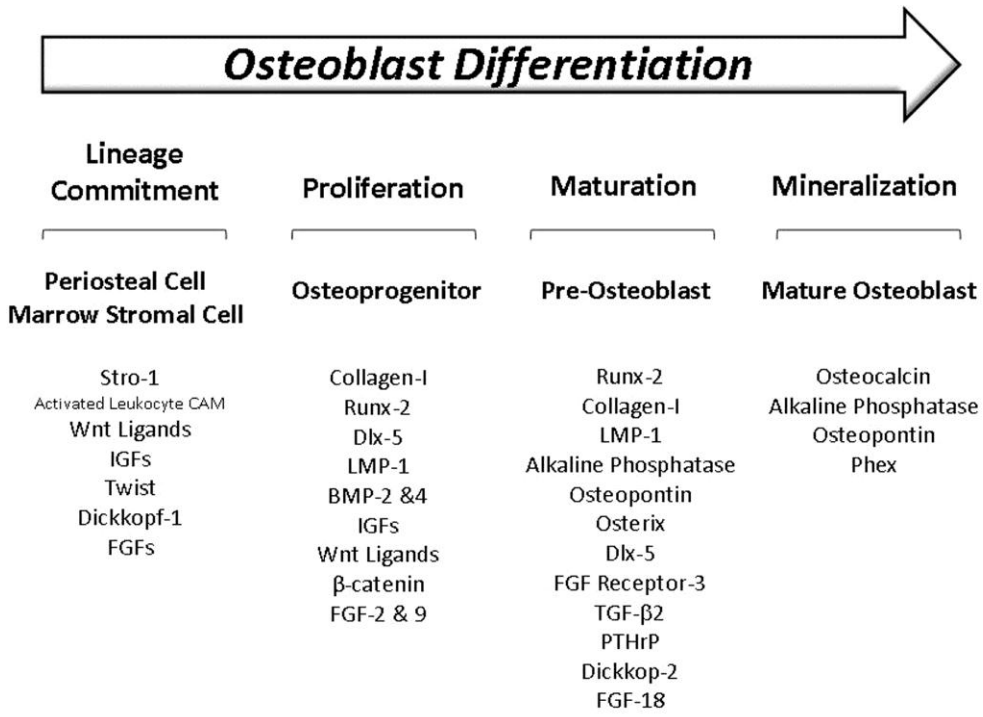

Figure 1.2. The stages of osteoblast development. The major transcription factors and growth factor in each stages of osteoblast differentiation are illustrated. The diagram taken from Strohbach, C.A., D.D. Strong, and C.H. Rundle (2011) [57].

There are three factors required to differentiate stem cell to bone cell for regenerative application, including morphogenetic signal, responding stem cells and extracellular matrix scaffolding [48]. The signals should be capable to modulate cellular activity and induce osteogenic process for bone formation. Growth factors or drugs could be used as the signals to either stimulate or inhibit cell proliferation, differentiation, migration and genes expression [58]. Term “growth factor” has been

used for natural protein that encourages cell proliferation and differentiation, usually refers to cytokines or hormones that bind into specific cell membrane receptor. In addition, some drugs such as statin, bisphosphonate, corticosteroids and antibiotics can be used to stimulate growth factor activity [55]. The list of growth factors and drugs that can be used as signals for bone formation are laid out in Table 1.4.

Growth factors usually bind to the specific receptor on the surface membrane of the cell target. In order to activate, they may need proteolytic activation and binding to matrix molecules for stabilisation. Their short half-life, relatively large molecular-size and slow penetration into cells or tissues make it difficult to deliver them through the conventional route such as adding them to culture media. This problem can be solved by incorporating them into a polymeric carrier which can facilitate the release of the bioactive molecules over extended periods [58].

Table 1.4. Several Growth Factors and Drugs for Morphogenetic Signals to Induce Bone Formation in Stem Cells.

Growth Factor or Drug	Function
Basic Fibroblast Growth Factor (bFGF)	Stimulate cell proliferation and increase production of mineralized matrix by enhance intrinsic osteogenic potential [55, 59, 60].
Vascular Endothelial Growth Factor (VEGF)	Stimulate proliferation, cells migration and osteoblast formation and control survival of stem cell by prevent inhibitor to penetrate the plasma membrane [61].
Platelet Derived Growth Factor (PDGF)	Increase population of bone forming cells by involved in cell division, migration and growth [55, 62]. Stimulates osteochondral progenitor and modulate response to BMP[63].
Nerve Growth Factor Beta (NGF-β)	Accelerated maturation in bone formation [64] and reducing apoptosis in osteoblast [55].
Transforming Growth Factor (TGF) family (TGF-β1, TGF-β_2 and TGF-β_3)	Induce cell growth, proliferation, differentiation and apoptosis [55, 65], regulating extracellular matrix formation [55], increase osteocytes density and bone formation [65, 66].
Bone Morphogenetic Protein (BMP-2 and BMP-4)	Initiate and promote stem cell osteogenesis [48, 55, 58, 67].
Wnt/ β-catenin	Controlling homeostasis of bone-forming osteoblast and bone-resorbing osteoclast [62, 68]
Insulin-like Growth Factor (IGF-I and IGF-II)	Local regulator in osteoblastic function and formation [62, 69, 70].
Corticosteroid	Stimulate expression of genes involved in bone formation and mineralization [71-73].
Statin	Involve in BMP2 up regulation and bone matrix mineralization production [55], increase anabolic effect and genes expression involving in osteogenic differentiation [74-76].
Ascorbic acid	Act as antioxidant [55], initiate extracellular matrix formation [77], stimulated ALP and osteocalcin for osteoblast formation [78, 79].
Biphosphonate	Inhibit bone-resorbing osteoclast activity [55, 80], enhance proliferation and initiate osteogenic differentiation [80-82].
Dihydropyridine	Increase collagen type I and osteoid calcification by stimulation calcium channel [55, 83, 84]
Antibiotic	Reduce or inhibit microorganism such as bacteria to prevent bone cells infection [55, 85]

1.3. Microparticles

Microparticles are small particles ranging in size from 1 to 1000 μm, with one or multiple core substances (solid or liquid) that are surrounded by polymer matrices [36, 86]. Microparticles offer several benefits such as controlling delivery and release of the drugs, they are easy to produce and biochemically stable. The incorporation of drugs can be achieved by encapsulation. The drug encapsulation into microparticles could be useful to deliver drugs with a sustained release profile over a period of time [87].

1.3.1. Microparticle Production

The method of microparticle production plays an important role in microparticle characteristics and drug loading. There are several techniques to create microparticles, such as emulsification, polymer phase separation (coacervation), spray drying and the use of supercritical fluid (SF).

1) Emulsification

An emulsion of two or more immiscible liquids can be used to produce microparticles. Usually, a volatile organic solvent with low water miscibility such as dichloromethane (DCM) or chloroform are used. In the initial step, polymer and drug are dissolved in organic solvent. Then, it is emulsified into a bulky aqueous phase containing tensioactive molecules, for example poly(vinyl alcohol) (PVA) [86, 88]. Microparticles are generated by solvent removal through an evaporation or extraction process and become free-flowing injectable microspheres after drying or lyophilization [88]. The emulsion type can be varied depend on the solubility of drug in water and encapsulating polymer [86].

Hydrophobic drugs can be encapsulated into microparticles by an oil-in-water (O/W) emulsification process. The amount of drug loading in the non-polar polymer matrix can be increased by adding sodium chloride (1 M NaCl solution) into the aqueous phase. Sodium chloride increases the polarity of aqueous phase and reduces the solubility of the drug in aqueous phase and improves encapsulation of the drug in non-polar polymer matrix [89]. However, the oil-in-water (O/W) emulsification process is not suitable for encapsulating a hydrophilic drug as it leads to poor encapsulation efficiency. Hydrophilic drug also can be deposited on the surface of microsphere and lead to rapid release of drug at the beginning or burst release[88]. Moreover, hydrophilic substances are drained during the intense solvent elimination and concentrate on the surface of microparticles then contribute to the initial burst release [90].

Modifications have been made to encapsulate hydrophilic drugs using water-oil-water (W/O/W) emulsion. In this particular method, a volatile organic solvent has been used to dissolve the polymer. Then, an aqueous solution containing the drugs is added to the organic phase under high shear to form water-in-oil (W/O) emulsion. Subsequently, the mixture is added into a large volume of water containing tensio-active molecules (e.g., PVA) to form a W/O/W emulsion under rapid stirring. Solvent removal is completed using evaporation or extraction with the formation of solid microparticles [88].

In this multiple emulsion method, the stability of the primary emulsion is an essential requirement to stabilize the multiple emulsions and it also influences the loading of the drug in solid microparticles. A high loading of hydrophilic drug can be obtained

from a stable primary emulsion. Stable primary emulsion can be reached by increasing the concentration of the emulsifier. Consequently, the average size of microparticles is also reduced in a higher concentration of emulsifier [91].

2) Polymer phase separation (coacervation)

The phase separation technique is based on solubility of the encapsulating polymers in an organic solvent by varying the temperature, or by adding the third component that interacts with the organic solvent but not with the polymer, it is called a coacervating agent (CA) [88]. Depending on the number of polymers that are involved in the formation of microparticles, coacervation can be categorized into simple and complex coacervation. Simple coacervation involves only one polymer and phase separation can be stimulated by desolvation (or dehydration) of the polymer phase. In contrast, complex coacervation involves two hydrophilic polymers of reverse charges. Separation of the polymers is obtained by neutralization of the overall positive charges on one of the polymers using the negative charge on the other polymer [86].

The coacervation process is suitable for encapsulation of both hydrophilic and hydrophobic drugs. Phase separation and the solidification stages in coacervation process are affected by CA. The CA should not dissolve the polymer and the drug, but should be soluble in the solvent. Coacervation is induced gradually when CA agent is added to the stirred polymer-drug-solvent system [86].

Thote *et al* (2005) demonstrated fabrication of dexamethasone phosphate microparticles, a hydrophilic drug, by using coacervation technique with silicon oil to

generate microparticles of PLGA polymer. Dry microparticles have been obtained by extracting silicone oil with hexane [89]. In contrast, microparticles of lipophilic drugs can be prepared by adding an aqueous hydroxypropyl methylcellulose (HPMC) solution into an organic polymer solution to separate the polymer and induce the formation of microparticle as established by Dong and Bodmeier (2006). The aqueous HPMC solution acted as a stabilizer for the coacervate droplets by preventing coalescence [92].

3) Spray drying

Spray drying is a single step microparticle production based on the atomization of drug and carrier solutions, using compressed air or nitrogen. This process includes three consecutive steps: formation of the aerosol, contact the aerosol with the warm air to dry the aerosol and separation of dried product. The spray drying method is a continuous process, easy to scale up and inexpensive [86, 88]. In the spray drying process, a high viscosity solution will create the formation of fibres instead of microspheres as the sprayed solution is not completely broken up into droplets. In addition, it also occurs when using inappropriate geometry of nozzle or at lower flow rates. Moreover, it will denature thermally labile drugs such as proteins due to the high temperatures (over 100°C) used to dry particles [88].

Chaw *et al* (2003) successfully entrapped physostigmine into microparticles using a spray drying method due to the absence of the water during the process [93]. Other research showed the highest encapsulation amount from poly(lactic acid) (PLA) polymer was obtained by spray drying PLA in dimethyl carbonate solution. The use of

dimethyl carbonate solution and carbon dioxide for the microencapsulation preparation would reduce concerns over excess solvent in the product [94].

4) Supercritical fluid

Supercritical fluid (SF) results in microparticles with no or very low amounts of residual organic solvent and provides a feasible and clean way to process thermo labile or unstable biological compounds [88]. In a supercritical process, the active compound and polymer are dissolved in an organic solvent and then sprayed into the column containing the supercritical gas phase. The organic solvent will be dissolved in the supercritical gas phase and subsequently extracted directing the formation of solid microparticles. The condition of gases such as pressure and temperature will produce a difference in gas density. The difference in gas density, in some case, can influence the size and shape of microparticles [95].

Supercritical anti-solvent precipitation was shown to be an effective process for manufacture of a water-insoluble drug since it produces smaller particles to improve the dissolution rate of poorly soluble drugs [96]. In this method, the organic solution containing drug and polymer were sprayed into supercritical fluid. The miscibility of organic solvent and supercritical fluid gas allow the drug particles to precipitate [97]. Supercritical anti-solvent precipitation produces spherical microparticles over pressures from 75 to 250 bar and temperatures between 35 and 60°C. Decrease in pressure would increase particle size distribution, while increase of solute concentration produces bigger particle [98].

1.3.2. Release of Active Drugs from Microparticle

The term “release” describes how the drug molecules are transported or released from microparticles, including mechanism and rate. The release of drug from microparticles is influenced by physico-chemical properties of polymer, physico-chemical properties of encapsulated molecules, properties of the microparticle itself and the surrounding environment e.g., *in vitro* or *in vivo* [87, 99]. Several release mechanisms of microparticles have been proposed, which include diffusion, osmotic pressure and erosion of the polymer matrix or combination of these [99, 100].

Most of drug release from microparticles is by a diffusion process. The release rate also can be regulated depending on microparticle properties like pore size, polymer molecular weight, crystallinity and copolymer composition [101]. High porosity microparticles provided high release of lidocaine from PLGA microparticles due to rapid mobility of the diffusing molecules (drug molecules, acids and bases) [38]. The effect of molecular weight of polymer on drug release from microparticle was shown in felodipine release from chitosan-tripolyphosphate cross-linked polymer. High molecular weight and high concentration of chitosan give a significant decrease of felodipine release from microparticles [39]. Crystalline microstructure also influenced the release of papaverine from poly(ε-caprolactone) (PCL) microparticles. As molecular weight increases in PCL, the crystallinity of polymer is considerably reduced to form amorphous regions which allow the drug to diffuse rapidly [102]. The effect of copolymer composition on drug released showed on release kinetics of levonorgestrel and estradiol from copolymers of caprolactone and DL-lactide.

Permeation rates and release fluxes of levonorgestrel and estradiol increased as the ratio of caprolactone in copolymer was increased [103].

Drug molecules could be released by convection, which is driven by osmotic pressure or by an osmotic pump. This is the mechanism usually given for release of drug from ethyl cellulose polymer [99]. The molecules of drug can be released from the microparticle upon contact with water. Water diffuses through microparticle pores and polymer swelling generates an internal pressure to drive the release of drug from the polymer [104]. The release rate of drug using this system depends on the permeability of the polymer and osmotic pressure of the core formulation, but it is pH independent [104, 105].

The release of drug molecules from microparticles may also occur by dissolution of the microparticle i.e., erosion. The mechanism of erosion involves weight loss from the microparticle mass. The erosion process begin with solvent penetration into the matrix of microparticle then the matrix starts to degrade by hydrolysis [106]. Pores are also created in the erosion process, therefore, the rate of drug release with erosion mechanism is not only influenced by rate of hydrolysis but also rate of pore formation [99]. In addition, drug properties and drug-polymer interaction highly affect the rate of release of proteins with different isoelectric points [107] .

1.3.3. Determination of Drug Release from Microparticles

The effectiveness of microparticle formulations is dependent on drug release and it is useful to gain information on the amount of release, the rate and mechanism of release to understand the behaviour of formulation at the molecular level. Release of

drug from microparticles can be evaluated either *in vivo* or *in vitro*. However, *in vitro* techniques are more promising due to lower cost than *in vivo*. The important points for *in vitro* release studies are selection of media and temperature. Selection of media is related to drug solubility and stability, whereas, selection of temperature is related to physiological conditions. In addition, an appropriate drug release study should be conducted in a sufficient volume of medium to dissolve the expected amount of drug. This condition is known as *sink conditions* and it can be maintained by apply media replacement to ensure solubility of drug and avoid accumulation of polymer degradation products in the system [108]. Adding surfactant into media can be used to increase solubility of drug to achieve sink conditions during drug release evaluation [109]. The common methods for *in vitro* drug release are the sample and separate (SS) method, the continuous flow (CF) method and dialysis [108, 110].

In the sample and separate (SS) method, microparticles are placed into a vessel containing medium and assessed at certain intervals. Medium for release study is selected based on drug solubility and stability during the period of evaluation. Medium is taken at certain intervals, separated from disperse microparticles (usually by centrifugation or filtration) and then the release of drug is assayed in the supernatant or filtrate [108, 110]. Replacement of medium is needed to maintain sink conditions in the system. Size of vessel or container depends on the volume of medium used to maintain sink conditions. During the period of study, continuous or intermittent agitation may be applied to the system to prevent aggregation of microparticles [38, 108, 111]. This technique gives satisfactory results for *in vitro* release. However, separation of medium from disperse microparticles is the major

issue, particularly if the size of microparticle is very small as it will be difficult to filter or to precipitate by centrifugation [108, 110].

The continuous flow (CF) method is adopted from USP apparatus 4. In this method microparticles are loaded into the base of cells containing media and a filter is placed on the base of cell. Medium is continuously pumped into the cell during the period of study and samples are taken by filtration from the base of the cells. Fresh medium is added to the system to keep the volume constant after sampling [108, 110]. Continuous medium flow mimics *in vivo* conditions in which microparticles are exposed to a continuous flow of biological fluid. Hence, this method demonstrates a good *in vitro –in vivo* correlation [112].

In the dialysis method, a dialysis membrane or bag is used to separate a suspension of microparticles from the bulk medium in a vessel. The drug diffuses out of sample and through the dialysis membrane to the outer bulk medium. Release of drug is assessed by sampling the bulk medium at intervals. Agitation may be applied to increase diffusion of drug to the bulk medium and prevent accumulation of drug at certain locations in bulk medium [108, 110]. The volume of outer bulk medium used should be approximately 6-10 fold higher than the volume of medium inside dialysis bag, to provide a driving force for drug molecules to move into the outside media. This method is not appropriate for protein release since a large pore size is needed for the protein to diffuse through the membrane and the protein can also adsorb to the membrane. In addition, detection of protein released may be a problem due to dilution in the bulk medium [108, 112]. This method offers advantage in sampling and medium replacement because the sample is separated by dialysis membrane.

However, this technique can be ambiguous as the partition of drug molecules to outer medium is controlled by concentration of drug in inner medium and the rate of diffusion of molecules through the dialysis membrane, not by the microparticle itself [110].

1.3.4. Microparticles in Tissue Engineering

A delivery approach using microparticles can be applied in the tissue engineering field including the encapsulation of growth factors or living cells within the scaffold. Microparticles can be used as a carrier to control a site-specific and time-specific release profile. Microparticles may act as supporting matrices for cell attachment and/or as a carrier for bioactive agents and provide controlled release kinetics [35]. In addition, microparticles are small enough to be used as an injectable scaffold and deliver through a syringe [36, 113].

A 3D construct for tissue replacement can be achieved using microparticles as a carrier. The schematic diagram for 3D construct using microparticles for tissue replacement is presented in Figure 1.3. In this figure, cellular aggregates are formed using microparticles and differentiated by culturing the cells aggregates *in vitro* and then injected at the later stage for tissue reconstruction *in vivo*. Tan *et al.,* demonstrated the use of poly (L-lactide) (PLLA) microparticles as a micro-carrier to promote formation of cell aggregates. The 3D shape of cell aggregates would be able to be injected into the defect site for cartilage repair [114]. Mixing microparticles with chondrocytes as a mouldable scaffold has been used for cartilage tissue engineering. The presence of microparticles increased total tissue-mass and glycosaminoglycan production [115].

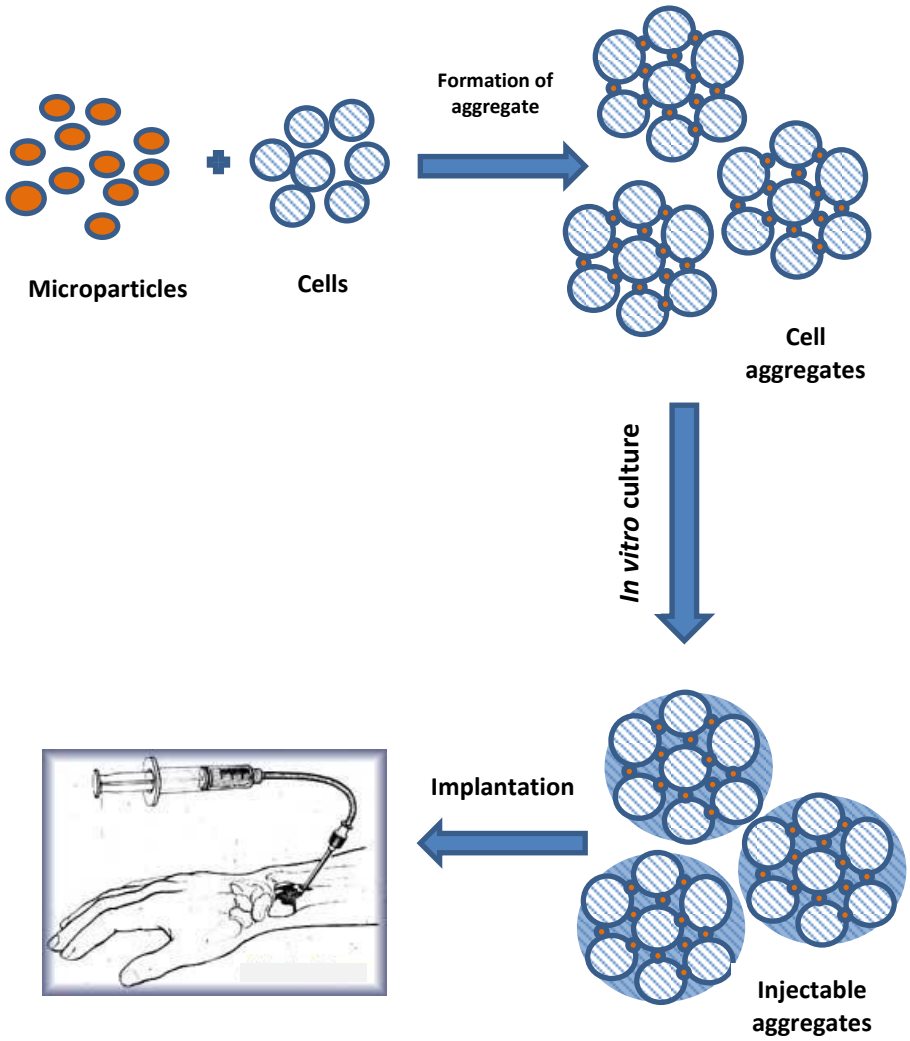

Figure 1.3. A schematic diagram of the formation of cell aggregates using microparticle for injectable tissue replacement

Microparticle matrices prepared from PLGA have been used in intra-cerebral transplantation to enhance cell attachment and provide structural support to form new tissue [116]. Sahoo *et al* (2005) also reported use of a PLGA microparticle scaffold to support 3D growth of breast cancer cells. The 3D system of breast cancer cell can then be potentially used as a model for preclinical evaluation of anticancer agents [117].

Most reports on the use of microparticles in tissue engineering focus on the encapsulation of bioactive molecules to support cell development. In this case, microparticles have been used as a reservoir that releases bioactive molecules at a repair site for particular length of time. Additionally, the structure of microparticles is advantageous in protecting encapsulated bioactive molecules from degradation [36, 40]. Microparticles can be used as injectable scaffold by incorporating microparticles with other materials or living cells. Incorporation of PLGA microparticles with calcium-phosphate cement in an injectable scaffold was used to control release of rhBMP-2 up to 28 days [118]. A mixture of microparticle and fibroblast cells showed promising results as an injectable scaffold for muscular tissue [119].

1.4. Functionalized Polymer for Tissue Engineering Scaffold

1.4.1. Introduction

Polymeric biomaterials have been used in tissue engineering for matrices and carriers for drugs. Surface interactions between biomaterials and cells play an important role for cell growth and development. Changing the biomaterial surface may improve cell behavior with respect to individual processes of cell like proliferation, differentiation and motility, hence, modification of polymer properties are needed to achieve biocompatibility, biodegradability and interconnectivity in the formation of the new tissue [120-122].

Understanding the influence of polymeric material on cell behavior is needed to select suitable polymers for tissue engineering. In this evaluation, cell and polymer should be in contact. Some different techniques have been used to evaluate cell

interaction with polymer *in vitro* such as adhesion and spreading, cell migration, cell aggregation and evaluation of cell phenotype. In addition, *in vivo* techniques also can be used to evaluate the interactions of cells with polymers, such as the wound chamber model which is adopted from intra-peritoneal or subcutaneous implantation technique in rodent and large animals. Most polymers implanted *in vivo* induce an inflammatory response or a foreign-body response (FBR). Response of cells to polymer are assessed by short-term studies (0-72 hours) of protein adsorption, inflammatory cell recruitment and adhesion, and macrophage fusion [123].

A potential polymer for tissue engineering scaffold is poly(glycerol adipate) (PGA). This novel polymer prepared from non-toxic monomers, divinyl adipate and glycerol, and synthesized by an enzymatic reaction. Biocompatibility of the polymer to several cells is promising for the scaffold to mimic the structure and properties of human tissue [124, 125]. Nanoparticles from poly(glycerol-adipate) has capability to degrade within the lysosomal compartment of cell. The ester bonds in the polymer backbone are expected to be unstable in the lysosomal environment [126] due to the presence of enzymes capable of reversing the synthetic reaction. Pendant hydroxyl groups in polymer backbone are potentially used for modification. The highest drug loading have been achieved in modified PGA nanoparticles with 40% acylation of C_{18}. High levels of drug interaction will be useful for encapsulation of growth factors into microparticles. PGA can be modified by tethering a functional group for ligand attachment such as poly(ethylene glycol). Addition of PEG molecules in the end group of polymer could reduce immunological interactions and increase *in vivo*

stability. Microparticles prepared from functionalized PGA polymer with diamino PEG-maleimide linker for attachment of RGD ligand demonstrated cellular aggregation in C6 and 3T3 cells [127].

1.4.2. Modified Polymer for Tissue Engineering Scaffold

Surface characteristics of polymers, for instance hydrophilicity, density of surface charge, micro-morphology of surface, free energy and specific chemical groups influence cell adhesion, spreading and signaling and thus regulate a broad variation in biological functions. Surface chemistry and surface topography of polymers play significant role for the biocompatibility of biomedical devices. Consequently, surface modification is needed to eliminate undesired effects and produce specific biological responses *in vivo* [15].

Specific interactions between polymers and their corresponding cell surface receptors could be obtained using ligands [121]. Ligands integrate into the material to produce chemically defined bioactive surfaces (Figure 1.4). This model involves the immobilization of biologically active ligands from extracellular matrix proteins such as fibronectin, laminin, vitronectin and collagen. In addition, the tripeptide adhesion sequence Arg-Gly-Asp (RGD) also contributes as cell adhesion proteins because it interacts with the integrin family of cell surface adhesion receptor [128].

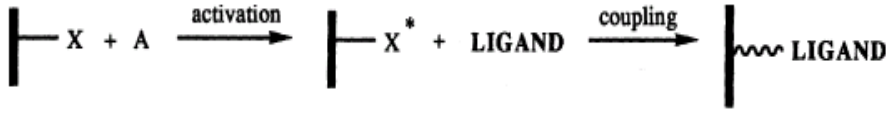

Figure 1.4. General chemical scheme for immobilized ligand onto a surface [128].

Hydroxyls, amines, carboxylic acid and thiols are typical chemical groups in protein as ligands for cell surfaces studies [128]. Polymer bioconjugates were prepared by modifying polymers with protein-reactive end-groups. The amine-bearing side-chains of lysine residues have been targeted for conjugation with polymer as it has excellent reactivity towards a wide range of electrophiles [129]. Modification of polymers using thiol-reactive end-groups has also been used. Thiol-reactive end groups create well-defined protein-polymer conjugates with the sulfhydryl group of cysteine, an amino acid in many proteins. The functional groups that have been demonstrated to be effective for conjugation with sulfhydryl group are vinyl sulfone, maleimide and activated disulfide end-groups. The recent progress of protein-polymer conjugates is the use of protein-reactive initiators to synthesis polymers. These polymers are reactive towards proteins directly after polymerization [129].

Nevertheless, several factors must be considered to retain maximum bioactivity. The ligand may not have optimum cell-receptor interactions due to physical constraints imposed by the surface. Thus, ligand surface immobilization may proceed in low yield due to sterically inaccessible reactive sites on the ligand molecule. The density of ligands immobilized upon a surface can be measured using radiolabelling, surface analysis or gravimetry [128]

1.4.3. Functionalized Polymer with Poly(ethylene glycol)

Polymer as a drug carrier can be modified to improve delivery of drug to target of site. One strategy of polymer modification is conjugating the polymer with poly(ethylene glycol) (PEG). PEG is a FDA approved-non-toxic polymer, hydrophilic, soluble in water and many organic solvents [130, 131]. The important characteristics of PEG conjugating are increasing solubility in water and circulation time *in vivo*, decrease of enzymatic degradation and immunogenicity. Moreover, PEG conjugation could be used to prevent unwanted adsorption of serum proteins and cellular recognition [130, 132]. Due to its benefits, PEG is highly suitable for functionalized polymer in targeted delivery.

PEG attachment on the surface of hydrophobic carriers increases their solubility in aqueous media and inhibits aggregation of drugs *in vivo* as well as *in vitro*. It occurs due to steric hindrance of PEG chains through formation of a “conformational cloud”. The “conformational cloud” of PEG also protects from interaction with blood component and enzymatic degradation as well as uptake by the reticuloendothelial system (RES). Consequently, conjugation of PEG demonstrates prolonged half-life in the body and enhanced bioavailability of the active molecules. The other advantage of the “conformational cloud” in PEGylated products is they perform steric hindrance to interact with charge-induced components within the body, so immune recognize systems can be diminished [133].

Conformation of attached PEG to the surface is influenced by relation between the distance of two adjacent chains (D) and the radius of gyration (R_g). Attached PEG to the surface becomes “mushroom” conformation if $D>2R_g$, while a “brush”

conformation appears at $D<<R_g$. (Figure 1.5). Radius of gyration (R_g) is related to the chain length of PEG [130]. Repellence capacity of PEG towards unwanted protein depends on chain length, chain density and the conformation of attached PEG to the surface. The efficiency of protein repellence becomes increased if more PEG chains overlap. Theoretically, protein can adsorb onto the surface by two mechanisms. Primary adsorption is at interface between PEG and substrate, while secondary adsorption is at the top of PEG brush. Increasing chain density of PEG would decrease the primary adsorption. However, for larger proteins, they may go through secondary adsorption. Therefore, they require a sufficient thickness of PEG to shield electrostatic forces interaction between protein and substrates [130, 133].

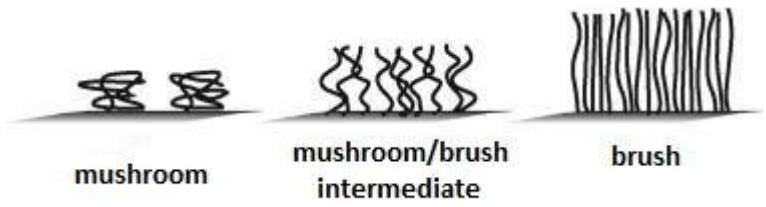

Figure 1.5. A schematic diagram represent different conformation of PEG grafted to the surface. Image is taken from Wattendorf and Merkle (2008) without any modification [130].

Microparticle can be conjugated with PEG polymer to gain several advantages of PEGylated products. In this case, PEG moieties may be presented in the bulk and on the surface of microparticles to ensure the availability of PEG moieties during biodegradation and erosion process. Preparation of microparticles typically involve aqueous media where PEG moieties are preferably oriented towards water phase and leading to microparticle with PEG enriched surfaces. For the purpose of cell or

tissue targeting, PEG moieties can be equipped with targeting ligands for specific cell surface receptor [130]. PEG conjugation using thiol-PEGylating agents are reported as the most specific method for conjugation with proteins and peptide as cysteine are rarely present in proteins or peptides. PEG-pyridylsulphide, PEG-maleimide, PEG-vinylsulfone and PEG-iodo-acetamide have been use as thiol-PEGylating agents [130, 131].

1.4.4. Role of proteins for cell attachment

In order to bind with other cells or ECM, cells are equipped with several types of proteins as cell adhesion molecules which are an integral part of membrane proteins. The adhesion molecules have ability to bind with cells or matrices *via* other adhesion molecules in the same type (homophilic binding), other adhesion molecules in a different type (heterophilic binding) or with an intermediary linker which binds itself to other adhesion molecules. Adhesion molecules can be divided as four major classes. They are cadherin, immunoglobulin-like adhesion molecules, selectin and integrin [134].

Cadherin are involved in cells adhesion by homophilic binding to other cadherin in calcium dependent manner, therefore removal of calcium from extracellular components disrupts binding. While, immunoglobulin-like adhesion molecules perform both homophilic and heterophilic binding and they have been found in nervous tissue and intracellular cell adhesion molecules. Another cells adhesion molecule is selectin, which binds to carbohydrate ligands on cells. It expresses mainly on the surface of endothelial cells, leukocytes and platelets. Interaction between selectin and carbohydrate allows leukocytes to roll along vascular endothelium in the

direction of blood flow as an introduction to integrin-mediated adhesion. Lastly, integrins as adhesion molecules play important roles for interaction between actin in cytoskeleton and extracellular matrix to regulate cell migration and activate a number of intracellular signaling pathways [134, 135].

Most adhesive interactions between cell and extracellular matrix are directed primarily by integrins. Integrin consist of α (alpha) chain to provide information for ligand binding and β (beta) chain to provide link to cytoskeleton. The ability of cells to identify adhesive substrate is determined by integrin expression profiles. Most of cells express $\alpha_1\beta_1$, $\alpha_2\beta_1$, $\alpha_3\beta_1$, and $\alpha_6\beta_1$ which are involved for adhesion to collagen and laminin [135]. The role of integrin is to facilitate a signaling cascade to allow efficient interaction between signaling components. Proper integration of these signals provides appropriate cellular growth, differentiation and tissue morphogenesis [136].

Adequate interaction between cells and matrices is needed to assemble cells in 3D structure. The interaction can be mediated using proteins or peptides as cell adhesion molecules. Therefore, several techniques have been used to improve biomaterials for cell attachment by adsorption of specific protein or immobilization of cell recognition motives. Introduction of protein as a cell adhesion molecules to matrices could be achieved by chemical modification, i.e. co-polymerization, and physical modification, i.e. plasma treatment [16, 137, 138]. Chemical modifications are more preferable than physical attachments as they lead to more stable and strong anchoring to the surface of materials [137].

1.4.5. Methods of Polymer Modification

Polymer surface modification can be achieved by several methods including chemical methods, photo induced grafting methods, and plasma treatment methods.

1) *Chemical methods*

For biodegradable aliphatic polyesters such as poly(glycolic acid) and poly (lactic acid), the cleavage of the ester bonds of the polymers result in the generation of carboxylic acid and hydroxyl groups at the ends of chain. Exposure of polymers to an alkaline solution can be used to modify the surface of biodegradable polymer to produce a hydrophilic and rough surface for cell attachment [122]. Thissen *et al.* (2006) reported that surface modification of PLGA by partial hydrolysis using sodium hydroxide could improve the proliferation rate of articular cartilage chondrocytes. Partial hydrolysis and covalent immobilization of amine-terminated dendrimer exhibited the maximum proliferation rate of chondrocytes [139].

Modification of poly(methyl methacrylate) (PMMA) with diamino poly(ethylene glycol) (PEG) by hydrolysis and aminolysis lead to amide formation has been used to produce a specific region for cell adhesion. The functionalization of PMMA-diamino-PEG with RGD peptide restored cell adhesion and enhanced cell attachment compared to unmodified PMMA [140].

2) Photo induced grafting

Photo-induced grafting polymerization is surface modification using irradiation in the presence of monomer in the vapor solution state. Ultraviolet (UV) light is typically use for source of irradiation [141]. The UV irradiation technique offers several

advantages like economic operation, mild reaction condition, rapid reaction, selective absorption without altering the bulk polymer and permanent modification on surface chemistry [15, 141].

Photo-induced grafting followed with polymerization have been used to increase hydrophilicity of the surface of poly(L-lactide) (PLLA) polymer using several combination of hydrophilic polymers. A single monomer of vinyl acetate, acrylic acid and acrylamide or a combination of those monomer, were grafted onto PLLA film surfaces by polymerization process using UV-light. As the result, the hydrophilicity of the film surface of PLLA increased when copolymerized with vinyl acetate or acrylic acid [15].

Several hydrophilic groups such as hydroxyl (-OH), carboxyl (-COOH) or amide (-$CONH_2$) could be presented onto PLLA surfaces *via* photo-induced grafting copolymerization. The modified PLLA membranes with hydroxyl or amide groups enhanced chondrocyte compatibility compared to the unmodified PLLA membrane. In contrast, the PLLA membrane modified with carboxyl groups had even worse cytocompatibility though it possessed a similar hydrophilicity [15].

3) Plasma grafting and plasma treatment methods

Plasma treatment has been extensively used to modify the surface of biomaterials. Polymer surfaces can be modified by physical and chemical techniques since they have good interaction with plasma containing electrons, ions, radicals and neutral molecules. Various cell culture devices such as petri dishes, microcarriers and membranes can be treated with plasma to improve cell adhesion. A hydrophobic

surface can be modified to a hydrophilic surface by treatment with oxygen plasma. On the other hand, modification of hydrophilic surface to hydrophobic surface can be achieved by treating with tetrafluoromethane (CF_4) plasma [15].

Cationized gelatin (CG) could be used to improve compatibility of PLLA nanofibres with chondrocytes. The –COOH groups on the surface were introduced to the PLLA fibers with oxygen plasma, then CG molecules were covalently grafted onto the fiber surface. Chondrocytes formed a tight attachment to CG-PLLA nanofibers. The research indicated that CG grafting onto the PLLA nanofibers could enhance viability, proliferation and differentiation of rabbit articular chondrocytes *in vitro*. The cell differentiation on CG-PLLA nanofiber was proven by an increased glycoaminoglycan and collagen secretion [142].

1.5. Project Overview

Poly(glycerol-adipate) (PGA) (Figure 1.6) is a potential polymer for use as a tissue engineering scaffold. The ester bonds in the polymer backbone would be expected to be unstable in the lysosomal environment due to the presence of acid hydrolase enzymes that capable to break down materials including polyesters such as polyurethane, poly(lactic acid) and poly(glycolic acid). Nanoparticles from poly(glycerol-adipate) showed a rapid breakdown within the lysosomal compartment of cells [143].

PGA polymer backbone has pendant hydroxyl group that could be substituted to provide maximum drug interaction in the polymer [125]. High level of drug interaction will be useful for encapsulation of growth factors into microparticle based

scaffolds. The PGA polymers showed good results for incorporation of drugs such as dexamethasone phosphate. PGA nanoparticles had the highest dexamethasone phosphate loading when acylated with 40% stearoyl (C_{18}) in the backbone of polymer. Although dexamethasone phosphate is water soluble, it has a hydrophobic steroid ring which interacts very strongly with the polymers [125]. Wahab *et al* (2012) found that the 100% acylated polymer with C_{18} also increased encapsulation efficiency of ibuprofen sodium within a PGA nanoparticle [144].

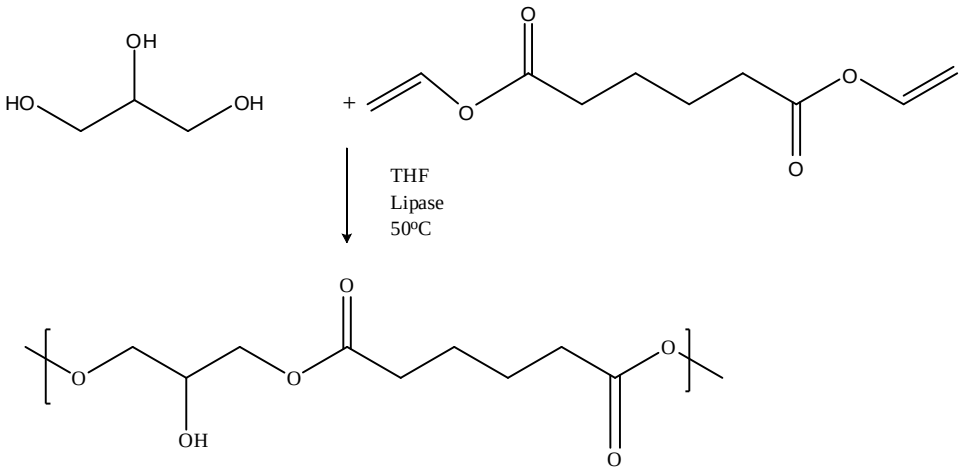

Figure 1.6. Poly(glycerol-adipate) backbone was formed from polycondensation of glycerol and divinyl adipate [125].

In order to allow specific region of cell adhesion, PGA microparticle is functionalized using cell adhesion peptides. A maleimide-poly(ethylene glycol) (MIHA-PEG-NH_2) linker then tethered into 40%C_{18}-PGA polymer to provide hybrid formation with a peptide onto polymer surface. PEG is considered non-toxic and non-adhesive polymer towards protein. Attachment of PEG onto the PGA polymer provides PEG

moieties on the surface of MP to prevent particle aggregation. In addition, PEG can be equipped with the maleimide group, a thiol-reactive-group, which has specific interaction with sulfhydryl group in ligand [130, 131].

Microparticles (MPs) for 3D assembly of cells are then prepared from modified PGA polymers, 40%C_{18}-PGA and 40%C_{18}PGA-PEG-MIHA. A MIHA-PEG-NH_2 chain onto microparticles hypothesizes to prevent the MP from aggregating each other by providing the spacer between the microparticles and ligand. Thus, it can allow optimum aggregation between cells (Figure 1.7). Moreover, the PEG hydrophilic layer reduces the immune response on parenteral delivery of MP [41]. Cell adhesion on the microparticle can be mediated using extracellular matrix protein such as collagen [128].

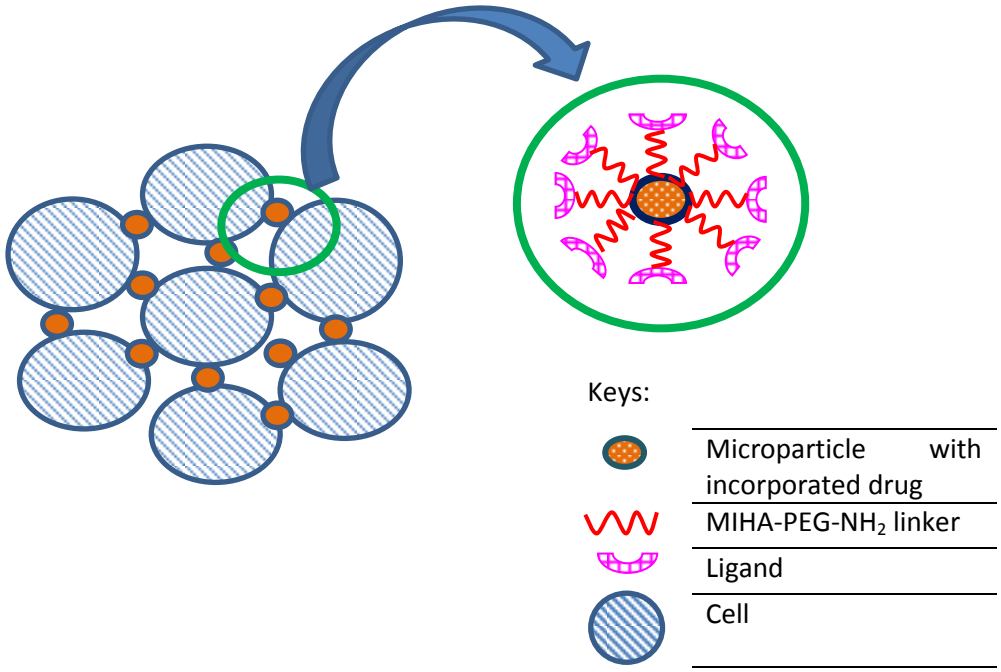

Figure 1.7. A schematic of ligand-functionalized PGA microparticles for cellular agregation

Collagen has been used as a ligand in this system to encourage cell attachment. Collagen, particularly type IV collagen, is a major constituent of mammalian basement membranes. Collagen type IV forms a spider web-like suprastructure that interacts with other components of molecules such as laminins, perlecans, and nidogen (entactin) to form a highly cross-linked and insoluble basement membrane on the basolateral of various cells. The interaction occurs *via* adhesion molecules and important for creating a productive cell-matrix interaction and subsequent intracellular signaling [145].

Bioactive molecules for osteogenic formation have been encapsulated within modified PGA microparticle. The microparticle would act as reservoir to release drug molecules in controlled manner. The ability of the microparticle to deliver bioactive molecules to targeted cells will be evaluated through evaluation of osteogenic development on mouse embryonic stem (mES) cell and osteoblast cell.

1.6. Aims of the Project

The overall aim of the project is to modify the poly(glycerol-adipate) (PGA) polymer for MP to create a 3D construct in tissue engineering and evaluate the use of MP to deliver bioactive molecules for osteogenic differentiation in mouse embryonic stem cells (mES) and osteoblast cells. It can be divided into four objectives.

The first objective is to modify poly(glycerol adipate) (PGA) polymer for high efficiency of encapsulated drug by 40% stearoylation (C_{18}) of the polymer backbone. The highest drug loading has been achieved in modified poly(glycerol adipate) nanoparticles with 40% acylation of C_{18}. Furthermore, acyl-substituted poly(glycerol

adipate) was further functionalized using maleimide-poly(ethylene glycol linker (MIHA-PEG-NH_2) for ligand attachment. Addition of PEG molecule in the end group of polymer reduces immunological interactions and encourages polymer scaffold attachment *in situ*. Maleimide group was added to facilitate conjugation of the polymer with peptide and react selectively with the sulfidryl group on the ligand.

The second objective is to develop a method for production of MP and ligand attachment into the surface of MP. The emulsification method will be the main method used to create MP due to its adaptability to different polymer matrix. Control of the emulsification processes will be investigated together with specific conditions needed to attach ligand into microparticle surface. Density of ligand attachment onto MP will be considered to maximise bioactivity with cells.

The third objective is the development of a microenvironment for stem cells using functionalized PGA MP as matrices to encourage cell aggregation. The specific conditions for cell aggregation, incorporation of MPs within cell aggregates, effect on cell proliferation in the presence of microparticles will also be investigated.

The last objective is to evaluate the drug release profile of MP prepared from modified PGA and ability of MP to deliver bioactive molecule for osteogenic differentiation. The extent and length of drug release from MPs will be tailored to meet the requirement for inducing bone formation. Osteogenic development in mES and osteoblast cells will be evaluated by determining alkaline phosphatase level, bone-protein formation and mineralization.

CHAPTER 2

2. EXPERIMENTAL METHODS

2.1. Introduction

The first step in this study was PGA polymer modification by substituting 40% pendant hydroxyl group in PGA polymer with stearoyl (40%C_{18}-PGA). The next step of polymer modification is attaching MIHA-PEG-NH_2 linker onto one of the the carboxyl group on the end of PGA polymer backbone. The MIHA-PGA-NH_2 linker is synthesized from *N*-maleimidohexanoic acid (MIHA) and diamine poly(ethylene glycol) (diamine PEG).. Besides the PGA polymer modification, collagen was also modified by providing iminothiolane functional group on the molecule of collagen for attachment with maleimide functional group. The iminothiolane-modified collagen was attached on the surface of 40%C_{18}-PGA-PEG-MIHA MP as a ligand to improve interaction between the microparticle and cells.

Second step of this study was using the modified PGA polymer, 40%C_{18}-PGA and 40%C_{18}-PGA-PEG-MIHA, for microparticles (MP). The particle size, zeta potential and shape of microparticles prepared from 40%C_{18}-PGA and 40%C_{18}-PGA-PEG-MIHA were characterized. In addition, the interaction between polymers and drugs was evaluated by determining encapsulation efficiency of dexamethasone phosphate (DXMP) and simvastatin (SIM) within the MP. The release of drug from MP *in vitro* is

also evaluated in phosphate buffer saline (PBS) medium. The ability of 40%C_{18}-PGA-PEG-MIHA MP to attach with iminothiolane-modified collagen was evaluated.

The next step of this study was evaluation of aggregate formation using modified PGA microparticle in mouse embryonic stem (mES) and osteoblast cells. The process of aggregate formation in various ratios of empty MP to cells was evaluated. Moreover, ability of modified PGA MP to act as matrix for cell proliferation was assessed by evaluating cell metabolic activity.

The last part of this study was incorporation of MP containing active drug within mES and osteoblast cells. The ability of modified PGA polymer to deliver drug for osteogenic differentiation was evaluated by determining alkaline phosphatase level, staining of osteocalcin expression and staining of mineralisation in cell using von Kossa staining. The schematic diagram for this study is laid on Figure 2.1.

All chemicals were purchased from Sigma Aldrich, UK while all solvents were obtained from Fisher Scientific, UK, unless otherwise stated.

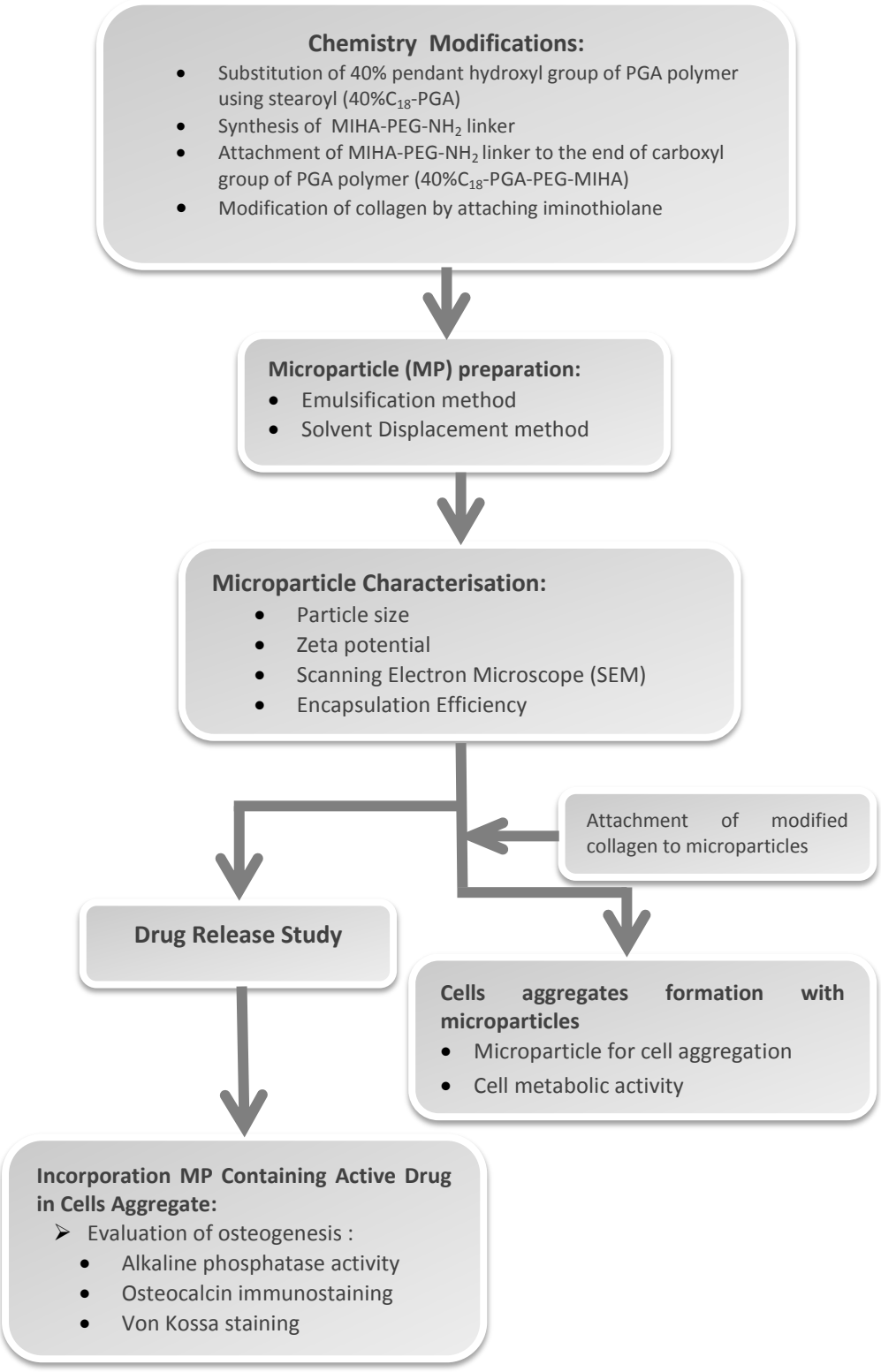

Figure 2.1. A schematic diagram of experimental methods from PGA polymer modification to application of microparticle for osteogenic differentiation.

2.2. Modification of Poly(glycerol adipate) Polymer

2.2.1. Materials and Equipments

The materials used for polymer modification were poly(glycerol- adipate) (PGA) 8 and 12 kDa, which was provided by Dr.G.Hutcheon, Liverpool John Moores University, UK; stearoyl chloride (C_{18}); dried tetrahydrofuran (THF); dichloromethane (DCM); dried pyridine; hydrochloric acid (HCl); chloroform; diamine poly(ethylene glycol) (diamine PEG, MW 2000); *N*-maleimidohexanoic acid (MIHA); dicyclohexylcarbodiimide (DCC); *N*-hydroxysuccinimide (NHS); 2-iminothiolane hydrochloride (Traut's); collagen type IV (type VI Sigma); Trizma® hydrochloride buffer solution pH 8; Fluorescein-5-isothiocyanate (FITC) from Molecular Probe; 5-5'-dithiobis-2-nitrobenzoic acid (DNTB); Bradford Reagent; paraformaldehyde (PFA) for cells fixation and Bovine Serum Albumin (BSA). The buffer used in the experiment was Phosphate Buffered Saline (PBS) tablets (Fisher Scientific, UK). The water used in the experiments was ultrapure deionized water (ELGA water).

The equipments used for polymer characterisation were Bruker Avance 400MHz Spectrometer and Nicolet FTIR spectrometer. The UV spectrophotometer DU800 from Beckman Coulter was used for qualitative and quantitative characterisation of modified collagen. Purification of the collagen was carried out by size exclusion chromatography using PD-10 column from GE Healthcare. The ability of modified collagen to attach to cells was assessed using a Beckman Coulter EPICS Altra flow cytometer.

2.2.2. General Methods for Polymer Modification

The synthesis of functionalized polymer was characterized using thin layer chromatography (TLC), proton nuclear magnetic resonance (^{1}H-NMR) spectroscopy, and fourier transformed infrared (FTIR) spectroscopy.

2.2.2.1. Thin Layer Chromatography (TLC)

Thin layer chromatography (TLC) was carried out on Merck 60 F254 silica gel plates and visualised using UV irradiation 254 nm or by staining the samples using potaasium permanganate ($KMnO_4$).

2.2.2.2. Proton Nuclear Magnetic Resonance (^{1}H-NMR) Spectroscopy

The ^{1}H-NMR spectra were recorded on a Bruker Avance 400MHz Spectrometer. The sample was dissolved in deuterated solvent in a 5-mm tube. Deuterated acetone ($(CD_3)_2CO$, δ_H = 2.05 ppm) was used as solvent for PGA polymer backbone, stearoyl chloride (C_{18}) and 40% C_{18} substituted PGA. While, deuterated chloroform ($CDCl_3$, δ_H = 7.28 ppm) was used as solvent for MIHA-PEG-NH_2 and 40%C_{18}-PGA-PEG-MIHA polymer.

2.2.2.3. Fourier Transformed Infrared (FTIR) Spectroscopy

Fourier transformed infrared (FTIR) spectrum was obtained using a Nicolet FTIR Spectrometer**.** The samples were dissolved in chloroform (2 mg samples in 100 µl chloroform) and prepared on sodium chloride (NaCl) disks. The scanning range was 400–4000 cm^{-1}. Sample analysis was carried out by the OMNIC software.

2.2.2.4. Analytical Data of Poly(glycerol adipate)

Poly(glycerol adipate) (PGA) is a copolymer of divinyl adipate and glycerol which is synthesized by a lipase catalysed polycondensation reaction. PGA polymer backbone was synthesized and characterized using ^{1}H-NMR and FTIR by Dr. G. Hutcheon as followed:

^{1}H-NMR (300 MHz, $(CD_3)_2CO$): δ (ppm) 1.66 (bs, 4H, -C(O)CH_2CH_2 from diacid), 2.36 (bs, 4H, -C(O)CH_2 from diacid), 2.85 (br, 1H, -OH), 4.38-3.54 (m, 5H, -O-CH_2CHCH_2-O from glycerol). IR: *v* (cm^{-1}): 3443, 2948, 2873, 1727, 1455, 1416, 1382, 1165, 1133, 1078, 1061, 940, 755.

2.2.3. 40% of acylation on poly(glycerol adipate) (40%C_{18}-PGA)

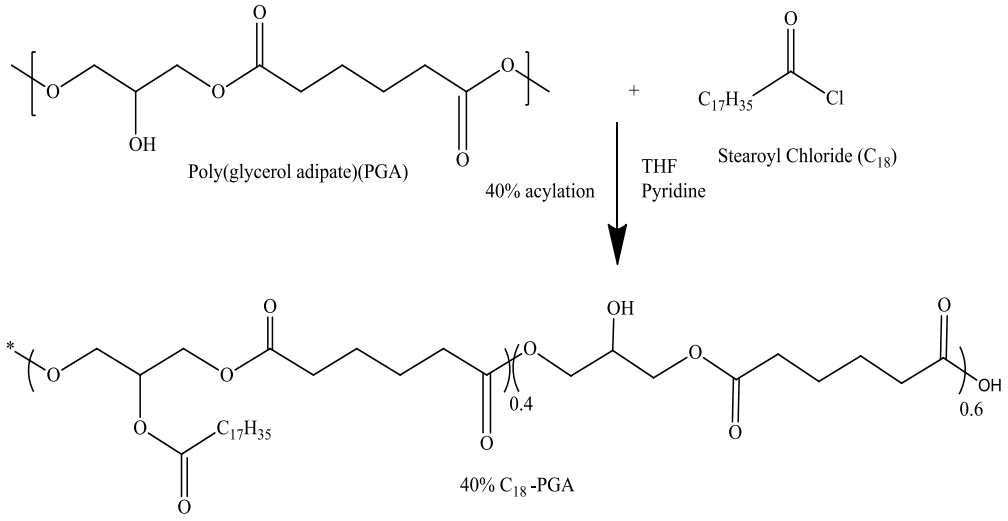

Figure 2.2. Acylation of poly(glycerol adipate) using stearoyl chloride

Poly(glycerol adipate) was substituted by 40% stearoyl acid (C_{18}) to increase the amount of drug loading into the microparticles (Figure 2.2). The percentage of acyl substitution was calculated using the repeat unit size of the backbone polyester

(202.21 g mol^{-1}). Poly(glycerol adipate) (PGA) (10.38 mmol, i.e. 2.10 g for 12 KDa) was dissolved in dried THF (10 ml). The mixture was warmed to reflux to dissolve the polymer and then stearoyl chloride (4.11 mmol, 1.4 ml,) was added. After those steps, pyridine (2 ml) was added to the mixture, producing acid fumes and white precipitate. The mixture was refluxed for 2 hour and then poured into 2 M HCl (100 ml). The aqueous solution was extracted with DCM (3 x 50 ml). The organic phase was then collected and extracted with water (100 ml). It was then dried over magnesium sulfate and the solvent was evaporated to dryness *in vacuo* to form a white waxy solid. The material was then washed with petroleum ether (10 ml) to remove the excess of stearic acid. The excess of petroleum ether was removed by evaporation under nitrogen gas for 2 hours followed by drying it in a vacuum desiccator until dried (2.48 g, 79% yield). R_f 0.40 (DCM/MeOH, 97.5: 2.5, $KMnO_4$ staining). ^{1}H-NMR (400 MHz, $(CD_3)_2CO$): δ (ppm): 0.86 (t, *J* 6.83 Hz, 72H, CH_3), 1.37 (s, 677H, CH_2), 1.65 (s, 252H, CH_2CH_2), 2.36 (bs, 240H, $CH_2C(O)$), 2.85 (br, 36H, OH), 4.21 (m, *J* 5 Hz, 250H, OCH_2CHCH_2O). IR : *v* (cm^{-1})3472, 2917, 2849, 1739, 1170, 1080, 757.

2.2.4. *N*-maleimide hexanoyl- diamine poly(ethylene glycol) (MIHA-PEG-NH_2)

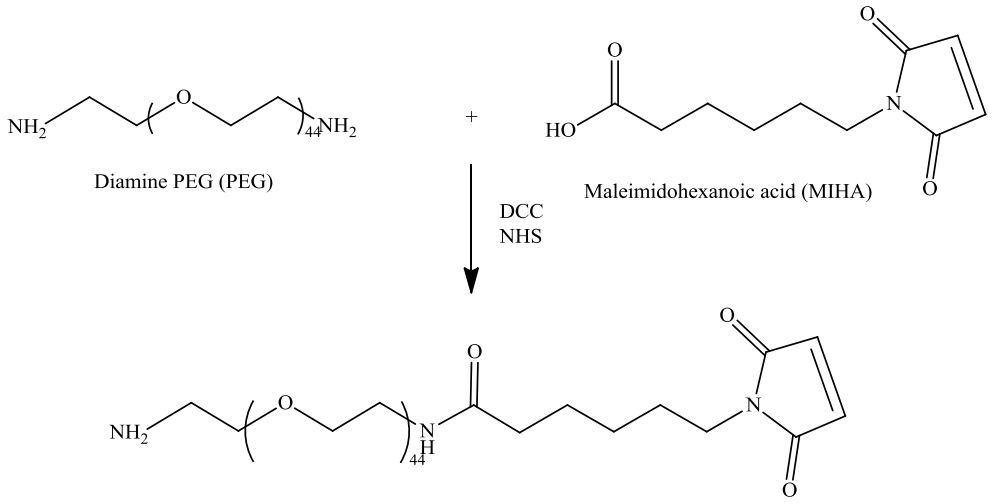

Figure 2.3. Synthesis of N-maleimidohexanoyl diamine poly(ethylene glycol) (MIHA-PEG-NH_2)

MIHA-PEG-NH_2 linker for the attachment of ligand on the microparticle was synthesized from maleimidohexanoic acid (MIHA) and diamine PEG (PEG) (Figure 2.3). The *N-m*aleimidohexanoic acid (MIHA) (0.20 mmol, 43.4 mg) was dissolved into chloroform (10 ml). Dicyclohexylcarbodiimide (DCC) (0.24 mmol, 49.8 mg) and *N*-hydroxysuccinimide (NHS) (0.25 mmol, 28.9 mg) were then added to the solution. The mixture was stirred overnight at room temperature. The insoluble dicyclohexyl urea was removed by filtration. After that, the organic solvent was removed under vacuum evaporator *in vacuo*.

The residual material was dissolved in chloroform (10 ml), the solution was then added to diamine PEG (0.20 mmol, 403 mg) in dropwise. The solution was stirred overnight at room temperature. The reaction was monitored using TLC. The mixture was then filtered and evaporated *in vacuo*. The resultant solid was triturated using diethyl ether followed by a filtration. The collected solid was dissolved into

chloroform (10 ml) and extracted using distilled water (10 ml) and saturated NaCl solution (10 ml). The organic phase was collected and evaporated *in vacuo* to afford a waxy, brownish-yellow solid (302.6 mg, 69% yield); R_f = 0.60 (DCM/MeOH, 90:10, $KMnO_4$ staining). ^{1}H-NMR (400 MHz, ($CDCl_3$): δ (ppm) : 1.30 (m, *J*=5 Hz, 2H, CH_2), 1.60 (m, *J*=7.6 Hz, 4H, CH_2CH_2), 3.50 (m, *J*=5 Hz 4H, CH_2-N), 3.55 (m, *J*=5 Hz, 2H, CH_2N), 3.6 (bs, 196 H, CH_2CH_2O), 6.7 (s, 2H, CH=CH). IR: *v* (cm^{-1}): 3325, 2884, 1626, 1467, 1105.

2.2.5. Attaching N-maleimidohexanoyl diamine poly(ethylene glycol) (MIHA-PEG) to 40%C_{18}-PGA (40%C_{18}-PGA-PEG-MIHA)

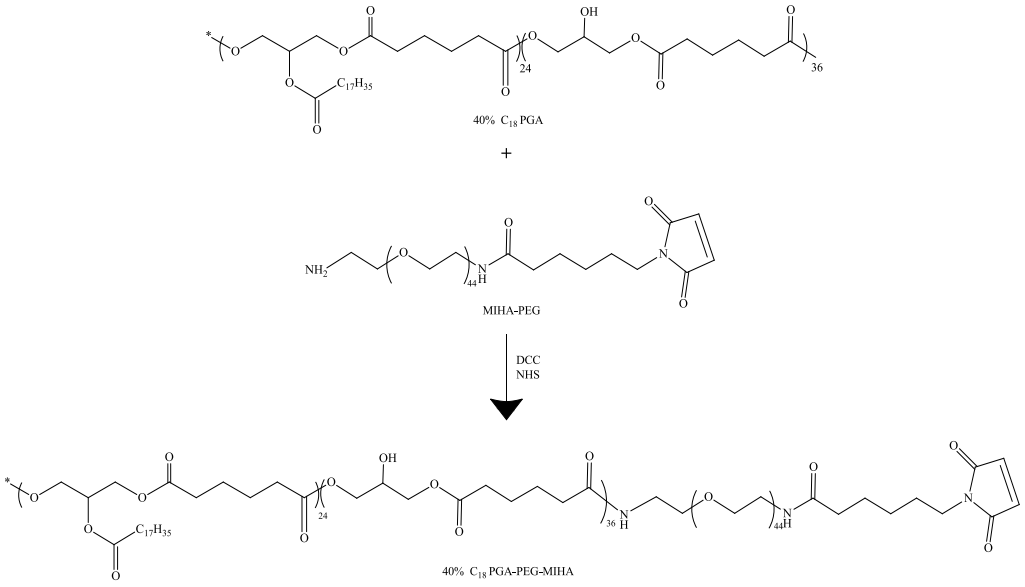

Figure 2.4. Synthesis of *N*-maleimidohexanoyl acid diamino PEG (MIHA-PEG-NH_2) coupled to 40% C_{18}-PGA (40%C_{18}-PGA-PEG-MIHA).

MIHA-PEG-NH_2 linker was tethered to 40%C_{18}-PGA for ligand attachment (Figure 2.4). A 40%C_{18}-PGA (0.05 mmol, 0.93 g,) was dissolved in 10 ml chloroform. After that, DCC (15.7 mg, 0.06 mmol) and NHS (6.9 mg, 0.06 mmol) were added to the PGA

solution. The mixture was stirred overnight at room temperature. MIHA-PEG-NH_2 (109.66 mg, 0.05 mmol) was added to the mixture and stirred continuously for 3 days at room temperature. Reaction was monitored using TLC. Following 3 days, the insoluble dicyclohexyl urea was then removed using filtration and the organic solvent was evaporated *in vacuo*. The solid compound was dissolved with chloroform (10 ml) and extracted using distilled water (10 ml) and saturated NaCl (10 ml). Organic solvent was evaporated *in vacuo* to obtain a brownish-yellow semisolid (579.6 mg, 56% yield); R_f = 0.40 (DCM/MeOH, 97.5:2.5, UV 254 nm). ^{1}H-NMR (400 MHz, ($CDCl_3$): δ (ppm): 0.90 (t, *J*=8.1 Hz, 72H, CH_3), 1.37 (bs, 675H, CH_2), 1.67 (bs, 260H, CH_2CH_2), 2.37 (m, 240H, CH_2CO), 3.45 (m, *J*=5.6 Hz, 10H, CH_2-N), 3.56 (m, *J*=5.6 Hz, 4H, CH_2N), 3.6 (bs, 135 H, CH_2CH_2O), 4.15 (m, *J*=7 Hz, 250H, OCH_2CHCH_2O), 6.7 (s, 2H, CH=CH). IR: *v (*cm^{-1}): 3473, 3323, 2924, 2849, 1739, 1621, 1465, 1169, 948.

2.2.6. **Modification of Collagen for Ligand**

2.2.6.1. Preliminary study for determination amount of thiol group

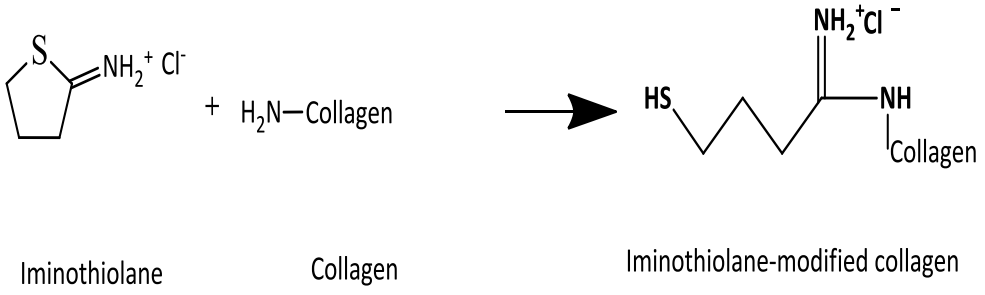

Figure 2.5. Attachment of 2-iminothiolane hydrochloride (**Traut's reagent) to collagen**.

Collagen was modified to provide a thiol group on its molecule (Figure 2.5). Due to the small amount of iminothiolane needed for conjugation with collagen, the amount

of thiol group cannot be analysed using spectrophotometer. Therefore, it was estimated by preliminary studies (Table 2.1).

Table 2.1. Preliminary study estimate the amount of thiol group attached to collagen

Batch	Amount of Collagen (nmol)	Amount of Trauts added (nmol)
AS008DD	1	100
AS009DD	1	500

Collagen (5 mg/ml) was dissolved in phosphate buffered saline (PBS) by continuous stirring for a minimum of 4 hours. Collagen solution (100µl, 1 nmol,) was added to tris buffer pH 8 (1.5 ml). The 2-iminothiolane hydrochloride (Traut's reagent) in solution was added to the mixture as amount stated in Table 2.1. The mixture was stirred at room temperature for 1 hour. Excess Traut's reagent was removed by passage through a PD-10 column (GE Healthcare). The collagen-SH fraction (fraction 3-5) was collected after detection using UV-spectrophotometer (Beckman Coulter DU800). The amount of thiol group was determined using 5-5'-dithiobis-2-nitrobenzoic acid (DTNB) (Ellman's reagent).

Ellman's reagent (50 µl) was added to the sample of collagen-Traut's fraction (30 µl). Tris buffer (1M) pH 8 (100 µl) and water (820 µl) were added to the mixture. The mixture was mixed and measured using UV-spectrophotometer (Beckman Coulter DU800) at λ 412 nm. The concentration of thiol group was calculated by two methods: 1). calculated using Equation 2-1 and 2). plotted the absorbance onto an acetyl cysteine calibration curve.

Equation 2-1: -SH (thiol) concentration.

$$-SH\ (thiol)\ concentration\ (M) = \frac{total\ volume\ (\mu l)}{sample\ volume\ (\mu l)}\ x\ \frac{absorbance\ at\ \lambda\ 412nm}{\varepsilon}$$

Where ε is the extinction coefficient of DTNB (13.6 x 10^4 M^{-1}. cm^{-1})

The acetyl cysteine calibration curve was produced using samples with known concentration of acetyl cysteine ranging from 10 to 50 µM and mixed with Ellman's reagent (50 µl) and Tris buffer (1M) pH 8 (100 µl). The volume of each concentration then adjusted with water to 1 ml. The mixture then scanned using UV-spectrophotometer at 412 nm.

2.2.6.2. *Attach collagen to FITC and 2-iminothiolane (Traut's)*

FITC was dissolved in DMSO to a concentration of 1 mg/ml. FITC (50 nmol, 20 µl) was taken from the stock solution and the solvent was dried to give solid FITC in glass vial. The collagen was dissolved in PBS to a concentration of 5 mg/ml. The collagen (10 nmol, 1 ml,) and sodium carbonate buffer 0.1 M, pH 9.5 (970 µl) was added to the glass vial. The mixture was incubated at room temperature for 4 hours in darkness. After 4 hours, the pH of the solution was adjusted to 8 using monobasic sodium phosphate (0.1 M). Then, Traut's reagent (200 nmol, 20 µl) was added and stirred for 1 hour at room temperature. Amount of the Traut's reagent to be added was estimated from the amount of thiol group provided in the previous step (section 2.2.6.1). The reaction steps of collagen modification can be found in Figure 2.6

The mixture was purified by desalting through PD-10 column using phosphate buffer saline (PBS) as eluent to remove the excess collagen, Traut's reagent and FITC. Fraction number 3-5 was collected to get 3 ml of product. Amount of FITC was

determined using spectrophotometer at λ 495 nm and the amount of collagen was determined using Bradford method at λ 595 nm.

FITC concentration on the sample was calculated using Equation 2-2:

Equation 2-2: Concentration of FITC

$$Concentration\ FITC = \frac{A_{495}}{\varepsilon}$$

Whereas A_{495} is the absorbance at λ 495 nm and ε is the extinction coefficient of FITC ($7.97 \times 10^4\ M^{-1}.\ cm^{-1}$).

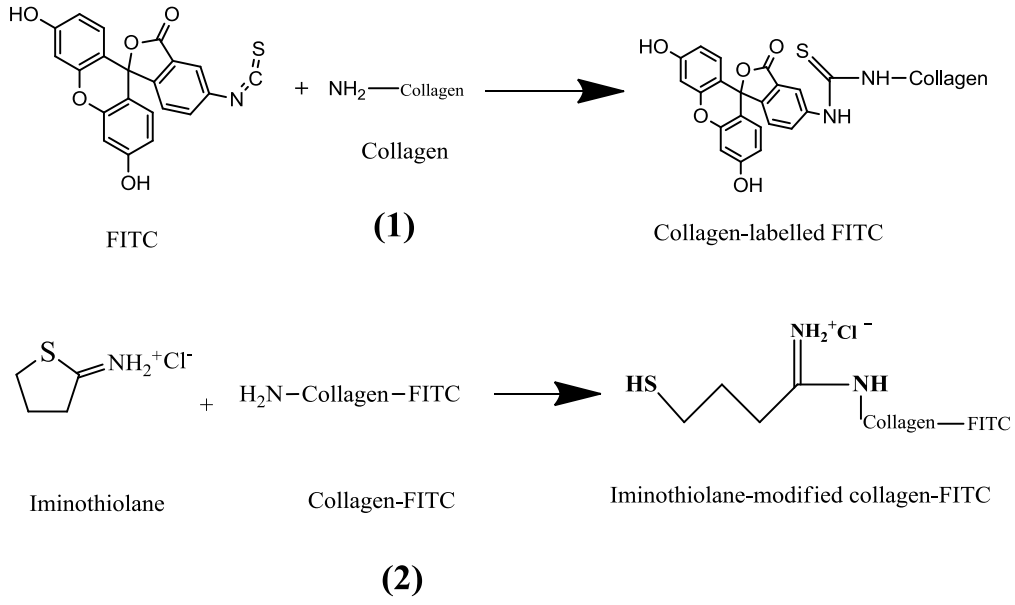

Figure 2.6. Collagen was modified with FITC and iminothiolane. FITC was attached for fluorescence (1) and iminothiolane was tethered to collagen to provide a thiol group in the collagen molecule (2).

The concentration of collagen in the solution was determined using the Bradford method. The method is based on the proportional binding of the Brilliant Blue G dye to proteins. The protein-dye complex causes a shift in the absorption maximum of

the dyes from 465 nm to 595 nm. Sample (100 µl) and water (400 µl) were added to Bradford reagent (500 µl) then incubated at room temperature for 10 minutes. The absorbance of the sample was measured using a spectrophotometer at λ 595 nm. Collagen concentration was calculated by plotting the absorbance of the sample into a collagen calibration curve.

2.2.6.3. *Cells attachment on modified collagen*

The ability of iminothiolane-modified collagen to attach to cells was evaluated using a flow cytometry assay. Briefly, mouse embryonic stem (mES) cells (passage 23-30) were trypsinized, harvested and fixed with 4% paraformaldehyde solution (2 ml, 10 minutes) continued by rinsing with PBS+0.1% BSA (3 x 2 ml). The cells were then adjusted to concentration of 10^5/ml in PBS. For flow cytometry assay, the cells (0.5 ml) were added to flow cytometry tubes. Various concentrations of modified collagen were then added to each tube and allowed to bind on the cells for half an hour in the dark. The mixture was then centrifuged (180 x g, 5 minutes) and the supernatant was discarded to remove unbound collagen. The pellet of cells was dispersed in PBS+0.1% BSA (0.5 ml) by gently pipetting. The number of cells tagged with modified collagen was evaluated using flow cytometry by determining the fluorescence intensity ($\lambda_{emission}$ 495 nm, $\lambda_{excitation}$ 521 nm) .

2.3. Microparticles production and characterization

2.3.1. Materials and equipment

The materials used for MP preparation and release studies were 40%C_{18}-PGA polymer and 40%C_{18}-PGA-PEG-MIHA polymer, which was modified from PGA polymer backbone, poly(vinyl alcohol) (PVA) (87-89% hydrolyzed, MW 85,000-

146,000), DCM, acetone, dexamethasone 21-disodium phosphate (DXMP), dexamethasone (DXM), simvastatin (SIM) from Merck Biosciences UK, phosphate buffer saline (PBS) tablet for PBS buffer, HEPES buffer, rhodamin B, tween 20.

The equipments used for MP preparation were Ultra-Turrax T25 Basic (IKA®), Magnetic Multi Stirrer RT 10 (IKA®) and centrifuge (Centaur 2). The characteristics of the microparticles were determined using Particle Size Analyser (Beckman Coulter LS230), Zetasizer (Malvern Zetasizer Nanoseries ZS90) and Scanning Electron Microscope (JEOL JSM 6060). The drug loading determination was carried out using HPLC Hewlett Packard (HP) Agilent 1050 equipped with an auto sampler. The fluorescence intensity measurement was obtained using a Fluorescence Spectrophotometer (Hitachi F-4500).

The equipment for the drug release study are included shaking water-bath DMS 360 (Fisher Scientific UK), centrifuge (Centaur 2), microcentrifuge (Eppendorf type 5430), and 15 ml Greiner centrifuge tubes. Quantitative analyses of drugs were carried out using HPLC Hewlett Packard (HP) Agilent 1050.

2.3.2. Manufacture of the Microparticles

Three different methods were applied to prepare MP from modified PGA polymer. The method was selected based on the properties of the encapsulated drugs and the modified PGA polymer.

2.3.2.1. Single emulsion method

The single emulsion method was used to prepare the MP from 40%C_{18}-PGA and 40%C_{18}-PGA-PEG-MIHA containing SIM as a drug. The polymer (100 mg) was

dissolved in 2 ml or 20 ml of DCM to give 0.5% and 5% polymer concentrations, respectively. SIM (200 µl, containing 1 mg of simvastatin in methanol) was added to the polymer solution and homogenised for 3 minutes at 22,000 rpm using the Ultra-Turrax. A small amount of rhodamine B (50 µl of 10mg/ml stock solution) was added to label the MP for cell work. The mixture was then added to PVA solution (5 ml) and mixed for 3 minutes at 22,000 rpm. PVA solution was provided by dissolving PVA in water and stirred for a minimum of 4 hours. The concentration of PVA used in the experiment varied from 0.005% to 2.5%. Organic solvent was evaporated by slowly stirring in a fume hood overnight. The MP was collected using centrifugation at 1818 x g for 5 minutes followed by rinsing with ultrapure water (3 x 10 ml). Supernatants were collected to determine the amount of free drug. The microparticles were freeze dried and kept in a fridge.

2.3.2.2. Double emulsion method

DXMP was incorporated in 40%C_{18}-PGA and 40%C_{18}-PGA-PEG-MIHA polymers using the double emulsion method. The polymer (100 mg) was dissolved in DCM (20 ml) to give 0.5% polymer concentration. A small amount of rhodamine B (50 µl of 10mg/ml stock solution) was added to label the MP for cell work. DXMP (1 mg in water) was added to the polymer solution and homogenized for 3 minutes using the Ultra-Turrax to form a primary emulsion. Volume of DXMP as a solution was varied towards organic phase to perform the primary emulsion as described in Table 2.2. Two variations of mixer speeds were used to prepare the microparticles. Those speeds were 11,000 rpm and 13,000 rpm. The mixture was then added with 2.5 % PVA solution (20 ml) and continued to homogenise for 3 minutes at 13,000 rpm to

complete the secondary emulsification process. PVA solution was prepared by stirring PVA in water for a minimum of 4 hours. The organic solvent was evaporated by stirring the mixture slowly in a fume hood overnight. The MP was collected by centrifugation at 1818 x g for 5 minutes followed by rinsing with ultrapure water (3 x 10 ml) to remove free DXMP from the microparticles. Supernatants were collected to determine the amount of free drug. The microparticle was freeze dried and kept in a fridge.

Table 2.2. Volume ratio of primary emulsion for DXMP encapsulation within modified PGA microparticle using double emulsion method.

Volume ratio of aqueous to organic phase	Volume of aqueous phase (ml)	Volume of organic phase (ml)
1 : 200	0.1	20
1 : 20	1	20

2.3.2.3. Solvent displacement method

The solvent displacement method was used to produce MP from 40%C_{18}-PGA without PVA. SIM was used as encapsulated drug. Briefly, a 40%C_{18}-PGA (100 mg) was dissolved in acetone (2 ml). A small amount of rhodamin B (50 µl of 10mg/ml stock solution) was added to label the MP for cell work. SIM (200 µl, containing 1 mg of simvastatin in methanol) was added to the polymer solution and homogenised for 3 minutes at 22,000 rpm. The mixture was then added dropwise to 5 ml water under homogenisation at speed setting 5. The organic solvent was evaporated by continuous stirring in a fume hood for overnight. The microparticles were obtained by centrifugation at 1818 x g for 5 minutes followed by rinsing with ultrapure water

(3 x 10 ml). Supernatants were retained to analyses drug loading using the indirect method. The microparticles were then freeze dried and kept in a fridge.

2.3.3. Characterisation of Microparticles

2.3.3.1. Particle size

The particles size was determined using a Beckman Coulter LS230 instrument. A microparticle suspension (100 µl) was placed in the fluid module and circulated through a sample cell at a constant speed. A beam of laser light passed through the cell was diffracted by particles within the sample cell, and the forward scattered (or diffracted) light was collected by a series of detectors. The distribution of light falling on the sensors enables the size distribution of the sample to be calculated. The measurement of particle size was taken at 8-12% obscuration.

2.3.3.2. Zeta potential

The zeta potentials of the MP were determined using Malvern Zetasizer Nanoseries ZS90. The sample of the MP was suspended in 1 mM HEPES buffer pH 7 to give a concentration of 1 mg/ml. The sample was then filtered through a 5µm filter to get particle size below 5 µm. The suspension of MP (1 ml) was then placed into a disposable folded capillary cell and inserted into the instrument. An electric field was applied to the suspension of the MP to move the microparticles with a certain velocity related to the zeta potential of the particle. The electrophoretic mobility was measured using Phase Analysis Light Scattering to determine the zeta potential of the MP.

2.3.3.3. Scanning Electron Microscope Images

A small amount of dried MP was placed on a carbon disk and positioned into a low vacuum sputter machine for gold coating. The sample was coated with gold for 5 minutes under vacuum then was placed into the vacuum-sample chamber. Images were taken from 15 mm working distance using a voltage of 40 KV. A high energy of electrons beam applied through the sample and interacted with the electron within the samples to produce back-scattered electrons that can be detected to give a high-resolution image.

2.3.4. Determination of Drug loading in Microparticle

2.3.4.1. Indirect method

Determination of drug loading using the indirect method was based on the amount of free drug in the supernatant. The supernatant was diluted in ultrapure water or methanol. The diluted sample then centrifuged at 19,466 x g for 5 minutes in a microcentaur microcentrifuge to precipitate the excess of polymer before injected to High Performance Liquid Chromatography (HPLC) HP 1050 for analysis.

For DXMP determination, supernatant was diluted in ultrapure water then centrifuged at 19,466 x g for 5 minutes to precipitate the excess of polymer in the supernatant. The supernatant was taken and injected into HPLC system as described in section 2.3.4.3. The DXMP concentration was calculated by plotting the peak area obtained on DXMP calibration curve.

For determination of SIM, supernatant was diluted five times using methanol then spun down using a centrifuge at 19,466 x g for 15 minutes. The clear supernatant was

then analysed using HPLC as described in section 2.3.4.4. The SIM concentration was calculated by plotting the peak area obtained on SIM calibration curve.

2.3.4.2. Direct method

Preliminary studies for validation of drug extraction method from MP were done by using various ratio of DCM: water and DCM: MeOH for DXMP and SIM, respectively. A known amount of drug was mixed homogenously with 40%C18-PGA polymer and then extracted with the solvents. For DXMP extraction, DCM and water was used in ratio 1:1, 1:2 and 1:4, while in SIM extraction the combination DCM and MeOH was used in the same ratio as used for DXMP extraction.

According preliminary study for extraction method, the ratio 1:4 of DCM: water was used to extract DXMP from modified PGA MP. The MP containing DXMP (10 mg) was dissolved in DCM (2 ml). Then, DXMP was extracted from MP with distilled water (8 ml). The solution was kept to equilibrate overnight. The water phase was then taken for determination of DXMP using HPLC. The organic phase was diluted in methanol then injected into HPLC system as described in section 2.3.4.3 to determine the amount of dexamethasone (DXM) as degradation product of DXMP in organic phase. The DXMP and DXM concentration was calculated by plotting the peak area obtained on their calibration curve.

The 1:4 ratio of DCM: MeOH was used to extract SIM from modified PGA MP containing SIM. The MP (10 mg) was dissolved in DCM (2 ml) followed by adding methanol (8 ml) to precipitate the polymer. The mixture was centrifuged at 19,466 x g for 5 minutes to get a clear supernatant. The supernatant was taken for HPLC

analysis as described in section 2.2.4.4. The SIM concentration was calculated by plotting the peak area obtained on SIM calibration curve.

2.3.4.3. Method for DXMP determination using HPLC

The determination of DXMP was carried on using eluent 0.01 M KH_2PO_4 : Methanol (35:65) in isocratic mode (1 ml/minute) at ambient temperature. The Lichrosphere 100 RP-18 (25 cm × 4.6 µm; 5µm) column was fitted into the HPLC HP 1050 system. The DXMP standard solution or sample containing DXMP was injected to the system using auto sampler. The volume of the injection was 20 µl. The peak of DXMP was eluted at 3.1 minutes and detected using UV at λ 240 nm. The HPLC analysis for DMP was carried out using the same method with DXMP and the peak of DXM is eluted at 6.6 minutes.

The calibration curve of DXMP was obtained by prepared series concentration of DXMP in water ranging from 0.39 -100 µg/ml and analysed by HPLC using the method described above. The calibration curve of DXM was obtained with the same method for DXMP but DXM was dissolved in MeOH.

2.3.4.4. Method for SIM determination using HPLC

The analysis was conducted using 1 mM ammonium acetate pH 4.4: methanol (10:90) as eluent in isoctratic mode (1 ml/minute). The Lichrosphere 100 RP-18 (25 cm × 4.6 µm; 5µm) column was fitted into HPLC HP 1050 system. Volume of sample injection is 5 µl and the temperature of the system was maintained at 40°C. The SIM peak was detected using UV at λ238 nm and eluted at 4.4 minutes.

The calibration curve of SIM was obtained by prepared series concentration of SIM in MeOH ranging from 0.20 -200 µg/ml and analyzed by HPLC using the method described above.

2.3.5. Manufacture of Solid Dispersion

2.3.5.1. Materials and equipments

The materials used for solid dispersions preparation were 40%C_{18}-PGA polymer and 40%C_{18}-PGA-PEG-MIHA polymer, which was modified from PGA polymer backbone, DCM, simvastatin (SIM) from Merck Biosciences UK.

The equipments used for solid dispersions preparation were Ultra-Turrax T25 Basic (IKA®). The drug loading in solid dispersion was determined using HPLC Hewlett Packard (HP) Agilent 1050 equipped with an auto sampler.

2.3.5.2. Preparation of Solid Dispersions

A polymer (100 mg) was dissolved in DCM (2 ml) and then SIM (200 µl, containing 1 mg of drug) was added to the solution. This solution was homogenized at 13,000 rpm for 3 minutes. The organic solvent was evaporated overnight in a fume hood to obtain a waxy solid. This solid material was then rinsed with methanol to remove unbound SIM. The solid dispersions were then freeze dried for 2 x 24 hours to obtain a brittle waxy solid.

2.3.5.3. Determination SIM loading in solid dispersions

The solid dispersions (10 mg) was dissolved in DCM (2 ml) followed by adding methanol (8 ml) to precipitate the polymer. The mixture was centrifuged at 19,466 x g for 5 minutes to get a clear supernatant. The supernatant was taken for HPLC analysis as described in section 2.3.4.4.

2.3.6. Drug Release Study

Drug release studies were applied to 40%C_{18}-PGA microparticle (MP), 40%C_{18}-PGA-PEG-MIHA MP and 40%C_{18}-PGA-PEG-MIHA MP coated with collagen as well as solid dispersion of SIM in 40%C_{18}-PGA and 40%C_{18}-PGA-PEG-MIHA. PBS tablet (Fisher Scientific UK) dissolved in distilled water was used as drug release medium. Tween 20 was added into the medium for simvastatin (SIM) release to increase the solubility of the active drug in the system and ensure sink conditions were obtained.

The drug release from the MP was evaluated using the Sample and Separate (SS) method. In a 15 ml centrifuge tube, 10 mg of MP or solid dispersions was placed within 1 ml PBS as a medium for drug release. For MP containing SIM, 0.1% tween 20 was added to PBS to improve the solubility of released SIM in PBS. The tubes were placed in shaking water-bath at 37°C. Gentle agitation (100 rpm) was applied to prevent MP precipitation. At a predetermined time point, the tubes were centrifuged at 1818 x g for 5 minutes to precipitate MP. A 1 ml sample was taken and fresh media was added for replacement at each time point. The sample for the drug release study was examined using HPLC HP 1050 using the methods described at section 2.3.4.3 and 2.3.4.4.

2.3.7. Collagen attachment onto microparticle

2.3.7.1. Preliminary study to evaluate collagen attachment onto microparticle

Preliminary study had been carried out to evaluate ability of iminothiolane-modifified collagen to attach on 40%C_{18}-PGA-PEG-MIHA MP. Various amount of iminothiolane-modified collagen (Table 2.3) were added to the microparticle (5 mg) in PBS (1 ml). The mixture was stirred in darkness for 24 hours. The microparticles were isolated by centrifugation at 20,187 x g for 10 minutes followed by rinsing with ultrapure water (3 x 1 ml). Amount of iminothilane-modified collagen was determined by measuring fluorescence intensity of FITC attached to collagen.

Table 2.3. Amount of collagen added to evaluate collagen attachment onto 40%C_{18}-PGA-PEG-MIHA microparticle.

Sample	Microparticle (mg)	Amount of collagen added (nmol)
A	5	0.1
B	5	0.2
C	5	0.4
D	5	0.8
E	5	1.6

2.3.7.2. Attach iminothiolane-modified collagen onto microparticle

Iminothiolane-modified collagen (500 µl) was added to MP (10 mg) in PBS (1 ml). The mixture was stirred in darkness by wrapping the container with aluminium foil for a minimum 24 hours. MP coated with collagen were isolated by centrifugation at 20,187 x g for 10 minutes followed by rinsing with ultrapure water (3 x 1 ml). Microparticles coated with collagen were then freeze dried for 2 days to get dried microparticle and were kept in a freezer.

2.3.7.3. Determination of collagen attachment onto microparticle

The amount of collagen attached onto MP was determined by both an indirect method and direct method.

2.3.7.3.1. Indirect method

The amount of modified collagen attached to the MP was determined using the fluorescence intensity of the unbound collagen in the solutions obtained from the supernatant and the washing steps. The fluorescence intensity of unbound collagen in the liquid phase was determined using fluorescence spectrophotometer at $\lambda_{excitation}$ of 495 nm and $\lambda_{emission}$ of 521 nm. The concentration of FITC in the unbound collagen was determined using the fluorescence intensity which was plotted to the FITC calibration curve. Since the amount of collagen added and the ratio of FITC to collagen had been known, the amount collagen attached to the MP can be calculated

2.3.7.3.2. Direct method

A MP coated with collagen (5mg) was suspended in water. The amount of collagen attached to the MP was determined by measuring the fluorescence intensity of FITC in collagen using fluorescence spectrophotometer at $\lambda_{excitation}$ of 495 nm and $\lambda_{emission}$ of 521 nm. Since the ratio FITC to collagen had been known, the amount of collagen attached to the MP can be determined.

2.4. Cells Aggregate Formation using Microparticles

2.4.1. Materials and Equipment

2.4.1.1. Cell Culture Media

STO Neo-Leukemic (SNL) fibroblast was proliferated standard culture medium (SCM) containing Dulbecco's Modified Eagle Medium (DMEM) from Invitrogen, Paisley UK, supplemented with 10% Fetal Bovine Serum (FBS) from Biosera (Catalogue No. FB-1001); penicillin-streptomycin (50 units/ml) from Invitrogen, Paisley UK; L-Glutamine (1 mM) and β-mercaptoethanol (100 μM).

The medium for mouse embryonic stem (mES) cells was SCM supplemented with Leukemia Inhibitory Factor (LIF) (500 unit/ml) from Chemicon, Hampshire UK from Chemicon, Hampshire UK.

The medium for primary osteoblast cells was Alpha Modified Eagles Medium (Alpha MEM) from BioWhittaker, Belgium supplemented with 10% FBS from Sigma (Catalogue No. F9665), penicillin-streptomycin (50 units/ml), L-Glutamin (1 mM) and sodium pyruvate (1 mM) from Invitrogen, Paisley UK.

2.4.1.2. Other Materials

The other materials for cells culture preparation and maintenance were PBS; gelatin; trypsin 0.25% containing 0.02% EDTA (Trypsin/EDTA); mitomcyn C, S. caespitosus from Merck Biosiences Ltd. Resazurin in Hanks Balanced Salt Solution (HBSS) was used to determine the cells proliferation.

2.4.1.3. Equipments

The equipments used for performing and maintaining the cell culture experiments were Class II cabinet fitted with high efficiency particulate air (HEPA) filter; cell incubator (Sanyo, 37°C, 5% CO_2); multifunction rotator (Grant PS-M3D); microscope Nikon Eclipse TS100; plate reader (Tecan); disposable lab-ware for tissue culture included cell culture flasks T75 and T25, non-tissue culture treated 96-well plates, 7 ml bijoux, pipette tips, 1.5 ml microcentrifuge tubes from Scientific Laboratory Supplies (SLS); 20 ml universals tube from Starsted; 0.25µm filter from Sartorius, Epsom UK for sterilisation of cell medium; UV lamp for steriliation of microparticles.

2.4.2. Culture of SNL fibroblast

SNL fibroblasts were obtained from Miss Magdalen Self, Wolfson Centre for Stem Cell, Tissue Engineering and Modelling (STEM), University of Nottingham, UK. They are of unknown passages, however it is well established in Tissue Engineering Group for embryonic stem cell proliferation and pluripotency maintenance and used between passages 1-50 post receipt. SNL were maintained in SCM described in section 2.4.1.1 and cultured in T75 cell culture flask and incubated in humidified static condition at 37°C with 5% CO_2 until confluence was reached. Once at confluence, the cells were passaged. The medium was carefully aspirated from the flask and the cells were washed using 10 ml PBS. Trypsin/EDTA (2 ml) was added to the flask to detach cells from the flask for no longer than 5 minutes to minimize damage to cells. Medium (3 ml) was then added to inactivate the trypsin. The cell suspension was transferred to a 20 ml universal tube and was centrifuged at 180 x g for 5 minutes. The supernatant was then aspirated, leaving the pellet of cells. The

cells pellet was then diluted with 5 ml cells medium with typical ratio of 1:5 by gently pipetting to avoid cell clumps. The cell suspension (1 ml) was then cultured in T75 cell culture flask containing 9 ml cell media and was incubated for 4-5 days until reaching confluence and ready for subsequent passaging.

2.4.3. Preparation of Feeder Layer for mES cell culture

Confluent SNL cells were used for feeder layer preparation. The feeder layer was prepared in a T25 cell culture flask treated with 0.1% gelatin for 2 hours. The medium was aspirated from confluent SNL cell culture then treated with 10 ml mitomycin C solution (0.01 mg/ml). The cells treated with mitomycin were incubated at 37 °C with 5% CO_2 for 2 hours. The mitomycin C solution was then removed and the cells were washed twice with 10 ml PBS. Trypsin/EDTA (2 ml) was then added to detach the cells from the flask for no longer than 5 minutes. The flask was gently agitated to dissociate the cells and SNL medium (3 ml) was added. The cell suspension was then transferred to a 20 ml universal and centrifuged for 5 minutes at 180 x g. The supernatant was aspirated and the cells were diluted with SNL medium (2 ml) prior to cell counting using a haemocytometer. The cells were then seeded in a T25 cell culture flask-gelatin treated at density of $8x10^4$/ml in SCM medium (5 ml). The feeder layers were incubated in static condition at 37°C and 5% CO_2 in humidified atmosphere. The feeder layer was ready for mES cells culture by the next day and could be used as feeder layer until 14 days. The medium was replaced when the colour of the media became slightly yellow.

2.4.4. Culture of mouse embryonic stem (mES) cell

The mouse embryonic stem (mES) cells were cell line originally derived from mouse columnar epiblast epithelium (CEE) and maintained as stock in the Tissue Engineering Group. The mES cells were cultured in a T25 fibroblast feeder layer and proliferated in mES cell medium as described in section 2.4.1.1. The confluent mES cells were passaged to maintain pluripotency of the stem cells. The media was aspirated from the confluence mES culture flask followed by rinsing with PBS (5 ml). The cells were detached from the culture flask by adding trypsin/EDTA (2 ml) for no more than 5 minutes. The flask was gently agitated to completely dissociate the mES cells. The medium (3ml) was then added to deactivate trypsin/EDTA. The mES suspension was then transferred to a 20 ml universal tube and was pelleted using centrifugation at 180 x g for 5 minutes. The supernatant was aspirated to remove trypsin/EDTA. The pellet of mES cells was then suspended in 4 ml medium for splitting at ratio 1:4 and gently pipetted to break cell clumps. The cells suspension (1 ml) was then cultured in a T25 fibroblast feeder layer containing 4 ml mES cells media. The cells were incubated in static condition at 37°C and 5% CO2 in humidified atmosphere until reaching confluence and ready to use for cells experiment or for passaging. The mES cells typically reached confluence after 2-3 days. Mouse ES cells could be kept undifferentiated until passage 30.

2.4.5. Culture of primary osteoblast cells

The primary osteoblast cells were isolated from neonatal (1-5 day old) CD1 mouse calvariae. The primary osteoblast cells were proliferated in aT75 flask supplemented with primary osteoblast medium described in section 2.4.1.1. The primary osteoblast

cells from frozen stock (1 ml) was thawed and diluted in osteoblast medium (4 ml). The cells were then centrifuged at 300 x g for 5 minutes. The supernatant was removed and the cells were suspended in osteoblast medium (2 ml). The osteoblast suspension was seeded in T75 cell culture flask containing osteoblast medium (8 ml). The cells were incubated at 37°C with 5% CO2 in humidified atmosphere for 2-3 days to reach confluence and ready for experiments.

2.4.6. Aggregate formation with microparticle

The confluent cells were harvested using trypsinization, centrifuged and resuspended in appropriate cell culture media described in section 2.4.1.1. Passage 23-29 was used for an experiment with mES cells while the primary osteoblast cells were used without passaging. MP was sterilized under a UV light for 45 minutes prior to use. Microparticles (MP) suspension in phosphate buffer saline (PBS) was seeded in non-tissue culture treated 96-well plate then cells ($1x10^4$ cells per well) were seeded in ratio 1:1 cells to MP. The volume of media was adjusted to 200 µl per well. The plate was placed in a 15 rpm multifunction rotator in an incubator at 37°C and 5% CO_2 for 6 hours (for mES cells) or 3 hours (for primary osteoblast) then transferred to a static condition incubator. The cultures were maintained in a static incubator for 14 days. The cell culture medium was replaced every 2 days (for mES cells culture) and 5 days (for osteoblast cells culture) or when the colour of the cell medium turned to yellow.

2.4.7. Determination of the Diameter of Cell Aggregates

Aggregate formation images were taken using Nikon Eclipse TS100 microscope at day 3, 5 and 7. The cell aggregate images were taken at three random areas in each well. The images were labelled and the aggregate diameter was analysed using ImageJ

Software. Two perpendicular diameters diameter were measured across the centre of the aggregate and the average of these two measurements was calculated.

2.4.8. Determination of the amount of microparticle inside cell aggregates

The incorporation of MP inside the cell aggregates were evaluated by dissociating the cell aggregates at day 3. The cell aggregates were taken out from the well-plate and rinsed with PBS (3 x 1 ml) to remove unincorporated MP before dissociating using trypsin/EDTA. The number of microparticles inside the cell aggregates was counted by taking image of microparticle and cells at three random selected areas using fluorescence and bright field microscope, respectively. The number of particle and cell were counted by image analysis using ImageJ software. The incorporation of the microparticles inside cell aggregates was calculated using Equation 2-3.

Equation 2-3. Incorporation of microparticle inside cells aggregate (%)

$$\textbf{Incorporation of microparticle inside cells aggregate } (\%) = \frac{\textbf{number of microparticles in random selected area}}{\textbf{number of cells in random selected area}} \textbf{ x 100}$$

2.4.9. Determination number of single cells

The number of single cells was counted by image analysis using ImageJ software. The images was taken at three random selected areas each well under bright field microscope.

2.4.10. Alamar Blue assay for cell proliferation and metabolism activity

Cells proliferation and metabolism activity were evaluated using the Alamar Blue assay on 7-day and 14-day old cell cultures. The cell aggregates were washed using PBS then transferred to a 96-well plate. Resazurin (Alamar Blue) was dissolved in HBSS buffer to get 20µg/ml solution. The solution was filtered through 0.25 µm filter and was kept in the dark. Alamar Blue solution (200 µl) was added to the washed cell aggregates. The plate was incubated for 15 minutes at 37°C in the dark. The fluorescence intensity of the reduced form of resazurin was measured using a plate reader at $\lambda_{excitation}$ of 560 nm and $\lambda_{emmision}$ of 590 nm.

2.5. Microparticles for cell differentiation

2.5.1. Materials and Equipment

Microparticle (MP) containing simvastatin prepared from 40%C_{18}-PGA and 40%C_{18}-PGA-PEG-MIHA were used to induce osteogenesis in mES and primary osteoblast cells. Cells culture is maintained in an appropriate media as described in section 2.4.1.1.

The alkaline phosphatase was identified using p-nitrophenyl phosphate (pNPP) in 0.2 M Trizma® base pH 9.8.

Osteocalcin imunostaining was identified using anti osteocalcin polyclonal antibody from Millipore (Catalogue No. AB 10911, raised in Rabbit), Biotinylated Anti-Rabbit IgG H+L from Vector Laboratories (Catalogue No. BA-1000, raised in goat), and diaminobenzidine (DAB) histochemistry kit from Molecular Probes (Catalogue No. D22187). PBS with 1% Triton X-100 was used to permeabilize aggregates; PBS with

0.1% bovine serum albumin (BSA) was used as general solvent during staining process with antibody.

The mineralisation in cells was identified using the von Kossa staining method using silver nitrate and sodium thiosulfate.

The other materials for cells culture maintenance were deionized tissue culture water, phosphate buffer saline (PBS); trypsin 0.25% containing 0.02% EDTA (Trypsin/EDTA).

The equipments used for performing and maintaining cell culture experiments are described in section 2.4.1.3.

2.5.2. Incorporation of microparticles within cells for osteogenic differentiation

The osteogenic differentiation of mES cells was maintained in SCM supplemented with β-Glycerophosphate (50 mM) and L-ascorbic acid (50 μg/ml).

The osteogenic differentiation of primary osteoblasts was maintained in primary osteoblast medium supplemented with β-Glycerophosphate (50 mM) and L-ascorbic acid (50 μg/ml).

The microparticles (MP) were dispersed in phosphate buffer saline and sterilized under UV light for 45 minutes prior to use. The calculated amount of MP suspension was seeded into non-tissue culture treated 96-well plate, given the ratio 1:10 of MPs to cells. Then, cells were seeded to the plate at 10^4 cells per well and the volume of medium was adjusted to 200 μl per well. The plate was placed on 15 rpm multifunction rotator in 37°C incubator for 6 hour (for mES cell) or 3 hour (for

osteoblast cell) to induce aggregate formation then moved to a static incubator. The cells were maintained in the culture for 28 days. The media was changed every 2 days for mES cell and every 5 days for osteoblast cell.

2.5.3. **Alkaline phosphatase assay**

The samples of cells from day 7^{th}, 14^{th} and 21^{st} were collected and washed using PBS to remove the media. Alkaline phosphatase was lysed in 0.2 M Trizma® buffer by freezing down the cell aggregate in -80°C for 2 hours continued by sonication for 2 minute. The samples were centrifuged for 10 minutes at 14,420 x g to remove cellular debris. The supernatant was collected for alkaline phosphatase assay. The alkaline phosphatases in the samples were determined using pNPP as substrate. One tablet of pNPP substrate was dissolved in 0.2 M Trizma® buffer (20 ml). The supernatant (100 µl) was placed in 96-well assay plate and p-NPP (200 µl) solution was added to the sample. The alkaline phosphatase hydrolysed pNPP to the yellow end product, p-nitrophenol, which was soluble in buffer. The absorbance of the supernatant was measured at λ 405nm. The alkaline phosphatase in the samples was quantified using alkaline phosphatase enzyme as a standard.

2.5.4. **Imunostaining of osteocalcin**

Osteocalcin in the cell aggregates was detected using horseradish peroxidase-streptavidin (HRP-streptavidin) immunodetection. Diaminobenzidine (DAB) was used as substrate for HRP to give brown-coloured oxidation product.

A sample of 28-day cell aggregate was fixed with 4% paraformaldehyde for 1 hour and kept in fridge to preserve active proteins until ready for immunostaining. The

aggregates were permeabilized in PBS containing 1% Triton X-100 for 30 minutes at room temperature followed by rinsing with PBS (200 µl, 3 x 5 minutes). Endogenous peroxidase in the cell aggregates was blocked by incubating the aggregates in 3% H_2O_2 for 1 hour in room temperature followed by rinsing with PBS (200 µl, 3 x 5 minutes). After blocking the endogenous peroxidase, the aggregates were incubated in 0.5% goat serum (200 µl) for 1 hour at room temperature to prevent non-specific binding of secondary antibody. The blocking serum was rinsed away three times with PBS+0.1% BSA (200 µl, 3 x 5 minutes).

Primary antibody (anti osteocalcin polyclonal antibody, raised in rabbit) was diluted 1 to 200 using PBS+0.1% BSA. The diluted primary antibody was then added to cell aggregates and incubated at 4°C overnight. The washing out using PBS+0.1% BSA (200 µl, 3 x 5 minutes) was carried out to rinse out primary antibody from the aggregates. Secondary antibody (biotinylated anti-rabbit IgG (H+L), raised in goat, 1:500 dilution in PBS+0.1% BSA, 200 µl) was added to the cells aggregates. The cell aggregates were incubated in secondary antibody at room temperature for one hour. Subsequently, the secondary antibody was rinsed with PBS+0.1% BSA (200 µl, 3 x 5 minutes).

The osteocalcin labelling was then detected using HRP-streptavidin conjugate. The cell aggregate was incubated with HRP-streptavidin conjugate (1:500 dilution in PBS+0.1% BSA, 200 µl) for 1 hour at room temperature, then HRP-streptavidin conjugate was rinsed out three times with PBS+0.1% BSA (200 µl, 3 x 5 minutes). DAB solution (1 mg/ml) was mixed with the cell aggregates using gentle agitation for 15 minutes. Afterward, 0.03% H_2O_2 (200 µl) was added to the cells aggregates and

allowed to remain for 5 minutes. DAB solution was rinsed out with PBS (200 µl, 3 x 5 minutes). Staining in the cells aggregates was viewed under bright field microscope.

2.5.5. **Von Kossa staining for mineralisation**

The von Kossa staining was used to detect mineralisation in 28 day old cells aggregates. This technique was used to detect the calcium deposition in the cell aggregates using silver nitrate solution. The calcium in the sample was reduced using strong light and replaced with silver deposit. The sample of 28-day cells aggregates was fixed with 4% paraformaldehyde for 1 hour and kept in a fridge for the experiments.

The fixed cell aggregates were rinsed and dehydrated by placing the aggregates in deionized water (200 µl) for 2 hours. The aggregate was then exposed to 1% silver nitrate solution under strong light for 1 hour. Mineralised aggregates turned to brown or black colour to indicate a complete reaction. Subsequently, the aggregates were rinsed three times with deionized water (200 µl, 3 x 5 minutes). The unreacted silver nitrate was removed by mixing with 2.5% sodium thiosulfate for 5 minutes. The aggregates were then washed three times with deionized water. Mineralisation in the cell aggregates was indicated by brown colour visualized under a light microscope.

CHAPTER 3

3. MODIFICATION OF POLY(GLYCEROL ADIPATE)

3.1. Introduction

Microparticles (MP) can be applied as matrices in tissue engineering to facilitate 3D assembly of cells and act as a drug reservoir to release drug in controlled manner [16, 17, 35]. Poly(glycerol-adipate) (PGA) is a potential material for preparation of microparticles for 3D tissue engineering as it is biodegradable and biocompatible with several cells [124, 125, 146]. However, modifications of the polymer are useful to meet the requirement for delivering bioactive molecules to cell for tissue engineering.

Many bioactive molecules have hydrophobic properties and tend to interact with lipid environment in biological membrane [147, 148]. Consequently, it is anticipated that material could be efficiently encapsulated within PGA polymer by creating lipophilic environment on the polymer backbone [149]. A lipophilic environment can be created by conjugation of lipophilic acyl chloride to the pendant hydroxyl group of PGA polymer. Previous studies showed that PGA with a 40% substitution of stearoyl groups ($C_{18}H_{35}O$-) to the hydroxyl group of PGA polymer exhibited the highest encapsulation efficiency for dexamethasone phosphate. The steroidal moiety on dexamethasone phosphate is expected to interact very well with the alkyl moieties of

stearic acid [125]. This result could be applied to encapsulate other hydrophobic bioactive molecules for modulating cell growth.

Further modification is needed for the microparticle to support cell aggregation for generating a 3D structure. The adhesiveness of the microparticle can be achieved by attaching ligand or extracellular matrix (ECM) proteins, as cell adhesion molecules, onto the surface of microparticle. Moreover, attachment of ECM proteins can mimic an *in vivo* microenvironment to control the development of cells. The attachment of ECM using physical adsorption e.g. plasma coating seems not effective as desorption occurs after a period of time [138]. Thus, conjugation *via* covalent bonding offers stable attachment of ECM protein on the surface of MP. Therefore, a linker is needed to facilitate ECM protein conjugation to MP.

Poly(ethylene glycol) is an attractive linker to enable ECM protein conjugation. The PEG chain would produce a "conformational cloud" around the MP to prevent aggregation. In addition, PEG configuration protects MP from immune recognition, thus reducing immunological reactions [130, 132, 133]. The thiol-PEGylating agent, *N*-maleimidohexanoyl diamino-poly(ethylene-glycol) (MIHA-PEG-NH_2) linker, has been used to provide more specific conjugation with protein. MIHA-PEG-NH_2 linker only reacts with thiol functional groups on protein molecules. The thiol groups are rarely present in proteins, therefore, it offers a more selective attachment of proteins on the surface of MP [130, 131]. The PEGylation of MP can be prepared before fabrication of MP or after MP was formed. MIHA-PEG-NH_2 linker was attached to modified PGA polymer to ensure that PEGylation occurred on the bulk of MP.

The aims of the experiment presented in this chapter are functionalization of PGA polymer by substituting 40% of hydroxyl group of PGA with stearoyl moiety (C_{18}), attaching *N*-maleimidohexanoyl diamino-poly(ethylene-glycol) (MIHA-PEG-NH_2) to provide linker for ligand attachment to the 40% C_{18} substituted PGA (40%C_{18}-PGA) and installation of iminothiolane-modified collagen as ligand for cell attachment.

3.2. Stearoyl Substitution on Poly(glycerol adipate) (40%C_{18}-PGA)

The pendant hydroxyl group on PGA polymer backbone was substituted with C_{18} to provide a lipophilic environment for encapsulation of drug. Stearic acid (C_{18}) was conjugated on 40% of hydroxyl group in PGA backbone and the synthesis involved addition of stearoyl chloride into the polymer backbone and refluxed for 2 hours as described in Chapter 2, section 2.2.3. For 40% stearoyl substitution, 4 mmol of steroyl chloride was added to 10 mmol (2.02 gram) of PGA polymer. The yields from this procedure on several batches are around 76 % which is comparable to previous study by Kalinteri *et al* (2005) with reported yield of 79% [125].

The acylation of polymer was confirmed using ^{1}H-NMR and FTIR. The following figures (Figure 3.1 and Figure 3.2) are ^{1}H-NMR spectra of poly(glycerol adipate) backbone and 40% C_{18} substituted poly(glycerol adipate) (40%C_{18}-PGA). The percentage of the o-acylation was confirmed using the CH_3 peak at δ 0.86 which is assigned to terminal of the C_{18} and CH_2CO at δ 2.36 assigned to PGA. The percentage of the polymer acylation from several batches showed that the percentage of the acylation was varied from 38% to 42%. This result was also confirmed using FTIR spectrum.

The FTIR spectrum showed the functional groups in both polymer backbone and 40% C_{18}-PGA (Figure 3.3). The peak of –OH group at 3472 cm^{-1} from polymer backbone was still present in 40% C_{18} substituted polymer since acylation was not intended to be completed. However, the -OH group in the 40%C_{18}-PGA appeared in lower intensity than unsubstituted PGA.

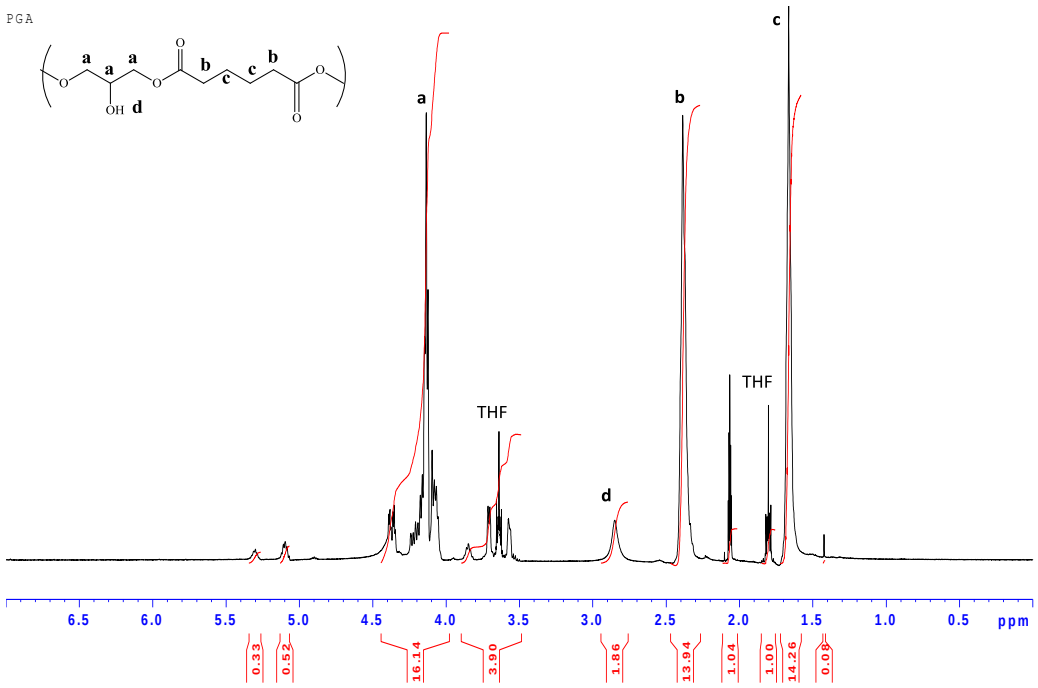

Figure 3.1. ^{1}H-NMR spectrum of poly(glycerol adipate) (PGA) backbone

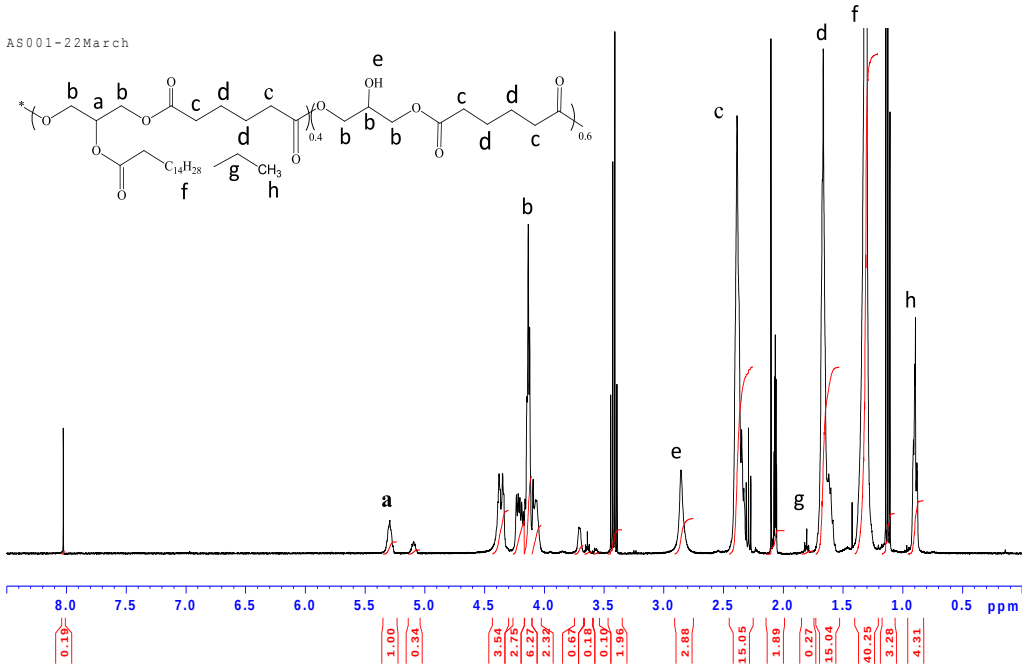

Figure 3.2. ^{1}H-NMR spectrum for 40% C_{18} acylation of poly(glycerol-adipate) (40%C_{18}-PGA)

(a)

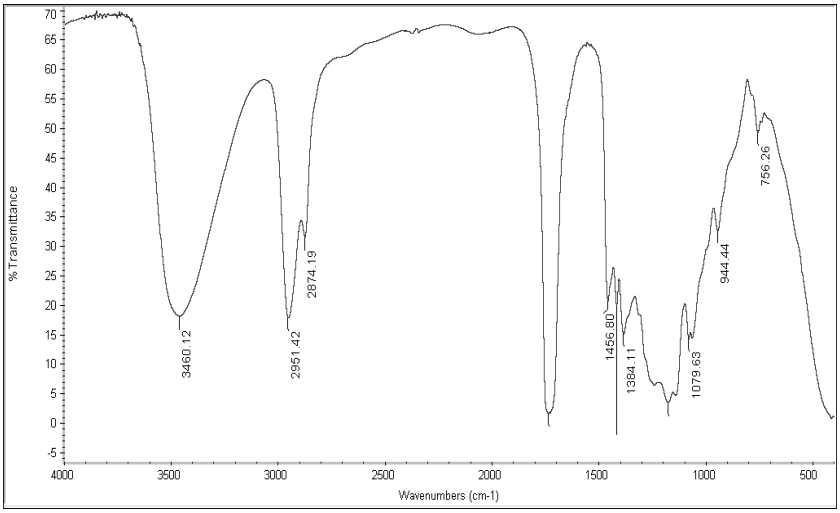

(b)

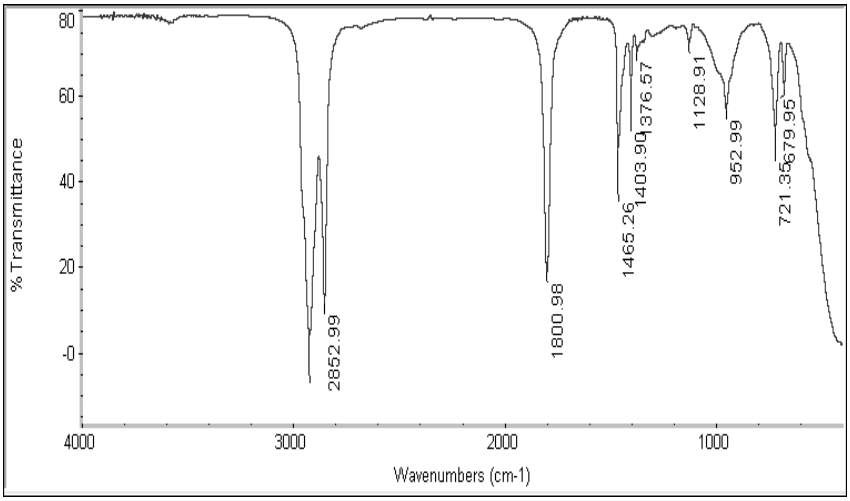

(c)

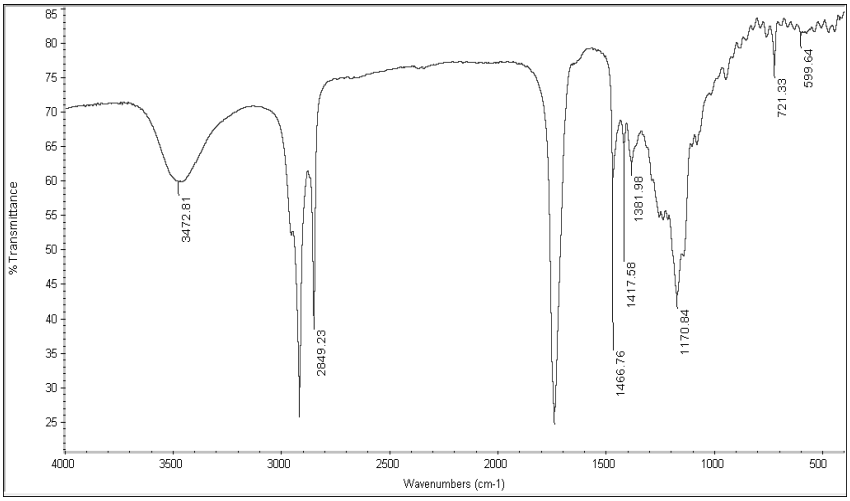

Figure 3.3. FTIR spectrum of (a) poly(glycerol adipate (PGA), (b) stearoyl chloride (C_{18}) and (c) 40% C_{18}-PGA

3.3. Synthesis of *N*-maleimidohexanoyl diamino-poly(ethylene-glycol) (MIHA-PEG-NH_2) linker

In order to attach ligand onto the surface of microparticles, PGA polymer was functionalized with *N*-maleimidohexanoyl diamino-poly(ethylene-glycol) (MIHA-PEG-NH_2) linker. The conjugation of ligand on polymer surface can be achieved using maleimido functionality. The MIHA-PEG-NH_2 linker was synthesized from N-maleimidohexanoic acid (MIHA) and diamine poly(ethylene glycol) (H_2N-PEG-NH_2, MW 2000) by amide formation. Diamine PEG has a functional amine at each end of the PEG chain and each of the amine groups in the end of PEG chains has the ability to react with activated maleimidohexanoic acid. Thus, the diamine PEG was used in high molar excess in order to ensure mono-substitution.

The formation of an amide bond between the terminal carboxylic acid group in maleimidohexanoic acid and an amine on diamine-PEG can be accomplished by carbodiimide-mediated coupling as mentioned in Chapter 2, section 2.2.4. Thus, *N*-maleimidohexanoic acid was activated using combination of *N,N*-dicyclohexylcarbodiimide (DCC) and *N*-hydroxysuccinimide (NHS). This combination was reported as an efficient way of creating active ester necessary for formation of amide linkage [150].

The activation of *N*-maleimidohexanoic acid took overnight. During the process, the mixture became cloudy as the by-product, *N,N*-dicyclohexylurea, was produced. Dicyclohexylurea was removed from the activated maleimidohexanoic acid (MIHA) by filtration. The activated MIHA was then added to diamine PEG dropwise to ensure that only one end of the amine group react with the carboxylic acid from

maleimidohexanoic acid. Following an overnight reaction, again, the dicyclohexylurea was removed from the product using filtration and the product was triturated with diethyl ether to remove the excess of DCC. After that step, the excess of NHS was removed by aqueous extraction of the organic phase using water. The yield of MIHA-PEG-NH_2 synthesis after the purification was 68% and confirmation of MIHA-PEG-NH_2 synthesis was established by ^{1}H-NMR (Figure 3.4) and FTIR (Figure 3.5).

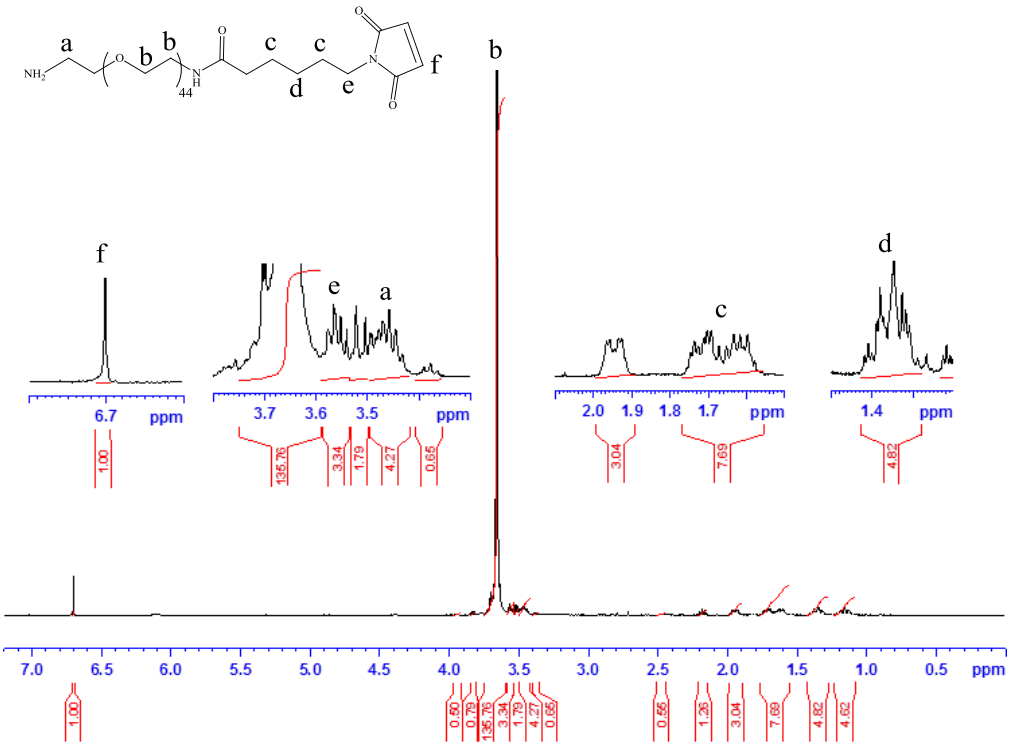

Figure 3.4. ^{1}H-NMR spectrum for N-maleimidohexanoyl diamino poly(ethylene-glycol) (MIHA-PEG-NH_2)

(a)

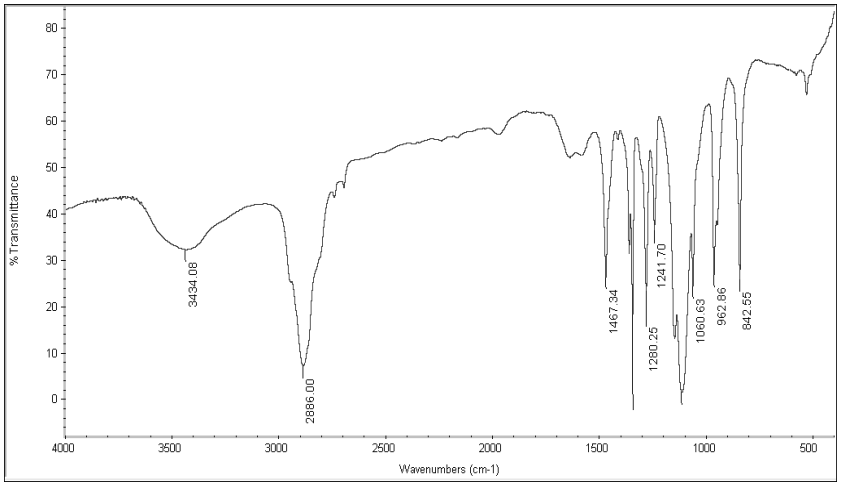

(b)

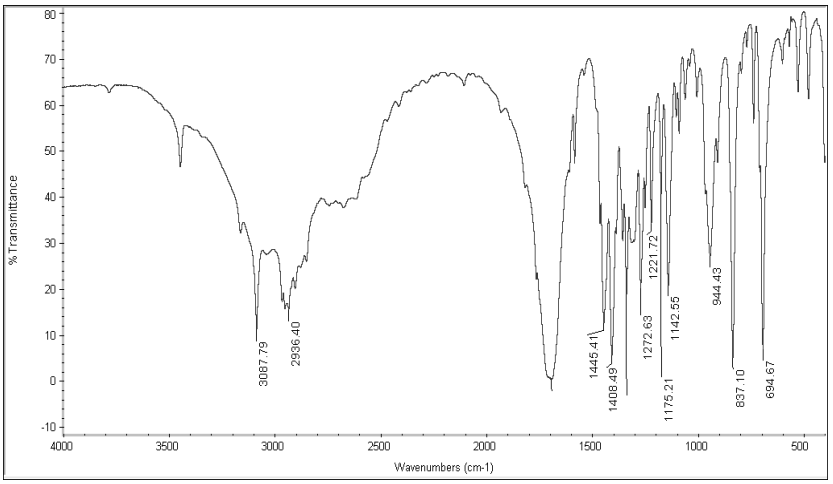

(c)

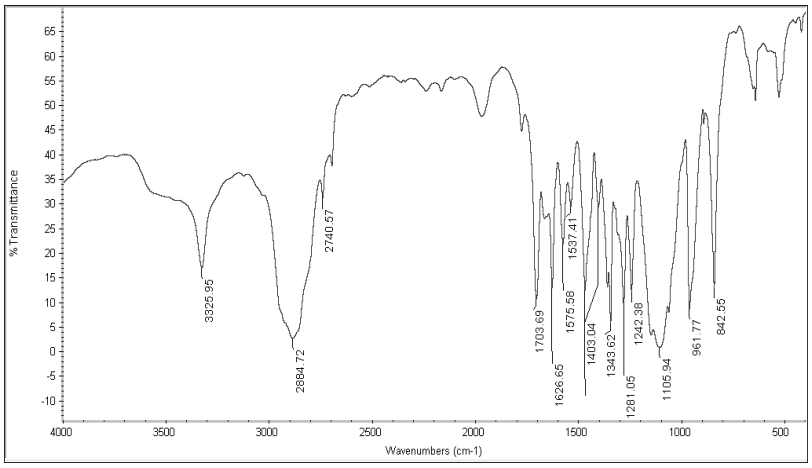

Figure 3.5. FTIR spectrum of (a) diamine poly(ethylene glycol) (PEG), (b) *N*-maleimidohexanoic acid (MIHA (c) *N*-maleimidohexanoyl diamino Poly (ethylene-glycol)(MIHA-PEG-NH_2)

The comparison of the relative peak area of –O-CH_2-CH_2 group in diamine PEG (δ 3.6-3.7) and the peak area of –CH of maleimide ring (δ 6.7) showed that the ratio of PEG to MIHA was 1:1. The NH_2 stretching broad spectrum from diamine PEG at 3434 cm^{-1} was shifted to 3327 cm^{-1} indicated the amide bond formation in MIHA-PEG-NH_2. In addition, a sharp peak around 1626 cm^{-1} in MIHA-PEG-NH_2 spectrum from O=C-N- indicated that one of NH_2 of diamine PEG substituted to carboxyl group of MIHA and became O=C–NH.

3.4. Attachment of MIHA-PEG-NH_2 linker to 40%C_{18}-PGA

The next stage of functionalizing the poly(glycerol adipate) polymer is attachment of MIHA-PEG-NH_2 to 40%C_{18}-PGA. The target of this reaction is coupling the amine group from MIHA-PEG-NH_2 to the terminally located carboxylic acid group in PGA (Chapter 2, section 2.2.5). Since the amide formation to afford a 40%C_{18}-PGA-PEG-MIHA is similar to the formation of PEG-MIHA-NH_2, the combination of the coupling agents, DCC and NHS, were again used to activate the carboxylic acid in the end chain of polymer.

The 40%C_{18}-PGA was activated overnight using DCC and NHS. The activated 40%C_{18}-PGA with MIHA-PEG-NH_2 were left for 3 days at room temperature. The purification of desired product was done by extraction of organic phase using water to remove the excess NHS. The final product of 40%C_{18}-PGA-PEG-MIHA is a brownish-yellow semisolid and the yields of several batches were varied from 65-83%. The polymer was analysed using ^{1}H-NMR and FTIR to confirm the final product of 40%C_{18}-PGA -PEG-MIHA.

^{1}H-NMR spectrum (Figure 3.6) was used to confirm 40%C_{18}-PGA-PEG-MIHA structure. The spectrum was difficult to analyse due to relatively small amount of PEG-MIHA added to 40%C_{18}-PGA. Consequently, the important peaks were only visible in small intensities. The comparison of the relative peak area of –CH_2 group near carbonyl in PGA polymer (δ 2.3-2.4) and the peak area of –CH on maleimide ring (δ 6.7) showed that PGA was coupled with PEG-MIHA.

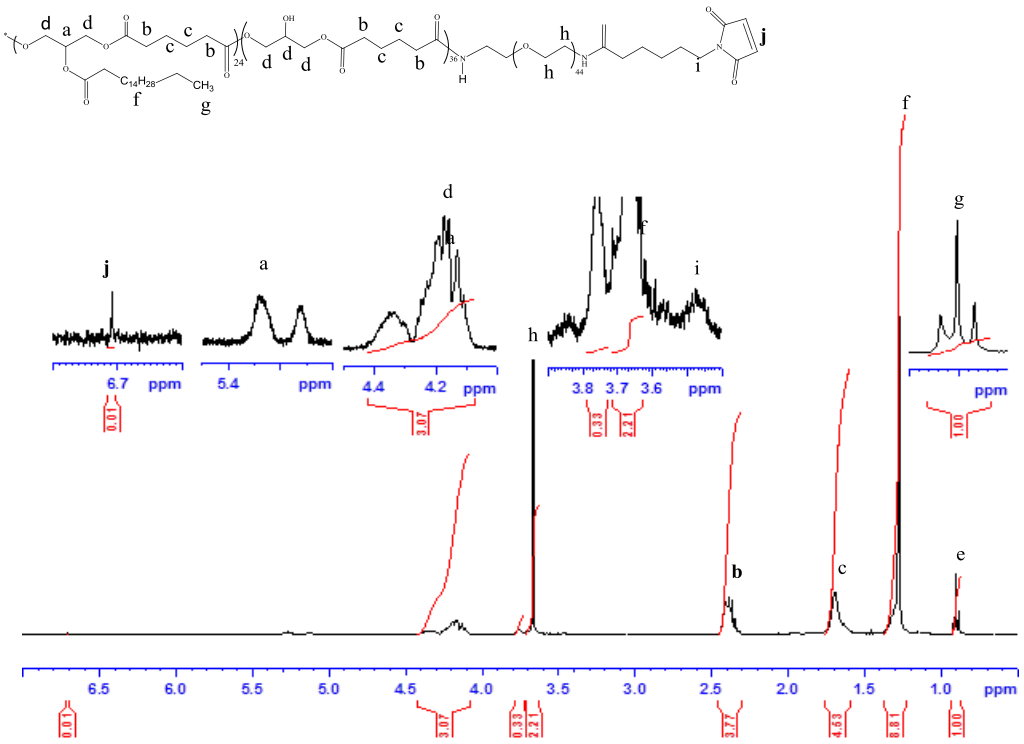

Figure 3.6. ^{1}H-NMR spectrum for 40%C_{18}-PGA-PEG-MIHA

The FTIR spectrum of 40%C_{18}-PGA-PEG-MIHA (Figure 3.7) showed that the sharp peak at 3323 cm^{-1} came from N-H stretching. The broad -OH band of PGA polymer at 3473 cm^{-1} still presented since acylation was not intended to be completed. In addition, there was a sharp peak around 1621 cm^{-1} assigned to O=C-N- in 40%C_{18}-PGA-PEG-

MIHA spectrum. It confirmed that NH_2 from PEG-MIHA was substituted to carboxylic acid of PGA polymer and created the newly amide bond.

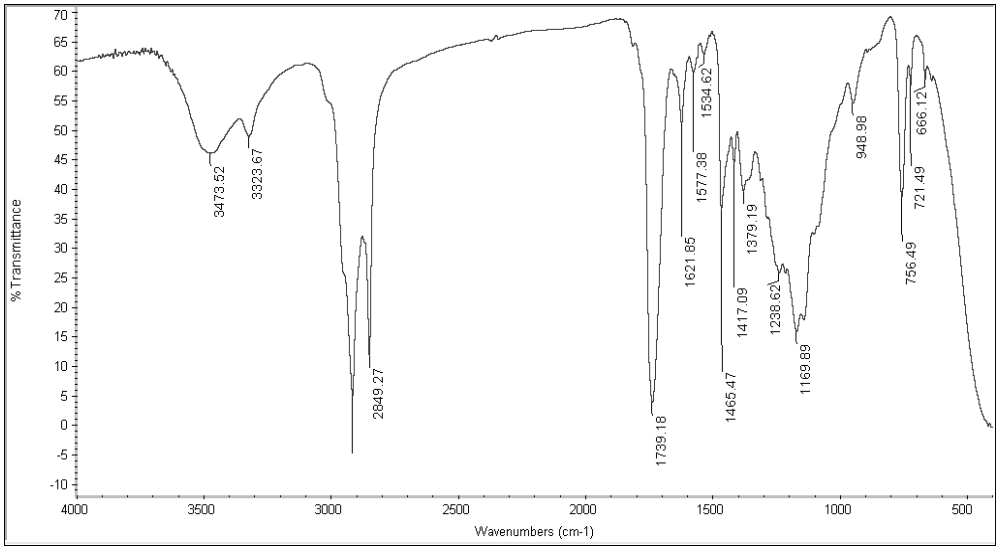

Figure 3.7. FTIR spectrum of N-maleimidohexanoyl diamino PEG (MIHA-PEG) coupled to 40%C_{18}-PGA (40%C_{18}-PGA-PEG-MIHA)

3.5. Preparation of Iminothiolane-modified collagen as ligand

Collagen was proposed as a ligand on the surface of MP for cell adhesion. Collagen, as ECM protein, provides structural support for cell growth and proliferation. Despite mediation by matrix glycoprotein, cells have an ability to attach directly to collagen through an integrin receptor on cell membrane [151-153]. In order to attach to 40%C_{18}-PGA-PEG-MIHA polymer, a thiol functional group must be present on collagen. Since free cysteine residues are not present on collagen, a thiol group was installed by reacting collagen with 2-iminothiolane (Traut's reagent) [154]. In this experiment, two molecules of thiol were attached to collagen.

Due to the small amount of 2-iminothiolane needed to attach with collagen, the amount of thiol group cannot be analysed by spectrophotometry. Therefore, it was estimated by Ellman's assay as described in Chapter 2, section 2.2.6.1. The amount of –SH group in preliminary studies was determined by using Ellman's reagent. The amount of thiol group was calculated using Equation 2-1 and plotting the absorbance at acetyl cysteine calibration curve (Figure 3.8). The calculation using both methods gave the same result for thiol group concentration in sample. According to the result from preliminary study, 2 molecules of thiol per mole of collagen can be obtained by reacting 200 nmole of 2-iminothiolane to 10 nmole of collagen (Table 3.1).

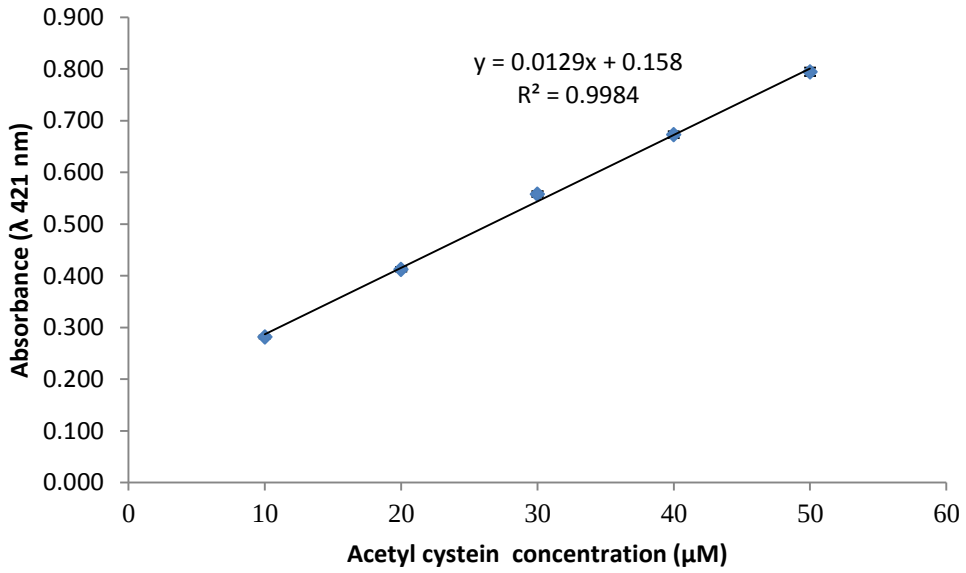

Figure 3.8. Acetyl cysteine calibration curve in Tris buffer. The calibration curve was created using standard concentration of acetyl cysteine ranging from 10 to 50 µM and reacted with Ellman's reagent. The absorbance was measured using spectrophotometer UV. All samples are taken triplicate and averages calculate.

Table 3.1. Calibration to estimate the amount of thiol group attached to collagen

Batch	Amount of Collagen (nmol)	Amount of Trauts added (nmol)	Amount of thiol group attached	Amount of thiol group per mol collagen
AS008DD	1	100	10	10
AS009DD	1	500	55	55
AS010DD*	10	200	≈20	≈2*

**) estimate amount of thiol group conclude from AS008DD and AS009DD.*

For the next stages of the experiments, fluorescein-5-isothiocyanate (FITC) needs to be reacted with collagen. The attachment of FITC is necessary in order to determine the amount of collagen attached to MP. Collagen was labelled by adding FITC (50 nmole) to 10 nmole collagen. The attachment of collagen with FITC and iminothiolane was carried out in consecutive reactions (Figure 3.9) and the procedure was described in Chapter 2, section 2.2.6.2. FITC was attached to proteins *via* primary amines in sodium carbonate buffer pH 9.5. Subsequently, after FITC reaction, the solution was adjusted to pH 8 for attachment of 2-iminothiolane to collagen as described in literature [155]. The reaction for 2-imnothiolane attachment was for 1 hour. The 2-iminothiolane reacts with primary amine to provide thiol group in the peptide. The purification of iminothiolane-modified-collagen-FITC was carried out by size exclusion chromatography using a PD-10 (Sephadex G-25) column. The amount of collagen was determined using Bradford method by plotting the absorbance at λ 595 nm to calibration curve of collagen (Figure 3.10). The amount of FITC attached to collagen was determined using equation 2-2 at λ 495 nm as described in Chapter 2. The FITC attached at ratio 4 to 1 collagen (Table 3.2).

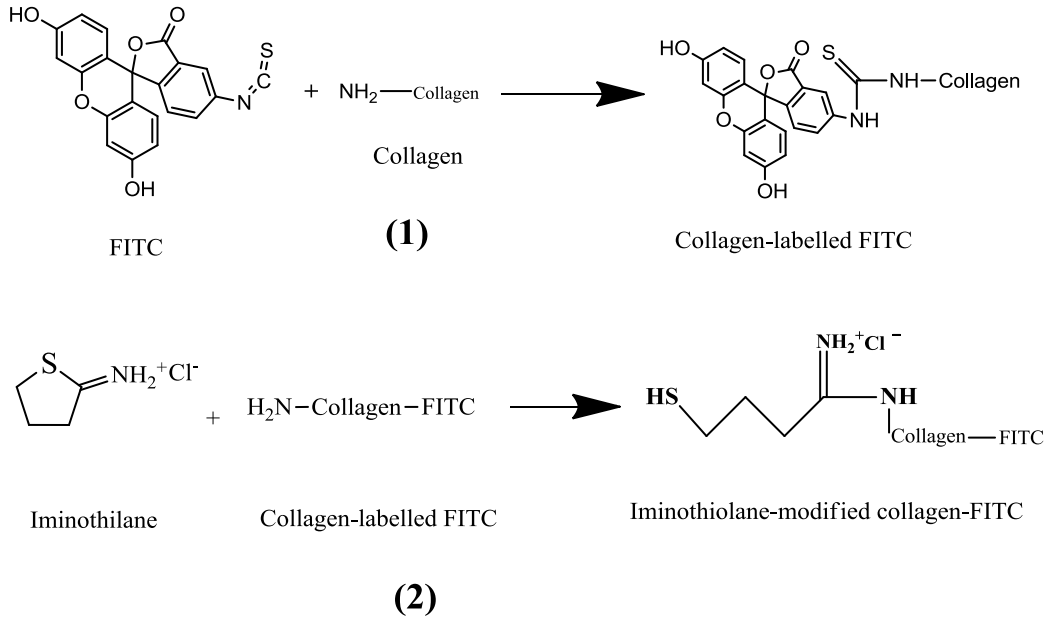

Figure 3.9. Collagen was modified with FITC and iminothiolane. FITC was attached for fluorescence (1) and iminothiolane was tethered to collagen to provide thiol group in collagen molecule (2).

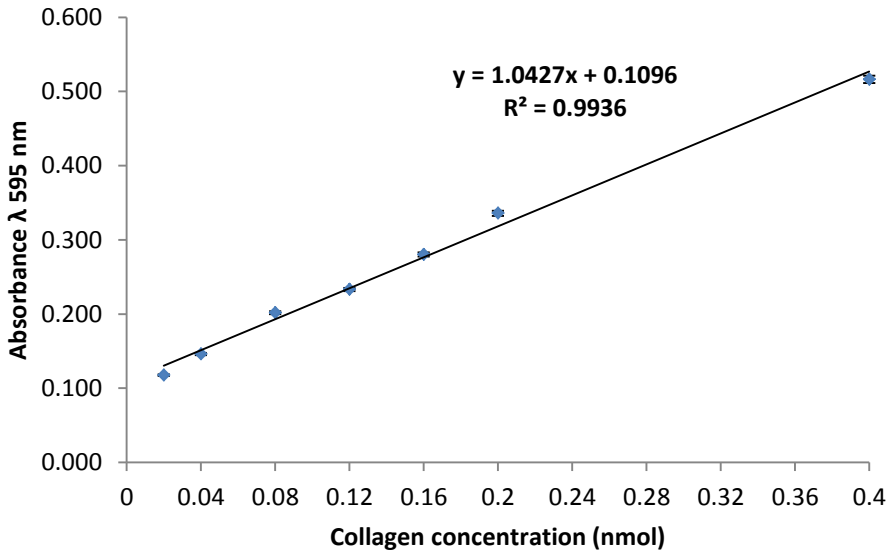

Figure 3.10. Collagen calibration curve in PBS. The calibration curve was created using Bradford method with known amount of collagen ranging from 0.02 to 0.4 nmol. The absorbance was measured using spectrophotometer UV. All samples are taken triplicate and averages calculate.

Table 3.2. The amount of FITC and collagen determined in iminothiolane-modified-collagen-FITC.

	Amount added (nmole)	Amount determined*) in iminothiolane-modified-collagen-FITC (nmole)±SD	Ratio
Collagen	10	7.07±0.89	1
FITC	50	27.88±0.09	4

*) Collagen was determined by measuring collagen absorbance with Bradford reagent at λ 595 nm while FITC was determined by measuring FITC absorbance at λ 495 nm and calculated using Equation 2-2.

In order to ensure that iminothiolane-modified collagen-FITC have an ability to attach to the cells, the fluorescence intensity of collagen attached to cells was evaluated using flow cytometry as described in Chapter 2 section 2.2.6.3. Fixed mouse embryonic stem (mES) cells were used in this experiment. The cells were mixed with a series of concentrations of iminothiolane-modified collagen-FITC for half an hour. Unbound modified collagen was removed from the cells by discarding the supernatant after centrifugation. The suspensions of cells attached with collagen in PBS+0.1% BSA were passed through the flow chamber of the flow cytometry. The amount of collagen attached to the cells was determined by the fluorescence intensity attached to each cell. The result from the flow cytometry showed that the amount of modified collagen attached to the cells increased proportionally with the amount of collagen added (Figure 3.11). The figure presented that collagen retained its ability for cells attachment although it had been modified by attaching FITC and iminothiolane onto its molecule. However, fluorescence intensity declined when more than 18 picomoles collagen was added. It indicated that the surface of the cells became saturated with collagen and was not able to interact any further.

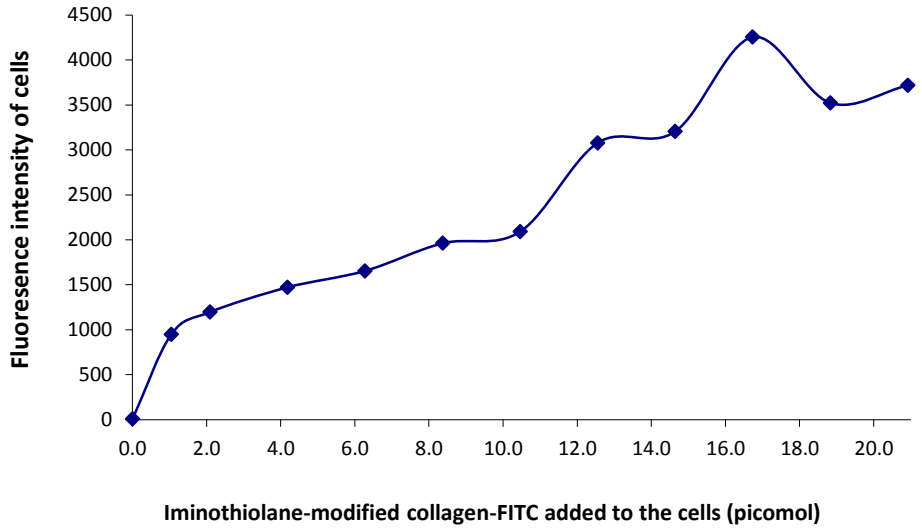

Figure 3.11. The fluorescence intensity of iminithiolane-modified-collagen-FITC attached to mES cell. The mES was fixed with 4% paraformaldehyde solution before attached with collagen. The $5x10^4$ mES cell was used to interact with the each amount of iminothiolane-modified-collagen-FITC. The fluorescence intensity was measured using flow cytometer at λemmision 495 nm and λexcitation 521 nm

3.6. Discussion

Acylation of PGA polymer backbone could be completed with pyridine as catalyst or without pyridine as described in Figure 3.12. Since the –Cl is a good leaving group, PGA substitution could be accomplished without pyridine. However, pyridine was involved in this reaction as acid scavenger [125]. In addition, pyridine was used as a nucleophile for stearoyl chloride ($C_{18}H_{35}OCl$). Pyridine donated a pair of electron on acyl chloride and provided active carboxyl group in stearoyl chloride, therefore became ready to attach with hydroxyl on polymer backbone. The acylation of PGA polymer was indicated by formation of acid fume. The reaction was carried out for 2 hours to ensure complete substitution of hydroxyl group on PGA polymer. The

substitution of hydroxyl group using pyridine resulted in a basic environment for the polymer solution. The hydrochloric acid (2M, 100 ml) was added to neutralize polymer solution in order to stop the reaction. The polymer solution was then obtained by extraction using dichloromethane. In previous study by Kallinteri *et al,* the substituted polymer was used without further purification. In this experiment, the excess of stearic acid (C_{18}) was removed by washing the substituted polymer with petroleum ether followed by drying the substituted polymer with nitrogen. The acyl substitution with stearoic acid also changed the physical characteristics of PGA polymer from sticky semisolid polymer to white waxy solid.

The percentage of acylation was calculated by comparing the methyl peak at δ 0.86 ppm assigned to the end of acid chains of C_{18} and the methylene peak near the carbonyl group at δ 2.36 ppm assigned to PGA. Since the peak intensities on those peaks related to the number of hydrogen presented on molecule, the percentage of C_{18} substitution could be determined. The percentage of substitution could not be determined using FTIR spectrum. FTIR presented the fingerprint of each molecules but it was not related to the amount of functional groups on molecules. However, the substitution of stearoyl molecule to PGA polymer could be confirmed by the disappearing peak of O=C-Cl at 1800 cm^{-1} and C-Cl from stearoyl chloride at 721 cm^{-1}. As the substitution reaction was controlled under dry condition, the disappearing of O=C-Cl and C-Cl band can be used to confirm acyl substitution to PGA polymer. The hydroxyl group on PGA polymer still appeared at 3472 cm^{-1} since not all of hydroxyl group on PGA intended to be substituted by C_{18}.

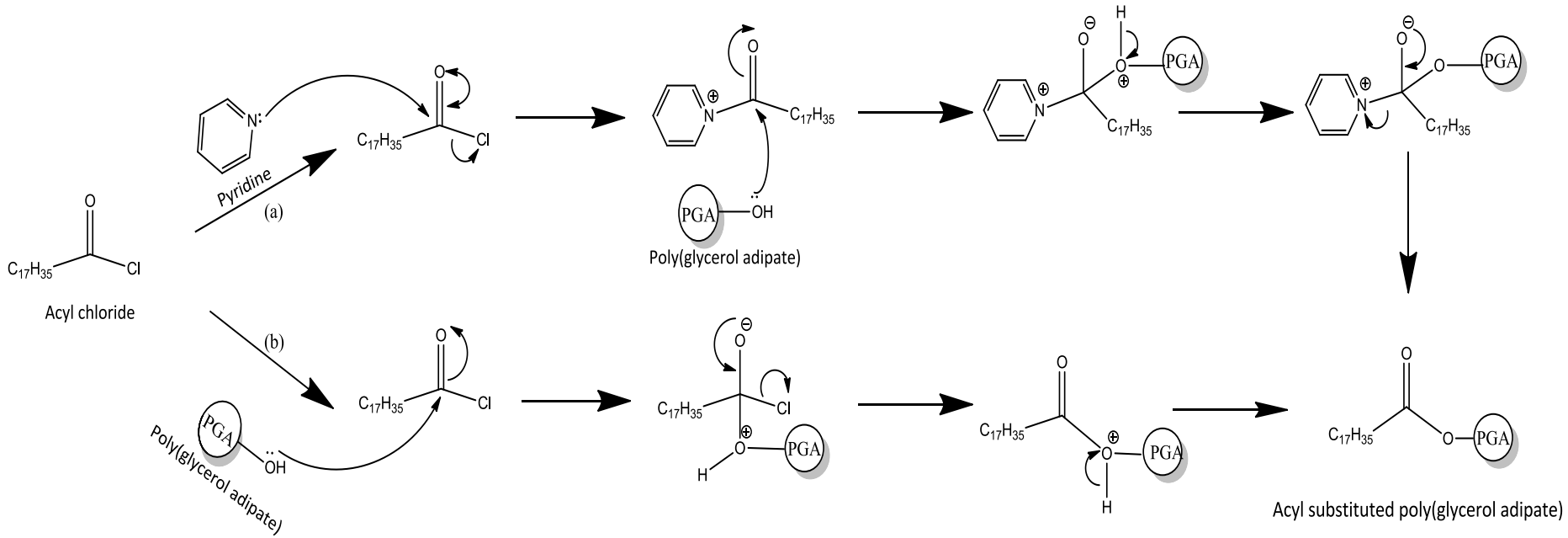

Figure 3.12. Proposed reaction mechanism of stearoyl acid substitution on hydroxyl groups of PGA polymer catalyzed by pyridine (a) and without pyridine (b).

Further modification on PGA polymer is attaching PEG-maleimide (MIHA-PEG-NH_2) linker to the polymer backbone. The amide formation on both MIHA-PEG-NH_2 linker and 40%C_{18}-PGA-PEG-MIHA were mediated using coupling agents, DCC and NHS. DCC and NHS are effective coupling agent to create amide linkage molecules [150, 156]. The DCC is widely used to create amide bond in peptide synthesis as reported by Han and Kim (2004). This carbodiimide coupling agents categorized as low cost and mild coupling reagents in peptide synthesis. The by-product from DCC is not dissolved in solvents, therefore it is easy to separate by filtration. However, since it produces insoluble by-product, DCC not suitable for polypeptides synthesis as it is difficult to separate from the product [157].

The carboxylic acid functional group on the end of PGA chain reacted with DCC to produce an intermediate product O-acylisourea and then reacted with NHS to form a stable-amine-reactive NHS-ester. The NHS-activated species was then ready to couple with the amine nucleophiles leading to amide bond formation (Figure 3.13) [156, 158, 159]. The MIHA-PEG-NH_2 attachment to the 40%C_{18}-PGA would be useful to prevent aggregation of MP. Since MIHA-PEG-NH_2 linker attached to the 40%C_{18}-PGA prior to microparticle fabrication, the PEG chain will present in the bulk of MP and oriented to aqueous phase leading to the formation of enriched PEG microparticle [130]. Thus, the maleimide functional group would be effectively attached with ligand on the surface of microparticle. Instead of attachment in bulk polymer, the PEG linker attachment could also be achieved by attaching the PEG linker to preformed microparticle as studied by Madani *et al* (2007). Madani *et al* demonstrated PEG attachment to preformed microparticle using DCC and NHS as coupling agents [160]. However, this technique may lead to incomplete PEG

attachment on the surface microparticle leaving PEG-unprotected microparticle surface.

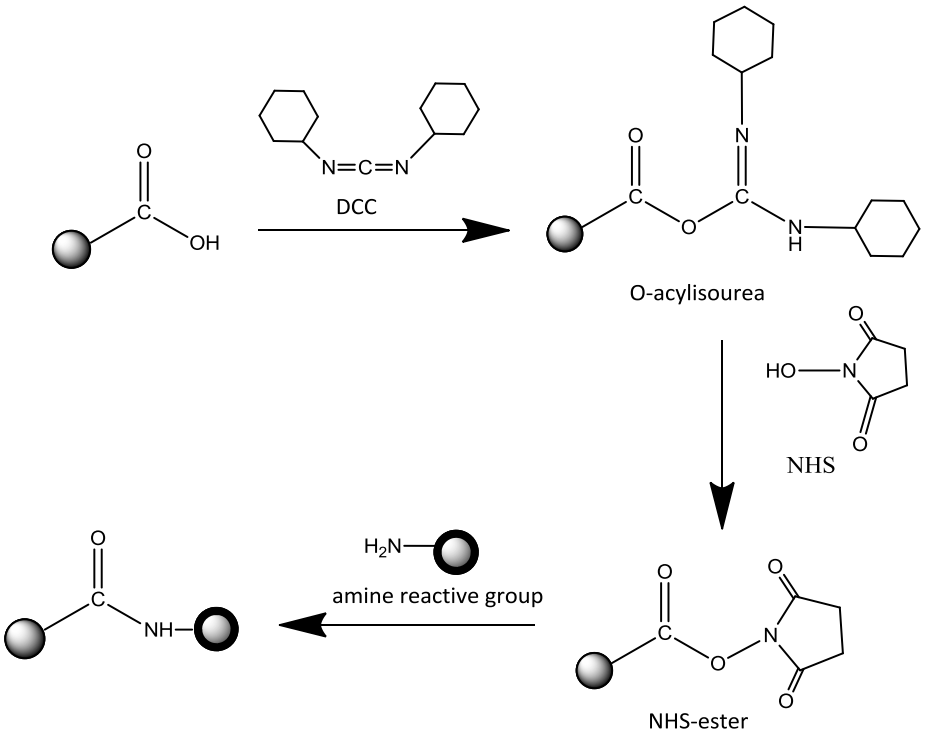

Figure 3.13. The carboxylic group was converted to active intermediate by DCC and then reacted with NHS to form stable-amine-reactive NHS-ester. The nucleophilic of amine group attacked to NHS-ester to form an amide bond [158, 159].

Amide formation on both on MIHA-PEG linker and 40%C_{18}-PGA-PEG-MIHA can be identified using FTIR by the sharp peak in area 1620-1630 cm^{-1}. While, the ratio of each component in coupling reactions could be identified using ^{1}H-NMR spectrum. The single peak of $–CH_2$ on maleimide ring (δ 6.7 ppm) is a specific peak to calculate ratio of coupling diamine PEG to MIHA and coupling MIHA-PEG-NH_2 to 40%C_{18}-PGA.

Collagen was modified by attaching with 2-iminothiolane and FITC for further experiments. The attachment of 2-iminothiolane on collagen molecule gave a thiol

functional group, while FITC acted as a labelling agent on collagen molecule. Both of the reactants were attached to collagen through primary amine of lysine on the collagen molecule. However, the conditions for the two consecutive reactions were different. The optimum pH for isothiocyanate conjugation was 9.5 while the optimum condition of for 2-iminothiolane conjugation was at a pH below 9 [155, 161]. In this experiment, the 2-iminothiolane conjugation was carried out at pH 8 in room temperature. This condition was adopted from Jue *et al* (1978) who successfully demonstrated the conjugation of 2-iminothilane to 30S ribosome at pH 8 in room temperature (22°C). The 2-iminothiolane could also be attached to macromolecule, such as human serum albumin (HSA) under the similar condition (pH 8.5) as demonstrated by Langer *et al* (2000). The iminothiolane-labelled HSA nanoparticle had specific interaction with maleimide-activated avidin. However, amount of sulfhydryl group attached to HSA nanoparticle reduced after four weeks of preparation due to an oxidative formation of disulfide cross-links during storage [162]. Therefore, iminothiolane-modified collagen should be prepared freshly prior to use to avoid the degradation of thiol active group.

After modification, iminothiolane-modified collagen-FITC still maintained its ability to interact with cells since only 4 molecules of FITC and 2 molecules of 2-iminothiolane attached to the collagen. However, there was a maximum amount of collagen to interact with cell. The surface of cell would be saturated with collagen in certain concentration. In this experiment, the surface of cells reached saturation on the concentration 18 picomole of collagen for 50,000 cells. Consequently, in a further addition of collagen, the molecule was not able to interact with the surface of cell.

3.7. Conclusion

A 40% substitution of C_{18} on PGA polymer backbone was effectively catalysed with pyridine as a nucleophile for acyl chloride. In addition, further purification on 40%-C_{18}-PGA was established to remove the free stearoyc acid from substituted PGA. The percentage of acyl substitution was mainly identified by ^{1}H-NMR spectrum instead of using FTIR spectrum. However, FTIR could be used to identify the main functional group prior to substitution. Although percentage of stearoyl substitution from several batches not exactly reached 40% substitution, but it is acceptable to provide lipophilic environment for encapsulation of hydrophobic drug.

The amide linkage on MIHA-PEG-NH_2 and 40%C_{18}-PGA-PEG-MIHA was successfully formed using combination of DCC and NHS as coupling agent. The ratio of diamine PEG attached to *N*-maleimidohexanoic acid was determined by ^{1}H-NMR spectrum while the amide bond formation was identified using FTIR spectrum. However, the identification using ^{1}H-NMR spectrum was facing difficulties for analysis of 40%C_{18}-PGA-PEG-MIHA due to small intensities of important peaks on the spectrum. The amide linkage formation on 40%C_{18}-PGA-PEG-MIHA was clearly determined based on FTIR spectrum.

The immobilized thiol group on collagen molecule was provided by attaching iminothiolane to collagen at pH 8. The FITC molecule was also successfully attached to collagen for further cell experiment. Although it has been modified by attaching 2-imiothiolane and FITC, the iminothiolane-modified collagen still maintained its ability to interact with the surface of cell. The interaction of iminothiolane-modified

collagen with cells reached saturation at a certain concentration indicated by inability of collagen to attach to cells.

CHAPTER 4

4. MICROPARTICLE PREPARATION AND CHARACTERISATION

4.1. Introduction

Microparticles (MP) can be applied to tissue engineering for encapsulation of bioactive molecules and delivery active molecules to the cells. In addition, MP may act as supporting matrices to help form three dimensional (3D) structures with cells [35]. Controlled release of bioactive molecules can be tailored during the MP formulation processes and the method of MP formulation can be selected based on the characteristics of polymers used to form the MP and the bioactive molecules to be encapsulated. Several techniques have been introduced to generate MPs such as emulsification, polymer phase separation (coacervation), spray-drying and supercritical fluid.

Among those methods of MP preparation, the emulsification method is commonly used at the laboratory scale due to relative ease of processing [36, 163]. In this method, the polymer is dissolved in a suitable organic solvent and added to the aqueous external phase. The two immiscible solvents will perform a stable emulsion with the presence of emulsifier in the aqueous phase. As the organic solvent is evaporated, the MP will precipitate. The MP can be then collected by centrifugation followed by washing steps in ultrapure water and freeze drying [86, 88, 163].

The type of emulsion method, single emulsion or double emulsion, is selected depending on the solubility of the bioactive compound in the aqueous phase. An oil in water (O/W) emulsification process can be used to encapsulate hydrophobic drugs within the MP, while water-oil-water (W/O/W) emulsification process can be applied for hydrophilic drugs [88, 90]. Simvastatin (SIM) and dexamethasone phosphate (DXMP), as bioactive molecules for inducing bone formation, will be encapsulated within functionalized poly(glycerol adipate) (PGA) MP. Simvastatin (SIM), developed as a cholesterol lowering drug, has also been shown to have anabolic effects on bone tissue stimulating osteoblastic activity and mineralisation of bone matrix [55, 74-76]. Simvastatin may act as a stimulator of BMP2 expression in murine osteoprecursor cells at early stage of cell culture [75]. Dexamethasone phosphate (DXMP) is a corticosteroid and has been shown stimulate bone formation and mineralisation by stimulating transcription of osteoblast-specific genes [71-73]. *In vitro*, DXMP delivery by a polymer gel increased osteogenic differentiation of mesenchymal stem cells (MSCs) as suggested by increasing activity of alkaline phosphatase enzyme, osteopontin and core binding factor alpha expression [73].

Due to the hydrophobicity of SIM, oil-in-water (O/W) emulsification process was used to prepare modified PGA MP containing SIM. However, emulsification process had been modified to encapsulated water soluble drug, DXMP. Double emulsion, water-oil-water (W/O/W), is used to prepare MP containing DXMP. An emulsifier, poly(vinyl alcohol) (PVA) was used to reduce surface tension of immiscible phase during emulsification process and increase the stability of emulsion [164]. The manufacturing MP without surfactant was done using solvent displacement method.

In this method, organic solvent containing polymer is emulsified with the aqueous external phase and then precipitated followed by diffusion of organic solvent to aqueous medium. A water-miscible solvent normally used in this method in order to perform spontaneous emulsification. Fast diffusion of the organic solvent results in the formation of a colloidal suspension. Particles are then generated by removal of organic phase and aqueous phase through evaporation. [165, 166].

Modified PGA polymer with 40% stearoyl substitution (40%C_{18}-PGA) and 40%C_{18}-PGA with MIHA-PEG-NH_2 linker (40%C_{18}-PGA-PEG-MIHA) was used for formation of biodegradable MP and mixing with cells to promote 3D assembly of cells. Kallinteri *et al.,* (2005) showed that 40% stearoyl substitution on PGA polymer backbone increased the encapsulation efficiency of DXMP within PGA nanoparticles. The encapsulation efficiency of DXMP within 40%C_{18}-PGA nanoparticles reached 35-38% compare to un-substituted PGA [125]. In MP preparation, physicochemical properties of the active compound and critical factors such as polymer concentration, ratio dispersed phase to continuous phase, and concentration of emulsifier during manufacturing process affected encapsulation efficiency, physical characteristics of MP and release of drug from MP [164, 167]. Moreover, attachment of MIHA-PEG-NH_2 linker to PGA polymer will significantly affect the chemical properties of PGA and might affect the physical characteristics and encapsulation efficiency of MP overall.

The aim of this chapter was to evaluate the influence of critical factors during manufacturing process of MP prepared from modified PGA polymers in terms of MP size and size distribution, surface charge, encapsulation efficiency and drug release.

Furthermore, the ability of MP to be attached with iminothiolane-modified collagen was also investigated.

4.2. Particle Size

In order to promote the formation of 3D cells matrices, the size of MP should meet the requirement of matrices for cells in tissue engineering. The size should be small enough to be incorporated within the cell aggregate but not to be taken up by the cells. These requirements are important to maintain integrity of 3D constructs of the cells for tissue replacement. The size of particle that would be taken up through endocytosis, including phagocytosis, is varying from nanoscale up to 10 µm and also depends on physicochemical properties of the particle [168-170]. Wang *et al* (2010) explained that the optimum diameter of gold nanoparticle for being up taken by HeLa cells is around 45 nm and the efficiency of endocytosis reduces related to the increasing size of particle [171]. The critical factors that affected the size of MP are chemical properties of modified PGA polymers, properties of encapsulated drug, homogenisation speed during manufacturing process and concentration of PVA as emulsifier.

4.2.1. Effect of polymer type

The size of modified PGA MP is influenced by chemical properties of the polymer. To investigate the effect of PEG attachment on particle size, MPs were prepared by emulsification process with 2.5% PVA as emulsifier as described in Chapter 2 section 2.3.2.1. The sizes of MP are shown in Figure 4.1. The mean particle diameters prepared from 40%C_{18}-PGA and 40%C_{18}-PGA-PEG-MIHA were 9.0 ± 1.63 and 5.0 ±

0.50 µm, respectively. It showed that attachment of MIHA-PEG-NH_2 linker to PGA polymer exhibited the smaller particle size than the one without the linker.

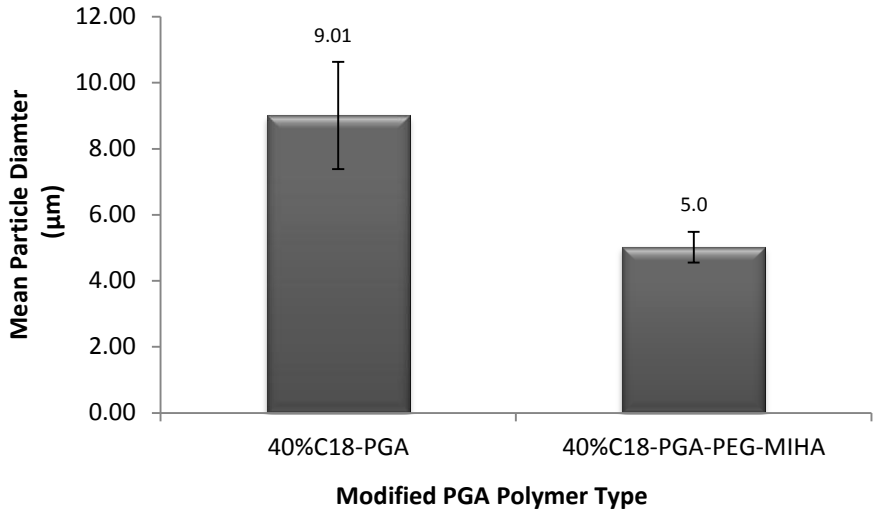

Figure 4.1. Size of microparticles prepared from modified PGA polymer. Microparticles were prepared using emulsification method with 2.5% PVA as emulsifier. The mean diameter was taken from different batches of MP (n=3). Bars represent SEM.

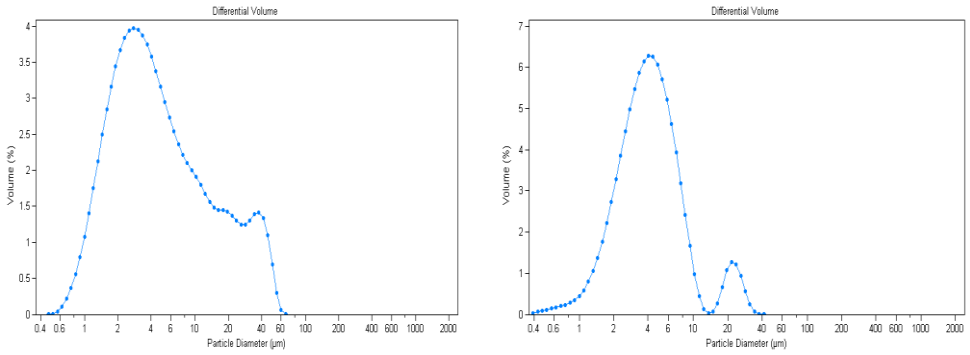

a) 40%C_{18}-PGA **b) 40%C_{18}-PGA-PEG-MIHA**

Figure 4.2. Particle size distribution of MP prepared from 40%C_{18}-PGA (a) and 40%C_{18}-PGA-PEG-MIHA (b) using emulsification method with PVA 2.5% as emulsifier.

The size distribution of particles showed bimodal poly-dispersed MP with diameter ranging from 0.4 µm to 60 µm (Figure 4.2). The bimodal peak on particle size distribution revealed that the aggregation of particle was occurring. MP prepared from 40%C_{18}-PGA showed a positively skewed population with high population of MP below 6 µm. In contrast, MP prepared from 40%C_{18}-PGA-PEG-MIHA displayed normal distribution, with the mean diameter at the highest population of MP. Microparticle prepared from 40%C_{18}-PGA-PEG-MIHA polymer exhibited narrow size distribution compared with the MP prepared from 40%C_{18}-PGA, indicating a smaller variation on particle size for 40%C_{18}-PGA-PEG-MIHA MP.

4.2.2. Effect of homogenizer speed

Particle size is also affected by the speed of the stirrer used during the manufacturing process. In this method, control of homogenisation speed was applied both during the formation of primary emulsion and mixing with PVA solution. Figure 4.3 presents the effect of homogenizer speed on particle size. Increasing homogenizer speed reduced the particle size. This result was seen for both MPs prepared from 40%C_{18}-PGA and 40%C_{18}-PGA-PEG-MIHA. Increasing homogenizer speed related to the formation of finer droplet of emulsion, so the smaller particles were formed [167, 172].

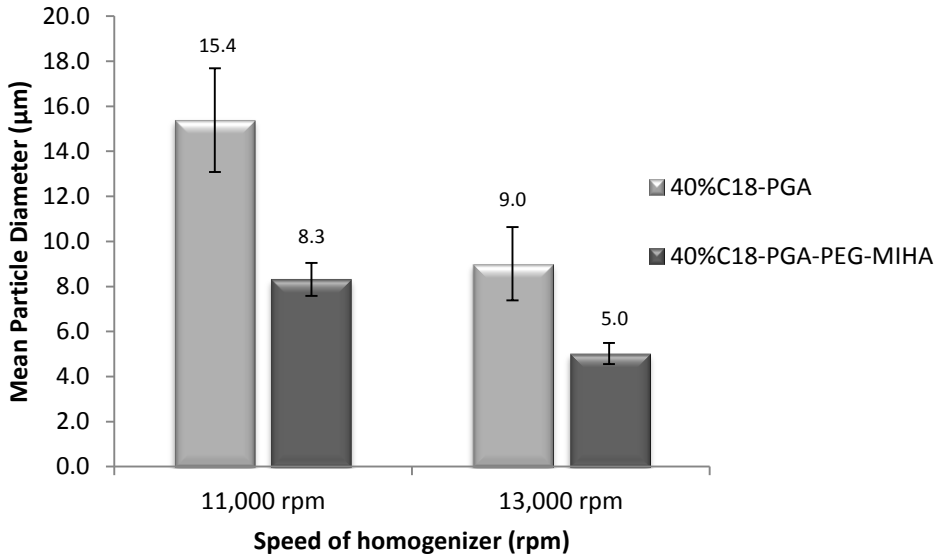

Figure 4.3. Effect of homogenizer speed on size of microparticles prepared from 40%C_{18}-PGA and 40%C_{18}-PGA-PEG-MIHA. Microparticles were prepared using emulsification method with PVA 2.5% as emulsifier. The mean was taken from different batches of MPs (n=3). Bars represent SEM.

4.2.3. Effect of PVA concentration

The size of particle is not only influenced by polymer type and speed of homogenizer during manufacturing process, but is also affected by concentration of surfactant used in preparation. Use of PVA as emulsifier act as a tensio active molecule to reduce interfacial tension between organic and aqueous phase [167]. The effect of emulsifier concentration on particle size was investigated in preparation of MP from 40%C_{18}-PGA.

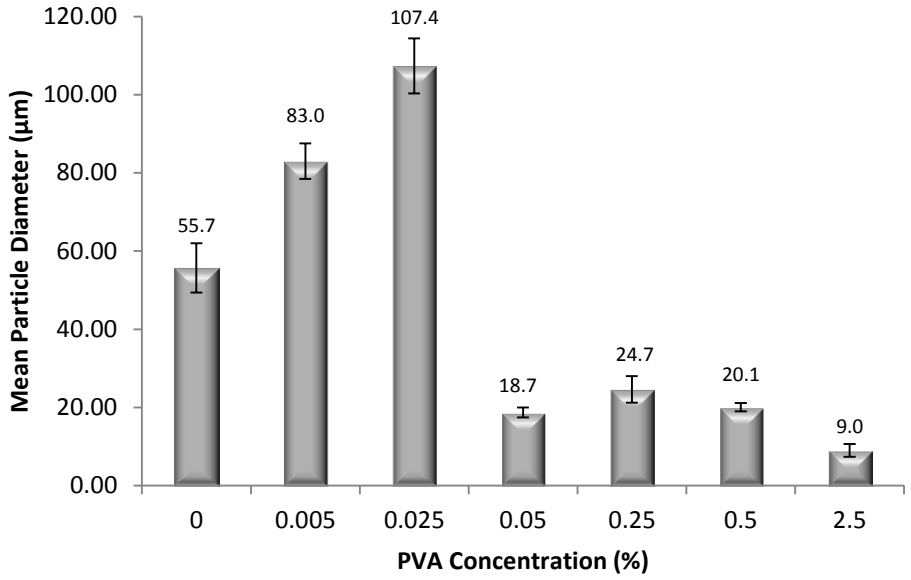

Figure 4.4. Effect of PVA concentration on the size of microparticles prepared from 40%C_{18}-PGA polymer. The mean diameter was taken from three different batches of MP except for PVA 2.5% which was taken from seven different batches. Bars represent SEM.

Figure 4.4 illustrates the effect of PVA concentration on particle size. The MP exhibited a bigger particle size as the concentration of PVA increased from 0.005 % to 0.025%. However, the higher concentration of PVA used (above 0.05%) led to significantly smaller particle size. There is no significant difference on particle size of MPs prepared with PVA concentration 0.05 % to 0.5 % ($p > 0.05$, n=3).

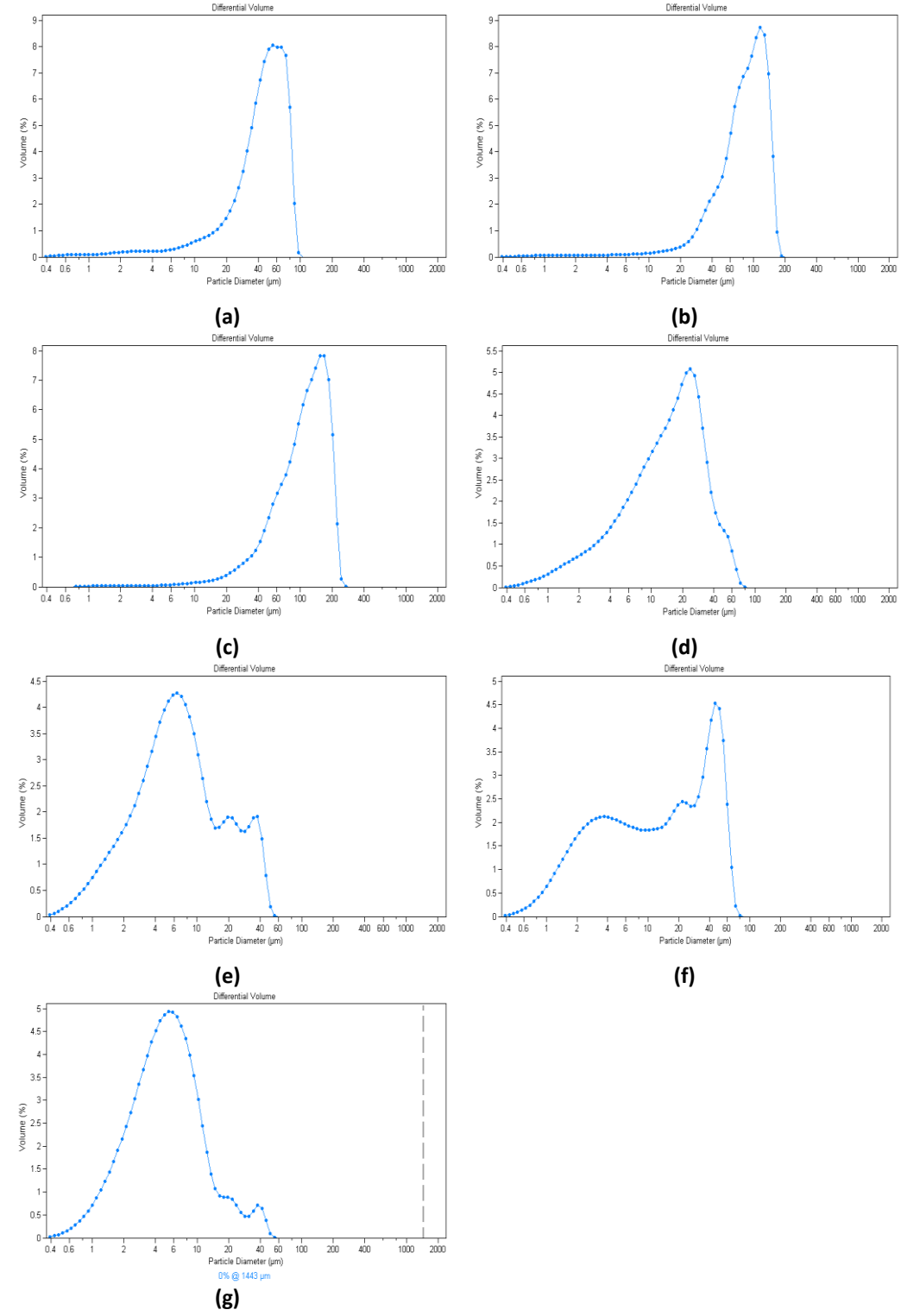

Figure 4.5. Particle size distribution of 40% C_{18}-PGA MPs prepared using emulsification method with PVA (a) 0%, (b) 0.005%, (c) 0.025%, (d)0.05%, (e)0.25%, (f)0.5% and (g) 2.5%.

The particle size distributions were also affected by concentration of PVA used in MP preparation as seen in Figure 4.5. The poly-dispersed particle distribution with negatively skewed distribution was seen with MP without PVA and with PVA 0.005% and PVA 0.025%. Negatively skewed distribution indicated coarser particles had been produced. Increasing PVA concentration to 0.05% shifted the distribution of MP to a more positive skewed distribution, indicating that finer particles had been produced above a critical minimum amount of emulsifier. In contrast, with PVA at a concentration of 0.25 % and above revealed multimodal size distribution with positively skewed distribution except for the MP prepared with PVA 0.5%.

The effect of PVA as emulsifier on particle size was also investigated on MP prepared from 40%C_{18}-PGA-PEG-MIHA. However, due to limited amount of the 40%C_{18}-PGA-PEG-MIHA polymer, the effect of PVA concentration on particle size was only investigated in PVA 0.005% and PVA 2.5% (Figure 4.6).

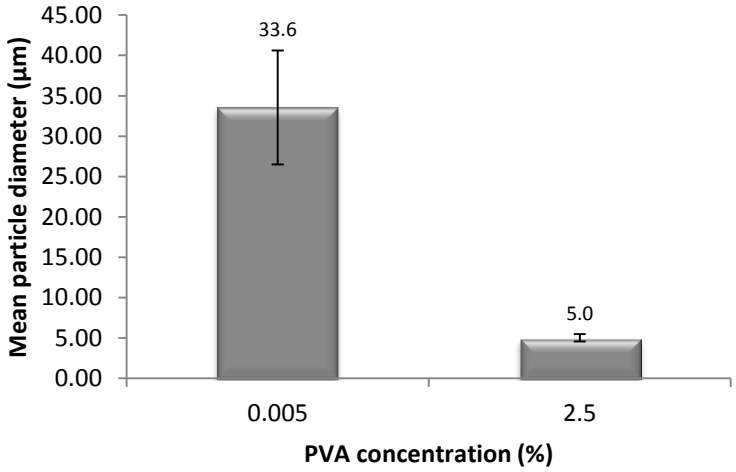

Figure 4.6. Effect of PVA concentration on the size of microparticles prepared from 40%C_{18}-PGA-PEG-MIHA. Emulsification method was used to prepare the microparticles. The mean diameter was taken from different batches of MP (n=3). Bars represent SEM.

Figure 4.6 shows the higher concentration of PVA in MP prepared from 40%C_{18}-PGA-PEG-MIHA produced a smaller diameter of MP. The size of particle prepared with PVA 0.005 % was 6 fold bigger than particle prepared with PVA 2.5%. Furthermore, a higher PVA concentration used to prepare MP from 40%C_{18}-PGA-PEG-MIHA shifted the size distribution from negatively skewed bimodal curve to the normal distribution of particle (Figure 4.7).

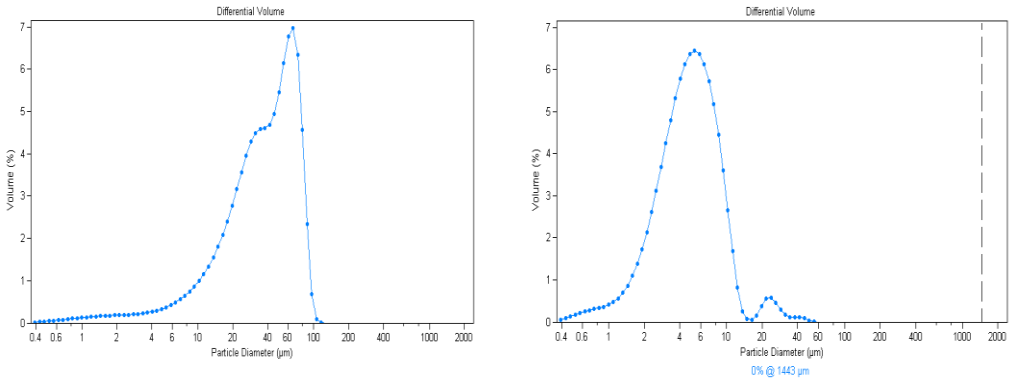

a b

Figure 4.7. The particle size distributions of 40% C_{18}-PGA-PEG-MIHA MP prepared using emulsification method with (a) 0.005%, (b) 2.5% of PVA.

Comparing the effect of PVA concentration to particle size in 40%C_{18}-PGA and 40%C_{18}-PGA-PEG-MIHA MPs, an increasing PVA concentration generated the fine particle size for MP prepared from 40%C_{18}-PGA and 40%C_{18}-PGA-PEG-MIHA (Figure 4.8). The increasing PVA concentration contributed more impact to reduce particle size in 40%C_{18}-PGA MP. By increasing PVA concentration to 2.5%, the 40%C_{18}-PGA could generate particles with a diameter almost one tenth of that produced with PVA 0.005%. However, increasing the PVA concentration from 0.005% to 2.5% in MP preparation from 40%C_{18}-PGA-PEG-MIHA resulted in only reduced particle size to one sixth.

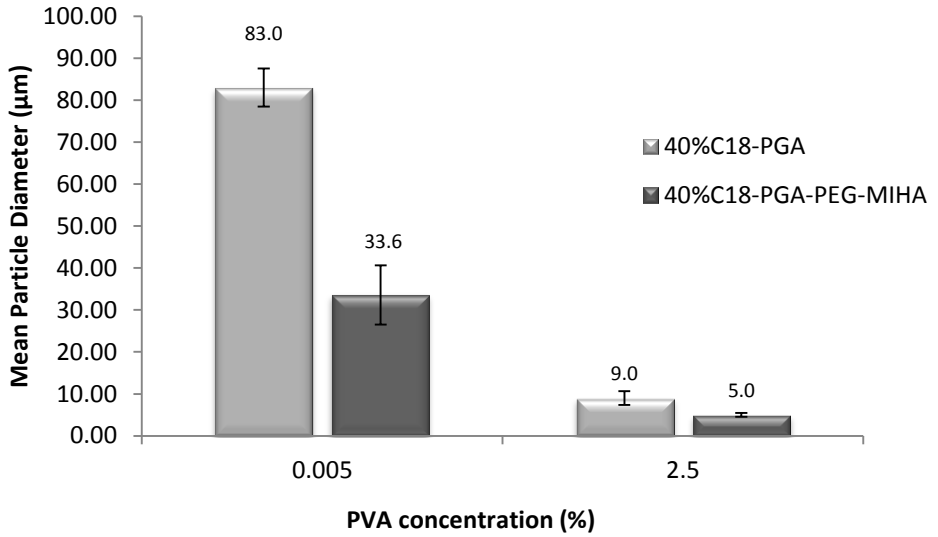

Figure 4.8. Effect of PVA concentration on size of microparticles made from modified PGA polymer. The mean diameter was taken from three different batches of MP except for MP prepared from 40%C_{18}-PGA with PVA 2.5% (n=7). Bar represents SEM.

4.3. Zeta Potential

Zeta potential of empty microparticles from modified PGA polymer was determined in order to investigate the effects of acylation, PEG attachment and ligand attachment on MP properties. Empty particles were produced using the method described in Chapter 2 section 2.3.2.1 without any drugs encapsulated. Empty MP from unsubstituted PGA was produced as a reference to evaluate effect of polymer modification on zeta potential. Since the yield of MP produced from unsubstituted PGA was not sufficient and physically sticky, the other characterisations such as particle size, SEM image and encapsulation efficiency were not applied with unsubstituted PGA MP.

Table 4.1 shows zeta potentials of modified PGA polymer in 1 mM HEPES buffer pH 7. The unsubstituted PGA MP exhibited negative zeta potential, which is related to the carboxyl group at the end of polymer chain. The 40% stearoyl substitution on pendant hydroxyl group of PGA backbone shifted the zeta potential of 40%C_{18}-PGA MP to lower negative value than unsubstituted PGA MP, while 40%C_{18}-PGA-PEG-MIHA MP revealed a higher negative value of zeta potential compared to zeta potential of 40%C_{18}-PGA MP.

Table 4.1. Zeta potentials of modified PGA microparticles in 0.1 mM HEPES buffer pH 7. The measurement was taken from different batches of microparticles (n=3)

Type of Microparticle	Zeta potential (mV)±SD
Unsubstituted PGA	-27.2 ± 3.00
40%C_{18}-PGA	-18.3 ± 1.60
40%C_{18}-PGA-PEG-MIHA	-25.2 ±2.19
40%C_{18}-PGA-PEG-MIHA + collagen	-20.1 ± 1.30

Zeta potential relates to the electrical charge of MP in liquid systems. The zeta potential determined the potential difference between the surface of MP and the aqueous medium. Therefore, attachment of collagen as a ligand on the surface of 40%C_{18}-PGA-PEG-MIHA resulted in a significant reduction in zeta potential of the MP compared to the MP without iminothiolane-modified collagen attachment ($P < 0.05$, n=3).

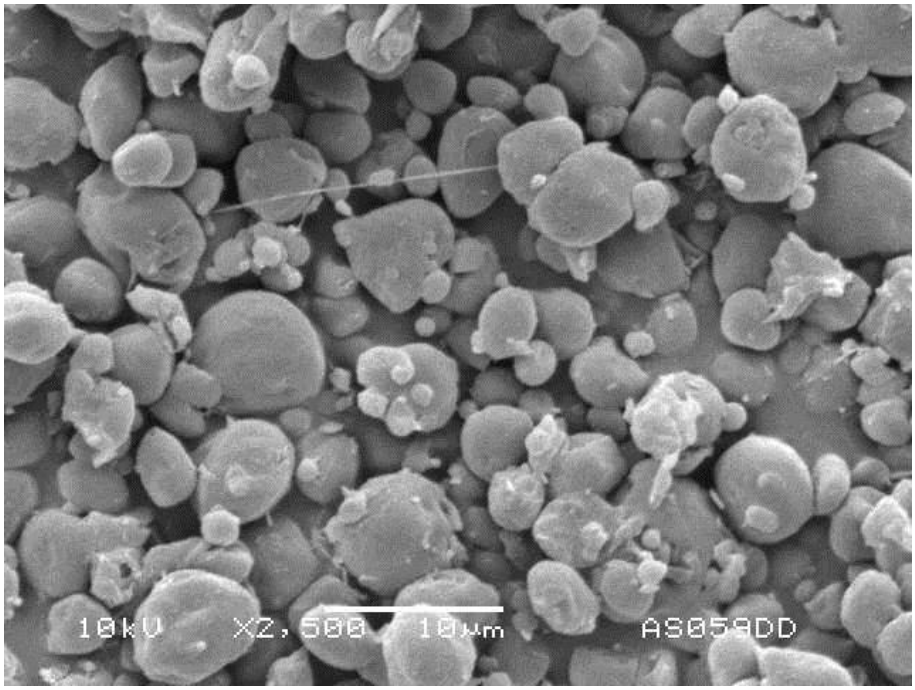

a) 40%C_{18}-PGA MP

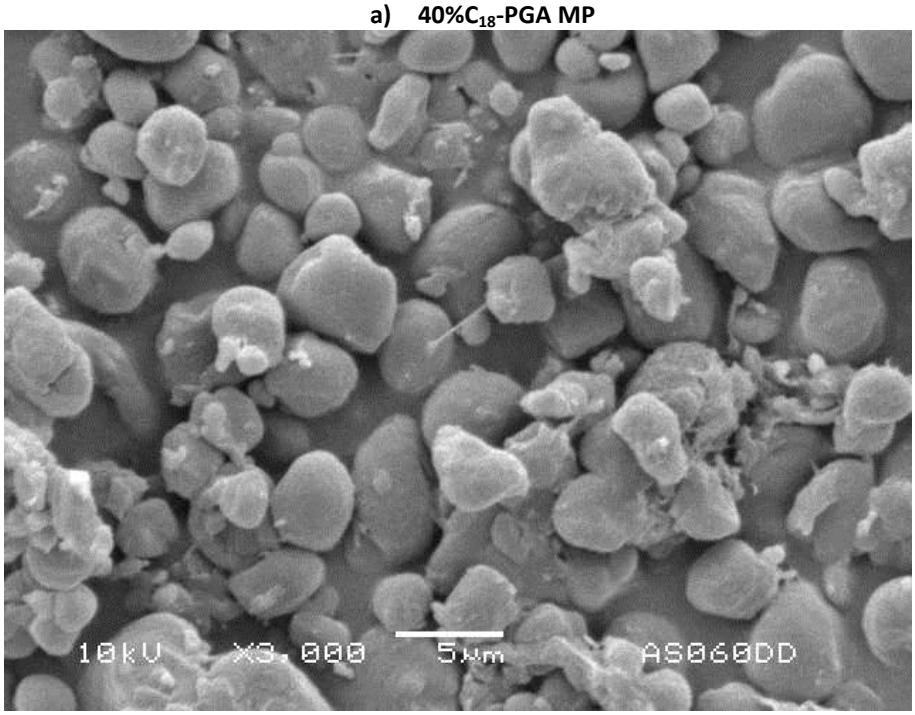

b) 40%C_{18}-PGA-PEG-MIHA MP

Figure 4.9. Scanning Electron Microscope images of microparticles prepared from modified PGA polymer using emulsification method with PVA 2.5% as emulsifier.

4.4. Scanning Electron Microscope Images

Scanning electron microscope images were obtained to assess the shape of MP prepared from modified PGA polymers. The empty MP without drug were prepared using emulsification method with PVA 2.5% as surfactant. The MP prepared from both 40%C_{18}-PGA and 40%C_{18}-PGA-PEG-MIHA exhibited poly-dispersed particles with smooth surfaces and non-spherical shape. However, the 40%C_{18}-PGA-PEG-MIHA MP showed a more homogenous and smaller size compared to 40%C_{18}-PGA MP. Figure 4.9 showed that aggregation had occurred in MP prepared from both polymers.

4.5. Encapsulation Efficiency

Dexamethasone phosphate (DXMP) and SIM were used as drug molecules to be incorporated within modified PGA MPs. In the initial studies, the double emulsion method was used to incorporate DXMP into modified PGA MP, while single emulsion method was used to generate modified PGA MP containing SIM. Poly(vinyl alcohol) (PVA) was used for emulsification in these processes. Several critical factors relating to encapsulation efficiency of drugs within MPs were investigated such as, volume ratio of inner phase (O/W) to perform primary emulsion, concentration of PVA as emulsifier and concentration of polymer in organic phase.

The drug loading and encapsulation efficiency was determined using indirect and direct methods. The indirect method determined the amount of free drug in supernatant and the result was confirmed with a direct method. In the direct method, the drugs were extracted with appropriate solvent prior to analysis by HPLC. Validation of drug extraction is needed in order to obtain adequate data from direct method.

The extraction of DXMP from MP was carried out using various combinations of dichloromethane (DCM) and water as solvents as stated in Chapter 2, section 2.3.4.2. A known amount of DXMP was added to 40%C_{18}-PGA polymer and homogenized. The DXMP was then extracted from the polymer using various combinations of DCM and water. The amount of DXMP extracted was determined using HPLC to calculate efficiency of extraction. The concentration of DXMP was calculated by plotting the peak area obtained to DXMP calibration curve in Figure 4.10. The water phase was also analysed to determine DXM, a possible degradation product of DXMP. The calibration curve of DXM is presented in Figure 4.11.

(A)

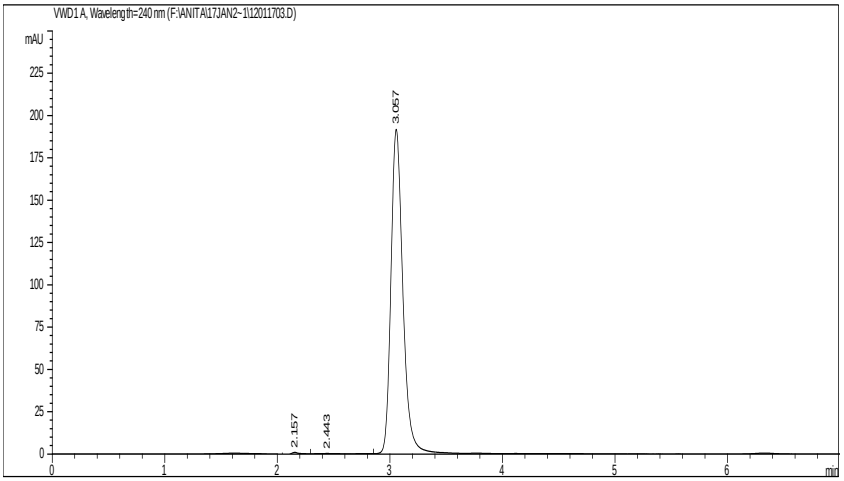

(B)

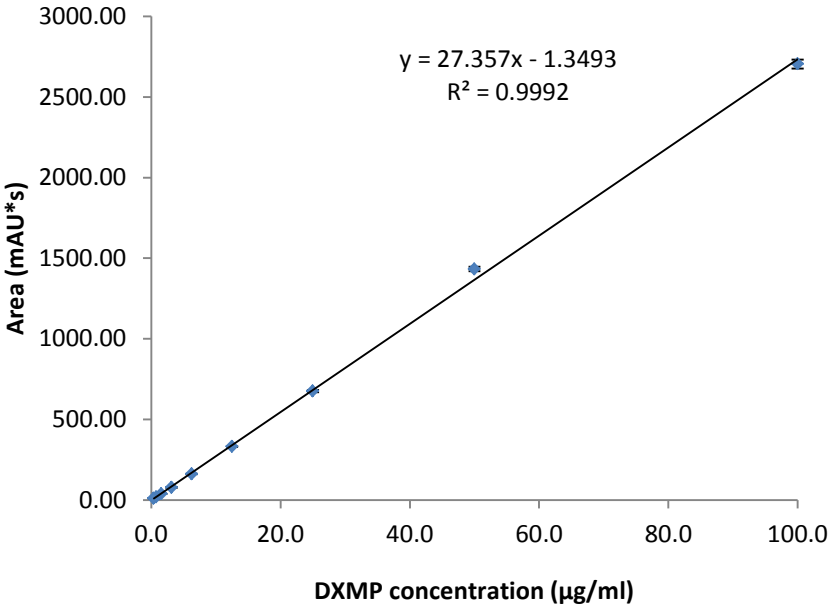

Figure 4.10. HPLC analysis of DXMP using 0.01 M KH_2PO_4 :MeOH (35:65) as eluent in isocratic mode. The Licrosphere 100 RP-18 column (5 µm) was used as stationary phase. DXMP was eluted at 3.1 minutes (A). DXMP calibration curve (B) was obtained by preparing a series of concentration of DXMP ranging from 0.4-100 µg/ml in water. All samples are taken triplicate and averages calculated. Bars represent SD.

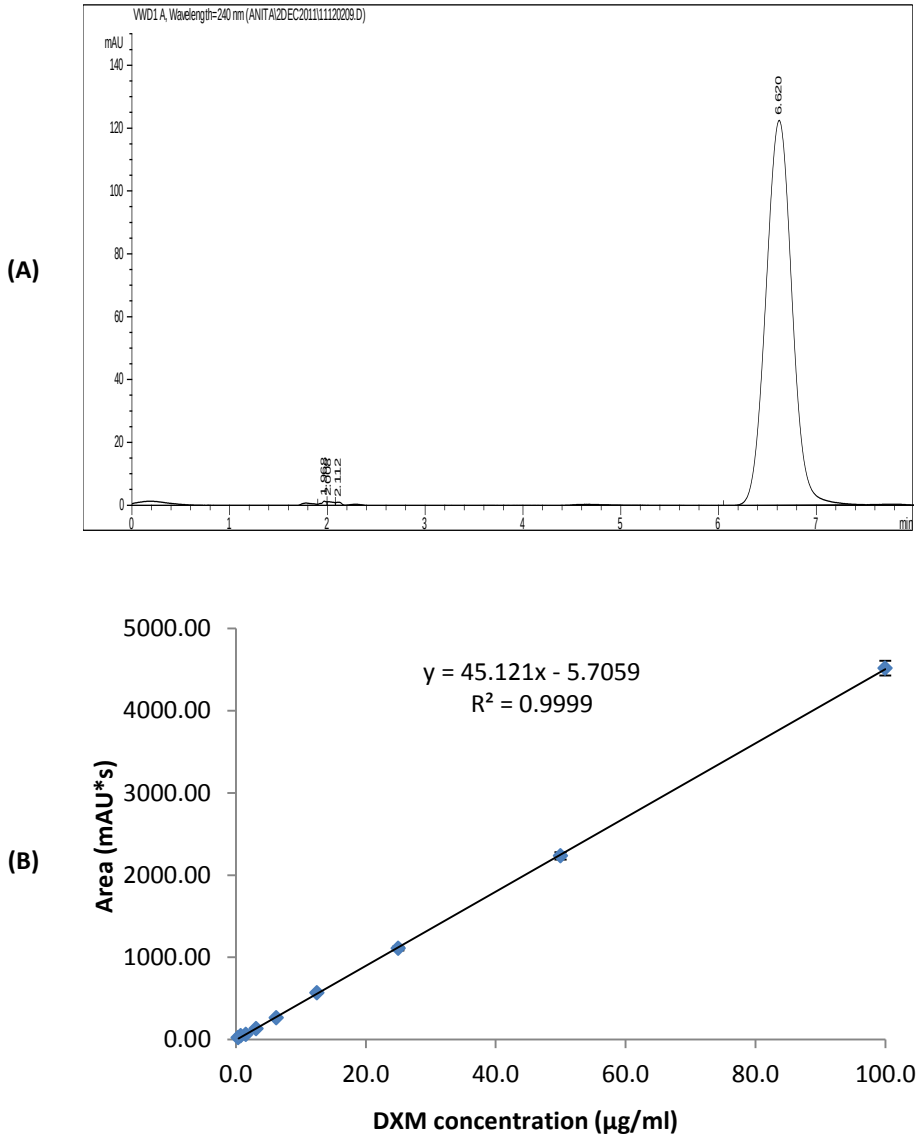

Figure 4.11. HPLC analysis of DXM using 0.01 M KH_2PO_4 :MeOH (35:65) as eluent in isocratic mode. The Licrosphere 100 RP-18 column (5 µm) was used as stationary phase. DXM was eluted at 6.6 minutes (A). DXM calibration curve (B) was obtained by preparing a series of concentration of DXM stock solution ranging from 0.4-100 µg/ml in water. All samples are taken triplicate and averages calculated. Bars represent SD.

Table 4.2 presents the extraction efficiency of DXMP from modified PGA polymer using various combinations of DCM and water. The result showed 97.0± 1.64 % of DXMP could be recovered from 40%C_{18}-PGA by extraction using DCM:water (1:4) which then became the standard method used.

Table 4.2. Efficiency of extraction of DXMP from 40%C_{18}-PGA polymer using various combination of dichloromethane and water (DCM:water).

Sample Code	DXMP added (µg)	Ratio DCM: water	DXMP recovered (µg)	Recovery (%)	Average Recovery (%)± SD
AS62-1	103	1 : 1	62.5	60.7	
AS62-2	103	1 : 1	63.1	61.2	60.5± 0.83
AS62-3	103	1 : 1	61.4	59.6	
AS62-4	103	1 : 2	70.5	68.5	
AS62-5	103	1 : 2	70.9	68.8	69.7 ± 1.89
AS62-6	103	1 : 2	74.1	71.9	
AS62-7	103	1 : 4	98.3	95.4	
AS62-8	103	1 : 4	99.9	96.9	97.0 ± 1.64
AS62-9	103	1 : 4	101.7	98.7	

Method validation was also carried out for extraction of SIM from 40% C_{18}-PGA MP. A known amount of SIM was mixed with 40%C_{18}-PGA. The SIM was then extracted using various combinations of DCM and methanol as solvents. The amount of SIM extracted was determined by HPLC analysis and eluted at 4.4 minutes. The concentration of SIM obtained was plotted on the SIM calibration curve in Figure 4.12.

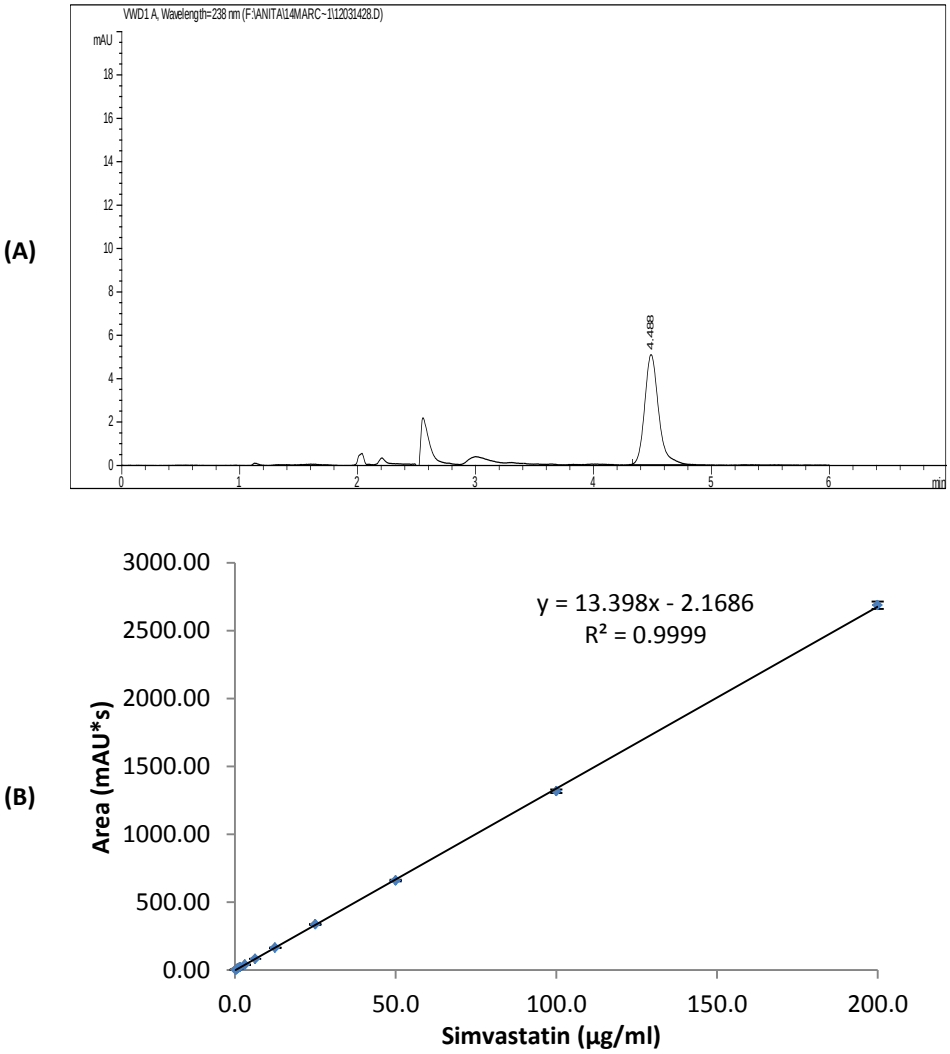

Figure 4.12. HPLC analysis of SIM using 1 mM ammonium acetate pH 4.4 : MeOH (10:90) as eluent in isocratic mode. The Licrosphere 100 RP-18 column (5 µm) was used as stationary phase. SIM was eluted at 4.4 minutes (A). SIM calibration curve (B) was obtained by prepared series concentration of SIM ranging from 0.2-200 µg/ml in MeOH. All samples are taken triplicate and averages calculated. Bars represent SD.

Table 4.3 shows that the highest extraction efficiency of SIM from 40%C_{18}-PGA (96.11 ± 3.34 %) was obtained using a combination of DCM and methanol (DCM:MeOH) 1: 4.

Table 4.3. Efficiency of extraction SIM from 40%C_{18}-PGA polymer using various combination of dichloromethane and methanol (DCM:MeOH).

Sample Code	SIM added (µg)	Ratio DCM: MeOH	SIM recovered (µg)	Recovery (%)	Average Recovery (%)± SD
AS63-1	100.3	1 : 1	68.8	68.6	
AS63-2	100.3	1 : 1	64.1	63.9	68.3 ± 4.22
AS63-3	100.3	1 : 1	72.6	72.4	
AS63-4	100.3	1 : 2	78.2	77.9	
AS63-5	100.3	1 : 2	80.2	79.9	77.6 ± 2.44
AS63-6	100.3	1 : 2	75.3	75.1	
AS63-7	100.3	1 : 4	98.5	98.2	
AS63-8	100.3	1 : 4	98.2	97.9	96.1 ± 3.34
AS63-9	100.3	1 : 4	92.5	92.3	

4.5.1. Effect of volume ratio of inner phase

The effect of inner phase volume ratio on encapsulation efficiency was investigated in DXMP. Incorporation of DXMP into modified PGA polymer was carried out using double emulsion method with PVA 2.5% as emulsifier as described in Chapter 2 section 2.3.2.2. In the double emulsion method (W/O/W), the term “inner phase” was used to define the primary emulsion. The primary emulsion acts as a dispersed phase and undergoes secondary emulsion with the outer phase or continuous phase. The 1:200 and 1:20 inner volume ratio of water to organic (W/O) phase was used to make the primary emulsion. The result is shown in Figure 4.13 reveals that the 1:200 inner volume ratio established a higher encapsulation efficiency of DXMP in 40%C_{18}-PGA MP and 40%C_{18}-PGA-PEG-MIHA MP with value 2.6 ± 0.40 % and 5.3 ± 0.10 %, respectively. However, the encapsulation efficiency of DXMP in 40%C_{18}-PGA MP and

40%C_{18}-PGA-PEG-MIHA MP was decreased to 0.9 ± 0.05 % and 3.6 ± 0.14 % when inner volume ratio was 1:20. The DXMP had higher encapsulation efficiency in 40%C_{18}-PGA-PEG-MIHA MP than in 40%C_{18}-PGA MP and seems be related to the tethering of MIHA-PEG-NH_2 linker on polymer backbone.

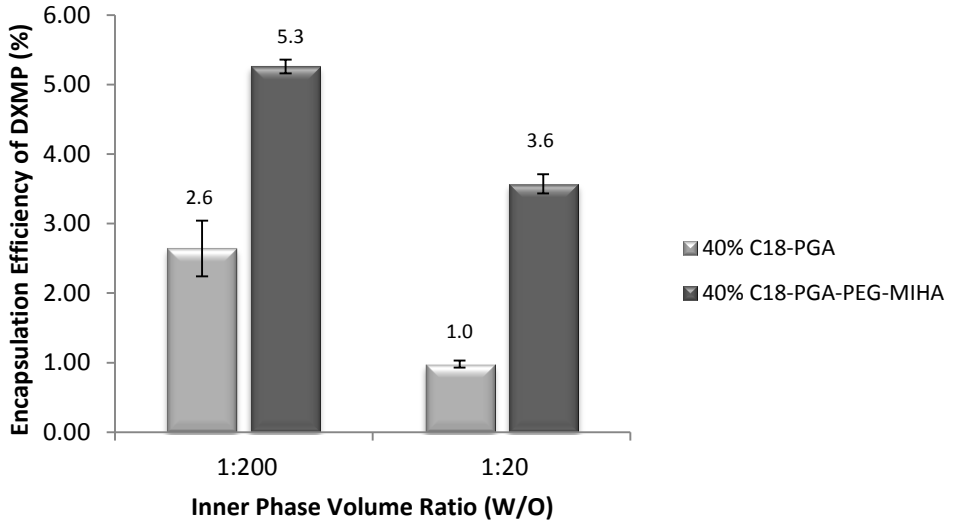

Figure 4.13. Effect of inner phase volume ratio (W/O) ratio to encapsulation efficiency of dexamethasone phosphate (DXMP) in modified PGA microparticles. The initial drug loading is 1 mg per 100 mg polymer. Bars represent SD (n=3).

4.5.2. Effect of drug on encapsulation efficiency

Encapsulation efficiency within modified PGA polymer was also investigated using SIM as an encapsulated drug. SIM was incorporated within modified PGA MP using the single emulsion method with PVA 2.5% as emulsifier. Incorporation of SIM exhibited greater encapsulation than DXMP in 40%C_{18}-PGA MP and 40%C_{18}-PGA-PEG-MIHA MP in the value 53.5 ± 6.13 % and 54.5 ± 4.83 %, respectively (Figure 4.14). The efficiency of encapsulation of SIM reached 25 and 10 times higher than DXMP in 40%C_{18}PGA and 40%C_{18}-PGA-PEG-MIHA MPs, respectively.

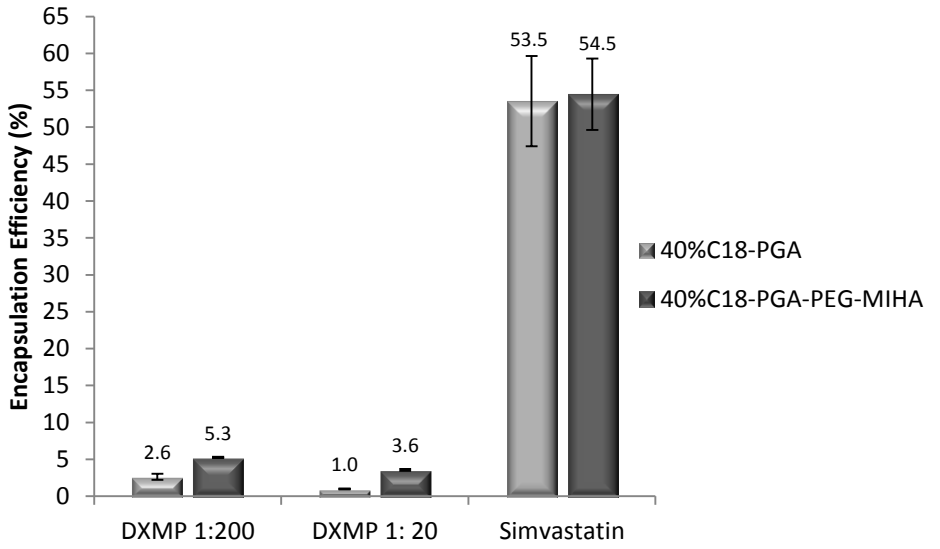

Figure 4.14. Encapsulation efficiencies of DXMP and SIM into modified PGA microparticles. Incorporation of DXMP into the polymer was carried out in double emulsion method, while SIM was incorporated using single emulsion method. The 1:200 and 1:20 W/O inner phase volume ratio were used to perform primary emulsion of DXMP. The initial drug loading is 1 mg per 100 mg polymer. Bars represent SD (n=3)

Since establishing good incorporation, the effect of PVA concentration as emulsifier on encapsulation efficiency was studied in the MPs containing SIM. Due to limited amount of 40%C_{18}-PGA-PEG-MIHA polymer, this study only investigated 40%C_{18}-PGA polymer.

4.5.3. Effect of PVA concentration

Effect of PVA concentration on encapsulation efficiency was investigated using PVA 0.25% and 0.5% with the former achieving the highest encapsulation efficiency as seen in Figure 4.15.

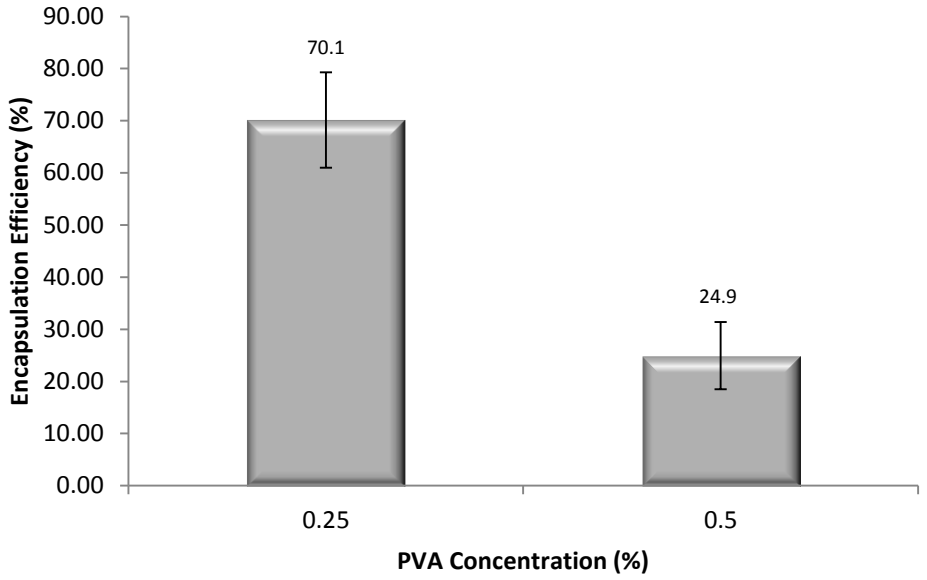

Figure 4.15. Encapsulation efficiency of simvastatin in 40%C_{18}-PGA microparticle prepared using single emulsion method with PVA 0.25% and 0.5%. The initial drug loading is 1 mg per 100 mg polymer. The encapsulation efficiency was determined from different batches of microparticle. Bars represent SEM (n=9).

4.5.4. Effect of polymer concentration in organic phase

Encapsulation efficiency also was influenced by polymer concentration in organic phase used in preparation. Microparticle prepared from 0.5% polymer in organic phase achieved encapsulation efficiency 20.4± 0.11 %, while 5% polymer exhibited 70.1 ± 12.81 % of encapsulation efficiency (Figure 4.16).

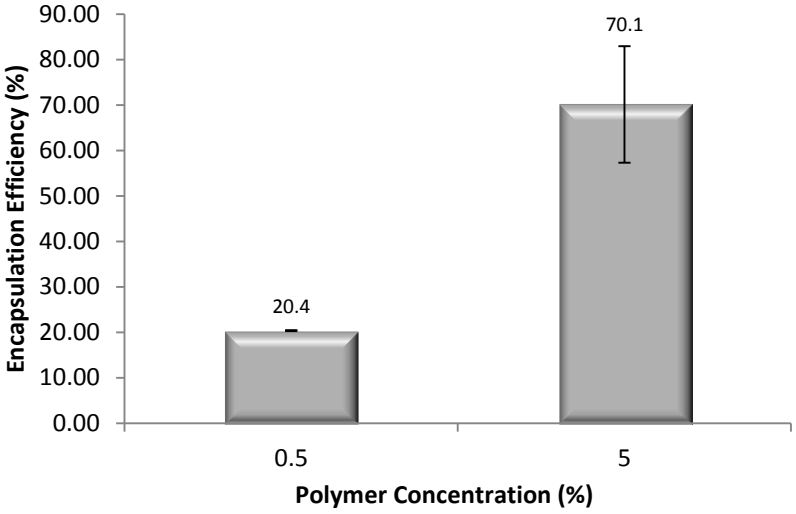

Figure 4.16. Encapsulation efficiency of simvastatin in 40%C_{18}-PGA microparticles prepared using single emulsion method with PVA 0.25 %. The initial drug loading is 1 mg per 100 mg polymer. The encapsulation efficiency was determined from different batches of microparticle. Bars represent SEM (n=9).

4.6. Drug Release from Microparticles

The release of drug from MP is influenced by the formulation. According to physical characterisation, the MPs prepared with PVA 2.5% met the size requirement for the incorporation into cell aggregates. The release studies were carried out for MP containing DXMP and SIM as active drugs. The sample and separate (SS) method was used to evaluate amount of drug release from microparticles as described in Chapter 2 section 2.3.6. Phosphate buffer saline (PBS) was used as a release medium for MP containing DXMP, while 0.1% of Tween 20 was added to the release medium for MP containing SIM.

Polymer concentration in organic phase	:	0.5%
PVA concentration	:	2.5%
Initial drug loading	:	10%
MP yield (%)		
40% C_{18}-PGA	:	52
40% C_{18}-PGA-PEG-MIHA	:	49
Drug loading (%)±SD		
40% C_{18}-PGA	:	0.3 ± 0.06
40% C_{18}-PGA-PEG-MIHA	:	0.4 ± 0.05
Particle size (µm)±SD		
40% C_{18}-PGA	:	7.2 ± 0.10
40% C_{18}-PGA-PEG-MIHA	:	5.6 ± 0.29
Encapsulation Efficiency (%)±SD		
40% C_{18}-PGA	:	2.9 ± 0.87
40% C_{18}-PGA-PEG-MIHA	:	3.6 ± 0.14

(A)

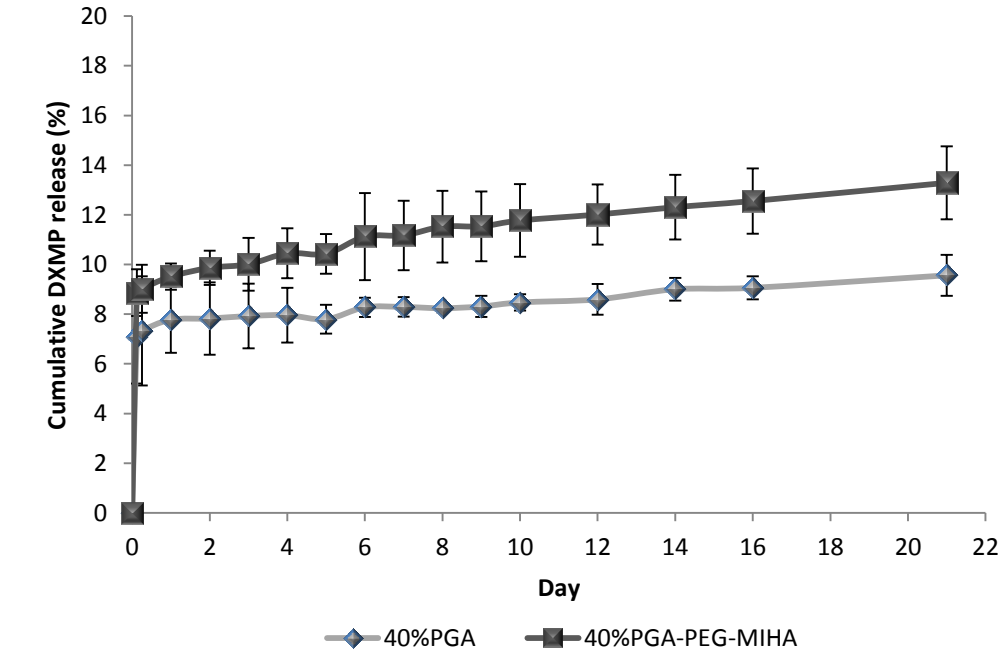

Figure 4.17. DXMP release profile from modified PGA microparticles. The release study was established at 37°C using PBS as a medium for 21 days. Table (A) showed the specification of microparticles used for the study. Bars represent SD (n=3)

The release profile from MP containing DXMP is presented in Figure 4.17. Almost 10% of drug was released from 40%C_{18}-PGA-PEG-MIHA MP containing DXMP, while the 40%C_{18}-PGA MP only released around 8% of DXMP within the first day of study.

The release of drug was remained constant after day 1. The 40%C_{18}-PGA-PEG-MIHA MP released higher amount of DXMP compared to 40%C_{18}-PGA MP. On the 21st day of the release study no further DXMP was found to be released in the medium, therefore, the release study was terminated on day 21. Only 9.6± 0.73 % and 13.3± 1.47 % of DXMP had been released from 40%C_{18}-PGA and 40%C_{18}-PGA-PEG-MIHA MPs after 21 days, respectively.

A further investigation was conducted on the amount of DXMP that remained within the MP. The DXMP was extracted from MP and analysed using HPLC. Around 56% and 37% of DXMP remained within 40%C_{18}-PGA and 40%C_{18}-PGA-PEG-MIHA MPs (Table 4.4). These data suggested that DXMP has a strong interaction within the modified PGA polymer. On the other hand, the lower amount of DXMP remaining in 40%C_{18}-PGA-PEG-MIHA MP indicated that attachment of MIHA-PEG-NH_2 linker to 40%C_{18}-PGA could enhance the release of drug from modified PGA MP.

Table 4.4. DXMP released from and remaining in modified PGA MPs after 21-day release study (n=3).

Type of microparticle	40%C_{18}-PGA	40%C_{18}PGA-PEG-MIHA
Initial amount of DXMP per 10 mg MPs (µg) ± SD	29.1 ± 0.32	36.3 ± 0.49
DXMP released from MP (µg) ± SD	2.7 ± 0.21	4.5 ± 0.47
DXMP released from MP (%)± SD	9.6 ± 0.73	13.3 ± 1.47
DXMP remaining in MP (µg) ± SD	16.4 ± 2.36	13.5 ± 1.28
DXMP remaining in MP (%)± SD	56.7 ± 8.56	37.2 ± 3.36

Polymer concentration in organic phase	:	0.5%
PVA concentration	:	2.5%
Initial drug loading	:	10%
MP yield (%)		
40% C_{18}-PGA	:	56.7
40% C_{18}-PGA-PEG-MIHA	:	47.9
Drug loading (%)±SD		
40% C_{18}-PGA	:	4.8 ± 0.24
40% C_{18}-PGA-PEG-MIHA	:	4.7 ± 0.31
Particle size (µm) ±SD		
40% C_{18}-PGA	:	12.4 ± 1.54
40% C_{18}-PGA-PEG-MIHA	:	10.3 ± 0.24
Encapsulation Efficiency (%)±SD		
40% C_{18}-PGA	:	46.4 ± 2.32
40% C_{18}-PGA-PEG-MIHA	:	45.8 ± 2.99

(A)

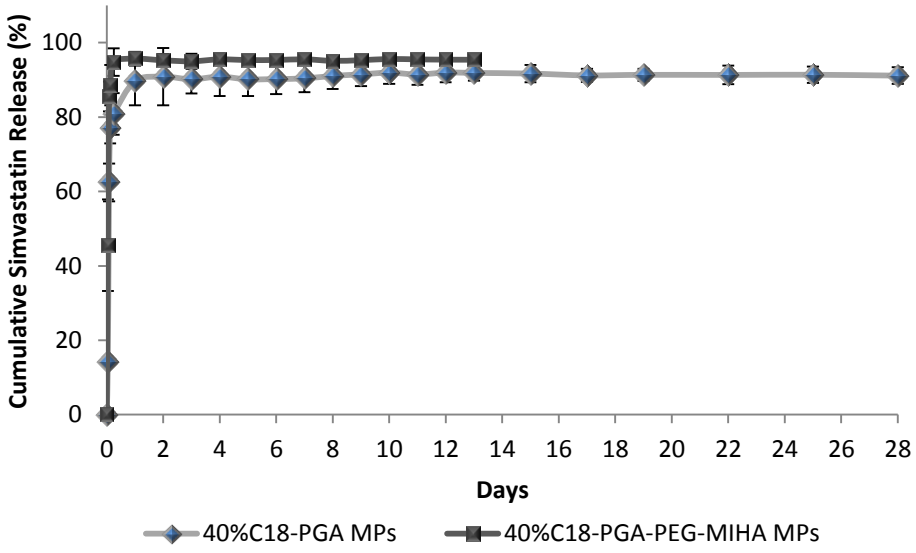

Figure 4.18. SIM release profile from modified PGA microparticles. The release study was established at 37 C using PBS+0.1% Tween 20 as a medium. Table (A) showed the specification of microparticles used for the study. Bars represent SD (n=3).

The drug release profile was also investigated with MP containing SIM as active drug. The release profile is shown in Figure 4.18. A high amount of SIM was released from the MPs on the first day of experiment, around 90% of SIM had been released from 40%C_{18}-PGA MP, while 95% had been released from 40% C_{18}-PGA-PEG-MIHA MP. The

SIM presented more rapid release from 40%C_{18}-PGA-PEG-MIHA MP compare to 40%C_{18}-PGA MP. The release study was terminated at day 13 for 40%C_{18}-PGA-PEG-MIHA MP since no more SIM was detected in the medium. Conversely, the release of SIM from 40%C_{18}-PGA continued up to 28 days of experiment. The remaining MPs were analyzed to determine amount of SIM remaining in MPs after release study. The signal of SIM was to low and not be able to detect with HPLC.

The initial rapid release of drugs from modified PGA MPs would not be useful for extended release of bioactive molecule to encourage cell differentiation. The differentiation of cells involved several phases over the defined period of time. Hence, the MP should be able to retain drug for longer periods and deliver a moderately slow release of the drug. In addition, the rapid release of drug at the early period may induce toxic effects for the cells due to high concentration drug released directly to the cells. Most of initial rapid release, known as burst release, caused by diffusion of drug through the preformed water channels on MP [164]. The burst release from MP could be related to the nature of polymer itself or microparticle formulation. To identify this problem, the solid dispersions of SIM in modified PGA polymers were prepared and the release of SIM was investigated.

4.6.1. Drug release from modified PGA solid dispersion

The solid dispersions of modified PGA polymer with SIM was prepared using solvent evaporation method as stated in Chapter 2 section 2.3.5.2. Figure 4.19 illustrates the release profile of SIM from modified PGA SDs. At the first day, only 24% of SIM had been released from 40%C_{18}-PGA solid dispersion, while 36% of SIM had been released from 40%C_{18}-PGA-PEG-MIHA solid dispersion. The SIM could be retained

within the solid dispersion up to 16 days in 40%C_{18}-PGA solid dispersion and up to 18 days in 40%C_{18}-PGA-PEG-MIHA solid dispersion. The 40%C_{18}-PGA-PEG-MIHA solid dispersion exhibited a higher drug release than 40%C_{18}-PGA solid dispersion. The total SIM released from 40%C_{18}-PGA and 40%C_{18}-PGA-PEG-MIHA solid dispersion at the end of release studies were around 45% and 56%, respectively.

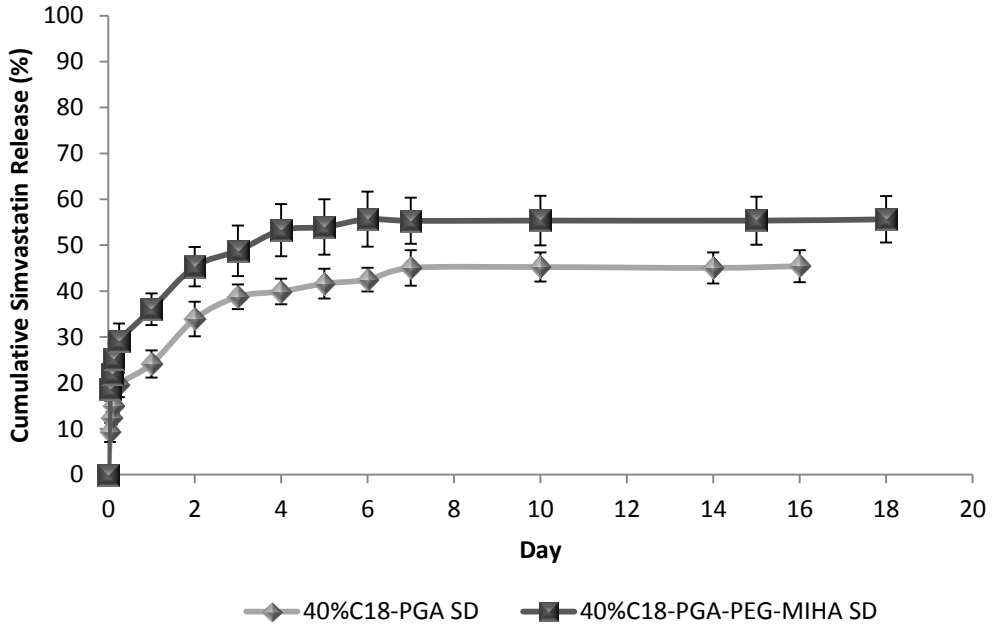

Figure 4.19. SIM release profile from modified PGA solid dispersions. The solid dispersions were prepared using solvent evaporation method containing 1% (w/w) of SIM within 100 mg of modified PGA polymers. The release study was established at 37°C using PBS+0.1% Tween 20 as a medium (n=3). Bar represents SD.

At the end of release study for the solid dispersions, the SIM was extracted to determine amount of drug retained within the polymer. Table 4.5 shows the summary of release study of modified PGA solid dispersions. Although the SIM released from solid dispersions are around 50%, it was found that the retained SIM within solid dispersions were less than 2% of the initial amount. It indicates that SIM

could not be completely extracted from the polymers due to strong interaction within polymers. It was also noticed that the initial high release of drug from modified PGA MPs seems to be mainly caused by its formulation.

Table 4.5. SIM release from and remaining in modified PGA solid dispersions at the end of released study. The release study was carried out for 16 days on 40%C_{18}-PGA and 18 days on 40%C_{18}-PGA-PEG-MIHA (n=3)

Type of solid dispersions	40%C_{18}-PGA	40%C_{18}PGA-PEG-MIHA
Initial amount of SIM per 5 mg SDs (µg) ± SD	42.7 ± 0.94	51.3 ± 4.45
SIM released from solid dispersion (µg) ± SD	19.5 ± 1.21	28.6 ± 3.74
SIM released from solid dispersion (%)± SD	45.4 ± 3.50	55.7 ± 5.23
SIM remaining in solid dispersion (µg) ± SD	0.7 ± 0.16	0.6 ± 0.11
SIM remaining in solid dispersion (%)± SD	1.8 ± 0.04	1.2 ± 0.14

Several critical factors relating to MP formulation had previously been identified. According to Yeo and Park (2004), the burst release could be controlled by modifying polymer concentration and composition of continuous phase during MP preparation [164]. Hence, experiments had been established to evaluate effect of polymer concentration and PVA concentration in continuous phase on release profile of drug from modified PGA MPs. Since SIM showed good incorporation within modified PGA MP, further studies were carried out with the MP containing SIM. Due to limited amount of 40%C_{18}-PGA-PEG-MIHA polymer, these two critical factors were investigated on 40%C_{18}-PGA.

4.6.2. Effect of polymer concentration

Effect of polymer concentration during preparation was studied with 40%C_{18}-PGA prepared by emulsification method using PVA 0.25%. Figure 4.20 shows that the amount of drug released was affected by polymer concentration in the organic phase. Initial burst released still occurred in both concentrations of polymer. At day one, MP prepared from 0.5% and 5% polymer concentration released 86.3 % and 78.2 % of SIM, respectively. The increasing polymer concentration did not affect the initial amount of drug release from MP at the first day of experiment ($P > 0.05$, n=3). However, the 5% polymer concentration exhibited lower amount of drug release than 0.5% polymer concentration after 14 days of experiment ($P < 0.05$, n=3).

Polymer concentration in organic phase		0.5%	5%
PVA concentration (%)	:	0.25	0.25
Initial drug loading (%)	:	1	1
MP yield (%)	:	55.0	60.1
Drug loading (%)± SD	:	0.2 ± 0.01	0.7 ± 0.0
Particle size (µm)± SD	:	10.2 ± 0.49	21.8 ± 0.15
Encapsulation Efficiency (%)± SD	:	20.4 ± 0.11	70.1 ± 1.28

(A)

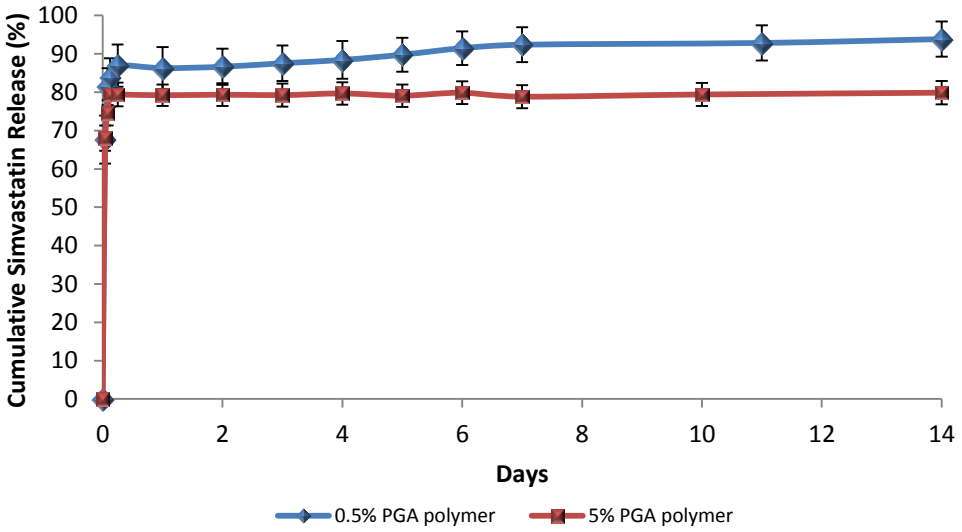

Figure 4.20. The release profiles of SIM from 40%C_{18}-PGA microparticles. Microparticles were prepared using emulsification method with PVA 0.25% as emulsifier (table A). Two concentration of polymer in organic phase were used in formulation, 0.5% and 5%. The release study was established in PBS+0.1% at 37°C. Bars represent SD (n=3).

Amount of SIM remaining in MP after 14 days of study was analysed and the result are presented in Table 4.6 showing 2.1 ± 0.29 % of SIM remained in 40%C_{18}-PGA MP while 5.9 ± 0.16 % was remained in 40%C_{18}-PGA-PEG-MIHA MP. The higher polymer concentration seems to provide stronger interaction with SIM as it retained more drug inside the MP.

Table 4.6. SIM released from and remaining in 40%C_{18}-PGA MPs prepared from 0.5% and 5% polymer in organic phase after 14-day release study

Concentration of polymer	0.5%	5%
Initial amount of SIM per 5 mg MPs (µg) ± SD	16.2 ± 0.37	34.9 ± 0.99
SIM released from MP (µg) ± SD	15.4 ± 0.61	27.8 ± 0.05
SIM released from MP (%)± SD	93.8 ± 4.61	79.9 ± 3.03
SIM remaining in MP (µg) ± SD	0.2 ± 0.16	2.1 ± 0.08
SIM remaining in MP (%)± SD*	2.1 ± 0.29	5.9 ± 0.16

4.6.3. Effect of PVA concentration

Effect of PVA concentration on drug release was investigated in MP prepared from 0.5 % and 5 % polymer. Figure 4.21 describes the release profile of SIM from MP prepared with 0.5% polymer concentration. Based on the Figure 4.21, the difference in PVA concentration did not affect the total amount of drug released from MPs ($P>0.05$, n=3). Although the MP prepared with PVA 0.25% exhibited lower drug release at the beginning, there was no significant difference between the MP prepared with PVA 0.25% and PVA 0.5% ($P>0.05$, n=3). This result also applied to the total amount of SIM released from microparticles at the end of the study (Table 4.7).

Polymer concentration in organic phase		0.5%	
PVA concentration (%)	:	0.25	0.5
Initial drug loading (%)	:	1	1
MP yield (%)	:	54.2	45.0
Drug Loading (%)±SD	:	0.2 ± 0.01	0.3 ± 0.03
Particle size (µm)±SD	:	25.1 ± 0.67	20.1 ± 1.15
Encapsulation Efficiency (%)±SD	:	20.4 ± 0.11	31.3 ± 1.31

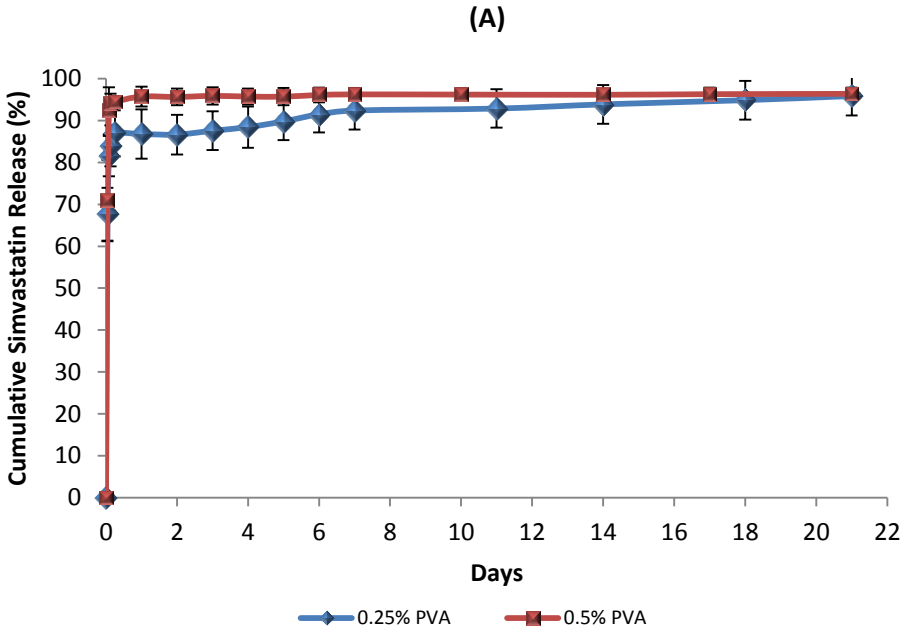

Figure 4.21. The release profiles of SIM from 40%C_{18}-PGA microparticles. Microparticles were prepared using emulsification method with 0.5 % polymer concentration. Two concentrations of PVA, 0.25% and 0.5%, were used in formulation (A). The released study was established in PBS+0.1% tween 20 at 37°C. Bars represent SD (n=3).

Table 4.7. SIM released from and remaining in 40%C_{18}-PGA MPs prepared from 0.5% polymer in organic phase with PVA 0.25 and 0.5% after 21-day release study

Concentration of PVA	0.25%	0.5%
Initial amount of SIM per 5 mg MPs (µg) ± SD	11.2 ± 0.25	18.5 ± 0.74
SIM released from MP (µg) ± SD	10.9 ± 0.33	17.9 ± 0.45
SIM released from MP (%)± SD	95.8 ± 4.65	96.4 ± 1.50
SIM remaining in MP (µg) ± SD	0.2± 0.06	0.7 ± 0.06
SIM remaining in MP (%)± SD	1.9 ± 0.16	3.6 ± 0.19

The effect of PVA concentration on drug release from MP was also investigated in MP prepared from 5% polymer concentration in organic solvent. Various concentrations of PVA were used to prepare MP from 40%C_{18}-PGA. The release profile of MP prepared with 5% polymer and various concentration of PVA is shown in Figure 4.22. It can be clearly seen that PVA concentration above 0.005% influenced the release of SIM from the MPs. There was no significant difference of drug release from MP prepared without PVA and with PVA 0.005% ($P>0.05$, $n=3$). On the first day of release study, the MP prepared with 0.005% released 47.8 ± 5.04% of SIM, while increasing PVA to 0.05% could increase release to 57.9 ± 1.68 % of SIM. Further increases in PVA concentration to 0.25% increased the drug release up to 78.2 ± 2.79 % at the first day of study.

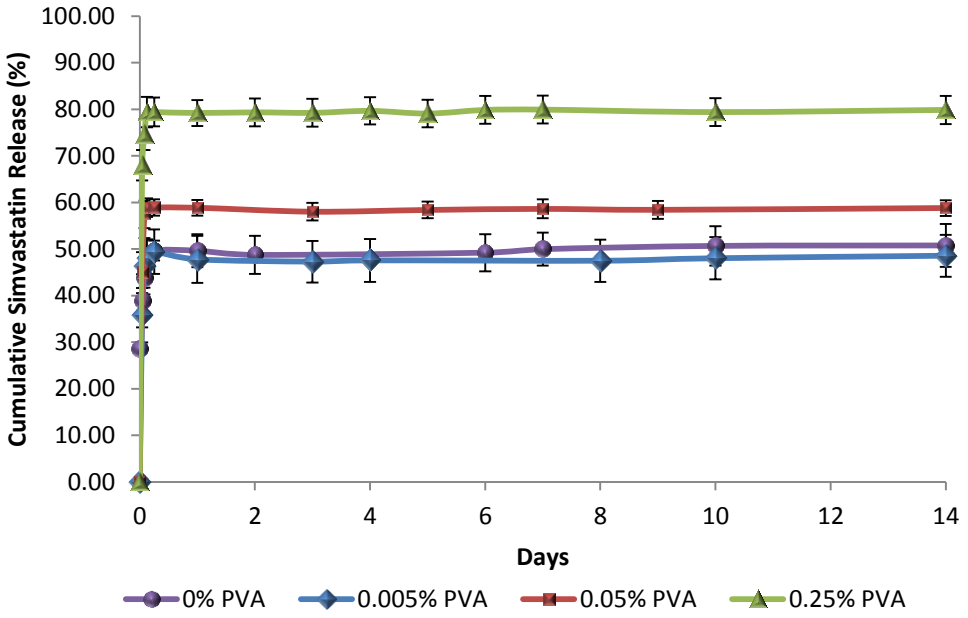

Figure 4.22. The release profiles of SIM from 40%C_{18}-PGA microparticles. Microparticles were prepared using emulsification method with 5 % polymer concentration with and without PVA. Various concentration of PVA were used in the formulation. The release study was established in PBS+0.1% tween 20 at 37°C. Bars represent SD (n=3).

Table 4.8. SIM released from and remaining in 40%C_{18}-PGA MP prepared with various concentration of PVA. Emulsification method was used to prepare MP with PVA while solvent displacement method was used to prepare MP without PVA.

	PVA concentration (%)			
	0	**0.005**	**0.05**	**0.25**
MP yield (%)	52.1	45.1	57.1	50.1
Initial amount of SIM per 5 mg MPs (μg) ± SD	32.5 ± 0.03	30.0 ± 0.66	30.9 ± 1.43	34.9 ± 0.99
SIM released from MP (μg) ± SD	17.3 ± 0.43	14.6 ± 1.69	17.7 ± 1.27	27.8 ± 0.05
SIM released from MP (%)± SD	50.7 ± 4.62	48.6 ± 4.49	57.8 ± 1.68	79.9 ± 3.03
SIM remaining in MP (μg) ± SD	0.6 ± 0.01	0.5 ± 0.14	0.6 ± 0.03	0.7 ± 0.08
SIM remaining in MP (%)± SD	1.70 ± 0.19	1.7 ± 0.50	1.9± 0.18	2.1 ± 0.29

The remaining MP were then analysed to determine amount of SIM retained inside MP after release study. It is seen from Table 4.8 that only a small amount of SIM (<2%) could be extracted from MP. The result was surprising since the amount of SIM released was around 50%. It was supposed that around 50% should be retained in MPs. Amount of SIM could be extracted is related to the PVA concentration during MPs formulation. A higher PVA concentration generated a higher amount of SIM could be extracted from MPs, i.e. 1.70, 1.71, 1.97, 2.11 % for MP prepared without PVA, with 0.005%, 0.05%, and 0.25% PVA respectively.

4.7. Ligand Attachment to Microparticles

Collagen was attached to MP prepared from 40%C_{18}-PGA-PEG-MIHA as a ligand to encourage cell attachment. Collagen had been modified with iminothiolane and FITC as described in Chapter 2, section 2.3.7. The thiol group on collagen molecule attached to maleimide active group on 40%C_{18}-PGA-PEG-MIHA MP *via* covalent

bonding. The amount of collagen attached to the MP was determined by fluorescence intensity of collagen.

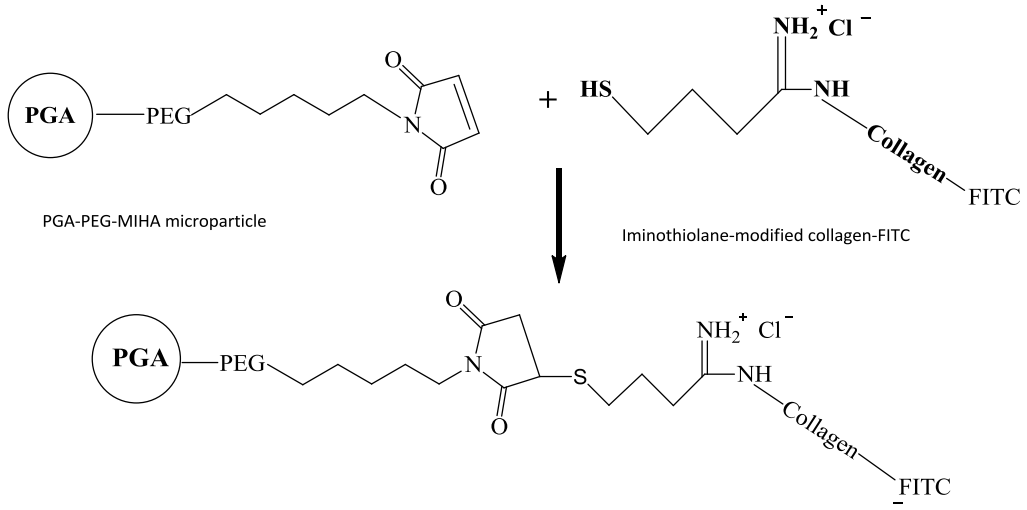

Figure 4.23. Reaction scheme of iminothiolane-modified collagen attached to 40%C_{18}-PGA-PEG-MIHA MP.

Reaction between 40%C_{18}-PGA-PEG-MIHA MP and iminothiolane-modified collagen is illustrated in Figure 4.23. In order to evaluate the specific bond of thiol with maleimide group on 40%C_{18}-PGA-PEG-MIHA MP, various amounts of iminothiolane-modified collagen was added to the MP (5 mg).

The amount of iminothiolane-modified collagen attached to MP was determined by measuring fluorescence intensity of FITC in attached MP. The FITC calibration curve as presented in Figure 4.24 was used to determine the amount of FITC attached to MP. Since the ratio of FITC to the iminothiolane-modified collagen was known, the amount collagen attached to the MP could be calculated.

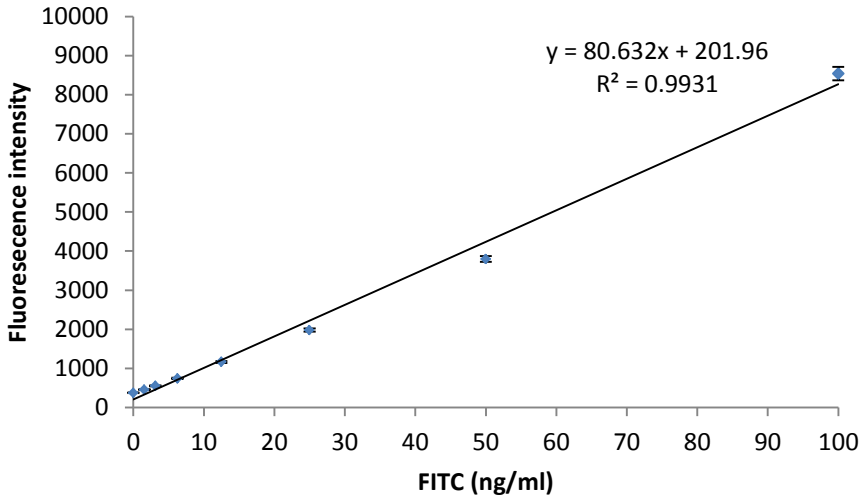

Figure 4.24. FITC calibration curve in phosphate buffer saline. A range of concentrations of FITC from 1.6 – 100 ng/ml was prepared from FITC 1 mg/ml stock solution in acetone. Fluorescence intensity was measured using fluorescence spectrophotometer at λ_{exc} of 495 nm and λ_{emm} of 521 nm. All samples are taken triplicate and averages are calculated.

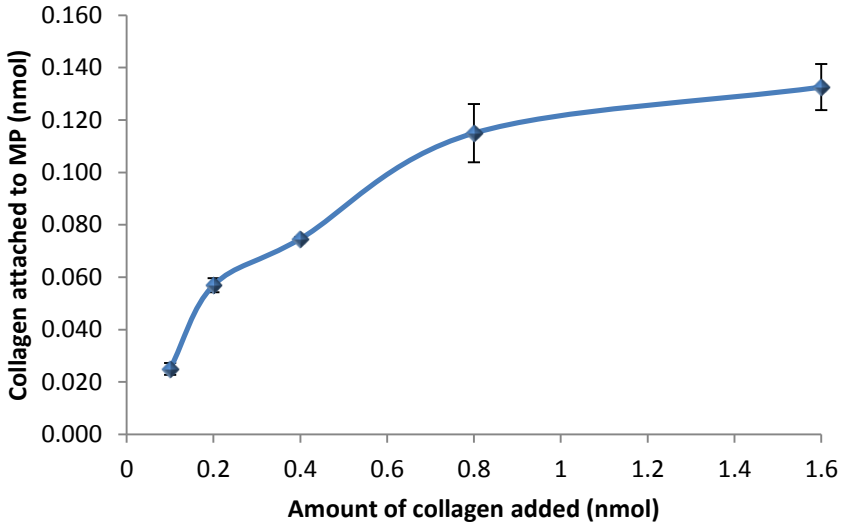

Figure 4.25. Iminothiolane-modified collagen attached to 40%C_{18}-PGA-PEG-MIHA MP. Amount of collagen attached was determined by measuring fluorescence intensity of FITC attached to collagen. FITC was attached to the collagen in ratio 1.6 : 1 (FITC : collagen). All samples are taken triplicate and averages are calculated. Bars represent SD (n=3).

The amount of iminothiolane-modified collagen attached to the MP is presented in Figure 4.25. The amount of iminothiolane-modified collagen attached to the MP was increased proportionally with amount of collagen added and reached a plateau at 1.6 nmol of iminothiolane-modified collagen added. It demonstrated that all active maleimide groups on 40%C_{18}-PGA-PEG-MIHA MP had reacted with thiol active group on iminothiolane-modified collagen molecule and became saturated. Therefore, it is probably related to the specific covalent bond between thiol group and maleimide. Further addition of iminothiolane-modified collagen would not be able to attach on the surface of 40%C_{18}-PGA-PEG-MIHA MP. The highest efficiency of iminothiolane-modified collagen attachment was achieved when 0.2 nmol collagen added to 5 mg of microparticle (Table 4.9). Although higher amounts of collagen attached to MP could be achieved with increasing amount of collagen added, the efficiency of attachment became lower.

Table 4.9. Efficiency of iminothiolane-modified collagen attachment to 40%C18-PGA-PEG-MIHA microparticle in phosphate buffer saline medium pH 7.2 (n=3).

Collagen added (nmol)	MP (mg)	FITC attached to MP (ng/ml))±SD	FITC attached to MP (nmol)±SD	Collagen attached to MP (nmol)±SD	Efficiency of Attachment (%)±SD
0.1	5	15.7 ±1.41	0.04 ±0.004	0.03 ±0.002	25.0 ± 2.24
0.2	5	35.8 ±0.68	0.09 ±0.004	0.06 ±0.003	28.5 ± 1.33
0.4	5	46.9 ±0.40	0.12 ±0.001	0.07 ±0.001	16.4 ± 3.92
0.8	5	72.4 ±6.99	0.19 ±0.018	0.11 ±0.011	14.4 ± 1.39
1.6	5	83.4 ±5.54	0.21 ±0.014	0.13 ±0.009	7.7 ± 1.13

Further investigation was conducted to evaluate the possibility of physical absorption of iminothiolane-modified collagen attachment to MP. A defined amount of iminothiolane-modified collagen was added to 40%C_{18}-PGA MP as well as to 40%C_{18}-PGA-PEG-MIHA. Figure 4.26 illustrates amount of iminothiolane-modified collagen

attached to 40%C_{18}-PGA MP and 40%C_{18}-PGA-PEG-MIHA MP after purification step to remove unbound collagen. It showed that there was some iminothiolane-modified collagen which could be strongly adsorbed to 40%C_{18}-PGA MP. However, the amount of collagen adsorbed was less than half the amount of specifically attached to 40%C_{18}-PGA-PEG-MIHA MP.

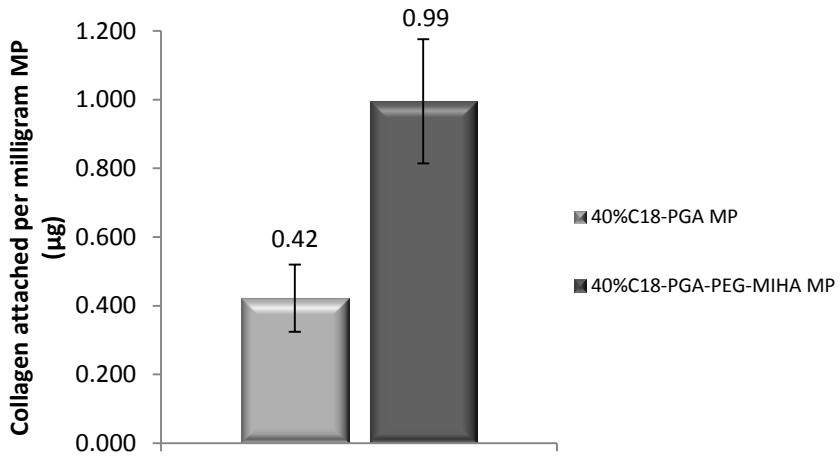

Figure 4.26. Iminothiolane-modified collagen adsorbed and attached to 40%C_{18}-PGA and 40%C_{18}-PGA-PEG-MIHA microparticles. Amount of collagen adsorbed or attached to microparticles was determined by fluorescence intensity of FITC on collagen molecule. Bars represent SD (n=3).

4.8. Discussion

4.8.1. Characterisation of microparticles

Several critical factors have been investigated relating to physical characteristics of MP, encapsulation efficiency and release of drug from MP. According to this study, the size of MP was influenced by type of polymer, homogenizer speed and concentration of PVA used as emulsifier in continuous phase. The MP prepared from 40%C_{18}-PGA-PEG-MIHA exhibited a smaller particle size compared to MP prepared

from 40%C_{18}-PGA. This phenomenon could be explained by two possibilities. First, the attachment of MIHA-PEG-NH_2 linker to 40%C_{18}-PGA could reduce the aggregation of polymer. It could occur due to formation of steric hindrance around the MP in the presence of PEG. The steric hindrance could act as a "conformational cloud" to prevent MP interactions with each other [133, 173]. Another possibility is that the presence of PEG increases the solubility of polymer in aqueous media as mentioned in literature [133]. The increasing solubility of 40%C_{18}-PEG-MIHA polymer in aqueous phase facilitated the formation of finer emulsion droplets hence reducing the size of particle. Moreover, the presence of PEG acts as a surfactant to stabilize emulsion droplets [174, 175]. This result seems to be similar with the other studies by Lee *et al* (2005) showing that the presence of PEG in peptide nanoparticles reduced the size of particle prepared by emulsification method [174, 176].

The particle size in both 40%C_{18}-PGA and 40%C_{18}-PGA-PEG-MIHA MPs was affected by homogenization speed during emulsification. Increasing the speed of stirrer to 13,000 rpm gave the size reduction on of particle related to formation of a finer emulsion [172]. A relationship between homogenisation speed and particle size had been investigated by Sansdrap and Moes (1993) [167]. According to this study, increasing stirring speed provides high energy to reduce interfacial tension between organic and aqueous solvent during emulsification process. Therefore, the interaction between two phases could be maximised to produce small droplets leading to small particle size. In addition, increasing stirrer speed also accelerates translational movement of surfactant on the aqueous-organic interface to perform particle in emulsion system [177].

As mentioned in the literature, the size of MP could be influenced by variation of emulsifier concentration during MP formation. Increasing emulsifier concentration is commonly related to the reduction of particle size [167, 172, 174, 177]. Contrary to this expectation, the addition of PVA as emulsifier at concentration 0.005% and 0.025% resulted in the larger particle size than the MP prepared without emulsifier. The solvent displacement method was used to prepare the MP without emulsifier. According to this finding, it can be seen that solvent displacement method could produce a smaller particle size compared to emulsification method even without emulsifier.

The unexpected result was shown with PVA 0.005% and 0.025%. Increasing PVA concentration from 0.005% to 0.025% resulted in the formation of a bigger particle. According Lee *et al* (1999), the size of particles is influenced by amount of PVA per specific surface area of particle. However, the increased PVA concentration in continuous phase might not change the surface of PVA density, particularly in larger particle [178]. Therefore, the 5 fold increasing of PVA concentration in the continuous phase might not affect particle size.

Further increases in PVA concentration during MP preparation, not only reduce particle size but also influence the particle size distribution. This may arise due to the PVA reducing surface tension between organic and aqueous medium to perform emulsion droplet, resulting in small particle [167]. Although the PVA 0.25% seems to produce larger particles compared to PVA 0.05%, there was no overall significant difference on particle size ($p > 0.05$, $n=3$). The distribution of particles was shifted from negatively skewed distribution to positively skewed distribution, indicating that

more fine microparticles were formed with increasing emulsifier concentration. This result also applied for MP prepared from 40%C_{18}-PGA-PEG-MIHA.

The zeta potentials of MPs are affected by the modification of PGA backbone. The unsubstituted PGA demonstrated negative zeta potential and is related to carboxyl group at the end of polymer [125, 179]. The acylation using stearoyl (C_{18}) on PGA backbone shifted the zeta potential to a low negative value. However, this result was the opposite of the effect of acylation on PGA polymer made in nanoparticles described in previous research by Kallinteri *et al* (2005) and Puri *et al* (2008) [125, 180] where an increase in zeta potential was seen. The difference in the method of preparation between nanoparticle and MP might influence the zeta potential value. Interfacial deposition method (IDP) was used to perform nanoparticle in Kallinteri *et al* (2005), while the emulsification method was used to prepare MP in this study. The method of nano or MP preparation would affect the structural rearrangement within the particle, therefore influenced the surface charge of MP.

The attachment of MIHA-PEG linker shifted the zeta potential to the higher negative value. The zeta potential of 40%C_{18}-PGA-PEG-MIHA MP is -25.2± 2.19, while 40%C_{18}-PGA revealed -18.3 ± 1.60. According to previous studies, attachment of PEG or PEG coating to particle would be able to bring zeta potential to lower negative value [181-183] since carboxyl group was reacted with PEG molecules resulted in charge neutralization and steric effect of PEG. In contrast with earlier findings, the attachment of MIHA-PEG linker in this study increases the negative value of zeta potential.

The 40%C_{18}-PGA-PEG-MIHA MP decorated with iminothiolane-modified collagen led to a lower negative zeta potential value. Since collagen molecule contains a net positive charge, the zeta potential of the MP was shifting to the positive direction [179]. This result also indicated that MP is well covered with iminothiolane-modified collagen.

Scanning electron microscope images illustrated that a smooth surface of MP had been obtained. It is seen that both types of MP form non-spherical shape. The 40%C_{18}-PGA-PEG-MIHA MP were small and more homogenous in size of particle. This finding supported the result for particle size and size distribution in Figure 4.1 and Figure 4.2.

4.8.2. Encapsulation Efficiency of Microparticles

The encapsulation efficiency was determined by both indirect methods. The indirect method determined amount of free drug in supernatant, but could not determine the exact amount of drug incorporated within the microparticle, so the direct method was developed for this study.

The substituted PGA polymer has a good solubility in dichloromethane (DCM) while DXMP was soluble in water. Several ratios between DCM and water were applied to get optimum extraction of DXMP from modified PGA polymer. The 97 % recovery of DXMP could be obtained using solvent combination DCM : water (1:4). One part of DCM was used to dissolve the modified PGA polymer then 4 part of water was added to dissolve DXMP. The water phase was analysed using HPLC while the organic phase was diluted with methanol to obtained dexamethasone (DXM) which is the

degradation product of DXMP [184]. The method of DXMP determination using HPLC was adopted from Puri. S (2007) [184]. The total concentration of DXMP is the concentration of DXMP in water phase and the dexamethasone concentration in organic phase.

A similar method was applied to extract SIM from modified PGA polymer. Due to high solubility in methanol, SIM was extracted using methanol. The 96.1 % SIM was recovered by extraction using a combination of DCM:methanol (1:4). The method for SIM determination using HPLC was adopted from Qutachi (2012) [185].

Dexamethasone phosphate (DXMP) was encapsulated within modified PGA polymer using double emulsion method. This method was applied to encapsulated hydrophilic drugs as described in Tewes *et al* (2007) [88]. Two variations of inner phase (W/O) volume ratio were investigated to obtain the high encapsulation efficiency. The highest encapsulation efficiency was obtained in lower inner phase ratio (1:200 of water in organic). The strong relationship between ratio inner phase and encapsulation efficiency for hydrophilic drug had been reported by Liu (2006) [186]. In this research, the small volume of water as inner phase increased the encapsulation efficiency of insulin within poly(lactic acid)-poly(lactic glycolic acid) (PLA-PLGA) microparticle. The observed increase in DXMP encapsulation within modified PGA microparticles could be attributed to lower volume of aqueous inner phase. By using small volume of inner phase, the loss of drug during coalescence process with outer phase could be prevented [187]. Figure 4.14 also showed the encapsulation efficiency of DXMP was influenced by properties of polymer. The 40%C_{18}-PGA-PEG-MIHA MP exhibited a higher encapsulation efficiency of DXMP due

to presence of PEG as a hydrophilic linker. The presence of hydrophilic linker might increase precipitation and solidification rate of MP during preparation, hence improving encapsulation efficiency of drug. In addition, the presence of PEG could stabilize primary emulsion increasing encapsulation efficiency of DXMP [164].

Due to the lower encapsulation efficiency of DXMP into modified PGA MP, the encapsulation efficiency of SIM was investigated. SIM as an alternative active drug for inducing osteogenic formation was encapsulated within the MPs. A single emulsion method was used to prepare MP containing SIM. The interesting finding was that SIM had good incorporation within modified PGA polymers. The encapsulation efficiency of SIM within MP reached more than 50% in both 40%C_{18}-PGA and 40%C_{18}-PGA-PEG-MIHA MP. It is suggested that the encapsulation efficiency was also influenced by properties of encapsulated drug. Figure 4.27 illustrates that both DXMP and SIM had hydrophobic rings which could possibly interact with the stearoyl group in 40% stearoyl substituted PGA. As mentioned in several literatures, SIM has a higher log P compare to DXMP which is related to its hydrophobicity [188-192]. Based on this result, it is suggested that the high encapsulation efficiency of SIM within PGA microparticles was associated with hydrophobic interaction between modified PGA polymers with drug.

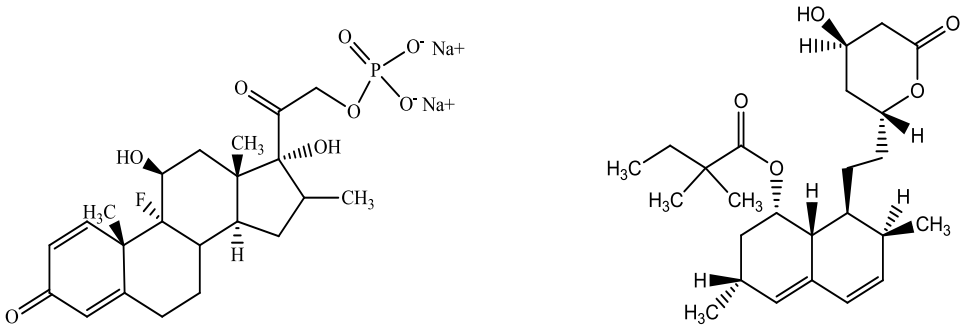

Dexamethasone sodium phosphate
Log P = 1.8
(a)

Simvastatin
Log P = 4.7
(b)

Figure 4.27. Chemical structure and Log P of DXMP (a) and SIM (b).

Beside the chemical properties of encapsulated drug, the encapsulation efficiency was influenced by concentration of emulsifier used during MP preparation. The MP preparation using PVA 0.25% exhibited a higher encapsulation efficiency of SIM within 40%C_{18}-PGA than PVA 0.5%. The effective PVA concentration has been reported by Feczko (2008) for encapsulation of bovine serum albumin (BSA) using double emulsion method. This study reported that the optimum PVA concentration to obtain the highest encapsulation efficiency of BSA is in the range 1-2%. Further increase in PVA concentration will decrease the encapsulation efficiency of BSA [193]. Other studies also reported that high emulsifier concentration is needed to stabilize the emulsion and obtained high encapsulation efficiency of BSA [164]. In contrast with two previous findings, the encapsulation of SIM was decreased with increasing PVA as emulsifier. It might be related to hydrophobicity of SIM. Since the

concentration of PVA increased, it would facilitate SIM to diffuse rapidly to the outer phase leading to lower encapsulation of SIM inside the microparticle.

The polymer concentration in organic phase also played an important role in encapsulation efficiency. As illustrated in Figure 4.16, the encapsulation efficiency increased more than 3 times when the polymer concentration in organic phase increased from 0.5 to 5 %. This present finding seems to be consistent with other research by Mehta *et al* (1996) which found that peptide incorporation increased from 53% to 71% with increasing polymer concentration from 20% to 32.5% [194]. It is related to the high viscosity of polymer in organic solvent leading to a rapid solidification of polymer to form MP [164].

4.8.3. Drug Release from Microparticles

The release study from MP containing DXMP showed less than 14% DXMP had been released from 40%C_{18}-PGA and 40%C_{18}-PGA-PEG-MIHA MP. More than 50% of DXMP was retained in 40%C_{18}-PGA MP and around 37% of DXMP was retained in 40%C_{18}-PGA-PEG-MIHA MP after 21 days release experiments. The stearoyl substitution in PGA polymer backbone might interact strongly with DXMP and prevent drug diffusion from MP. In previous study by Puri *et al* (2008) it was shown that increasing percentage of caprylic (C_8) substitution in PGA polymer would reduce burst release of DXMP due to strong interaction between DXMP and caprylic group in modified PGA polymer [180]. The strong interaction seems to have occurred between DXMP and stearoyl in substituted PGA polymer leading to high amount of DXMP retained in microparticle. However, MIHA-PEG-NH_2 linker attachment to modified PGA polymer showed a little enhancement of DXMP diffusion from MP as described in Table 4.4

An initial rapid release occurred in MP containing SIM. According to encapsulation efficiency, SIM interacts very well with modified PGA polymer and so burst release should not happen. This unexpected finding might be related to formulation of MP, hence the release study of SIM from solid dispersion was investigated. In solid dispersion, some critical factors in MP preparation such as polymer concentration and emulsifier were eliminated. Therefore, release of drug from polymer was mainly influenced by drug and polymer interaction.

The SIM was released slowly from solid dispersions and could be maintained up to 16 and 18 days in 40%C_{18}-PGA and 40%C_{18}-PGA-PEG-MIHA polymer, respectively. There was no burst release of SIM released from solid dispersions. However, only a low amount of SIM could be extracted from solid dispersions and the mass balance of SIM in solid dispersions was incomplete. Around 50% of SIM was released from the solid dispersions by the end of release study, but only less than 2% of SIM was remained in the polymers. It is hypothesised that SIM interacted strongly with the polymer and was not fully extracted from solid dispersions using DCM:MeOH (1:4). According to this hypothesis, the burst release of SIM from modified PGA MP was related to MP formulation. Yeo *et al* (2004) described that the reason of initial burst release cause by diffusion of drug through preformed water channel and related to solidification rate of dispersed phase during particle preparation. These factors related to molecular weight of polymer, hydrophilicity of polymer, drug loading, polymer concentration and PVA concentration in continuous phase [164].

The initial rapid release of SIM still occurred in 0.5% and 5% polymer concentration. However, MP prepared with 5% polymer concentration had a lower of total amount

of SIM released. The higher polymer concentration related to rapid solidification rate and high viscosity of polymer that could inhibit the drug diffusion from the matrix [164, 195]. The initial rapid release on the MP might be related to PVA as emulsifier in microparticle preparation.

Effect of PVA concentration in continuous phase was investigated in MP prepared with 0.5% and 5% polymer concentration. There was no significant difference ($P>0.05$, $n=3$) in release profile between PVA 0.25% and 0.5% prepared with 0.5% polymer concentration. Both of them showed rapid initial release (around 90%) at the first day.

In contrast, PVA concentration had a significant influence on SIM release from MP prepared with 5% polymer concentration. As illustrated in Figure 4.22, reducing PVA concentration could decrease initial release of SIM from MP prepared from 5% polymer concentration. The PVA as emulsifier might be entrapped within the microparticles, then, increasing of PVA concentration would enhance drug diffusion from MP and drug solubility in medium. This finding is in contrast to a previous finding by Mao *et al* (2007) where increasing PVA concentration is related to a reduced burst release in PLGA microparticle prepared with double emulsion technique. According to this study, increasing the PVA concentration could stabilize emulsion droplets that avoid mass drug transfer to the medium [195]. However, this explanation assumed that the PVA is located on the surface of MP, hence the diffusion of drug could be restricted by increasing viscosity of medium related to PVA concentration. Moreover, the different method of MP preparation investigated in

this research (single emulsion) and previous research (double emulsion) might influence the result obtained.

The concentration of PVA also influenced the extraction of SIM from MPs. As seen in Table 4.8, the amount of SIM could be extracted from modified PGA MPs prepared with various PVA concentrations are under 2%. However, there is a correlation between PVA concentration and amount of drug retained in MPs. Since the determination process involved SIM extraction from MPs, increasing concentration of PVA during MPs preparation would increase the SIM extracted from MPs. It is related to the increasing drug solubility in medium during extraction process due to addition of PVA in MPs formulation.

4.8.4. Ligand Attachment to Microparticles

Iminothiolane-modified collagen showed specific covalent attachment with 40%C_{18}-PGA-PEG-MIHA MP. The thiol group in modified collagen was attached to MP *via* maleimide group provided on polymer. In this study, the reaction was carried out in PBS buffer pH 7.2. According to Hermanson (2008), specific reaction between maleimide with sulfhydhryl group proceeds in pH range 6.5-7.5. In this reaction, one of the carbons in near the maleimide double bond is attacked with thiolate anion leading to the disappearance of maleimide double bond after sulfhydhryl addition [150]. As illustrated in Figure 4.25, as the amount of modified collagen increased, the amount of collagen attached also increased. However, the amount of collagen attached to microparticle reached a maximum suggesting that the maleimide group had been saturated with thiol group from modified collagen.

However, non-specific attachment of iminothiolane-modified collagen on 40%C_{18}-PGA MP was found. In 40%C_{18}-PGA MP, iminothiolane-modified collagen was attached to MP at around around 40% lower than amount attached to 40%C_{18}-PGA-PEG-MIHA MP. The non-specific attachment of protein on the surface of the MP was also found in maleimide-functionalized-poly(ethylene glycol)-poly(caprolactone) nanoparticle decorated with bovine serum albumin (BSA). Gindy *et al* (2008) reported in their study that BSA could be attached to non-functionalized poly(caprolactone) nanoparticle at approximately 15% lower than BSA attached to functionalized poly(caprolactone) nanoparticle. The research by Gindy *et al*.,(2008) was carried out in sodium chloride (NaCl) containing ethylene diamine tetraacetic acid (EDTA) pH 6.2-6.5 with efficiency of BSA attachment around 22% [196]. According to the result in Table 4.9, the efficiency of collagen attachment to 40%C_{18}-PGA-PEG-MIHA MP could reach 28% using PBS pH 7.2 as medium for reaction.

4.9. Conclusion

The MP has been prepared using two types of modified PGA polymers: 40%C_{18}-PGA and 40%C_{18}-PGA-PEG-MIHA. Physical characterisations including particle size, morphology, zeta potential, encapsulation efficiency as well as the release profile of drugs from microparticle have been investigated. In addition, the ability of 40%C_{18}-PGA-PEG-MIHA microparticle to bear maleimide functional group for ligand attachment had been successfully evaluated. However, the success of MP preparation is influenced by several critical factors during formulation process.

The attachment of MIHA-PEG-NH_2 linker to 40%C_{18}-PGA affected the particle size and size distribution of particle. Moreover, the speed of homogenisation needs to be controlled to achieve desirable size. The concentration of emulsifier such as PVA in continuous phase also affected the particle size. A higher of PVA concentration in continuous phase gave finer particle and better size of distribution. The increasing of PVA concentration in continuous phase had greater effect on size for MP prepared from 40%C_{18}-PGA.

The stearoyl substitution and MIHA-PEG-NH_2 linker attachment in PGA polymer backbone affected zeta potential value of formed MPs. The 40% stearoyl substitution decrease the zeta potential of MP to the lower negative value, however, further attachment with MIHA-PEG-NH_2 linker increase the zeta potential of MP to the higher negative value. The attachment of iminothiloane-modified collagen to 40%C_{18}-PGA-PEG-MIHA MP slightly changed the zeta potential of MP to lower negative value due to overall charge on the collagen molecule.

The volume ratio of inner phase for DXMP incorporation influenced the encapsulation efficiency. Reducing volume ratio of inner phase (W/O) from 1/20 to 1/200 increased the DXMP encapsulation efficiency in both 40%C_{18}-PGA and 40%C_{18}-PGA-PEG-MIHA MP as the small volume of soluble drug in water-inner phase prevented the loss of drug during coalescence process with outer phase. However, the interaction between polymer and drug also influenced the encapsulation efficiency. The modified PGA polymers showed a better interaction with SIM, indicated by a higher encapsulation efficiency of SIM within the MP. The encapsulation efficiency is also influenced by PVA concentration in continuous phase

and polymer concentration. In this study, a high PVA concentration would decrease SIM incorporation within MP while increasing polymer concentration in organic phase increase the encapsulation efficiency of SIM.

The release of drug from modified PGA MP strongly influenced by formulation process such as polymer concentration and PVA concentration in continuous phase. The modified PGA polymers themselves had ability to release drug slowly in controlled manner. The MP prepared from 5% polymer concentration had a lower diffusion of drug from MP than MP prepared from 0.5% polymer concentration. In addition, an increased PVA concentration in continuous phase during microparticle preparation encouraged rapid diffusion of drug from microparticle.

The maleimide functional group in 40%C_{18}-PGA-PEG-MIHA MP showed ability to interact specifically with thiol group provided on iminothiolane-modified collagen. The iminothiolane modified collagen attached to 40%C18-PGA-PEG-MIHA MP with the highest efficiency attachment of 28% in PBS medium pH 7.2.

CHAPTER 5

5. AGGREGATE FORMATION USING MICROPARTICLES

5.1. Introduction

The formation of aggregates as three dimensional (3D) structures of cells is useful to mimic *in vivo* behaviour of the cells and obtain functional substitutes for tissue replacement. Cell aggregates can be used as tools to evaluate tissue developments, cell interaction, viability and migration, cell differentiation [5, 197, 198] and to test drugs. Moreover, the formation of 3D structure of cells could be enhanced by extra cellular matrix (ECM) production and metabolic activity rather than in single cells [199].

The development of 3D culture system could be used as an *in vitro* technique to improve accuracy of analysis [5]. The formation of cell aggregates can be achieved using several methods such as the aggregation using spinner flasks, hanging drop method and manipulation of cell surface chemistry [7, 10, 200, 201]. However, these methods have several drawbacks including cell necrosis formation during spinning rotation, variable ability to deliver bioactive molecules due to difficulties with changing the medium in hanging drop method [202] and possibility of chemical toxicity in chemistry surface modification.

A possible alternative is to assemble cell aggregates using microparticles (MP). Microparticles can be used as micro-carriers to form cell aggregates as described in previous study by Rimmer (2009) and Tan *et al* (2010) [114, 127]. Microparticles are mixed with a suspension of the cells to form a 3D assembly of cell-MP aggregate. In this example, MP act as matrices for cells to aggregate, proliferate and differentiate. In addition, MP can be used as a reservoir for bioactive molecules and controlled release directly within the aggregate [36, 40].

However, the possibility of forming cell aggregates using MP is influenced by surface interaction between MP materials and cells. In this study, PGA polymer has been modified with 40% stearoyl (C_{18}) substitution and attachment of MIHA-PEG-NH_2 linker to the polymer backbone. Further modification by attaching collagen as ligand was done to encourage specific interaction between MP and cells. The influence of MP on cell behaviour is investigated to assess the suitability of these materials for cell aggregation, proliferation and differentiation.

The aim of this chapter is to evaluate interaction between cell and empty modified PGA MPs by investigating aggregate formation with mouse embryonic (mES) and primary osteoblast cells. The average MP diameters used in this experiment are ranging from 5.9 to 7.9 µm, while the cells size ranging from 10-15 µm (for mES) to 20-30 µm (for osteoblasts). Therefore, the MP hypnotized act as “glue” to mediated cell-cell interaction. The specific environment was created in order to incorporate modified PGA MPs within cell aggregate together with the evaluation of aggregate formation. Effect of cells to MP ratios on aggregate formation was also investigated.

Finally, the cell growth and proliferation within the cell-MP aggregates was evaluated through metabolic activity assay.

5.2. Interaction of Microparticles with Cells

5.2.1. Formation of aggregate with mES cells

The interaction between modified PGA MP and mES cell was investigated using empty MPs without active drug. The characteristics of MP used in the experiment are described in Table 5.1.

Table 5.1. Characteristics of microparticles used to interact with mES and osteoblast cells. The empty modified PGA microparticles were prepared using emulsification method.

Polymer concentration in organic phase	:	0.5%
PVA concentration	:	2.5%
Particle size (µm)±SD		
40% C_{18}-PGA MP	:	7.9 ± 0.56
40% C_{18}-PGA-PEG-MIHA MP	:	5.9 ± 0.64
40% C_{18}-PGA-PEG-MIHA MP+Collagen	:	6.5 ± 0.70
Zeta potential (mV)±SD		
40% C_{18}-PGA MP	:	-18.3 ± 1.60
40% C_{18}-PGA-PEG-MIHA MP	:	-25.2 ±2.19
40% C_{18}-PGA-PEG-MIHA MP+ collagen	:	-20.1 ± 1.30

The MP were added to non-tissue culture treated 96- well plate at a concentration of 10^4 MP per well. The mES cells were then seeded into the wells at ratio of 1:1 MP to cells. The total volume of medium in each well was 200 µl. Aggregate formation was investigated every 2 hours after the plate was placed on a multifunction rotator at 15 rpm in 37°C incubator (Chapter 2 section 2.4.6). The formation of aggregates in mES cell is shown in Figure 5.1.

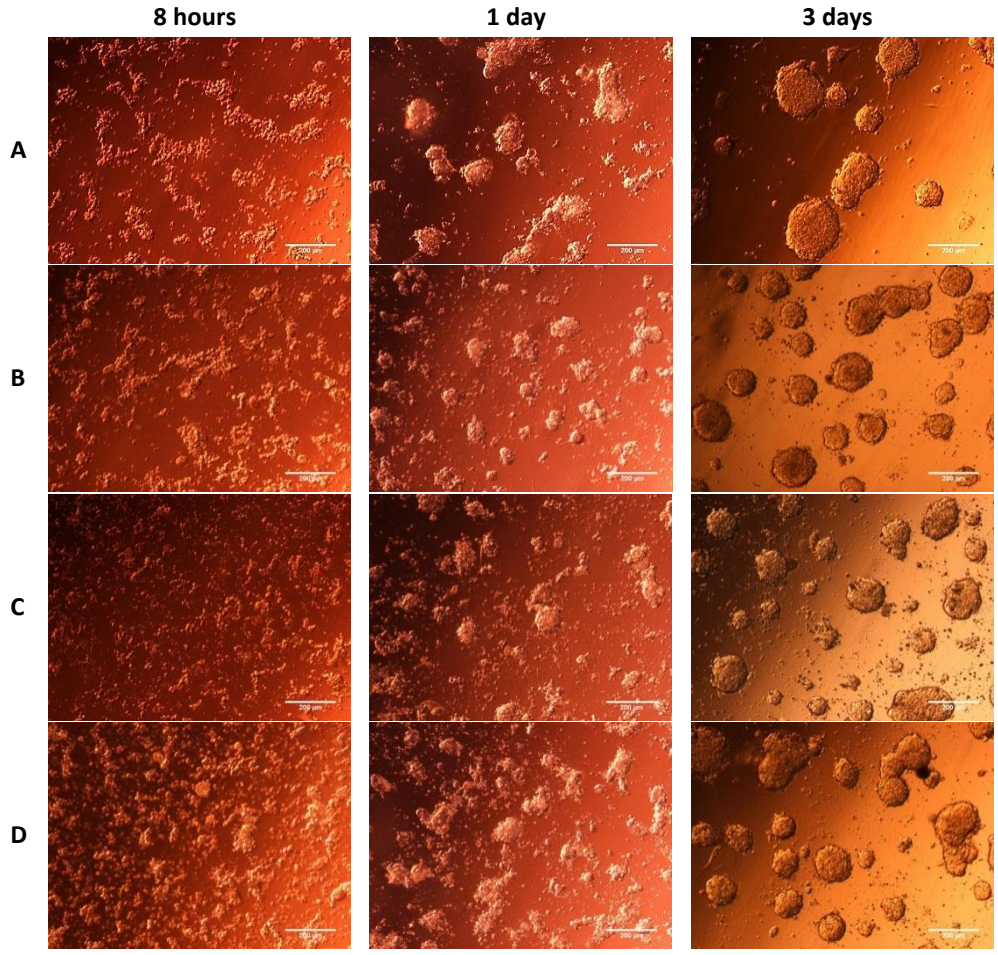

Figure 5.1. Aggregate formation of mES cell in control (without microparticles) (A), with 40%C_{18}-PGA MP (B), with 40%C_{18}-PGA-PEG-MIHA MP (C), and with 40%C_{18}-PGA-PEG-MIHA MP + collagen. The mES cells were mixed in mass suspension (at density 10^4 cells per well) with modified PGA MPs at ratio 1:1 in non-tissue culture treated 96-well plates. The plate was continuously rotated 15 rpm for 6 hours. Scale bar represents 200 µm.

Two hours after moving to static condition (8 hours), some cluster formation of cells had been found in all conditions. Since the mES have self-aggregating properties, the aggregates also formed in condition without MP (Figure 5.1-A). The highest number of single cell still appeared with 40%C_{18}-PGA-PEG-MIHA MP at 8 hour (Figure 5.1-C). Spheroid aggregates were formed in the control at day 1, whereas with modified PGA

MPs, the cells tended to form smaller and loose aggregates. At day 3, the aggregates became more compact in all conditions. Some aggregates coalesced to form larger irregular aggregates as shown in Figure 5.1-D. The control cell formed few aggregates compared to the cell with MPs. However, the aggregate in control group seemed to be larger suggesting the presence of more cells involved in individual aggregates.

The two perpendicular diameters were measured accros the centre of aggregate and the average value from each aggregates was taken as described in Chapter 2, section 2.4.7. The average diameters of mES aggregates over time in culture is shown in Figure 5.2 and reveal that the diameter of aggregates increased over the period of cell culture. The increase in diameter seems to be related to coalescence of several aggregates after several days of cell cultureand is also supported by data in Figure 5.3 which showing that the number of aggregates in each well decreased with the longer periods of cell culture.

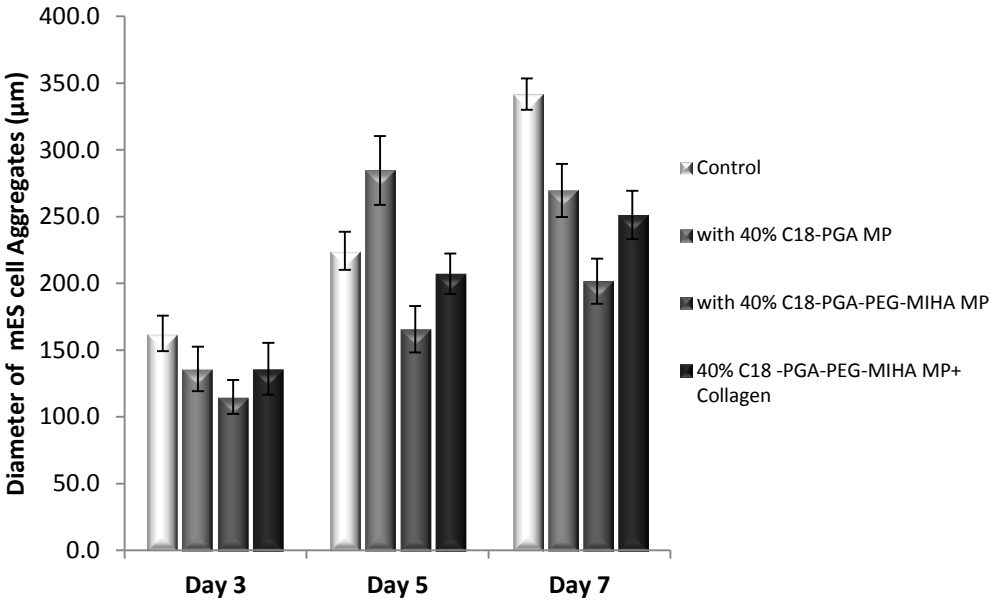

Figure 5.2. Diameter of aggregates in mES cell in the presence of modified PGA MP. The diameter is an average of two perpendiculars diameter on each aggregate in three random selected area of each well at day 3, 5 and 7 (n=15). Bars represent SEM.

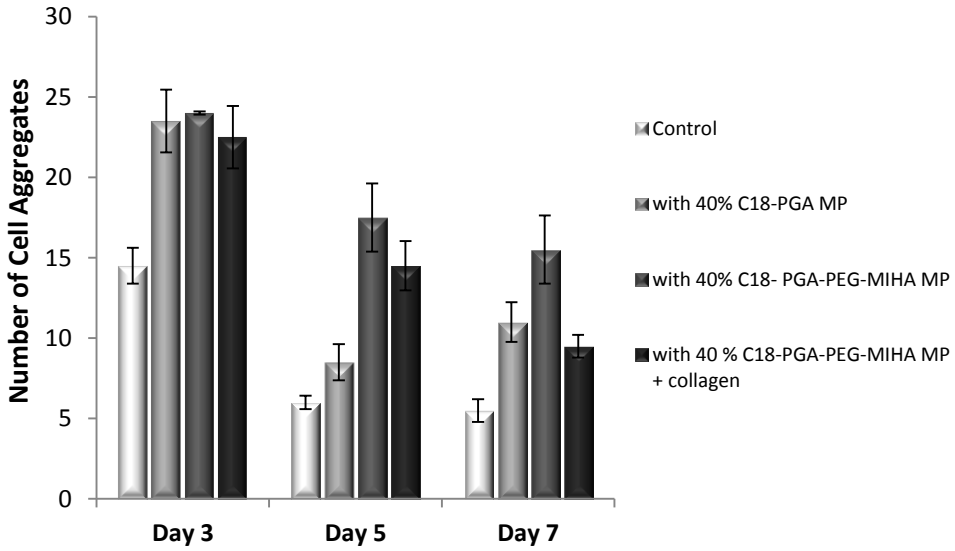

Figure 5.3. Number of mES cell aggregates in the presence of modified PGA MP. The number of aggregate was counted at three random selected area of each well at day 3, 5 and 7 (n=15). Bars represent SEM.

The incorporation of MP within cell aggregates was evaluated by dissociating 3-day old aggregates using trypsin (Chapter 2 section 2.4.8). The number of MP incorporated within cell aggregates was counted relative to the number of cells from the dispersed aggregates. This value could be useful to evaluate and estimate the interaction between MPs and cells by counting how many particles could be incorporated within a certain number of cells. The percentage of MP within mES cell–MP aggregates is shown at Figure 5.4.

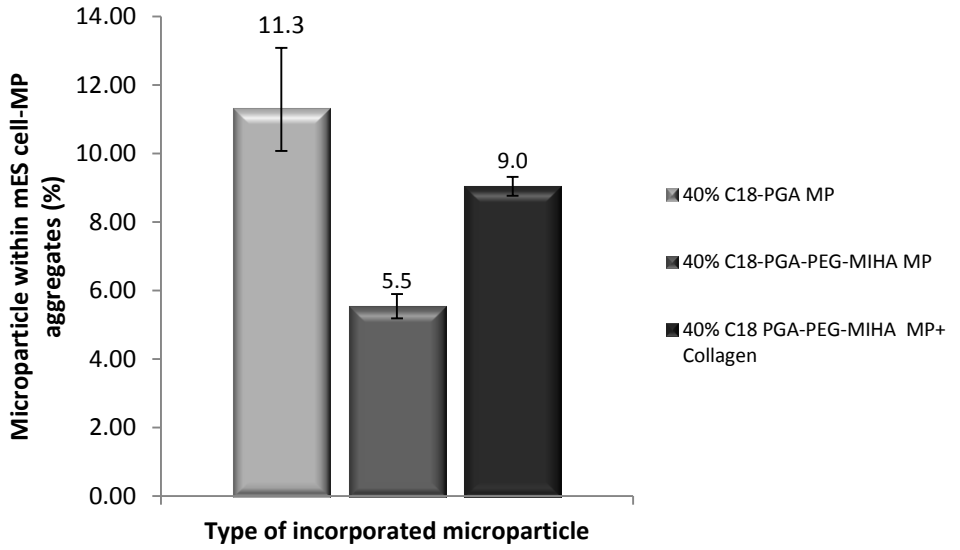

Figure 5.4. The percentage of microparticles within 3-day old mES cell-MP aggregates. The microparticles and cell were counted from three random selected areas in each well (n=15). The number of microparticle was calculated relatively to the number of cell which constructs aggregates. Bars represent SEM.

It can be seen from Figure 5.4 that the MP prepared from 40%C_{18}-PGA had the highest number of MP with the aggregates. However, the result showed no significant difference with MP prepared from 40%C_{18}-PGA-PEG-MIHA MP+ collagen ($P>0.05$, $n=5$). In contrast, the MP prepared from 40%C_{18}-PGA-PEG-MIHA showed the

lowest number with relative number of MP incorporated within aggregates being almost half as low as the two other formulations. By attaching the collagen on the surface of 40%C_{18}-PGA-PEG-MIHA MP, the percentage of microparticle within aggregates was increased. The increased percentage of 40%C_{18}-PGA-PEG-MIHA MP + collagen was almost double compare to the 40%C_{18}-PGA-PEG-MIHA MP without collagen attachment.

5.2.2. Aggregate formation with osteoblast cell

The empty modified PGA MPs were mixed with osteoblast cells to evaluate their interaction and ability of the MPs to encourage cell aggregation. Similar to studies with mES cells, osteoblast cells were seeded with MP in ratio 1: 1 and the plate was placed in a multifunctional rotator (15 rpm, 37° C) for 3 hours and then moved to static condition. The aggregate formation with osteoblast cells is shown in Figure 5.5.

The osteoblast in non-tissue culture treated plates formed a monolayer of cell a few hours after mixing with the MPs. The cells started to detach and pulled out from the edge of plate as a layer at 8 hours. At day 1, the area of cell detachment became wider. The osteoblast cells formed a clump with some of cell monolayer still attached to the plate. At day 3, the cells rolled over to form one spherical compact mass and fully detached from the plate except for control. Some small aggregates was found around the control of osteoblast without MP (Figure 5.5-A). Further evaluation was carried out to determine diameter of aggregate in osteoblast cell.

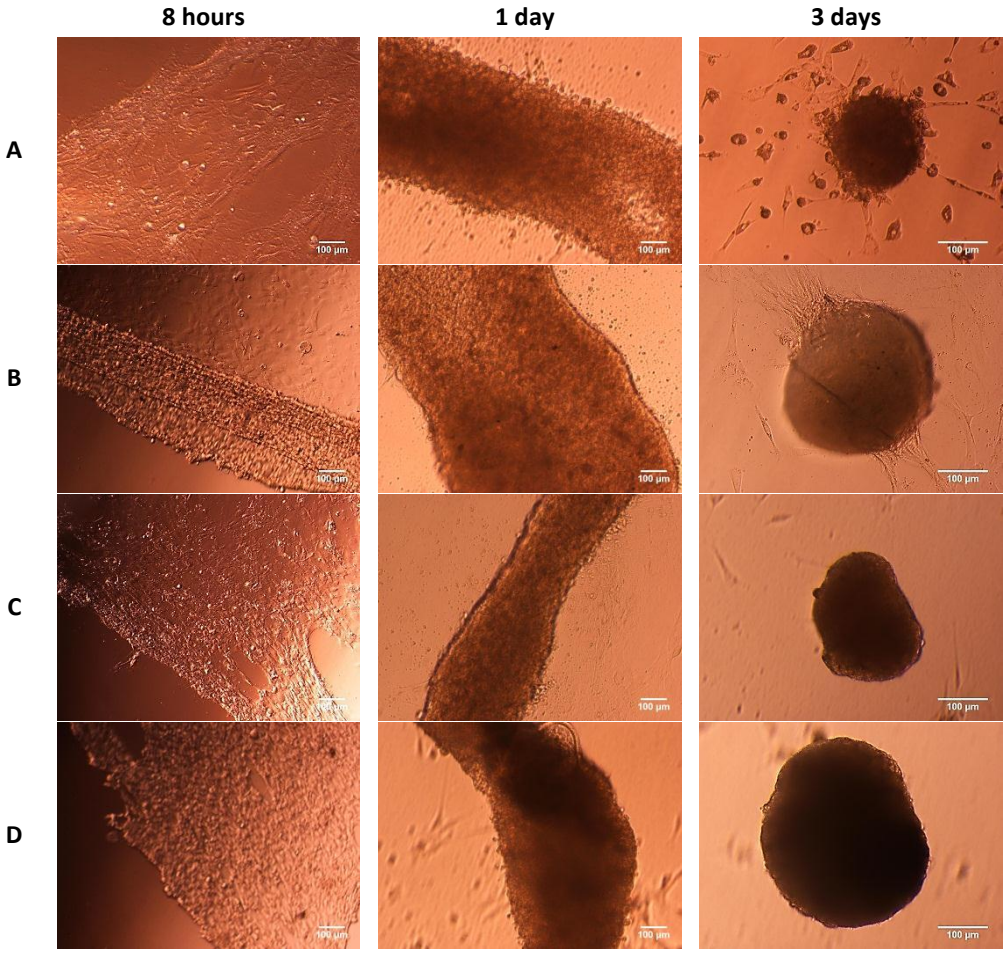

Figure 5.5. Aggregate formation with primary osteoblast cell in control (without microparticle) (A), with 40%C_{18}-PGA MP (B), with 40%C_{18}-PGA-PEG-MIHA MP (C), and with 40%C_{18}-PGA-PEG-MIHA MP + collagen. The primary osteoblast cells were mixed in mass suspension (at density 10^4 cells per well) with modified PGA MPs at ratio 1:1 in non-tissue culture treated 96-well plates. The plate was continuously rotated 15 rpm for 3 hours. Scale bars represent 100 µm.

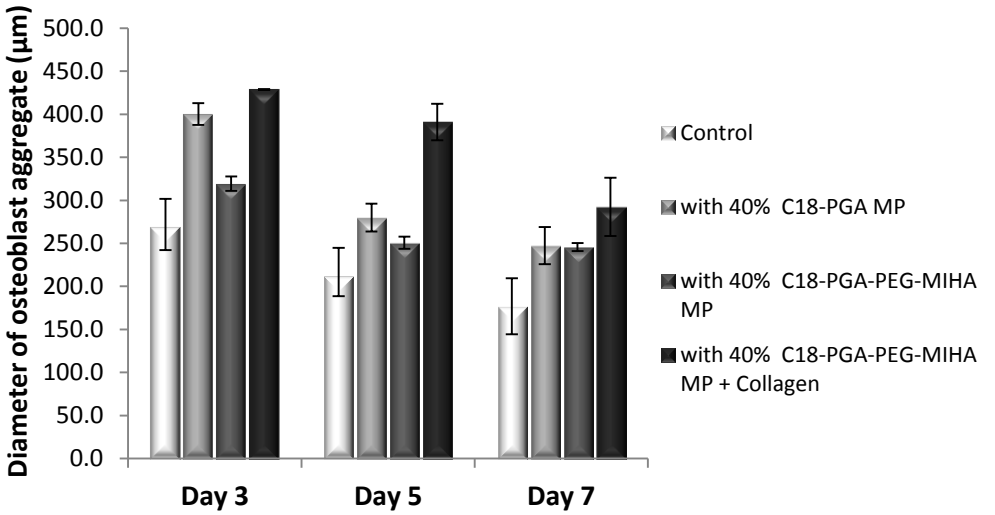

Figure 5.6. Diameter of aggregates from osteoblast cells in the presence of modified PGA MPs. The diameter is an average of two perpendiculars diameter on osteoblast aggregate at day 3, 5 and 7 (n=5). Bars represent SD.

The diameter of osteoblast aggregates was evaluated at day 3, 5 and 7. The diameter of osteoblast aggregate reduced gradually with longer time in culture. The aggregates seemed to form more compact mass of the cells. The mixing of MP within osteoblast cells generated larger aggregates compared to the control. The largest aggregates were formed with osteoblast cells and 40%C_{18}-PGA-PEG-MIHA MP+ collagen attachment, followed by the osteoblast cell with 40%C_{18}-PGA MP and the osteoblast cell with 40%C_{18}-PGA-PEG-MIHA MP. The numbers of MP incorporated within the aggregate also determined at day 3 by dissociating the osteoblast aggregate using trypsin.

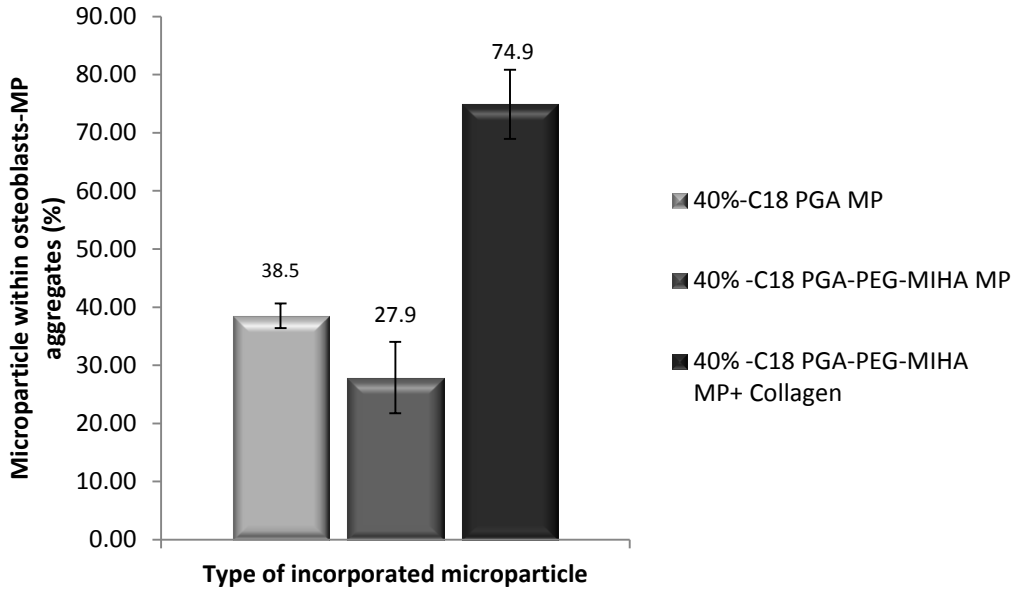

Figure 5.7. The percentage of microparticles within 3-day old osteoblast-MP aggregate. The microparticles and cell were counted from three random selected areas in each well (n=15). The percentage of microparticle was calculated relatively to the number of cell which constructs aggregates. Bars represent SEM.

The percentage of microparticle within osteoblast-MP aggregates was calculated relative to the number of osteoblast. As seen in Figure 5.7, the 40%C_{18}-PGA-PEG-MIHA MP+ collagen had the highest number within osteoblast cell. Without iminothiolane-modified collagen attachment on the surface of MP, the 40%C_{18}-PGA-PEG-MIHA MP exhibited the lowest number of MP within osteoblast aggregates. However, the percentage of 40%C_{18}-PGA-PEG-MIHA MP incorporated was similar to the percentage of 40%C_{18}-PGA MP incorporated within osteoblast at day 3 ($P>0.05$, $n=5$).

5.3. Effect of Microparticles/Cells Ratio on Aggregate Formation

The ability of modified PGA microparticle to encourage cell aggregation is difficult to evaluate since the mES cell naturally tend to aggregate to form embryoid bodies in

the absence of leukemia inhibitory factor (LIF) [202]. This natural aggregation is evident from Figure 5.1 but in the presence of MP there seems to be a change in aggregate formation with a general reduction in the diameter of aggregates.

In order to investigate effect of MP on mES cell aggregate formation, various MP to cell ratios were investigated based on diameters of aggregates, the number of aggregate formed and the number of single cells not involved in aggregate formation. This was done by microscopy analysis of the of mES cell aggregates in various MP: cell ratio.

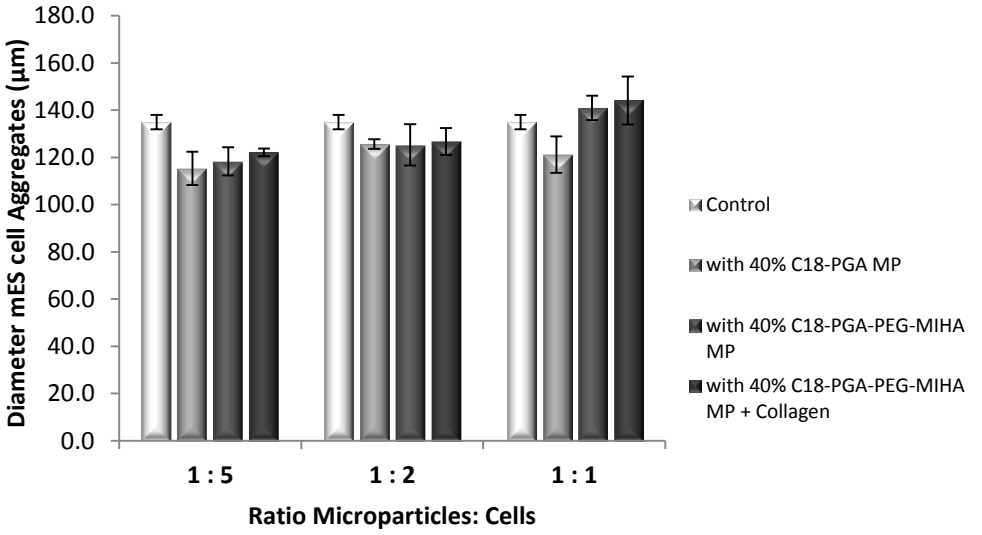

Figure 5.8. Diameter aggregates in mES cell in the presence of modified PGA MP with various ratios of microparticles to cells. The diameter is an average of two perpendicular diameters on each aggregate in three random selected areas of each well at day 3 (n=15) Bar represents SEM.

Figure 5.8 shows the diameter of mES aggregate with several MP to cells ratio. Incorporation of MP within mES resulted in aggregates with lower diameters compared to the control. This suggested that incorporation of microparticle might

disrupt aggregate formation in mES cell. Figure 5.8 shows that the diameter of mES cell aggregates was decreased with the reduction amount of MP mixed with the cells. It is suggested that increasing in diameter of aggregate in mES cell related to increasing number of particle entrapped in the mES cell aggregate. By reducing the amount of seeded MP to the mES cell, the aggregate exhibited lower diameter.

The number of aggregates and single cells from random selected areas in each well is presented in Figure 5.9 and Figure 5.10.

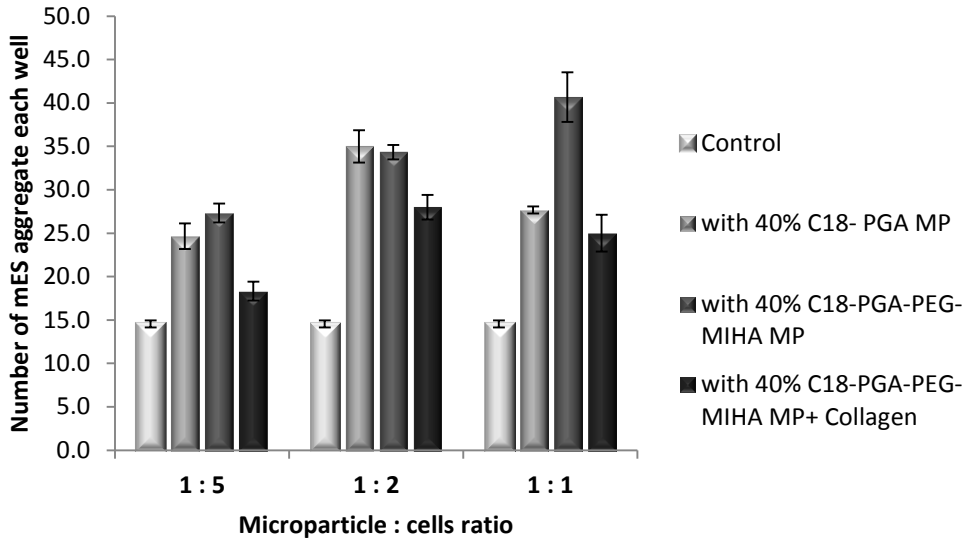

Figure 5.9. Number of mES-MP aggregates in each well. The number of aggregates was counted by image analysis in three selected random areas in each well at day 3 (n=15). Bar represents SEM.

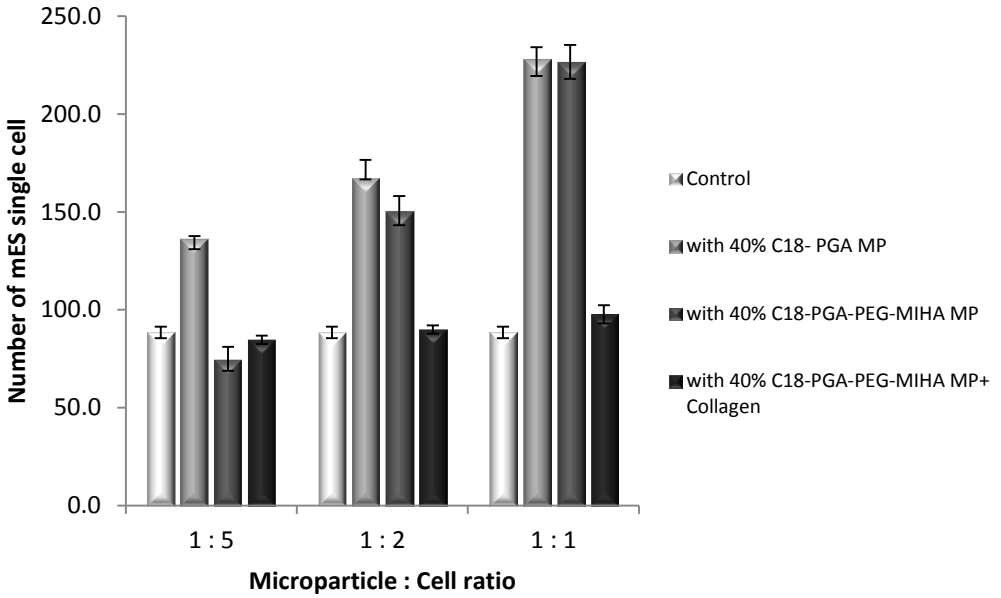

Figure 5.10. Number of single cell mES not involved in aggregation. The number of single cell was counted by image analysis in three selected random areas in each well at day 3 (n=15). Bar represents SEM.

The number of aggregates was reduced relative to lower ratio of microparticles to cells. This trend was clearly seen with 40%C_{18}-PGA-PEG-MIHA MP (Figure 5.9). However, although a high number of aggregate was found in mES with 40%C_{18}-PGA-PEG-MIHA MP, a high number of single cells was also found under the same conditions (Figure 5.10). The high number of single cells likely occurred due to the lack ability of 40%C_{18}-PGA-PEG-MIHA MP to support aggregate formation in mES. Control experiment, with cells and no MP exhibited the lowest number single cells and indicated that the aggregate formation in mES was more effective in the absence of MP. The control group formed less aggregates with larger diameter as shown in Figure 5.8 and Figure 5.9. It can be seen from Figure 5.10 that the number of single cell was reduced proportionally with the reduction in amount of MP to the cell except for the condition with 40%C_{18}-PGA-PEG-MIHA MP+ collagen. The condition

with 40%C_{18}-PGA-PEG-MIHA MP+ collagen revealed the number of aggregates and single cells was similar to the control. It is suggested that although the presence of MP might interrupt aggregate formation in mES cell, the attachment of iminothiolane-modified collagen on the surface of MP can help form aggregates better than the MP without attachment of collagen.

The effects of MP: cell seeding ratio was also investigated in aggregate formation with osteoblasts. The numbers of osteoblast single cells not involved with aggregates could not be determined and counted under microscope because osteoblast cells presented as thin monolayers on cell culture well-plates. The diameter of the aggregate in each condition was measured and presented in Figure 5.11.

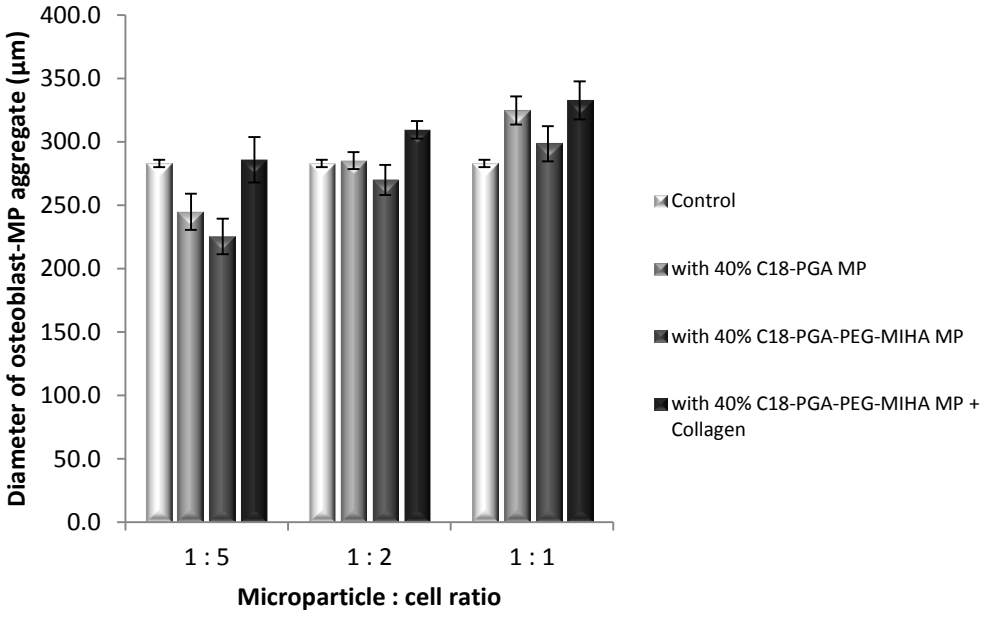

Figure 5.11. Diameter of osteoblast aggregates in the presence of modified PGA MPs with various ratios of microparticles to cells. The diameter is an average of two perpendiculars diameter on each aggregate in each well at day 3 (n=5). Bars represent SD.

The diameter of osteoblast aggregates decreased with reducing numbers of MP. The 40%C_{18}-PGA-PEG-MIHA MP+ collagen exhibited the largest aggregates in all ratios of MP to cells. In contrast, the 40%C_{18}-PGA-PEG-MIHA MP without collagen generated the lowest diameter aggregates. This result revealed that iminothiolane-modified collagen attachment on the microparticle surface could improve the ability of cell to interact with MP. Surprisingly, the good interaction between MP and osteoblast cell was also found with 40%C_{18}-PGA MP with 1: 1 microparticle to cell ratio. The cell aggregate with 40%C_{18}-PGA MP established the similar diameter with the cell aggregate containing 40%C_{18}-PGA-PEG-MIHA MP+ collagen.

5.4. Effect of Microparticles Incorporation on Cell Metabolic Activity

The cell metabolic activity was evaluated to investigate the effect of MP incorporation within cell aggregates. Metabolic activity is related to cell number as well as the viability of cells within aggregates. The Alamar Blue assay was used to determine the metabolic activity in mES and osteoblast cells aggregates as described in Chapter 2 section 2.4.10. The investigation was carried out in 7-day and 14-day old cell aggregates. The principle of Alamar Blue assay is the reduction of Alamar Blue (rezasurin solution, blue and non-fluorescent) to resorufin (pink and fluorescent) by lack of oxygen in the microenvironment during cellular metabolism [203]. The fluorescence intensity measured is related to the level of performed resorufin and indicative of the level of cell metabolic activity.

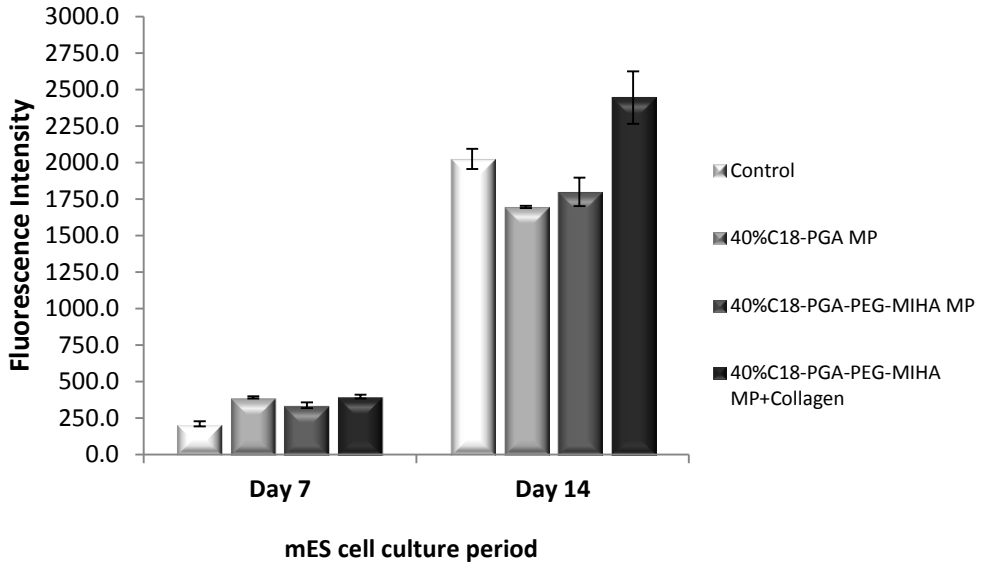

Figure 5.12. The metabolic activity of mES cell aggregates evaluated using Alamar Blue assay. The fluorescence intensity indicated the proliferation in aggregates. The Alamar blue was added to the 7 and 14-day old mES cell aggregates and incubated for 15 minutes at 37°C in the dark (n=3). Bars represent SD.

Figure 5.12 shows the fluorescence intensity measurement in mES cell aggregates. The increasing fluorescence intensity in this experiment was related to the formation of high level of resorufin which indicated more oxygen consumed in cell metabolic activity and suggesting cell proliferation. At day 7, the cell aggregates with MP had higher fluorescence intensity measurements compared with the control suggesting that the presence of MP within cell aggregate could support cell proliferation. However, the incorporation of 40%C_{18}-PGA-PEG-MIHA MP revealed the lower value of fluorescence intensity compare to the others microparticle at day 7.

Cell proliferation was also assessed on 14-day old mES aggregates. The effect of MP on supporting cell proliferation was seen with 40%C_{18}-PGA-PEG-MIHA MP+ collagen. The 40%C_{18}-PGA-PEG-MIHA MP+ collagen exhibited the highest fluorescence

intensity in 14-day mES cell aggregates. Conversely, proliferation was reduced in cell aggregate at day 14 with 40%C_{18}-PGA and 40%C_{18}-PGA-PEG-MIHA MPs, respectively.

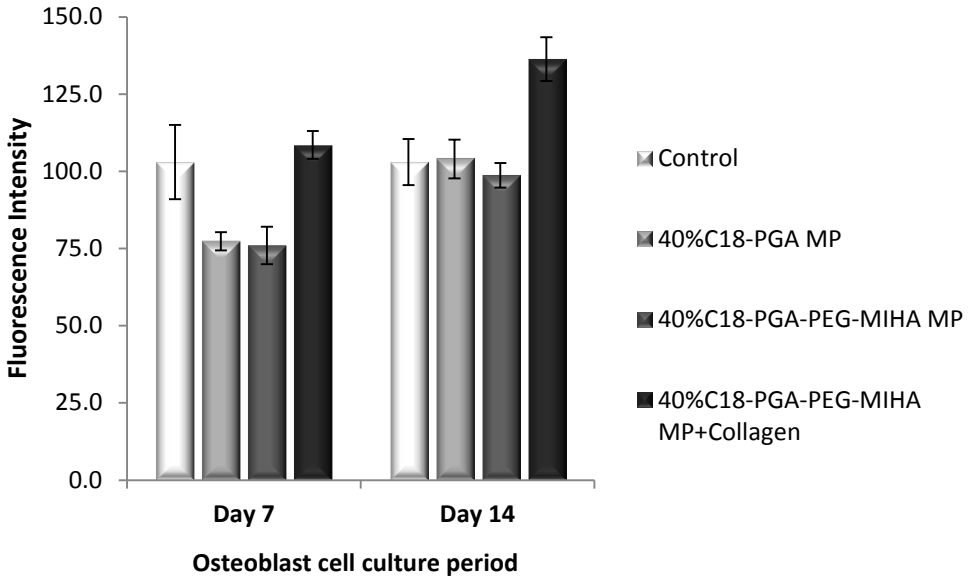

Figure 5.13. The metabolic activity of osteoblast cell aggregates evaluated using Alamar Blue assay. The fluorescence intensity indicated the proliferation in aggregates. The Alamar blue was added to the 7 and 14-day old osteoblast cell aggregates and incubated for 15 minutes at 37°C in the dark (n=3). Bars represent SD.

The cell metabolic activity in osteoblast cell aggregates was evaluated and results shown in Figure 5.13. At day 7, the metabolic activity of osteoblast aggregates with 40%C_{18}-PGA or 40%C_{18}-PGA-PEG-MIHA MPs were decreased as indicated by lower fluorescent intensity. Conversely, the cell metabolic activity was similar to the control with 40%C_{18}-PGA-PEG-MIHA MP+ collagen. Increased metabolic activity was seen with osteoblast aggregates with 40%C_{18}-PGA and 40%C_{18}-PGA-PEG-MIHA MPs at day 14 and for both was similar to the control. A significant increase in metabolic activity was seen in cell aggregates with 40%C_{18}-PGA-PEG-MIHA MP+ collagen suggesting

proliferation and increased cell numbers with 40%C_{18}-PGA-PEG-MIHA MP+ collagen on day 14 of culture.

Comparing the metabolic activities of mES and osteoblast cells, it is evident that a significant increase occurred in mES rather than in osteoblast cell. In mES, the fluorescence intensity was related to metabolic activity was increased almost 5 times within the 7 days period. At the same time, the metabolic activity of the osteoblasts increased only 1.25 times at the highest value. The 40%C_{18}-PGA-PEG-MIHA MP+ collagen showed similar effects on metabolic activity and suggested cell proliferation with both mES and osteoblast cells. However, 40%C_{18}-PGA and 40%C_{18}-PGA-PEG-MIHA MPs in mES cell led to the reduction of metabolic activity, while in osteoblasts the metabolic activity remained the same as control group.

5.5. Discussion

The formation of 3D aggregates is a useful approach to evaluate development of cells for tissue regeneration. The cell aggregates allow the investigation of cell interactions in 3D structure and the ability to support cell viability, proliferation and differentiation. The differentiation of pluripotent cell ES cells is often initiated by withdrawal of certain cytokines like LIF from cell culture medium to induce the spontaneous formation of cell aggregates, called embryoid bodies [197, 204]. Once formed cells within the aggregates proliferate and differentiate to various cell types. Although the ES cells can naturally form aggregates and differentiate without the addition of exogenous growth factors, the process needs to be controlled to develop desired cells.

Controlling the process of cell differentiation might be achieved by incorporating MP within cell aggregate. The PGA polymer used to make MP has been modified in this study to increase the exogenous bioactive molecule encapsulation within the MP. Also a collagen ligand for cell attachment has been tethered to the modified PGA polymer to increase specific interaction with cells. Here we present the ability of modified PGA microparticles to interact with mES cell and osteoblast cell to form 3D aggregates.

5.5.1. Aggregate formation in mES cell

The MP-cell aggregation was performed using mass suspension which has been widely used to perform cell aggregate in various cells type including stem cell [205-209]. Non-tissue culture treated plates were used to limit adherence to the well and to help promote cell to cell contact and encourage aggregation processes [202]. In order to optimize the aggregate formation, the plate was incubated with gentle rotatation at 15 rpm as described by Gothard *et al*.,(2009) to generate high numbers of ES aggregates in suspension culture [209].

Results from this study showed that the presence of MP with average diameter ranging from 5.9 to 7.9 µm seems to interrupt aggregate formation in mES (10-15 µm diameter) with 1: 1 MP to cell ratio and results in smaller diameter compared to control cell aggregates without MP. The presence of microparticle seems Fortunately, the diameter of aggregate in mES cell culture could be maintained below 300 µm. Previous study by Park *et al* (2007) presented that maintaining the initial size of ES aggregates below 300 µm size could be useful increasing gene expression as found in three major germ layers [204].

The diameter of MP-cell aggregates increased over time and correlated with a reduction in the number of aggregates. This suggested that agglomeration was occurring in mES aggregates. Although aggregate formation is important to induce cell differentiation, the formation of agglomerates of aggregates might inhibit cell growth as well as cell differentiation. Therefore, the balance between cell aggregation and agglomeration should be controlled in order to optimize cell growth and differentiation [210, 211]. The presence of modified PGA microparticles could be useful to prevent agglomeration in mES aggregates. As seen in figure 5.2 and figure 5.3, the increasing of diameter and decreasing of number of aggregates with MP is lower compared to control without MP.

The most obvious deviation from normal aggregation of control cells was found with 40%C_{18}-PGA-PEG-MIHA MP as shown by the lowest diameter of aggregates. This effect could be related to the effect of sterically stabilizing of MIHA-PEG-NH_2 on the surface of 40%C_{18}-PGA-PEG-MIHA MP. The hydrophilic layer of PEG on the surface of 40%C_{18}-PGA-PEG-MIHA MP provide as steric barrier to prevent interaction between cell and the microparticle and generate a low aggregate formation of mES cell.

The interaction between MP and cell also influenced the numbers of MP incorporated within the cell aggregate. The 40%C_{18}-PGA-PEG-MIHA MP exhibited the lowest percentage of MP within the aggregates and suggests lower interaction between 40%C_{18}-PGA-PEG-MIHA MP and mES cell (Figure 5.4). The incorporation of MP within cells aggregate mainly influence by surface interaction between MP and cells. The result showed that without ligand attachment, 40%C_{18}-PGA and 40%C_{18}-PGA-PEG-MIHA MP had ability to incorporate within cells aggregate indicate that the

surface of 40%C_{18}-PGA and 40%C_{18}-PGA-PEG-MIHA MP have a good interaction with mES cells. However, the best MP incorporation within cells was occurred with the presence of iminothiolane-modified collagen attached on the surface of 40%C_{18}-PGA-PEG-MIHA MP by improving the interaction between MP and cells. Collagen could be useful to mediate specific attachment between surface of MP and cell *via* integrin interaction since most of cells express integrin at their surface [135, 136]. Therefore, the 40%C_{18}-PGA-PEG-MIHA MP+ collagen showed a high proportion of MP within the aggregates. Surprisingly, the 40%C_{18}-PGA MP showed the highest proportion of MP within cell aggregate although overall there was no significance difference ($P>0.05$, $n=5$) with the percentage of 40%C_{18}-PGA-PEG-MIHA MP+ collagen within cell aggregate. The percentage of MP within cell aggregates is influenced by two factors. First, the percentage of microparticle within the aggregate is influenced by the interaction between MP with the cell. The better interaction between MP with cell leads to a higher proportion of MP. Secondly, the percentage of MP within cell aggregate is influenced by the number of cell involved in forming the aggregate. Since data on MP within aggregates was taken at day 3, there is a possibility of cells to proliferate. Hence, the increasing number of cells in aggregate would alter the ratio with MP. Further investigation is needed to evaluate the ability of MP within cell aggregate to encourage cell proliferation.

5.5.2. Aggregate formation in osteoblast cells

Unlike mES cells, osteoblasts do not typically spontaneously form aggregates in cell culture. Although this study used non-tissue culture treated plates, the osteoblasts did tend to adhere loosely and form a monolayer sheet. However, PGA MP in

osteoblast culture encouraged detachment of osteoblast cell sheet and aggregate formation in 15 rpm rotary agitation. The control group without MP in the same rotary agitation with could also form aggregates, but the cells did not fully detach from the culture plate. The formation of osteoblast aggregate has also been described in a study by Overstreet *et al* (2004) showing unexpected aggregation of osteoblasts after 3 days exposure to bear serum. The bear serum contained a molecule that could trigger cell detachment from the plate. Overstreet *et al*., (2004) explained that with the presence of bear serum in medium, the osteoblast adhered to each other and pulled as a layer from the plates. The osteoblast then aggregated and remained viable in cell medium [212]. In this study it is suggested that the modified PGA MPs acted as "glue" to mediate cell adherence and then pulled as a layer from the plate. The osteoblast could not fully detach from plate in control group since there was no MP to facilitate cell adherence.

The diameter of aggregates was determined to evaluate effect of MP on aggregate formation. The lowest diameter of aggregate was found in control group without modified PGA microparticle, while the highest diameter of aggregate was found in the presence of 40%C_{18}-PGA-PEG-MIHA MP+ collagen. The low diameter of cell aggregate in control group indicated the low number of cell involved in aggregate formation. As seen in Figure 5.5-A, some small cell aggregates presented around the main aggregate which indicated that some of the osteoblasts were not involved in constructing the main aggregate.

The presence of modified PGA microparticle exhibited larger diameter aggregates as shown in Figure 5.6 and might be explained by three reasons. First, the larger

aggregate formation related to the higher number of cells involved in aggregate formation. More cells involved would lead to the larger diameter of aggregate. Secondly, the presence of MP entrapped inside the aggregate would increase the bulk volume of aggregate as well as increasing the diameter of aggregate. The size of MP (diameter 5.9-7.9 µm) are around one third of the cells (diameter around 20-30 µm), hence incorporation of MP would increase the volume of cells aggregate. The last reason is the presence of MP could support cell proliferation in the aggregate. Since the diameter was determined in day 3, there is a possibility of osteoblast to proliferate within 3 days to form bigger aggregate. Although the MP entrapped within cell aggregate could increase the diameter of osteoblast aggregate, the incorporation of 40%C_{18}-PGA-PEG-MIHA MP with osteoblast exhibited low diameter of aggregate related to low incorporation of microparticle as illustrated in Figure 5.7. The possible effects and changes to osteoblast proliferation still remain to be investigated.

Looking at the proportion of MP within osteoblast aggregates, the highest entrapment within cell aggregate was shown by 40%C_{18}-PGA-PEG-MIHA MP+ collagen. The presence of collagen on the surface of MP could enhance interaction between MP and osteoblast as explained in section 5.5.1. The similar percentage of MP entrapment within osteoblast was obtained in 40%C_{18}-PGA and 40%C_{18}-PGA-PEG-MIHA MPs. It is revealed that the steric effect of MIHA-PEG-NH_2 linker on the surface of 40%C_{18}-PGA-PEG-MIHA MP did not affect the microparticle incorporation within osteoblast aggregate. However, since the percentage was calculated based on the

number of cell which constructs an aggregate, the proliferation of osteoblast cell might influence the result.

5.5.3. Effect of microparticles/cells ratio to aggregate formation

Due to disruption in aggregate formation in mES cell with the presence of MP, the MPs were added at lower numbers relative to cell numbers. Again analysis was performed on the diameter of the aggregates, number of aggregates in each well and also the number of single cells not involved in aggregate formation. The results show that higher amounts of MP mixed with the cells relates to lower formation of cell aggregates based on the high number of single cells not involved in aggregate formation. The number of single cell was reduced as the ratio of MP to cell was lowered. This result confirms that the efficiency of aggregate formation was influenced by the number of MP used as described in previous study by Hayashi and Tabata (2011) where aggregate formation by mesenchymal stem cell (MSC) was blocked due to excessive number of microparticle mixed with the cells. The excessive number of particle physically inhibiting contact and interaction between cells [199].

An interesting observation was noted with 40%C_{18}-PGA-PEG-MIHA MP+ collagen (Figure 5.10) where the number of single cell involved in aggregate was seemingly not affected by the number of MP. As the number of MP increase, the number of single cell not involved in aggregate formation remained constant and similar to the control. This finding supported statement in section 5.5.1 that the presence of collagen on the surface of microparticle could encourage specific interaction between microparticle and cell [135, 136].

Unfortunately, the effect of MP to cell ratio did not clearly influence osteoblast aggregate formation. The osteoblast still formed aggregates with the lower amount of MP. The decrease in diameter of osteoblast aggregates was related to the reduction in number of MP incorporated. However, the osteoblast with 40%C_{18}-PGA-PEG-MIHA MP+ collagen revealed the biggest diameter of aggregate even with the low amount of MP. It is suggested that 40%C_{18}-PGA-PEG-MIHA MP+ collagen had a good interaction and incorporation within osteoblast cell as described in Figure 5.7. This finding also supported the role of collagen to support interaction between microparticle and cell.

5.5.4. Effect of microparticle incorporation to cell metabolic activity

Since the percentage of MP within cell aggregates and diameter of aggregate in both mES and osteoblast cells were influenced by the number of cells involved in the aggregate construct, the ability of MP to support cell growth and proliferation was evaluated. The metabolic activity was related to the cell viability, cell proliferation and compatibility with biomaterial cells was assessed using the Alamar Blue assay. This method has been used widely in several studies to assess metabolic activity of cell [213-215], cell viability [215, 216] as well as cell proliferation [203, 217]. The use of Alamar Blue offers the advantage of being non-toxic to the cells with the exposure of reagent [203]. However, the accuracy of method is influenced by efficiency of reagent diffusion into the sample. Ng *et al* (2005) noted the importance of doing trials to optimize reagent concentration and incubation time to avoid saturation of signal [213]. Optimisation for incubation time had been done to avoid high fluorescent intensity produced in reduced sample (data for mES aggregate is shown

in appendix). In order to optimize the reagent diffusion to reach a whole sample, the sample was exposed to the reagent for 15 minutes in 37°C incubator.

The evaluation for cell metabolic activity was assessed at day 7 and 14 of cell culture. The fluorescence intensity related to cell metabolic activity was significantly increased at day 14 in all condition of mES cell aggregates. It is suggested that proliferation of mES was increased during 14 days of culture. Comparing the cell metabolic activity data at day 14, the highest activity was seen with 40%C_{18}-PGA-PEG-MIHA MP+ collagen. The presence of collagen on the surface of MP likely encouraged the interaction between microparticle and cell due to presence of integrin receptor on the surface of the cell which interact with collagen. As presented in previous study by Woo *et al* (2003), the presence of proteins from the material or cell itself could be useful to mediate cell growth [218].

The similar cell metabolic profile also was found in osteoblast cells culture. Although the increasing metabolic activity from day 7 to day 14 was lower than mES cells, the incorporation of modified PGA MPs increased metabolic activity of osteoblast cells. The highest metabolic activity was found with the 40%C_{18}-PGA-PEG-MIHA MP+ collagen within osteoblasts aggregate.

This result revealed the biocompatibility of modified PGA MP, particularly with iminothiolane-modified collagen attachment, could act as matrices to support the growth of cells in 3D constructs. Increasing the osteoblasts metabolic activity with the presence of MP is consistent with earlier finding by Hayashi and Tabata (2011). Hayashi and Tabata reported that the presence of particle within the cells aggregate

may increase the oxygen diffusion inside the aggregate. Hence, the number of live cells in aggregate with incorporation of microparticles is higher [199].

The other factor that influenced cell metabolic activity in both mES and osteoblast is the presence of collagen on the surface of microparticle. Collagen plays an important role to promote interactions between MP and cells. Collagen as component of ECM has the ability to interact with the cell through specific glycoprotein on the cells and influence the behaviour of cell including cell proliferation [151, 219]. The specific interaction between cell and collagen depends on the type of cell and collagen. Hence, certain types of cell can adhere to specific collagen [151]. Collagen type IV as a component of basement membrane [145, 219-221] was used in this study and it exhibited interesting effective interaction with mES as well as osteoblast cells. As the major component of basement membrane, the interaction between collagen and cell lead to promote cellular proliferation by formation “spider shape” structure [145, 221]. The ability of collagen type IV to support cells adhesion was reported in previous study conducted by Olivero and Furcht (1993). Olivero and Furcht conveyed that surface coating with collagen type IV endorses maximal adhesion with rabbit epithelial cells *in vitro* [222]. In addition, the role of collagen type IV for cell proliferation had been reported by Anbalagan and Rao (2004). Anbalagan and Rao informed that the presence of collagen type IV could stimulate the progenitor Leydig cells (PLC) proliferation *in vitro* by mediated intracellular signalling [223]

5.6. Conclusion

To summarize, the incorporation of modified MP at ratio of 1:1 with cells did not encourage aggregate formation in mES cells and seemed to disrupt the normal

aggregation process. In contrast, the addition of modified PGA MP at ratio 1: 1 with cell could enhance the formation of 3D structure in osteoblast cells indicated by fully detachment of osteoblast aggregate from cell culture plate.

However, the formation of aggregates with cells was determined by properties of MP and the ratio of MP to cells. The attachment of collagen on the surface of 40%C_{18}-PGA-PEG-MIHA MP could improve the aggregate formation in mES and osteoblast cells as well as increase the percentage of microparticle incorporated within cells aggregate. Surprisingly, the 40%C_{18}-PGA microparticle also exhibited a good incorporation within mES cells aggregate. In order to optimize the aggregate formation in mES and osteoblast cells, the number of microparticle should be adjusted to allow sufficient contact between microparticles and cells.

Although the presence of MP did not markedly change the aggregate formation in mES cells, the metabolism activity using Alamar Blue assay showed that the presence of 40%C_{18}-PGA-PEG-MIHA MP+ collagen increased metabolic activity of mES in 14 days culture of aggregates. The same finding also presented in osteoblast cells. The highest metabolic activity which might be related to cell proliferation was presented in osteoblasts aggregates with 40%C_{18}-PGA-PEG-MIHA MP+ collagen. In addition, the osteoblasts metabolic activity remained similar to the control group with 40%C_{18}-PGA MP and 40%C_{18}-PGA-PEG-MIHA MP. Those findings indicated that MP prepared from modified PGA polymer had ability to support cell growth in 3D constructs of cells aggregate.

CHAPTER 6

6. MICROPARTICLE INCORPORATION FOR OSTEOGENIC DIFFERENTIATION

6.1. Introduction

The control of cell differentiation and engineering of tissue formation using three dimensional (3D) cells aggregate is one approach to help obtain functional substitutes for tissue regeneration. Potentially, 3D cell aggregates formed *in vitro* can be injected at the later stage to fill a defect and restore function to the damaged tissue. This technique is a promising system for tissue regeneration particularly for bone replacement due to reducing of patient discomfort and low risk of infection [40, 41]. In order to enhance natural regeneration, the combination between cell sources, signals and extracellular matrix (ECM) should be provided. As a potential source of cell for bone replacement, the differentiation of stem cells could be induced by providing bioactive signals from growth factors or active drugs while ECM formation could be induced by formation of 3D constructs using material such as metals, ceramics, synthetic or natural polymers. The formation of 3D structure is a way for the cell to develop well-organized structure to imitate the functional characteristics of specific tissue.

Microparticle (MP) could be used as matrices for cell in 3D construct to produce ECM. Several studies had been conducted on formation of 3D cell constructs using MP for tissue replacement as described by Mercier *et al* (2005), Bible *et al* (2009) and Tan *et al* (2010) [114, 115, 224]. Most of those studies used MP as a micro-carrier to perform 3D cell aggregate for tissue transplantation. Besides acting as a matrix for cell attachment, MP could be used as a reservoir for bioactive molecules. By incorporating MP within cell aggregate, the amount of bioactive molecule incorporated could be easy to customize.

Simvastatin (SIM), a cholesterol lowering drug, is one of active molecule widely used to induce osteogenic differentiation *in vitro*. Simvastatin is a statin derivative which has ability to increase anabolic effect and gene expression for osteogenic differentiation. In addition, simvastatin involves Bone Morphogenetic Protein-2 (BMP-2) up regulation and induces production of bone matrix mineralisation [55, 74-76]. However, the effective dose and the mechanism of simvastatin for osteogenic differentiation still under investigation [75]. Active molecules or drugs usually interact with the cell through specific receptor on the surface membrane. In 3D aggregate, the delivery of molecule should be able reach not only on the surface of the aggregate but also inside the aggregate. The conventional route such as adding active molecules to the culture media is not effective way for delivery, as it is not be able to easily penetrate and reach all cells within the aggregate. Incorporating of active molecules within the polymeric microparticle is one way to facilitate the release of drug within an aggregate and could facilitate the release of drug over defined periods of time.

In this study poly(glycerol) adipate (PGA) has been modified with 40% stearoyl (C_{18}) to increase the encapsulation of drug within the polymer and attached with MIHA-PEG-NH_2 linker for specific ligand attachment on the surface of the MP. Based on studies in previous chapters, SIM had a high incorporation within the 40%C_{18}-PGA as well as 40%C_{18}-PGA-PEG-MIHA microparticles (MP). The 40%C_{18}-PGA-PEG-MIHA MP also showed ability to attach with collagen as ligand for specific interaction with cell. The release of drug from modified PGA polymer could be tailored by optimising formulation process. MP prepared from modified PGA polymers also exhibited the ability to form aggregates with mES and osteoblast cells and also seemed to enhance cell metabolic activity particularly with collagen attachment on the surface of microparticle. The aim of this chapter was to investigate delivery of simvastatin from modified PGA MPs and its effect for osteogenic differentiation in mouse embryonic stem (mES) and osteoblast cells. The osteogenic activity was assessed through alkaline phosphatase (ALP) assay, osteocalcin immunostaining and von Kossa staining for mineralisation.

6.2. Simvastatin and Osteogenic Differentiation

In order to evaluate the effect of simvastatin for osteogenic differentiation, the cells were cultured in osteogenic media containing simvastatin. The correlation between simvastatin concentration and alkaline phosphatase level was assessed on mES aggregates. The aggregate was formed by placed the mES cell in multifunctional rotator (15 rpm) for 6 hours. The alkaline phosphatase level was determined at day 7, 14 and 21 of culture. The effect of simvastatin addition to alkaline phosphatase level in mES cells is illustrated in Figure 6.1.

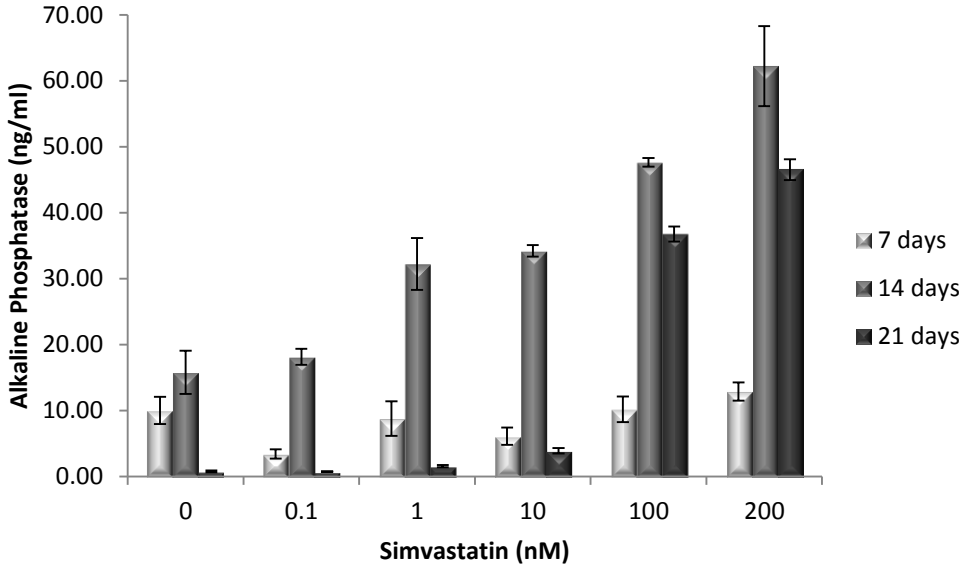

Figure 6.1. Alkaline phosphatase (ALP) level in mES cell culture treated with simvastatin ranging from 0.1 to 200 nM. The ALP was determined in 7, 14 and 21-day old cell culture using pNPP substrate. Bars represent SD (n=3).

The ALP was produced in the mES culture without simvastatin (control) at day 7 and the level is similar with the mES culture with 100 nM of simvastatin ($P>0.05$, n=3). The addition of simvastatin in the range concentration 0.1 to 10 nM to the medium reduced the level of ALP in mES below the alkaline phosphatase in control. Figure 6.1 showed that the level of alkaline phosphase at day 7 increased related to increasing of simvastatin concentration in medium.

The ALP level in mES cells culture reached the peak at day 14 of cell culture. There is positive correlation between simvastatin concentration and alkaline phosphatase level. However, there is no significant difference in mES cultured in 0.1 nM simvastatin and control ($P>0.05$, n=3). It is indicated that addition of 0.1 nM simvastatin on medium did not promote the osteogenic differentiation in mES cells.

In addition, there is also no significant difference on ALP level in mES cells at day 14 with addition of simvastatin 1 and 10 nM to the medium. Yet, the increasing concentration of simvastatin from 10 nM to 100 nM could increase alkaline phosphatase from 34.23 to 47.64 ng/ml. The level of ALP dropped to lower levels after 14 days of cell culture. This trend occurred in all level of concentration of simvastatin as well as in the control.

6.3. Simvastatin Release Profile from Modified PGA Microparticles

The optimum formulation was applied to prepare the MPs from modified PGA polymers. The release of drug for extended period was considered to be an important factor when deciding on the best formulation for MP preparation. The specification of modified PGA MP used to incorporate within cell aggregate is described in Table 6.1 and the particle size distribution illustrated in Figure 6.2.

Table 6.1. The specification of modified PGA MP used for mES and osteoblast differentiation. The microparticles were prepared using single emulsion method containing SIM as a drug.

Polymer concentration in organic phase (%)	:	5%
PVA concentration (%)	:	0.005%
Initial drug loading (%)	:	1%
MP yield (%)		
40% C_{18}-PGA MP	:	51.5
40% C_{18}-PGA-PEG-MIHA MP	:	43.0
SIM loading (%)±SD		
40% C_{18}-PGA MP	:	0.6±0.04
40% C_{18}-PGA-PEG-MIHA MP	:	0.6±0.01
40% C_{18}-PGA-PEG-MIHA MP+Collagen	:	0.5±0.01
Particle size (µm)±SD		
40% C_{18}-PGA MP	:	49.6± 2.97
40% C_{18}-PGA-PEG-MIHA MP	:	24.9± 0.43
40% C_{18}-PGA-PEG-MIHA MP+Collagen	:	27.6± 2.13
Zeta potential (mV)±SD		
40% C_{18}-PGA MP	:	-18.3 ± 1.60
40% C_{18}-PGA-PEG-MIHA MP	:	-25.2 ±2.19
40% C_{18}-PGA-PEG-MIHA MP+Collagen	:	-20.1 ± 1.30

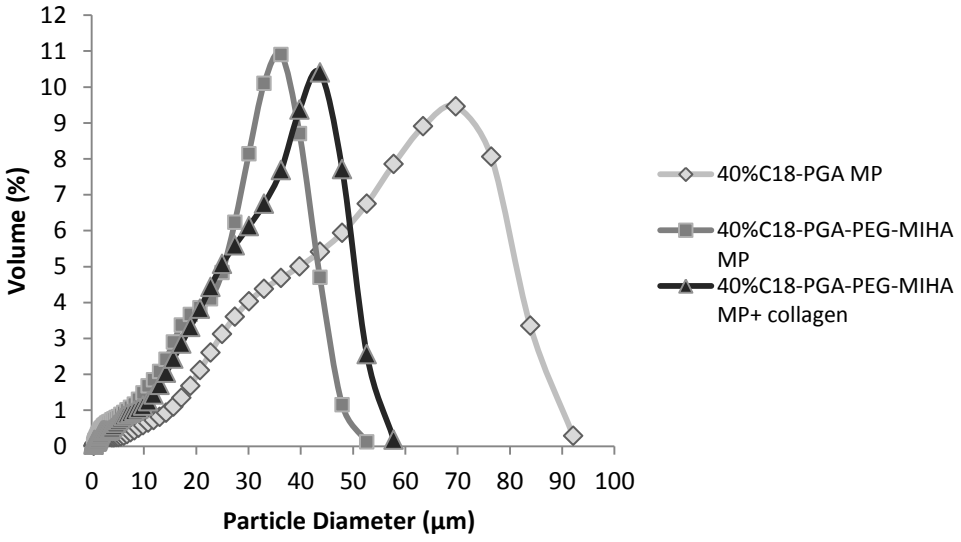

Figure 6.2. Particle size distribution of modified PGA MP. The 40%C_{18}-PGA MP and 40%C_{18}-PGA-PEG-MIHA MP were prepared using emulsification method with PVA 0.005% as emulsifier, while 40%C_{18}-PGA-PEG-MIHA MP+ collagen was prepared by attach collagen to 40%C_{18}-PGA-PEG-MIHA MP. Particle size was determined using Beckman Coulter LS 230.

The release profile of simvastatin from modified PGA MPs had been evaluated in phosphate buffer saline (PBS) containing 0.1% Tween 20. The effect of polymer modification and collagen attachment to MP on its release was determined. As illustrated in Figure 6.3, more than 50% of SIM was released from 40%C_{18}-PGA and 40%C_{18}-PGA-PEG-MIHA MPs within 6 hours of released study. The attachment of MIHA-PEG-NH_2 linker to 40%C_{18}-PGA increased the speed of simvastatin release from the MP. Surprisingly, the initial release was slower with attachment of collagen on the 40%C_{18}-PGA-PEG-MIHA MP. It is seen from the graph that the release of SIM from 40%C_{18}-PGA-PEG-MIHA MP+ collagen was 36% within the 6 hours of released study.

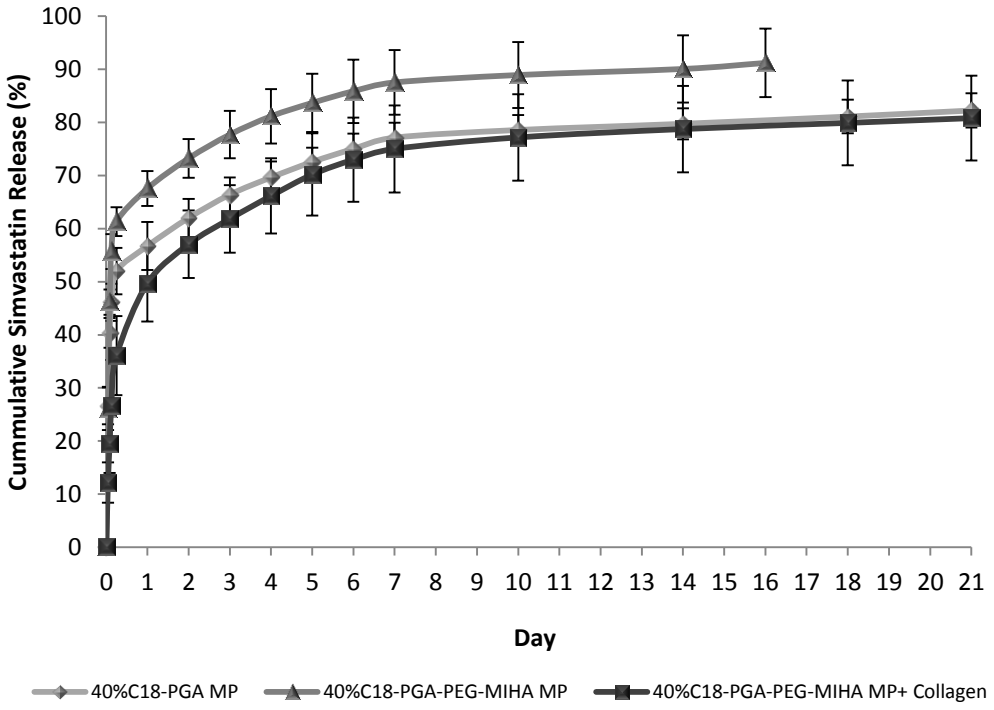

Figure 6.3. The release profiles of SIM from modified PGA MP. The MP was prepared using emulsification method with 5 % polymer concentration and 0.005% PVA. The release study was established in PBS+0.1% tween 20 at 37°C. Bar represents SD (n=3).

The release study ended at 16 days for 40%C_{18}-PGA-PEG-MIHA MP and 21 days for the others as there was no drug released from MP at those particular days. Around 90% of SIM had been released from 40% C_{18}-PGA-PEG-MIHA MP, while only 80% had been released from 40%C_{18}-PGA MP and 40%C_{18}-PGA-PEG-MIHA MP+ collagen at the end of study. The remaining microparticles were then analysed to determine the amount of SIM retained inside MP. Table 6.2 shows that a small amount of SIM is still retained MP and confirm that SIM was not completely released from MP.

Table 6.2. Percentage of SIM released from and remaining in modified PGA MP prepared using emulsification method with 0.05%PVA.

	Type of Microparticle		
	40%C_{18}-PGA	**40%C_{18}-PGA-PEG-MIHA**	**40%C_{18}-PGA-PEG-MIHA + Collagen**
Initial amount of SIM (µg) ± SD	29.6 ± 0.01	30.2 ± 1.08	26.2 ± 1.15
SIM released from MPs (µg) ± SD	24.4 ± 0.95	27.6 ± 1.75	21.1 ± 0.38
SIM released from MPs (%)± SD	82.3 ± 3.22	91.2 ± 6.46	80.8 ± 7.97
Release period (day)	21	16	21
SIM remaining in MPs (µg) ± SD	1.3 ± 0.26	0.7 ± 0.06	0.4 ± 0.02
SIM remaining in MPs (%)± SD	4.5 ± 1.90	2.5 ± 0.39	1.6 ± 0.36

The percentage of remaining drug in MP was determined by extraction of SIM from remained MP after release study ended. The MP prepared from 40%C_{18}-PGA showed the highest amount of SIM remained within the MP followed by 40%C_{18}-PGA-PEG-MIHA MP and 40%C_{18}-PGA-PEG-MIHA MP+ collagen. The attachment of MIHA-PEG-NH_2 linker to the 40%C_{18}-PGA polymer increased the amount of SIM released from MP, thus, SIM remaining in 40%C_{18}-PGA-PEG-MIHA MP was lower compared to 40%C_{18}-PGA. An interesting result is that 40%C_{18}-PGA-PEG-MIHA MP+ collagen had released 80% of SIM in 21 days, but the amount of SIM remaining in MP was only 1.6%. This amount was lower compared to the SIM remained in 40%C_{18}-PGA-PEG-MIHA MP and suggests that collagen attachment on the surface of MP also influenced the extraction of SIM from 40%C_{18}-PGA-PEG-MIHA MP+ collagen.

6.4. Interaction of microparticles with cells

The modified PGA MP containing simvastatin were mixed with cells in ratio 1:10 MP to cell. The low ratio of MP to the cells was applied as the MP has tendency to interrupt aggregate formation in mES cell. In addition, the low amount of MP was used to avoid SIM toxicity in cells as around 50% of SIM had released from MP at the first day. Based on the cell metabolic assay in Chapter 5, section 5.4, the 40%C_{18}-PGA MP and 40%C_{18}-PEG-PEG-MIHA MP+ collagen showed the ability to support cells proliferation in 3D aggregate culture. Therefore, these two types of MP containing SIM were used with the cells. The low ratio of MP was used in order to minimize possible cell toxicity which might initiated by release of SIM from MP. The aggregate formation in mES and osteoblast cells was carried out using the method as described in Chapter 2 Section 2.5.2. The incorporation of MP within cells was evaluated on day 3 of cell culture under the bright field and fluorescence microscope.

Figure 6.4 shows the incorporation of modified PGA MPs containing SIM within mES cell aggregate. The aggregation occurred in mES in the presence of modified PGA MP and without MP. Some of MP adhered on the surface of cells aggregate as shown in Figure 6.4-B and C. The 40%C_{18}-PGA-PEG-MIHA MP+ collagen showed better distribution within mES aggregate than 40%C_{18}-PGA MP.

The incorporation of modified PGA MP containing SIM was also evaluated in osteoblasts (Figure 6.5). Figure 6.5-B shows poor distribution of 40%C_{18}-PGA MP within MP-osteoblasts aggregate and some 40%C_{18}-PGA MP appeared to be aggregated each other and did not locate homogenously within the aggregate. The 40%C_{18}-PGA-PEG-MIHA MP+ collagen showed a better distribution within osteoblasts

aggregate (Figure 6.5-C) and a higher number of MP within osteoblasts aggregate compare to the 40%C_{18}-PGA MP (see also Table 6.3). However, some aggregation also occurred in 40%C_{18}-PGA-PEG-MIHA MP+ collagen.

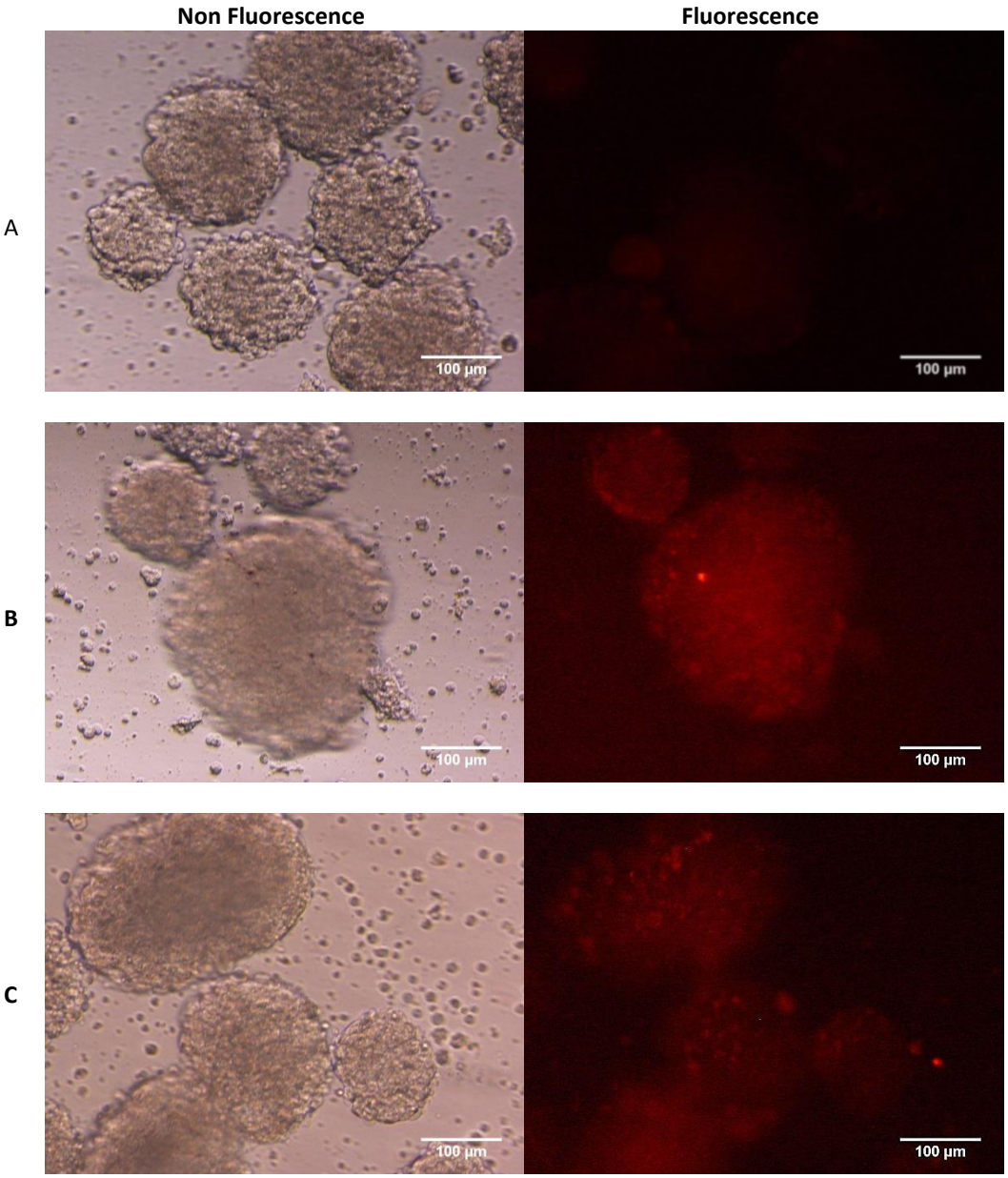

Figure 6.4. The mES cell aggregate without MPs (A), with 40%C_{18}-PGA MPs (B) and with 40%C_{18}-PGA-PEG-MIHA MP + collagen. MP were loaded with SIM and labelled with rhodamine. MP was mixed with the cells in ratio 1: 10 MPs to cells. Images were taken at 3 days of cell culture. Scale bars represent 100 µm.

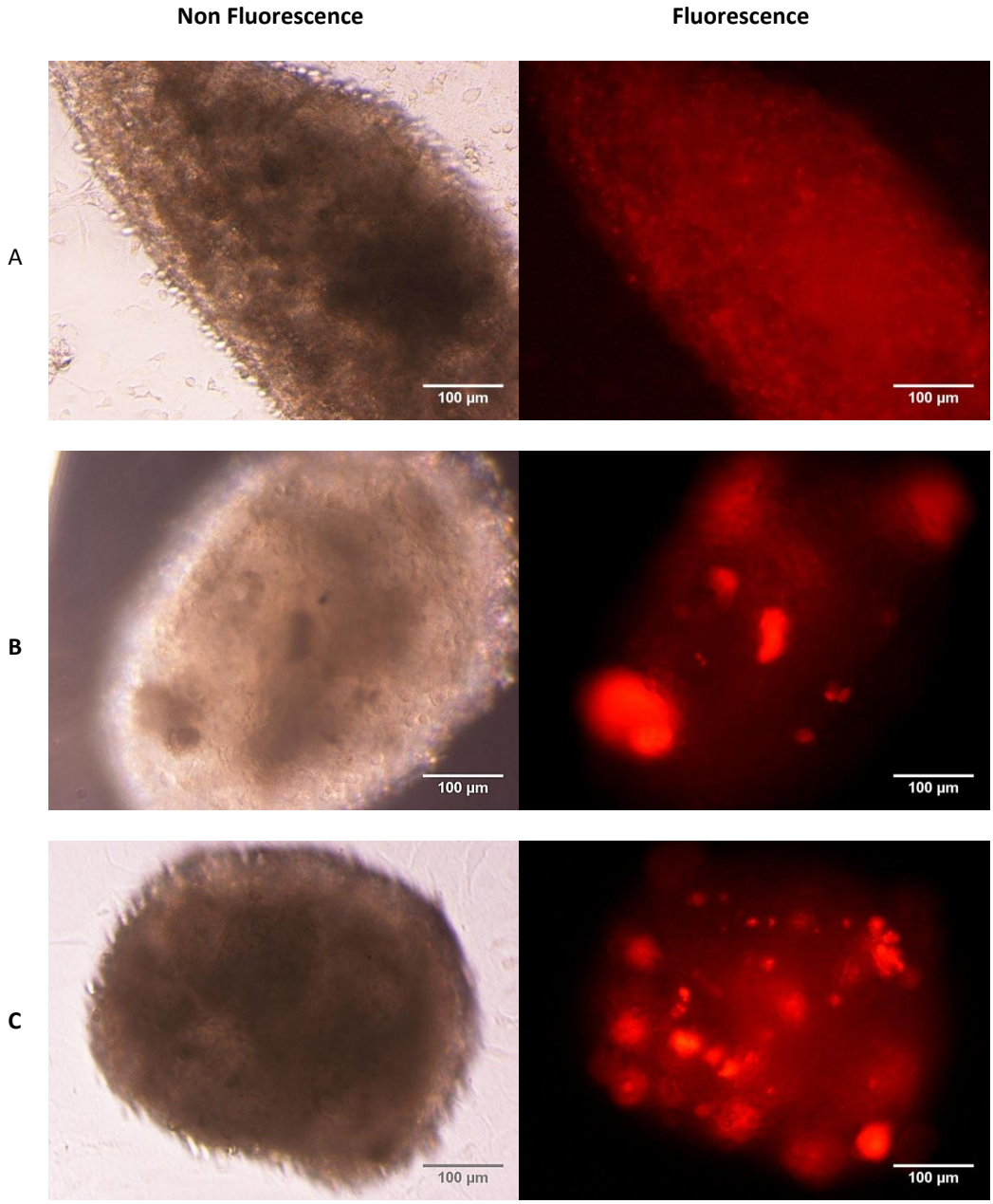

Figure 6.5. Osteoblast cell aggregate without MPs (A), with 40%C18-PGA MP (B) and with 40%C18-PGA-PEG-MIHA MP + collagen. MP was loaded with SIM and labelled with rhodamine. MP was mixed with the cells in ratio 1: 10 MP to cells. Images were taken at 3 days of cell culture. Scale bars represent 100 µm.

Table 6.3. Number of MP relative to the number of cells in aggregates (n=9)

Type of microparticle (MP)	Initial ratio MP : Cell	MP inside cell aggregates (%)± SEM	
		mES	osteoblast
40%C_{18}-PGA MP	1 : 10	3.1 ± 0.09	3.1± 0.03
40%C_{18}-PGA-PEG-MIHA MP+ collagen	1 : 10	7.7 ± 0.28	3.6± 0.14

In order to determine the effectiveness of MP incorporation within aggregates, the number of MP inside cells aggregate was evaluated by dissociating the aggregates at day 3 using trypsin. The number of fluorescence particles inside aggregates and the number of cells within the aggregates were counted and presented as percentage of MP within aggregates. It can be seen in Table 6.3 that 40%C_{18}-PGA-PEG-MIHA MP+ collagen exhibited high incorporation within mES and osteoblast aggregates. The percentage of 40%C_{18}-PGA-PEG-MIHA MP+ collagen incorporation in mES was two times higher compared to incorporation of 40%C_{18}-PGA MP, while the incorporation in osteoblast cell was only 0.44% higher than 40%C_{18}-PGA MP.

6.5. Alkaline Phosphatase activity

The release of SIM to cells for inducing osteogenic differentiation was evaluated using ALP assay (Chapter 2 section 2.5.3). ALP enzyme is a useful marker of osteogenic differentiation and was determined based on reaction of alkaline phosphatase with pNPP as substrate at 7, 14 and 21 days of cells culture. Based on the result of incorporation into cell aggregates and the ability to encourage cell proliferation, the 40%C_{18}-PGA MP and 40%C_{18}-PGA-PEG-MIHA MP+ collagen was used to deliver simvastatin (SIM) to mES and osteoblast cells. The MP was seeded with the cells to construct aggregates in ratio 1: 10 MP to cells.

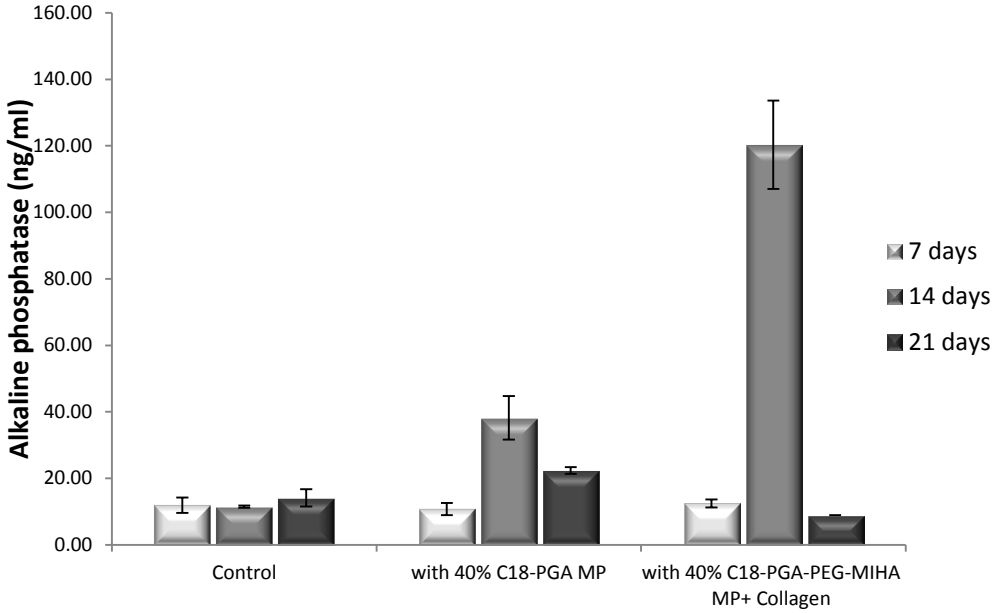

Figure 6.6. Alkaline phosphatase (ALP) level in mES cell at 7, 14 and 21 days of cell culture. The microparticles were mixed in ratio 1:10 microparticle to cell. Bars represent SD (n=3).

Figure 6.6 shows the alkaline phosphatase levels in mES cells aggregate at day 7, 14 and 21 of cell culture. The level of ALP is almost similar in all conditions at day 7. A significant increase in ALP level was seen at day 14 for mES aggregate with MPs. At day 14, the mES aggregate with 40%C_{18}-PGA MP showed an ALP activity of 38.17± 6.56 ng/ml while the mES aggregate with 40%C_{18}-PGA-PEG-MIHA MP+ collagen showed activity of 120.3 ± 13.30 ng/ml. ALP activity in control group at day 14 remained similar to day 7. The level of ALP activity was markedly lower at decreasing to 22.3 ±1.02 ng/ml and 8.9 ±0.01 ng/ml for mES cells aggregate with 40%C_{18}-PGA MP and 40%C_{18}-PGA-PEG-MIHA MP+ collagen, respectively.

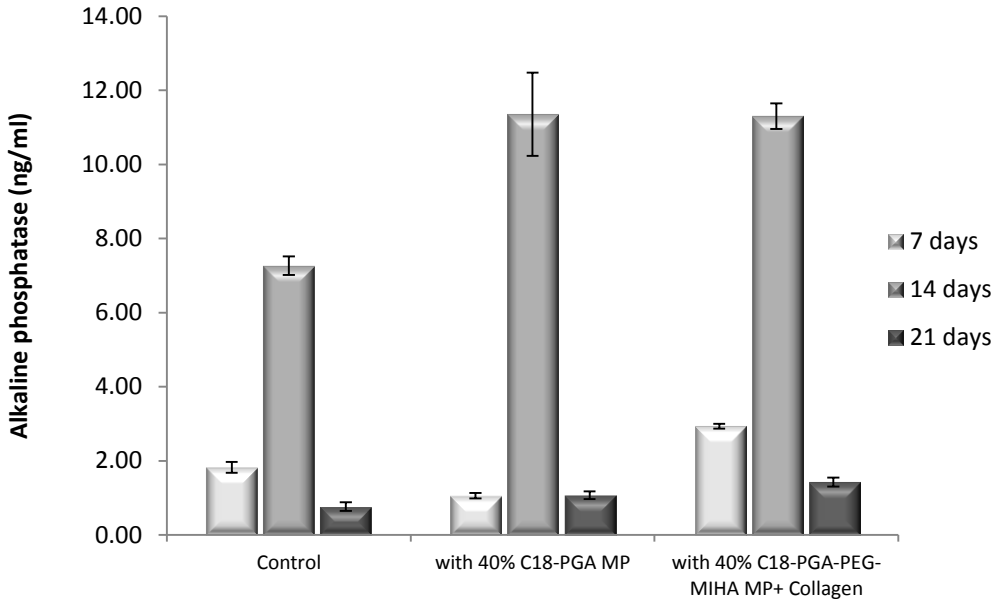

Figure 6.7. Alkaline phosphatase (ALP) level in osteoblast cell at 7, 14 and 21 days of cell culture. The microparticles were mixed in ratio 1:10 microparticle to cell. The alkaline phosphatase was determined based on the reaction of ALP with pNPP as substrate. Bars represent SD (n=3).

The ALP level was also evaluated in osteoblasts aggregates with modified PGA MPs. As shown in Figure 6.7, the highest ALP level at day 7 was found in osteoblasts aggregate with 40%C_{18}-PGA-PEG-MIHA MP+ collagen followed by ALP in control group and the osteoblasts aggregate with 40%C_{18}-PGA MP. The level of ALP activity increased significantly at day 14 with around 11 ng/ml ALP activity in osteoblast cells with 40%C_{18}-PGA MP and 40%C_{18}-PGA-PEG-MIHA MP+ collagen and 7.3 ±0.25 ng/ml for control (osteoblasts aggregate without MP). Again, as occurred in mES cells, the level of ALP decreased in day 21 in all conditions including control.

Comparing the ALP activity in mES and osteoblast cells, the mES had markedly higher levels of enzyme/activity than osteoblast cells. It was noted that the trend of increasing of alkaline phosphatase level from day 7 up to day 14 occurred in both

mES and osteoblast cells. The 40%C_{18}-PGA-PEG-MIHA MP+ collagen in mES revealed the higher ALP level than 40%C_{18}-PGA MP in mES while in osteoblast cells the levels of ALP activity were similar with both types of MP

6.6. Osteocalcin Immunostaining

The presence of osteocalcin as a marker for maturation osteoblast was evaluated in 28-day old of mES aggregates. The osteocalcin immunostaining was not evaluated in 28-day old osteoblasts aggregate as the aggregate could not be longer maintained and spreading to form monolayer cells on cell culture after 28 days of incubation. Osteocalcin was detected using antibodies and location revealed using secondary antibody conjugated to horseradish peroxide-streptavidin (HRP-streptavidin) and using diamino-benzidine (DAB) as substrate for HRP. The method for osteocalcin immunostaining on cell aggregates is described in Chapter 2 section 2.5.4. In order to determine specificity of reaction, controls were provided for primary antibody, secondary antibody and HRP as label. The list of treatment for the controls and samples is listed in Table 6.4.

The presence of osteocalcin as a non-collagenous bone matrix in mES aggregate is shown in Figure 6.8 and it can be seen that under all conditions osteocalcin protein was detected, as indicated by dark brown staining within cells aggregate. The osteocalcin was seen in cells aggregate with and without microparticle containing simvastatin. The intense brown staining in samples indicated abundant production of osteocalcin in mES aggregate at 28-day old cell aggregate.

Table 6.4. Treatment applied on controls and sample for osteocalcin imunostaining

Treatment	Control			Sample
	Primary antibody	Secondary antibody	HRP	
Blocking for endogenous peroxidase using H_2O_2	√	√	√	√
Blocking with secondary serum	√	√	√	√
Incubated with primary antibody	√	-	-	√
Incubated with secondary antibody	-	√	-	√
Incubated with HRP conjugate	-	-	√	√
Incubated with DAB	√	√	√	√

Keys: (√): treated; (-): not treated

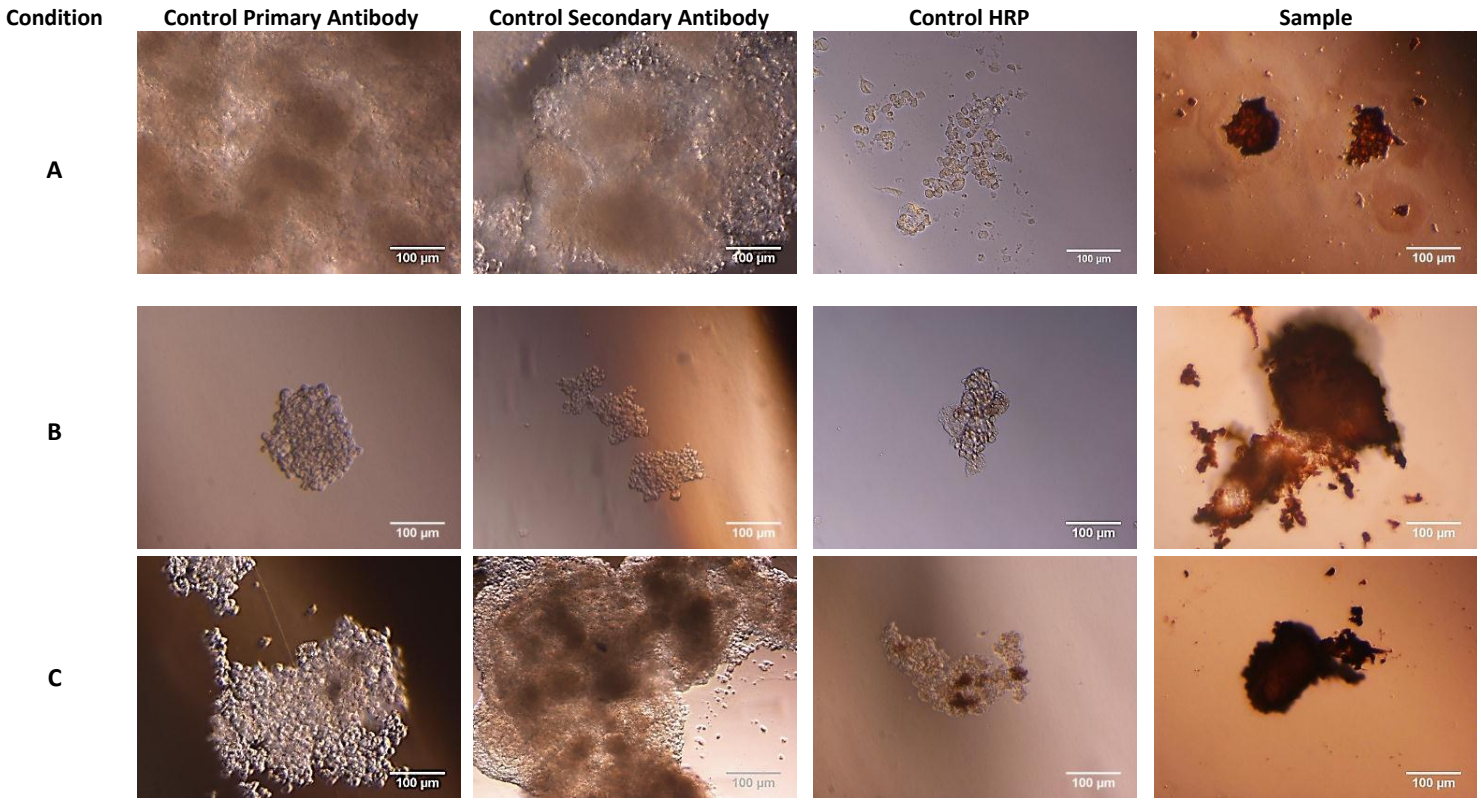

Figure 6.8. Osteocalcin imunostaining of mES cell aggregate using horseradish peroxide (HRP)-diamino-benzidine (DAB) detection. Sample is 28-day old mES cell without MP(A), with 40%C18-PGA-PEG-MIHA MP (B) and with 40%C18-PGA-PEG-MIHA-MP+ Collagen (C). The MP was loaded with SIM. Images were taken under brightfield microscope. Scale bars represent 100 µm.

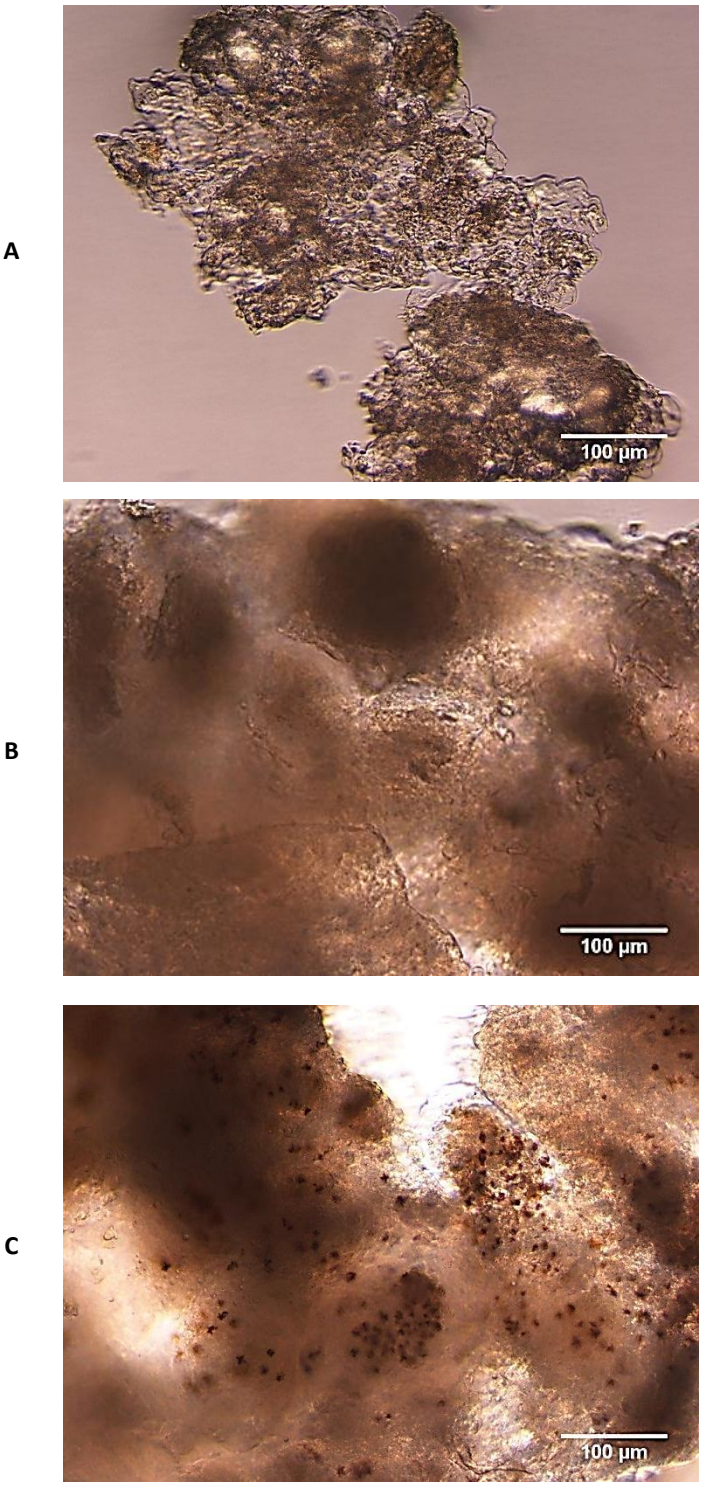

Figure 6.9. Von kossa staining on 28-day old mES cell. Samples are mES aggregate without microparticle (A), with 40%C_{18}-PGA-PEG-MIHA MP (B) and with 40%C_{18}-PGA-PEG-MIHA-MP+ Collagen (C). The MPs was loaded with SIM. Images were taken under light microscope. Scale bars represent 100 µm.

6.7. Mineralisation in Cells

Von Kossa staining for calcium salts was used to evaluate the mineralisation in 28-day old cells aggregate. The staining was carried out by incubating the aggregates with a 1% silver nitrate solution under strong light as described in Chapter 2 section 2.5.5. The staining in 28-day old mES aggregate is shown in Figure 6.9 and is seen as dark brown to black staining. Figure 6.9 shows that osteoclacin staining was seen in mES aggregate with 40%C_{18}-PGA-PEG-MIHA MP+ collagen but no staining was seen in control nor in mES aggregate with 40%C_{18}-PGA MP.

6.8. Discussion

Microparticles can be used as matrices to deliver active molecule for inducing cell differentiation in 3D constructs. Good interaction between cells and MP is needed to encourage cells differentiation. In this study, the PGA polymer had been modified by 40% stearoyl substitution and attachment of MIHA-PEG-NH_2 as ligand-bearing linker. The modified polymer showed high encapsulation efficiency of SIM and the attachment of MIHA-PEG-NH_2 linker showed the ability to hold collagen attachment on the surface of MP prepared from modified PGA polymer. Here we present the ability of MP prepared from modified PGA polymer to deliver SIM for inducing osteogenic differentiation in mES.

6.8.1. Simvastatin and osteogenic differentiation

Various 'effective' concentrations of SIM for inducing osteogenic have been reported. Kupcsik *et al* (2009) reported that the maximum concentration of SIM to induce calcification in mesenchymal stem cells is 1 µM, while Pagkalos *et al* (2010) reported the concentration for inducing osteogenic differentiation in mES cells ranged from

0.1 to 100 nM [76, 225]. The variation in SIM concentration might be influenced by several factors such as the type of cells, the density of cells and the condition of cell culture whether 2D or 3D. In order to evaluate osteogenic induction by SIM in cells aggregates, a range concentration of SIM were applied to aggregates.

The ability of SIM added directly to the culture medium to induce osteogenic differentiation in mES cells was assessed over a range of concentrations from 0.1 to 200 nM. The level of ALP activity for osteogenic differentiation was detected by reaction with the substrate of ALP enzyme, p-nitrophenyl phosphate (pNPP). The principle of this reaction is the development p-nitrophenol, by hydrolysis of pNPP using ALP enzyme and can be assessed by colorimetric change [226, 227]. It was found that untreated mES aggregate exhibited ALP activity and is linked to high intrinsic ALP activity in pluripotent cells [228]. By day 7, there was a reduction in level of ALP with SIM treatment in the range concentration of 0.1-10 nM. Hwang *et al* (2004) and Lee *et al* (2007) suggested that SIM treatments could reduce cell proliferation and disrupt cell self-renewal ability [229, 230] and consequently reduce ALP expression in embryonic stem cell [230]. On the other hand, treatment of SIM on murine osteoprecursor (MC3T3-E1) and bone marrow stromal (BMS) cells enhanced the ALP activity in dose dependent manner [75, 229, 231] by enhance bone morphogenetic protein-2 (BMP-2) expression and induction in estrogen receptor-alpha (ER-α) which involved in bone formation [75, 76, 231]. Based on the ALP assay at day 7, it can be seen that there is possibly some disruption on cells proliferation caused by SIM treatment.

The ALP activity in mES cells peaked at day 14 of cell culture and was related to the dose of SIM. This finding was consistent with the previous studies that describe increasing ALP activity related with the increasing dose of SIM in medium [75, 229, 231]. The level of ALP decreased at day 21 in all conditions including control. The decrease in ALP level is probably related to next stages of cells differentiation and also found in ALP expression of human embryonic stem (hES) cell and mesenchymal stem cell studied by Arpornmaeklong *et al* (2009) and Shafiee *et al* (2010) [232, 233].

6.8.2. Simvastatin release profile from modified PGA microparticles

The MP incorporated with cells aggregates should have ability to release the active molecule in controlled manner and if required over an extended period. Several studies on osteogenic differentiation using SIM showed the minimum period of 14 days for osteogenesis process in stem cell [75, 225, 233-235]. This period includes proliferation phase, matrix maturation and mineralization phases and is related to the mature differentiation of the osteoblast [56, 235]. Therefore, the MP should be able to extend the drug release minimum for 14 days to ensure sufficient amount of drug is delivered.

According to the studies in Chapter 4 section 4.6.3, the release of SIM from modified PGA MPs could be extended by reducing the concentration of PVA as emulsifier during the formulation process. The minimum concentration of PVA, 0.005%, was used to prepare MP from modified PGA polymer. Consequently, the preparation using emulsification method with PVA 0.005% generated the poly-disperse MP with a range of mean diameter depending of characteristics of the MP as shown in Table 6.1. The MP prepared from 40%C_{18}-PGA-PEG-MIHA polymer produced smaller diameter MP than those prepared from 40%C_{18}-PGA and is related to the MIHA-PEG-

NH_2 linker attachment at the end of carboxyl group of polymer backbone. Attachment of collagen on the surface of 40%C_{18}-PGA-PEG-MIHA MP resulted in larger size of MP. The presence of collagen on the surface increased the particle size by approximately 2.7 µm possibly related to small aggregation due to the presence of protein layer (Figure 6.2). The increasing of particle size after attachment with protein seems to be consistent with previous study by Gindy *et al* (2008) which found that attachment of bovine serum albumin (BSA) on the functionalized poly(caprolactone) nanoparticle increased the particle size [196]. The difference in zeta potential was also influenced by attachment of PEG-MIHA linker on the PGA polymer backbone and attachment of collagen as explained in Chapter 4, section 4.3.

The *in vitro* release study showed that the SIM release from 40%C_{18}-PGA MP and 40%C_{18}-PGA-PEG-MIHA MP+ collagen could be maintained for up to 21 days. It can be seen from Figure 6.3 that the presence of collagen on the surface of 40%C_{18}-PGA-PEG-MIHA MP extend the period of drug release from MP until day 21 compared to the MP without collagen attachment. Attachment of collagen on the surface of MP might reduce the diffusivity of drug from MP to medium and help to extend the time-course of release of drug from MP. It was noted that there was incomplete release of SIM from MP with only around 82.3 % and 80.8 % of SIM released from 40%C_{18}-PGA MP and 40%C_{18}-PGA-PEG-MIHA MP+ collagen, respectively. The extraction of SIM from remaining MPs after release study indicated 4.5 % of SIM remained within 40%C_{18}-PGA MP while 1.6 % remained within 40%C_{18}-PGA-PEG-MIHA MP+ collagen. The incomplete mass balance on SIM released might relate to the strong interaction between SIM and modified PGA polymer and the extraction of SIM from MP. The presence of collagen on the surface of the MP probably reduced the extraction

efficiency of SIM from the MP. Although the modified PGA polymer presented incomplete release of SIM *in vitro,* the drug is expected to completely release when applied to the cells. The research by Meng *et al* (2006) reported that the nanoparticle prepared from PGA polymer degraded when applied to the cells by the esther bonds breaking of polymer backbone [143].

6.8.3. Incorporation of microparticles with cells

The fluorescence images of modified PGA MPs in mES cells aggregate showed MP had distributed within the aggregate with some MP attached on the surface of aggregates. In mES cells aggregate, the 40%C_{18}-PGA-PEG-MIHA MP+ collagen showed more MP within cell aggregate (Table 6.3). The presence of collagen on the surface of 40%C_{18}-PGA-PEG-MIHA MP+ collagen likely encouraged the MP interaction with the cells. Although the percentage of MP within aggregates is also influenced by the number of cells which constructs the aggregate, cell metabolic activity assay data (Chapter 5, section 5.4) suggested that the presence of collagen on the surface of might also encourage increased cells proliferation. In addition, the 40%C_{18}-PGA-PEG-MIHA MP+ collagen had better distribution of particle within cells aggregate as shown in Figure 6.5. Some aggregation had appeared in 40%C_{18}-PGA-PEG-MIHA MP+ collagen in osteoblasts aggregate and but it was lower than had occurred in 40%C_{18}-PGA MP. The presence of MIHA-PEG-NH_2 linker on the molecule of PGA polymer provided a PEG layer to prevent interaction between particles [133, 173]. The research by Mishra *et al* (2004) also reported that the particle with PEG grafting exhibited non-aggregating particle when incorporated with cell aggregates and it remained on the surface of cells [236].

6.8.4. Osteogenesis Differentiation

The ALP activity, as marker for osteogenic differentiation, reached a peak at day 14 in mES. ALP is widely known as an important component expressed in mineralized cell and it is observed on the cell surface and matrix vesicle [237]. ALP expression/activity usually peaks near to the end of proliferation stage and during the matrix deposition stage [234]. In mES cells culture, the highest ALP activity was seen with 40%C_{18}-PGA-PEG-MIHA MP+ collagen. The ALP enzyme is expressed during the maturation stage of osteoblasts differentiation [56]. In this study, the maturation of cell is not only influenced by SIM as an active drug, but also influenced by MP as supporting matrix within aggregate. As described in Chapter 5, section 5.4, the 40%C_{18}-PGA-PEG-MIHA MP+ collagen revealed increases in cells metabolic activity, possibly related to cells proliferation. Since the 40%C_{18}-PGA-PEG-MIHA MP+ collagen gave a better support for cell proliferation, the incorporation of the MP containing SIM within mES cell with this MP achieved the higher ALP enzyme compare with mES aggregate with 40%C_{18}-PGA MP. Although the maturation stages reduces cell proliferation capacity [238], the proliferation stage at initial phase correlated with the further stage of cell differentiation. Turning into the ALP level in osteoblast cells, the ALP also reached the peak at 14 days as occurred in mES. The ALP level in osteoblast cells with 40%C_{18}-PGA MP and 40%C_{18}-PGA-PEG-MIHA MP+ collagen is produced at similar level and the ALP level peaked lower compare to mES aggregates.

The presence of osteocalcin was evaluated in 28-day old mES. In order to prevent non-specific binding between HRP and endogenous peroxide from the cells, sample was pre-treated with hydrogen peroxide (H_2O_2) [239]. Blocking the samples with the serum from the host of secondary antibody was applied in order prevent non-specific

binding of secondary antibody [240, 241]. The negative control also provided for primary antibody, secondary antibody and HRP label to show the specificity of reaction in each antibody and label as recommended by Burry (2011) [242]. The osteocalcin staining was detected using HRP enzyme. The HRP reacted specifically with the diamino-benzidine (DAB) substrate to produce brown colour on the sample [240].

The osteocalcin imunostaining and von Kossa staining for mineralization were not performed in osteoblast aggregate since the osteoblast aggregate failed to maintain its integrity and spread as monolayer on culture plate after longer period of incubation. Therefore, the maintenance condition and formation of aggregate in osteoblast should be optimized.

Positive osteocalcin staining was produced in mES cells at day 28 without and with MP containing SIM and was similar in all examples. Zur Nieden *et al* (2003) described the presence of osteocalcin in embryonic stem cell to represent the late stage of osteogenic differentiation and could be identified in the fourth week of ES cell culture [234]. The osteocalcin staining in mES cell aggregate showed the abundant level of osteocalcin in the condition without and with MP containing SIM. Thus, effect of PGA polymer modification on SIM delivery to the cell could not be distinguished by osteocalcin staining.

The von Kossa staining showed there was deposition of calcium salts and possibly indicating mineralization in mES cells aggregate with 40%C_{18}-PGA-PEG-MIHA MP+ collagen. The result revealed that the 40%C_{18}-PGA-PEG-MIHA MP+ collagen was able to effectively deliver SIM for osteogenic differentiation. There is no positive von

Kossa staining in mES without MP and with 40%C_{18}-PGA-MP. This result was contrary with the expectation about mineralization in mES cells. The osteocalcin immunostaining showed the abundant presence of osteocalcin particularly in mES with and without modified PGA MPs but the von Kossa staining only detect the mineralisation in mES cell aggregate with 40%C_{18}-PGA-PEG-MIHA MP+ collagen. Schroder *et al* (1999) mentioned that the mineralization phase was indicated with the expression of osteocalcin [56], thus the presence of osteocalcin in sample would correlate with the positive result using von Kossa staining. The previous studies by zur Nieden *et al* (2003) showed that the positive result of osteocalcin staining in differentiated ES cells also related with the positive result in von Kossa staining [234].

The result for mineralisation using von Kossa staining is unexpected and could be explained by two reasons. The first reason is the SIM could be delivered to the cells but the amount of SIM released is not sufficient enough to support mineralisation in mES cells. The release study of modified PGA MP *in vitro* showed that around 50% SIM was released at day 1 and then become slower after day 7. The release of SIM from the MP was ended in the period of 21 days. Since the mineralization phase was evaluated at fourth week, there is possibility that the amount of SIM not sufficient enough to support mineralisation phase in osteogenesis. Secondly, the amount of calcium phosphate in differentiated cells is not sufficient enough to be detected using von Kossa staining. Therefore, Bonewald *et al* (2003) suggested to confirm the result from osteocalcin staining using Alizarin red staining and mineralisation analysis using electron microscope analysis, X-ray diffraction and Fourier transform infrared spectroscopy [243].

6.9. Conclusion

In conclusion, the MP prepared from modified PGA polymer showed the ability to incorporate drug and deliver it for the 21-day period. The attachment of collagen on the surface of MP affected the initial release of drug from MP to become lower than the MP without collagen attachment. However, the incomplete release of drug from modified PGA microparticles had shown in 40%C_{18}-PGA MP and 40%C_{18}-PGA-PEG-MIHA MP+ collagen.

Although the formulation of MP using PVA 0.005% generated larger particles, the modified PGA MP could be incorporated within cell aggregate in ratio 1: 10 of MP to cells. The attachment of collagen on the surface of MP exhibited higher incorporation within cells aggregates and more homogeneous distribution within cells aggregate. The attachment of MIHA-PEG-NH_2 linker showed the ability to prevent aggregation of microparticle within cells aggregate.

The delivery of SIM from modified PGA polymer showed the ability to induce osteogenesis process in mES cells, particularly for maturation stage. The incorporation of 40%C_{18}-PGA-PEG-MIHA MP+ collagen within cells aggregate exhibited the higher ALP level on the cells than the cell aggregate with 40%C_{18}-PGA MP. However, the ability of modified PGA polymer to induce osteogenesis for mineralization stage needs to be reviewed using the others assay to support the result. In addition, the condition for aggregate formation in osteoblasts should be optimized.

CHAPTER 7

7. CONCLUSION AND FUTURE WORK

7.1. Conclusion

To summarize, poly glycerol adipate (PGA) polymer had been modified by 40% stearoyl (C_{18}) substitution on the pendant hydroxyl group of PGA polymer (40%C_{18}-PGA) to increase drug incorporation within the polymer. The acyl substitution increase the hydrophobicity of polymer, thus increases the interaction between hydrophobic drug and the polymer. This modification would be useful to generate microparticles containing active molecule for cells development process. The polymer also modified with a MIHA-PEG-NH_2 linker to bear a ligand for optimising the interaction between microparticles and cells.

The substitution of 40% hydroxyl group in poly(glycerol adipate) (PGA) with stearoyl (C_{18}) is effectively catalysed by pyridine. The percentage of substitution could be identified using ^{1}H-NMR spectrum by comparing the peak intensity of methyl group near carboxyl in PGA backbone with the methyl at the end of C_{18} molecule. Further attachment MIHA-PEG-NH_2 linker to the terminal carboxyl group of polymer backbone (40%C_{18}-PGA-PEG-MIHA) also identified using ^{1}H-NMR spectrum to assure that the attachment generated 1 to 1 ratio of PGA polymer to MIHA-PEG-NH_2 linker. All of these synthesis also confirmed by FTIR analysis to identify important functional

group related to substitution and attachment on modified PGA polymer. Together with these synthetic reaction steps, collagen as a proposed ligand was also modified by attaching iminothiolane group and FITC. The modification of collagen molecule using iminothiolane is necessary to provide thiol group on collagen molecule for attachment with maleimide group on the molecule of 40%C_{18}-PGA-PEG-MIHA polymer. In addition, FITC attachment on collagen would be useful for further analysis such as determination of collagen attachment as well as for cell work. The modified collagen with iminothiolane and FITC did not alter the ability of collagen to interact with the cells although the interaction of collagen and the cells is influenced by collagen concentration and density of the cells.

The modified PGA polymers, 40%C_{18}-PGA and 40%C_{18}-PGA-PEG-MIHA, were formulated into microparticle (MP) for tissue engineering purpose. The emulsification method was used to prepare the MP from modified PGA. Some critical factors in formulation process related to physical characteristics and release of drug from modified PGA MP had been identified. The attachment of MIHA-PEG-NH_2 linker to 40%C_{18}-PGA polymer generated a smaller particle size. In addition, the size of particle was also influenced by the speed of homogenizer and concentration of PVA as emulsifier. The attachment of MIHA-PEG-NH_2 linker on the 40%C_{18}-PGA polymer also affected the zeta potential value of microparticle as well as the attachment of iminothiolane-modified collagen on the surface of microparticle. The 40%C_{18}-PGA-PEG-MIHA MP exhibited a higher negative value of zeta potential than 40%C_{18}-PGA MP while the attachment of iminothiolane modified collagen on the surface of the 40%C_{18}-PGA-PEG-MIHA MP reduced the zeta potential to the lower negative value

due to the presence the amino group on the collagen molecule. The modification of PGA polymer by 40% stearoyl substitution on PGA polymer backbone (40%C_{18}-PGA) exhibited the good interaction with SIM indicated by more than 50% encapsulation efficiency of SIM as well as in 40%C_{18}-PGA-PEG-MIHA polymer. However, the encapsulation efficiency is also influenced by polymer concentration during preparation and concentration of PVA as emulsifier. The modified PGA polymers had ability to extend the release of drug from polymer as demonstrated in release of SIM from solid dispersions prepared from modified PGA polymer. The formulation of MP played important role for the release of drug from microparticle. As demonstrated in the result, the release of drug was influenced by polymer concentration in organic phase and the concentration of PVA as emulsifier. The attachment of MIHA-PEG-NH_2 linker on 40%C_{18}-PGA polymer resulted in a high release of drug at initial phase. Moreover, the MP prepared from 40%C_{18}-PGA-PEG-MIHA had the ability to attach with iminothiolane-modified collagen through maleimide functional group on the modified PGA polymer.

The modified PGA microparticle showed the ability to incorporate within mES and osteoblast cells. Although the presence of the MP did not encourage aggregate formation in mES cells, but it was be able to support aggregate formation in osteoblast cells. The formation of aggregate is determined by ratio of MP to cell as well as the properties of microparticle. The formation of aggregate using MP could be improved by using a low ratio of MP to the cells. In addition, the attachment of iminothiolane-modified collagen on the surface of MP improve the interaction between the microparticle and cells, therefore it could exhibited better aggregate

formation. The cells metabolism assay showed that the 40%C_{18}-PGA-PEG-MIHA MP+ collagen could act as a matrix for cell to grow and proliferate.

The release of SIM from modified PGA microparticles could be extended up to 21 days by using minimum amount of PVA involved in MP preparation. In addition, iminothiolane-modified collagen attachment on the surface of 40%C_{18}-PGA-PEG-MIHA MP could reduce initial high release caused by the presence of MIHA-PEG-NH_2 linker on the polymer backbone. The SIM was effectively delivered from modified PGA MP indicated by increasing of ALP level as a marker for ostegenesis process. The mineralisation of cells showed by positive staining on osteocalcin but presented unsatisfactory result using von Kossa staining.

In conclusion, the modification of PGA polymer by providing stearic moiety in PGA polymer backbone exhibited high encapsulation efficiency of SIM. However, the encapsulation efficiency of drug within the polymer not only influenced by interaction polymer with the drug but also influenced by formulation of MP. The formulation process could be tailored by adjusting the critical factors related to particle size, encapsulation efficiency and release of drug to achieve the desired physical properties and drug release. In addition, attachment of MIHA-PEG-NH_2 linker to the end of carboxyl group of PGA polymer showed the ability for ligand attachment on MP prepared from 40%C_{18}-PGA–PEG-MIHA polymer. The attachment of collagen as a ligand on the surface of MP improved the ability of microparticles to act as matrix for cells proliferation in 3D structures. Moreover, the attachment of collagen on the surface of modified PGA MP showed the better support for inducing osteogenesis in mES cells.

7.2. Future Work

Although the 40% stearoyl (C_{18}) substitution on pendant hydroxyl group of poly(glycerol adipate polymer) (PGA) successfully exhibited the high encapsulation efficiency of simvastatin (SIM), interaction between the polymer and other drugs and proteins particularly for tissue development need to be explored. According to Puri *et al* (2008), the acyl substitution containing more than 8 atoms carbon (C_8) with the high percentage of acyl group is effective in enhancing drug incorporation for hydrophobic drug due to increasing of hydrophobic interaction between drug and polymer [180]. Therefore, the different acyl substitution with alteration in degree of substitution could be useful to improve interaction between other drugs with the PGA polymer. Since most of growth factors for inducing cell differentiation consist of proteins that bind specifically to receptor in cell membrane, the further exploration is needed for protein encapsulation within substituted PGA polymer. Previous work by Rimmer (2009) presented unsatisfactory result for lysozyme incorporation within 40%C_{18}-PGA microparticle with the encapsulation efficiency less than 10% [127]. However, the encapsulation efficiency of protein within the polymer is not only influenced by interaction between drug and polymer but also affected by formulation parameters such as concentration of polymer in organic phase, ratio inner phase to outer phase, the rate of solvent removal and emulsifier concentration [164, 194]. For that reason, the formulation parameters should be precisely controlled to achieve the desired drug loading as well as release profile.

The attachment of MIHA-PEG-NH_2 linker with 1 to 1 ratio to PGA polymer showed the ability to attach specifically with iminothiolane-modified collagen, reduce the particle

size and minimize aggregation of MP when applied to the cell. In addition, the collagen attachment on the surface of 40%C_{18}-PGA-PEG-MIHA MP is also promising to use as a matrix for cell growth in 3D structure by increasing cells proliferation and generated better effect for cells differentiation. However, the identification of MIHA-PEG-NH_2 attachment on 40%C_{18}-PGA at 1 to 1 ratio using ^{1}H-NMR and FTIR spectrum was not easy due to small intensities of important peaks on the spectrum. In order to overcome this problem, gel permeation chromatography (GPC) analysis to estimate the ratio of attachment by identification polymer molecular weight is needed.

The properties of microparticle such as particle size, encapsulation efficiency and release of drug could be controlled by adjusting formulation parameters. Among those factors, controlling of MP size into monodispersed particle is the most important property related to drug loading, drug distribution within microparticle and release profile of drug as explained in Tran *et al* (2011) that the hydrophilic drugs tend to distributed near the surface of microparticle while the hydrophobic drugs distributed around the core of the microparticle larger than 40 µm. The homogenous distribution of drug in microparticle was found in small size microparticle (10-20 µm) [244]. Looking at the release profile, the smaller particle related to the larger surface area, thus the release of drug tend to be faster compare to larger particle. Therefore, the others methods for MP preparation and scale up production should be explored. Several novel methods are need to be explored to produce monodispersed MP such as using microfluidic systems [244-246] and electro spraying [244, 247].

The aggregate formation using suspension cell in non-treated plate was successfully to incorporate the modified PGA microparticle within mES and osteoblast cell

aggregate. However, the number of microparticle incorporated in each aggregate may vary as the number of cell and microparticle used to form aggregate depend on the probability of cells and microparticle to interact each other. As a result, the broad variation of size and shape in cells aggregate had been found. According Park *et al* (2007), the initial size of aggregate influence the extent of cell differentiation where the expression of ectodermal marker increased in the smaller aggregate (100 μm) while the mesodermal and endodermal marker expression increased in 500 μm aggregates [204]. Consequently, the size of aggregate should be controlled to achieve desired differentiation in reproducible manner. In addition, the agglomeration between aggregate should be noticed as the agglomeration might inhibit cell growth and differentiation [210] due to difficulties of oxygen transfer to cell aggregate. Controlling aggregate size and formation could be achieved using stirred-suspension culture in spinner flask as reviewed by Kurosawa (2007) and Sasitorn *et al* (2009). This system offers benefits related to simple design and easiness to monitor culture environment such as dissolved oxygen, pH and homogeneity of nutrient in medium. Moreover, the agglomeration could be prevented by a spinner flask equipped with an impeller [202, 248]. The spinner flask technique has been successfully used to differentiate human amniotic fluid stem cell (hAFSC) for cellular cardiomyoplasty [249] and re-differentiate chondrocytes [250]. The other benefit using spinner-flask method is the ability to scale up to meet the demand for therapeutic application. Spinner-flask method as part of bioreactor expected to generate a robust and well defined expansion of cell aggregate formation and differentiation [202, 248, 250].

REFERENCES

1. Li, S., *Stem Cell and Tissue Engineering*. 2011, River Edge, NJ, USA: World Scientific & Imperial College Press.
2. Yang, F., et al., *Tissue Engineering: The Therapeutic Strategy of The Twenty-First Century*, in *Nanotechnology and Tissue Engineering: The Scaffold*, C. Laurencin and L. Nair, Editors. 2008, CRC Press: Boca Raton. p. 3-32.
3. Nerem, R.M., *Chapter Two - The challenge of imitating nature*, in *Principles of Tissue Engineering (Third Edition)*, L. Robert, et al., Editors. 2007, Academic Press: Burlington. p. 7-14.
4. Lee, J., M.J. Cuddihy, and N.A. Kotov, *Three-Dimensional Cell Culture Matrices: State of the Art.* Tissue Engineering Part B: Reviews, 2008. **14**(1): p. 61-86.
5. Maltman, Daniel J. and Stefan A. Przyborski, *Developments in three-dimensional cell culture technology aimed at improving the accuracy of in vitro analyses.* Biochemical Society Transactions, 2010. **38**(4): p. 1072.
6. De Bank, P.A., et al., *Accelerated formation of multicellular 3-D structures by cell-to-cell cross-linking.* Biotechnology and Bioengineering, 2007. **97**(6): p. 1617-1625.
7. Layer, P.G., et al., *Of layers and spheres: the reaggregate approach in tissue engineering.* Trends in Neurosciences, 2002. **25**(3): p. 131-134.
8. El Haj, A.J. and S.H. Cartmell, *Bioreactors for bone tissue engineering.* Proceedings of the Institution of Mechanical Engineers, Part H: Journal of Engineering in Medicine, 2010. **224**(12): p. 1523-1532.
9. Lazar, A., et al., *Formation of porcine hepatocyte spheroids for use in a bioartificial liver.* Cell Transplantation, 1995. **4**(3): p. 259-268.
10. Kelm, J.M. and M. Fussenegger, *Microscale tissue engineering using gravity-enforced cell assembly.* Trends in Biotechnology, 2004. **22**(4): p. 195-202.
11. Wang, X. and P. Yang, *In vitro differentiation of mouse embryonic stem (mES) cells using the hanging drop method.* Journal of visualized experiments : JoVE, 2008(17).
12. Luo, Y., et al., *Chapter Twenty-Five - Three-dimensional scaffolds*, in *Principles of Tissue Engineering (Third Edition)*, L. Robert, et al., Editors. 2007, Academic Press: Burlington. p. 359-373.
13. Veiseh, M., E.A. Turley, and M.J. Bissel, *Top-Down Analysis of a Dynamic Environment: Extracellular Matrix Structure and Function*, in *Nanotechnology and Tissue Engineering: The Scaffold*, C.T. Laurencin and L. Nair, Editors. 2008, CRC Press: Boca raton. p. 33-51.
14. Chan, B.P. and K.W. Leong, *Scaffolding in tissue engineering: general approaches and tissue-specific considerations.* European Spine Journal, 2008. **17**(S4): p. 467-479.
15. Yan-Peng Jiao and Fu-Zhai, C., *Surface modification of polyester biomaterials for tissue engineering.* Biomedical Materials, 2007. **2**(4): p. R24.

16. Mano, J.F., et al., *Natural origin biodegradable systems in tissue engineering and regenerative medicine: present status and some moving trends.* Journal of The Royal Society Interface, 2007. **4**(17): p. 999-1030.
17. Dhandayuthapani, B., et al., *Polymeric Scaffolds in Tissue Engineering Application: A Review.* International Journal of Polymer Science, 2011. **2011**: p. 1-19.
18. Pan, Z. and J. Ding, *Poly(lactide-co-glycolide) porous scaffolds for tissue engineering and regenerative medicine.* Interface Focus, 2012. **2**(3): p. 366-377.
19. Gauvin, R., et al., *Microfabrication of complex porous tissue engineering scaffolds using 3D projection stereolithography.* Biomaterials, 2012. **33**(15): p. 3824-3834.
20. Jiang, X., et al., *Chapter Nineteen - Micro-scale patterning of cells and their environment*, in *Principles of Tissue Engineering (Third Edition)*, L. Robert, et al., Editors. 2007, Academic Press: Burlington. p. 265-278.
21. Murphy, M.B. and A.G. Mikos, *Chapter Twenty-Two - Polymer scaffold fabrication*, in *Principles of Tissue Engineering (Third Edition)*, L. Robert, et al., Editors. 2007, Academic Press: Burlington. p. 309-321.
22. Martins, A., et al., *Hierarchical starch-based fibrous scaffold for bone tissue engineering applications.* Journal of Tissue Engineering and Regenerative Medicine, 2009. **3**(1): p. 37-42.
23. Metter, R.B., et al., *Biodegradable fibrous scaffolds with diverse properties by electrospinning candidates from a combinatorial macromer library.* Acta Biomaterialia, 2010. **6**(4): p. 1219-1226.
24. Smith, L.A., X. Liu, and P.X. Ma, *Tissue engineering with nano-fibrous scaffolds.* Soft Matter, 2008. **4**(11): p. 2144-2149.
25. Smith, A.M., et al., *Engineering Increased Stability into Self-Assembled Protein Fibers.* Advanced Functional Materials, 2006. **16**(8): p. 1022-1030.
26. Ho, M.-H., et al., *Preparation of porous scaffolds by using freeze-extraction and freeze-gelation methods.* Biomaterials, 2004. **25**(1): p. 129-138.
27. Mohamad Yunos, D., O. Bretcanu, and A.R. Boccaccini, *Polymer-bioceramic composites for tissue engineering scaffolds.* Journal of Materials Science, 2008. **43**(13): p. 4433-4442.
28. Mourino, V. and A.R. Boccaccini, *Bone tissue engineering therapeutics: controlled drug delivery in three-dimensional scaffolds.* Journal of The Royal Society Interface, 2009. **7**(43): p. 209-227.
29. Kim, S.-S., et al., *Poly(lactide-co-glycolide)/hydroxyapatite composite scaffolds for bone tissue engineering.* Biomaterials, 2006. **27**(8): p. 1399-1409.
30. Steinhoff, G., et al., *Tissue Engineering of Pulmonary Heart Valves on Allogenic Acellular Matrix Conduits.* Circulation, 2000. **102**(suppl 3): p. Iii-50-Iii-55.
31. Atala, A., *Tissue engineering of human bladder.* British Medical Bulletin, 2011. **97**(1): p. 81-104.
32. Koh, C.J. and A. Atala, *Tissue Engineering, Stem Cells, and Cloning: Opportunities for Regenerative Medicine.* Journal of the American Society of Nephrology, 2004. **15**(5): p. 1113-1125.

33. Sandmann, G.H., et al., *Generation and characterization of a human acellular meniscus scaffold for tissue engineering.* Journal of Biomedical Materials Research Part A, 2009. **91A**(2): p. 567-574.
34. Eitan, Y., et al., *Acellular Cardiac Extracellular Matrix as a Scaffold for Tissue Engineering: In Vitro Cell Support, Remodeling, and Biocompatibility.* Tissue Engineering Part C: Methods, 2009. **16**(4): p. 671-683.
35. Singh, M., et al., *Microsphere-Based Seamless Scaffolds Containing Macroscopic Gradients of Encapsulated Factors for Tissue Engineering.* Tissue Engineering Part C: Methods, 2008. **14**(4): p. 299-309.
36. Chau, D.Y.S., K. Agashi, and K.M. Shakesheff, *Microparticles as tissue engineering scaffolds: manufacture, modification and manipulation.* Materials Science and Technology, 2008. **24**(9): p. 1031-1044.
37. Berkland, C., K. Kim, and D.W. Pack, *Fabrication of PLG microspheres with precisely controlled and monodisperse size distributions.* Journal of Controlled Release, 2001. **73**(1): p. 59-74.
38. Klose, D., et al., *How porosity and size affect the drug release mechanisms from PLGA-based microparticles.* International Journal of Pharmaceutics, 2006. **314**(2): p. 198-206.
39. Ko, J.A., et al., *Preparation and characterization of chitosan microparticles intended for controlled drug delivery.* International Journal Of Pharmaceutics, 2002. **249**(1-2): p. 165-174.
40. Hou, Q., P.A. De Bank, and K.M. Shakesheff, *Injectable scaffolds for tissue regeneration.* Journal of Materials Chemistry, 2004. **14**(13): p. 1915.
41. Kretlow, J.D., L. Klouda, and A.G. Mikos, *Injectable matrices and scaffolds for drug delivery in tissue engineering.* Advanced Drug Delivery Reviews, 2007. **59**(4-5): p. 263-273.
42. Choumerianou, D.M., H. Dimitriou, and M. Kalmanti, *Stem Cells: Promises Versus Limitations.* Tissue Engineering Part B: Reviews, 2008. **14**(1): p. 53-60.
43. Buttery, L. and K.M. Shakesheff, *A Brief Introduction to Different Cell Types*, in *Advances in tissue engineering*, S. Mantalaris, S.E. Harding, and J.M. Polak, Editors. 2008, Imperial College Press: GB.
44. Chandross, K.J. and É. Mezey, *Plasticity of adult bone marrow stem cells*, in *Advances in Cell Aging and Gerontology*, G.V.Z. Mark P. Mattson, Editor. 2002, Elsevier. p. 73-95.
45. Khademhosseini, A., et al., *Chapter Thirty-Two - Embryonic stem cells as a cell source for tissue engineering*, in *Principles of Tissue Engineering (Third Edition)*, L. Robert, et al., Editors. 2007, Academic Press: Burlington. p. 445-458.
46. Stein, G.S., *Human Stem Cell Technology and Biology : A Research Guide and Laboratory Manual*. 2011, Hoboken, NJ, USA: Wiley-Blackwell.
47. Robinton, D.A. and G.Q. Daley, *The promise of induced pluripotent stem cells in research and therapy.* Nature, 2012. **481**(7381): p. 295-305.
48. Reddi, A.H., *Chapter Nine - Morphogenesis and tissue engineering*, in *Principles of Tissue Engineering (Third Edition)*, L. Robert, et al., Editors. 2007, Academic Press: Burlington. p. 117-128.
49. Marolt, D., M. Knezevic, and G. Vunjak-Novakovic, *Bone tissue engineering with human stem cells.* Stem Cell Research & Therapy, 2010. **1**(2): p. 10.

50. Guillot, P.V. and W. Cui, *Stem Cells Differentiation*, in *Advances in tissue engineering*, S. Mantalaris, S.E. Harding, and J.M. Polak, Editors. 2008, Imperial College Press: GB.
51. Hassan, H.T. and M. El-Sheemy, *Adult bone-marrow stem cells and their potential in medicine.* JRSM, 2004. **97**(10): p. 465-471.
52. Sekiya, I., et al., *Expansion of Human Adult Stem Cells from Bone Marrow Stroma: Conditions that Maximize the Yields of Early Progenitors and Evaluate Their Quality.* Stem Cells, 2002. **20**(6): p. 530-541.
53. Bianco, P. and P.G. Robey, *Stem cells in tissue engineering.* Nature, 2001. **414**(6859): p. 118-121.
54. Bielby, R., et al., *In vitro differentiation and in vivo mineralization of osteogenic cells derived from human embryonic stem cells.* Tissue Eng, 2004. **10**: p. 1518 - 1525.
55. Cartmell, S., *Controlled release scaffolds for bone tissue engineering.* Journal of Pharmaceutical Sciences, 2009. **98**(2): p. 430-441.
56. Schoroder, H.C., et al., *Polyphosphate in Bone.* Biochemistry (Moscow), 2000. **65**(3): p. 296-303.
57. Strohbach, C.A., D.D. Strong, and C.H. Rundle, *Gene Therapy Applications for Fracture Repair*. Gene Therapy Applications. 2011.
58. Babensee, J.E., L.V. McIntire, and A.G. Mikos, *Growth Factor Delivery for Tissue Engineering.* Pharmaceutical Research, 2000. **17**(5): p. 497-504.
59. Valta, M.P., et al., *Regulation of Osteoblast Differentiation: A Novel Function for Fibroblast Growth Factor 8.* Endocrinology, 2006. **147**(5): p. 2171-2182.
60. Fakhry, A., et al., *Effects of FGF-2/-9 in calvarial bone cell cultures: differentiation stage-dependent mitogenic effect, inverse regulation of BMP-2 and noggin, and enhancement of osteogenic potential.* Bone, 2005. **36**(2): p. 254-266.
61. Liu, Y., et al., *Intracellular VEGF regulates the balance between osteoblast and adipocyte differentiation.* Journal of Clinical Investigation, 2012. **122**(9): p. 3101-3113.
62. Canalis, E., *Growth Factor Control of Bone Mass.* Journal of Cellular Biochemistry, 2009. **108**(4): p. 769-777.
63. Caplan, A.I. and D. Correa, *PDGF in bone formation and regeneration: New insights into a novel mechanism involving MSCs.* Journal of Orthopaedic Research, 2011. **29**(12): p. 1795-1803.
64. Wang, L., et al., *Locally applied nerve growth factor enhances bone consolidation in a rabbit model of mandibular distraction osteogenesis.* Journal of Orthopaedic Research, 2006. **24**(12): p. 2238-2245.
65. Janssens, K., et al., *Transforming Growth Factor-β1 to the Bone.* Endocrine Reviews, 2005. **26**(6): p. 743-774.
66. Erlebacher, A., et al., *Osteoblastic Responses to TGF-β during Bone Remodeling.* Molecular Biology of the Cell, 1998. **9**(7): p. 1903-1918.
67. Yamaguchi, A., T. Komori, and T. Suda, *Regulation of Osteoblast Differentiation Mediated by Bone Morphogenetic Proteins, Hedgehogs, and Cbfa1.* Endocrine Reviews, 2000. **21**(4): p. 393-411.

68. Kramer, I., et al., *Osteocyte Wnt/β-Catenin Signaling Is Required for Normal Bone Homeostasis.* Molecular and Cellular Biology, 2010. **30**(12): p. 3071-3085.
69. Laviola, L., et al., *Abnormalities of IGF-I signaling in the pathogenesis of diseases of the bone, brain, and fetoplacental unit in humans.* American Journal of Physiology - Endocrinology And Metabolism, 2008. **295**(5): p. E991-E999.
70. Palermo, C., et al., *Potentiating role of IGFBP-2 on IGF-II-stimulated alkaline phosphatase activity in differentiating osteoblasts.* American Journal of Physiology - Endocrinology And Metabolism, 2004. **286**(4): p. E648-E657.
71. Eijken, M., et al., *The essential role of glucocorticoids for proper human osteoblast differentiation and matrix mineralization.* Molecular and Cellular Endocrinology, 2006. **248**(1–2): p. 87-93.
72. Phillips, J.E., *Glucocorticoid-induced osteogenesis is negatively regulated by Runx2/Cbfa1 serine phosphorylation.* Journal of Cell Science, 2006. **119**(3): p. 581-591.
73. Nuttelman, C.R., M.C. Tripodi, and K.S. Anseth, *Dexamethasone-functionalized gels induce osteogenic differentiation of encapsulated hMSCs.* Journal of Biomedical Materials Research Part A, 2006. **76A**(1): p. 183-195.
74. Benoit, D.S.W., et al., *Synthesis and characterization of a fluvastatin-releasing hydrogel delivery system to modulate hMSC differentiation and function for bone regeneration.* Biomaterials, 2006. **27**(36): p. 6102-6110.
75. Park, J.-B., et al., *Simvastatin Maintains Osteoblastic Viability While Promoting Differentiation by Partially Regulating the Expressions of Estrogen Receptors α.* Journal of Surgical Research, 2012. **174**(2): p. 278-283.
76. Pagkalos, J., et al., *Simvastatin induces osteogenic differentiation of murine embryonic stem cells.* Journal of Bone and Mineral Research, 2010. **25**(11): p. 2470-2478.
77. Franceschi, R.T., B.S. Iyer, and Y. Cui, *Effects of ascorbic acid on collagen matrix formation and osteoblast differentiation in murine MC3T3-E1 cells.* Journal of Bone and Mineral Research, 1994. **9**(6): p. 843-854.
78. Torii, Y., K. Hitomi, and N. Tsukagoshi, *L-Ascorbic Acid 2-Phosphate Promotes Osteoblastic Differentiation of MC3T3-E1 Mediated by Accumulation of Type I Collagen.* Journal of Nutritional Science and Vitaminology, 1994. **40**(3): p. 229-238.
79. Xiao, G., et al., *Ascorbic Acid-Dependent Activation of the Osteocalcin Promoter in MC3T3-E1 Preosteoblasts: Requirement for Collagen Matrix Synthesis and the Presence of an Intact OSE2 Sequence.* Molecular Endocrinology, 1997. **11**(8): p. 1103-1113.
80. von Knoch, F., et al., *Effects of bisphosphonates on proliferation and osteoblast differentiation of human bone marrow stromal cells.* Biomaterials, 2005. **26**(34): p. 6941-6949.
81. Koch, F., et al., *The impact of bisphosphonates on the osteoblast proliferation and Collagen gene expression in vitro.* Head & Face Medicine, 2010. **6**(1): p. 12.
82. Maruotti, N., et al., *Bisphosphonates: effects on osteoblast.* European Journal of Clinical Pharmacology, 2012. **68**(7): p. 1013-1018.

83. Nishiya, Y., et al., *A Potent 1,4-Dihydropyridine L-type Calcium Channel Blocker, Benidipine, Promotes Osteoblast Differentiation.* Calcified Tissue International, 2002. **70**(1): p. 30-39.
84. Guggino, S.E., et al., *Bone remodeling signaled by a dihydropyridine- and phenylalkylamine-sensitive calcium channel.* Proceedings of the National Academy of Sciences, 1989. **86**(8): p. 2957-2960.
85. Popat, K.C., et al., *Decreased Staphylococcus epidermis adhesion and increased osteoblast functionality on antibiotic-loaded titania nanotubes.* Biomaterials, 2007. **28**(32): p. 4880-4888.
86. Park, K. and Y. Yeo, *Microencapsulation Technology*, in *Encyclopedia of Pharmaceutical Technology*, J. Swarbrick, Editor. 2007, Informa Healthcare: New York. p. 2315-2327.
87. Gaskell, E.E., et al., *Encapsulation and release of alpha-chymotrypsin from poly(glycerol adipate-co-omega-pentadecalactone) microparticles.* Journal of Microencapsulation, 2008. **25**(3): p. 187-195.
88. Tewes, F., F. Boury, and J.-P. Benoit, *Biodegradable Microspheres: Advances in Production Technology*, in *Microencapsulation: Methods and Industrial Applications*, J. Swarbrick, Editor. 2006, Taylor and Francis: London. p. 1-41.
89. Thote, A.J., et al., *Reduction in the initial-burst release by surface crosslinking of PLGA microparticles containing hydrophilic or hydrophobic drugs.* Drug Development and Industrial Pharmacy, 2005. **31**(1): p. 43-57.
90. Rosca, I.D., F. Watari, and M. Uo, *Microparticle formation and its mechanism in single and double emulsion solvent evaporation.* Journal of Controlled Release, 2004. **99**(2): p. 271-280.
91. Nihant, N., et al., *Polylactide Microparticles Prepared by Double Emulsion/Evaporation Technique .1. Effect of Primary Emulsion Stability.* Pharmaceutical Research, 1994. **11**(10): p. 1479-1484.
92. Dong, W. and R. Bodmeier, *Encapsulation of lipophilic drugs within enteric microparticles by a novel coacervation method.* International Journal of Pharmaceutics, 2006: p. 128-138.
93. Chaw, C.S., et al., *Design of physostigmine-loaded polymeric microparticles for pretreatment against exposure to organophosphate agents.* Biomaterials, 2003. **24**(7): p. 1271-1277.
94. Yin, W.S. and M.Z. Yates, *Encapsulation and sustained release from biodegradable microcapsules made by emulsification/freeze drying and spray/freeze drying.* Journal of Colloid and Interface Science, 2009. **336**(1): p. 155-161.
95. Bleich, J., B.W. Muller, and W. Wassmus, *Aerosol Solvent-Extraction System - A New Microparticle Production Technique.* International Journal of Pharmaceutics, 1993. **97**(1-3): p. 111-117.
96. Yasuji, T., et al., *Preliminary evaluation of polymer-based drug composite microparticle production by coacervate desolvation with supercritical carbon dioxide.* Journal of Pharmaceutical Sciences, 2006. **95**(3): p. 581-588.
97. Patomchaiviwat, V., O. Paeratakul, and P. Kulvanich, *Formation of Inhalable Rifampicin-Poly(L-lactide) Microparticles by Supercritical Anti-solvent Process.* Aaps Pharmscitech, 2008. **9**(4): p. 1119-1129.

98. Reverchon, E., et al., *Spherical microparticles production by supercritical antisolvent precipitation: Interpretation of results.* Journal of Supercritical Fluids, 2008. **47**(1): p. 70-84.
99. Fredenberg, S., et al., *The mechanisms of drug release in poly(lactic-co-glycolic acid)-based drug delivery systems—A review.* International Journal of Pharmaceutics, 2011. **415**(1–2): p. 34-52.
100. Makadia, H.K. and S.J. Siegel, *Poly Lactic-co-Glycolic Acid (PLGA) as Biodegradable Controlled Drug Delivery Carrier.* Polymers, 2011. **3**(3): p. 1377-1397.
101. Lee, S.H. and H. Shin, *Matrices and scaffolds for delivery of bioactive molecules in bone and cartilage tissue engineering.* Advanced Drug Delivery Reviews, 2007. **59**(4-5): p. 339-359.
102. Jeong, J.-C., J. Lee, and K. Cho, *Effects of crystalline microstructure on drug release behavior of poly([var epsilon]-caprolactone) microspheres.* Journal of Controlled Release, 2003. **92**(3): p. 249-258.
103. Chien, Y.W. and W.-P. Ye, *Dual-Controlled Drug Delivery Across Biodegradable Copolymer. I. Delivery Kinetics of Levonorgestrel and Estradiol Through (Caprolactone/Lactide) Block Copolymer.* Pharmaceutical Development and Technology, 2008. **1**(1): p. 1-9.
104. Keraliya, R.A., et al., *Osmotic Drug Delivery System as a Part of Modified Release Dosage Form.* ISRN Pharmaceutics, 2012. **2012**: p. 1-9.
105. Verma, R.K., D.M. Krishna, and S. Garg, *Formulation aspects in the development of osmotically controlled oral drug delivery systems.* Journal of Controlled Release, 2002. **79**(1–3): p. 7-27.
106. Bertrand, N., G. Leclair, and P. Hildgen, *Modeling drug release from bioerodible microspheres using a cellular automaton.* International Journal of Pharmaceutics, 2007. **343**(1–2): p. 196-207.
107. Blanco, D. and M.a.J. Alonso, *Protein encapsulation and release from poly(lactide-co-glycolide) microspheres: effect of the protein and polymer properties and of the co-encapsulation of surfactants.* European Journal of Pharmaceutics and Biopharmaceutics, 1998. **45**(3): p. 285-294.
108. D'Souza, S.S. and P.P. DeLuca, *Methods to Assess in Vitro Drug Release from Injectable Polymeric Particulate Systems.* Pharmaceutical Research, 2006. **23**(3): p. 460-474.
109. Jamzad, S. and R. Fassihi, *Role of surfactant and pH on dissolution properties of fenofibrate and glipizide—A technical note.* Aaps Pharmscitech, 2006. **7**(2): p. E17-E22.
110. Washington, C., *Drug release from microdisperse systems: a critical review.* International Journal of Pharmaceutics, 1990. **58**(1): p. 1-12.
111. Zhang, Z. and S.-S. Feng, *The drug encapsulation efficiency, in vitro drug release, cellular uptake and cytotoxicity of paclitaxel-loaded poly(lactide)–tocopheryl polyethylene glycol succinate nanoparticles.* Biomaterials, 2006. **27**(21): p. 4025-4033.
112. Giteau, A., et al., *How to achieve sustained and complete protein release from PLGA-based microparticles?* International Journal of Pharmaceutics, 2008. **350**(1–2): p. 14-26.

113. Howard, D., et al., *Tissue engineering: strategies, stem cells and scaffolds.* Journal of Anatomy, 2008. **213**(1): p. 66-72.
114. Tan, H., et al., *The Design of Biodegradable Microcarriers for Induced Cell Aggregation.* Macromolecular Bioscience, 2010. **10**(2): p. 156-163.
115. Mercier, N.R., et al., *Poly(lactide-co-glycolide) microspheres as a moldable scaffold for cartilage tissue engineering.* Biomaterials, 2005. **26**(14): p. 1945-1952.
116. Bible, E., et al., *Attachment of stem cells to scaffold particles for intra-cerebral transplantation.* Nat. Protocols, 2009. **4**(10): p. 1440-1453.
117. Sahoo, S.K., A.K. Panda, and V. Labhasetwar, *Characterization of Porous PLGA/PLA Microparticles as a Scaffold for Three Dimensional Growth of Breast Cancer Cells.* Biomacromolecules, 2005. **6**(2): p. 1132-1139.
118. Ruhe, P.Q., et al., *rhBMP-2 Release from Injectable Poly(DL-Lactic-co-glycolic Acid)/Calcium-Phosphate Cement Composites.* The Journal of Bone & Joint Surgery, 2003. **85**(suppl_3): p. 75-81.
119. Senuma, Y., et al., *Bioresorbable microspheres by spinning disk atomization as injectable cell carrier: from preparation to in vitro evaluation.* Biomaterials, 2000. **21**(11): p. 1135-1144.
120. Akdemir, Z.S., et al., *Photopolymerized injectable RGD-modified fumarated poly(ethylene glycol) diglycidyl ether hydrogels for cell growth.* Macromolecular Bioscience, 2008. **8**(9): p. 852-862.
121. Drotleff, S., et al., *Biomimetic polymers in pharmaceutical and biomedical sciences.* European Journal of Pharmaceutics and Biopharmaceutics, 2004. **58**(2): p. 385-407.
122. Jiao, Y.-P. and F.-Z. Cui, *Surface modification of polyester biomaterials for tissue engineering.* Biomedical Materials, 2007. **2**(4): p. R24-R37.
123. Saltzman, W.M. and T.R. Kyriakides, *Chapter Twenty - Cell interactions with polymers*, in *Principles of Tissue Engineering (Third Edition)*, L. Robert, et al., Editors. 2007, Academic Press: Burlington. p. 279-296.
124. Meng, W., et al., *Evaluation of poly (glycerol-adipate) nanoparticle uptake in an In Vitro 3-D brain tumor co-culture model.* Experimental Biology and Medicine, 2007. **232**(8): p. 1100-1108.
125. Kallinteri, P., et al., *Novel functionalized biodegradable polymers for nanoparticle drug delivery systems.* Biomacromolecules, 2005. **6**(4): p. 1885-1894.
126. Meng, W., et al., *Uptake and metabolism of novel biodegradable poly (glycerol-adipate) nanoparticles in DAOY monolayer.* Journal of Controlled Release, 2006. **116**(3): p. 314-321.
127. Rimmer, J., *Development of Ligand-Bearing Poly(Glycerol Adipate) Microparticles for Cellular Agregation*, in *School of Pharmacy*. 2009, University of Nottingham: Nottingham. p. 290.
128. Drumheller, P.D. and J.A. Hubbell, *Surface Immobilization of Adhesion Ligands for investigations off Cell-Substrate Interactions*, in *The Biomedical Engineering Handbook: Second Edition*, J.D. Bronzino, Editor. 2000, CRC Press LLC: Boca Raton.
129. Heredia, K.L. and H.D. Maynard, *Synthesis of protein-polymer conjugates.* Organic & Biomolecular Chemistry, 2007. **5**(1): p. 45-53.

130. Wattendorf, U. and H.P. Merkle, *PEGylation as a tool for the biomedical engineering of surface modified microparticles.* Journal of Pharmaceutical Sciences, 2008. **97**(11): p. 4655-4669.
131. Veronese, F.M. and G. Pasut, *PEGylation, successful approach to drug delivery.* Drug Discovery Today, 2005. **10**(21): p. 1451-1458.
132. Joralemon, M.J., S. McRae, and T. Emrick, *PEGylated polymers for medicine: from conjugation to self-assembled systems.* Chemical Communications, 2010. **46**(9): p. 1377-1393.
133. Knop, K., et al., *Poly(ethylene glycol) in Drug Delivery: Pros and Cons as Well as Potential Alternatives.* Angewandte Chemie International Edition, 2010. **49**(36): p. 6288-6308.
134. Seller, Z., *Cellular Adhesion and Adhesion Molecules.* Turkish Journal of Biology, 2001. **25**(1): p. 1-15.
135. Elangbam, C.S., C.W. Qualls, and R.R. Dahlgren, *Cell Adhesion Molecules--Update.* Veterinary Pathology, 1997. **34**(1): p. 61-73.
136. Aplin, A.E., et al., *Signal Transduction and Signal Modulation by Cell Adhesion Receptors: The Role of Integrins, Cadherins, Immunoglobulin-Cell Adhesion Molecules, and Selectins.* Pharmacological Reviews, 1998. **50**(2): p. 197-264.
137. Hersel and U., *RGD modified polymers: biomaterials for stimulated cell adhesion and beyond.* Biomaterials, 2003. **24**(24): p. 4385-4415.
138. Pakstis, L.M., et al., *Evaluation of polydimethylsiloxane modification methods for cell response.* Journal of Biomedical Materials Research Part A, 2010. **92A**(2): p. 604-614.
139. Thissen, H., et al., *Synthetic biodegradable microparticles for articular cartilage tissue engineering.* Journal of Biomedical Materials Research Part A, 2006. **77A**(3): p. 590-598.
140. Patel, S., et al., *Control of cell adhesion on poly(methyl methacrylate).* Biomaterials, 2006. **27**(14): p. 2890-2897.
141. Qiu, C., et al., *Nanofiltration membrane prepared from cardo polyetherketone ultrafiltration membrane by UV-induced grafting method.* Journal of Membrane Science, 2005. **255**(1-2): p. 107-115.
142. Chen, J.-P. and C.-H. Su, *Surface modification of electrospun PLLA nanofibers by plasma treatment and cationized gelatin immobilization for cartilage tissue engineering.* Acta Biomaterialia, 2011. **7**(1): p. 234-243.
143. Meng, W., et al., *Uptake and metabolism of novel biodegradable poly (glycerol-adipate) nanoparticles in DAOY monolayer.* Journal of Controlled Release, 2006. **116**(3): p. 314-321.
144. Wahab, A., et al., *Development of poly(glycerol adipate) nanoparticles loaded with non-steroidal anti-inflammatory drugs.* Journal of Microencapsulation, 2012. **29**(5): p. 497-504.
145. Kalluri, R., *Discovery of Type IV Collagen Non-collagenous Domains as Novel Integrin Ligands and Endogenous Inhibitors of Angiogenesis.* Cold Spring Harbor symposia on quantitative biology, 2002. **67**: p. 255-266.
146. Meng, W., et al., *A new in vitro 3-D brain tumor coculture model used to study nanoparticle uptake and tumor invasion.* Neuro-Oncology, 2006. **8**(4): p. 333-333.

147. Katzung, B., S. Masters, and A. Trevor, *Basic and Clinical Pharmacology, 11th Edition*. 2009: McGraw-Hill Companies,Incorporated.
148. Peetla, C., A. Stine, and V. Labhasetwar, *Biophysical Interactions with Model Lipid Membranes: Applications in Drug Discovery and Drug Delivery.* Molecular Pharmaceutics, 2009. **6**(5): p. 1264-1276.
149. Lee, H., et al., *Poly(vinyl pyrrolidone) conjugated lipid system for the hydrophobic drug delivery.* Macromolecular Research, 2007. **15**(6): p. 547-552.
150. Hermanson, G.T., *Bioconjugate techniques*. 2nd edition ed. 2008, London: Academic Press. 1202.
151. Kleinman, H.K., R.J. Klebe, and G.R. Martin, *Role of collagenous matrices in the adhesion and growth of cells.* The Journal of Cell Biology, 1981. **88**(3): p. 473-485.
152. Heino, J., *The collagen receptor integrins have distinct ligand recognition and signaling functions.* Matrix Biology, 2000. **19**(4): p. 319-323.
153. Heino, J., *The collagen family members as cell adhesion proteins.* BioEssays, 2007. **29**(10): p. 1001-1010.
154. Eastoe, J.E., *Amino Acid Composition of Mammalian Collagen and Gelatin.* Biochemical Journal, 1955. **61**(4): p. 589-600.
155. Jue, R., et al., *Addition of Sulfhydryl-Groups to Escherichia-coli Ribosomes by Protein Modification with 2-Iminothiolane (Methyl 4-Mercaptobutyrimidate).* Biochemistry, 1978. **17**(25): p. 5399-5406.
156. Pascual, S., et al., *Investigation of the effects of various parameters on the synthesis of oligopeptides in aqueous solution.* European Polymer Journal, 2003. **39**(8): p. 1559-1565.
157. Han, S.-Y. and Y.-A. Kim, *Recent development of peptide coupling reagents in organic synthesis.* Tetrahedron, 2004. **60**(11): p. 2447-2467.
158. Ju, S. and W.-S. Yeo, *Quantification of proteins on gold nanoparticles by combining MALDI-TOF MS and proteolysis.* Nanotechnology, 2012. **23**(13): p. 135701.
159. Thanh, N.T.K. and L.A.W. Green, *Functionalisation of nanoparticles for biomedical applications.* Nano Today, 2010. **5**(3): p. 213-230.
160. Madani, F., et al., *PEGylation of microspheres for therapeutic embolization: Preparation, characterization and biological performance evaluation.* Biomaterials, 2007. **28**(6): p. 1198-1208.
161. Baslé, E., N. Joubert, and M. Pucheault, *Protein Chemical Modification on Endogenous Amino Acids.* Chemistry & Biology, 2010. **17**(3): p. 213-227.
162. Langer, K., et al., *Preparation of avidin-labeled protein nanoparticles as carriers for biotinylated peptide nucleic acid.* European Journal of Pharmaceutics and Biopharmaceutics, 2000. **49**(3): p. 303-307.
163. Edlund, U. and A. Albertsson, *Degradable Polymer Microspheres for Controlled Drug Delivery* in *Degradable Aliphatic Polyesters*. 2002, Springer Berlin / Heidelberg. p. 67-112.
164. Yeo, Y. and K. Park, *Control of encapsulation efficiency and initial burst in polymeric microparticle systems.* Archives of Pharmacal Research, 2004. **27**(1): p. 1-12.

165. Fessi, H., et al., *Nanocapsule formation by interfacial polymer deposition following solvent displacement.* International Journal of Pharmaceutics, 1989. **55**(1): p. R1-R4.
166. Pinto Reis, C., et al., *Nanoencapsulation I. Methods for preparation of drug-loaded polymeric nanoparticles.* Nanomedicine: Nanotechnology, Biology and Medicine, 2006. **2**(1): p. 8-21.
167. Sansdrap, P. and A.J. Moës, *Influence of manufacturing parameters on the size characteristics and the release profiles of nifedipine from poly(DL-lactide-co-glycolide) microspheres.* International Journal of Pharmaceutics, 1993. **98**(1–3): p. 157-164.
168. Tomazic-Jezic, V.J., K. Merritt, and T.H. Umbreit, *Significance of the type and the size of biomaterial particles on phagocytosis and tissue distribution.* Journal of Biomedical Materials Research, 2001. **55**(4): p. 523-529.
169. Champion, J., A. Walker, and S. Mitragotri, *Role of Particle Size in Phagocytosis of Polymeric Microspheres.* Pharmaceutical Research, 2008. **25**(8): p. 1815-1821.
170. Garnett, M.C., *Nanomedicines and nanotoxicology: some physiological principles.* Occupational Medicine, 2006. **56**(5): p. 307-311.
171. Wang, S.-H., et al., *Size-dependent endocytosis of gold nanoparticles studied by three-dimensional mapping of plasmonic scattering images.* Journal of Nanobiotechnology, 2010. **8**(1): p. 33.
172. Freiberg, S. and X.X. Zhu, *Polymer microspheres for controlled drug release.* International Journal of Pharmaceutics, 2004. **282**(1-2): p. 1-18.
173. Shimmin, R.G., A.B. Schoch, and P.V. Braun, *Polymer Size and Concentration Effects on the Size of Gold Nanoparticles Capped by Polymeric Thiols.* Langmuir, 2004. **20**(13): p. 5613-5620.
174. Rosa, G.D., et al., *Influence of the co-encapsulation of different non-ionic surfactants on the properties of PLGA insulin-loaded microspheres.* Journal of Controlled Release, 2000. **69**(2): p. 283-295.
175. Chern, C.-S. and C. Lee, *Emulsion Polymerization of Styrene Stabilized with an Amphiphilic PEG-Containing Graft Copolymer.* Macromolecular Chemistry and Physics, 2001. **202**(13): p. 2750-2759.
176. Lee, W.-k., et al., *Preparation and characterization of biodegradable nanoparticles entrapping immunodominant peptide conjugated with PEG for oral tolerance induction.* Journal of Controlled Release, 2005. **105**(1-2): p. 77-88.
177. Aravand, M.A. and M.A. Semsarzadeh, *Particle Formation by Emulsion Inversion Method: Effect of the Stirring Speed on Inversion and Formation of Spherical Particles.* Macromolecular Symposia, 2008. **274**(1): p. 141-147.
178. Lee, S.C., et al., *Quantitative analysis of polyvinyl alcohol on the surface of poly(d,l-lactide-co-glycolide) microparticles prepared by solvent evaporation method: effect of particle size and PVA concentration.* Journal of Controlled Release, 1999. **59**(2): p. 123-132.
179. Zhang, L.I. and L. Zhang, *Lipid–Polymer Hybrid Nanoparticles: Synthesis, Characterization and Applications.* Nano LIFE, 2010. **01**(01n02): p. 163-173.

180. Puri, S., et al., *Drug incorporation and release of water soluble drugs from novel functionalised poly(glycerol adipate) nanoparticles.* Journal of Controlled Release, 2008. **125**(1): p. 59-67.
181. Hu, Y., et al., *Effect of PEG conformation and particle size on the cellular uptake efficiency of nanoparticles with the HepG2 cells.* Journal of Controlled Release, 2007. **118**(1): p. 7-17.
182. He, Q., et al., *The effect of PEGylation of mesoporous silica nanoparticles on nonspecific binding of serum proteins and cellular responses.* Biomaterials, 2010. **31**(6): p. 1085-1092.
183. Kreppel, F. and S. Kochanek, *Modification of Adenovirus Gene Transfer Vectors With Synthetic Polymers: A Scientific Review and Technical Guide.* Molecular Therapy, 2007. **16**(1): p. 16-29.
184. Puri, S., *Novel Functionalized Polymers for Nanoparticle Formulations with Anti Cancer Drugs*, in *Pharmacy*. 2007, University of Nottingham: Nottingham.
185. Qutachi, O., *A Three Dimensional Model for Osteogenesis using Controlled Released Simvastatin Loaded Polylactide-co-glycolide Microparticles within Embryoid Bodies*, in *Pharmacy*. 2012, University of Nottingham: Nottingham.
186. Liu, R., et al., *Preparation of insulin-loaded PLA/PLGA microcapsules by a novel membrane emulsification method and its release in vitro.* Colloids and Surfaces B: Biointerfaces, 2006. **51**(1): p. 30-38.
187. Boyd, N., et al., *Human embryonic stem cell-derived mesoderm-like epithelium transitions to mesenchymal progenitor cells.* Tissue Eng Part A, 2009. **15**: p. 1897 - 1907.
188. Bogman, K., et al., *HMG-CoA reductase inhibitors and P-glycoprotein modulation.* British Journal of Pharmacology, 2001. **132**(6): p. 1183-1192.
189. Arora, R., et al., *Analysis of Cholesterol Lowering Drugs (Statins) using Dried Matrix Spots Technology*, I. Agilent Technologies, Editor. 2011: Lake Forest, CA.
190. Lipinski, C.A., et al., *Experimental and computational approaches to estimate solubility and permeability in drug discovery and development settings.* Advanced Drug Delivery Reviews, 1997. **23**(1–3): p. 3-25.
191. *A Listing of Log P Values, Water Solubility, and Molecular Weight for Some Selected Chemicals*, in *Handbook of Biochemistry and Molecular Biology, Fourth Edition*. 2010, CRC Press. p. 747-750.
192. Wang, J.D., et al., *Quantitative Analysis of Molecular Absorption into PDMS Microfluidic Channels.* Annals of Biomedical Engineering, 2012. **40**(9): p. 1862-1873.
193. Feczkó, T., J. Tóth, and J. Gyenis, *Comparison of the preparation of PLGA–BSA nano- and microparticles by PVA, poloxamer and PVP.* Colloids and Surfaces A: Physicochemical and Engineering Aspects, 2008. **319**(1-3): p. 188-195.
194. Mehta, R.C., B.C. Thanoo, and P.P. Deluca, *Peptide containing microspheres from low molecular weight and hydrophilic poly(d,l-lactide-co-glycolide).* Journal of Controlled Release, 1996. **41**(3): p. 249-257.
195. Mao, S., et al., *Effect of WOW process parameters on morphology and burst release of FITC-dextran loaded PLGA microspheres.* International Journal of Pharmaceutics, 2007. **334**(1–2): p. 137-148.

196. Gindy, M.E., et al., *Preparation of poly(ethylene glycol) protected nanoparticles with variable bioconjugate ligand density.* Biomacromolecules, 2008. **9**(10): p. 2705-2711.
197. Dai, W., J. Belt, and W.M. Saltzman, *Cell-binding Peptides Conjugated to Poly(ethylene glycol) Promote Neural Cell Aggregation.* Nat Biotech, 1994. **12**(8).
198. Lee, J., M.J. Cuddihy, and N.A. Kotov, *Three-dimensional cell culture matrices: state of the art.* Tissue Eng Part B Rev, 2008. **14**(1): p. 61-86.
199. Hayashi, K. and Y. Tabata, *Preparation of stem cell aggregates with gelatin microspheres to enhance biological functions.* Acta Biomaterialia, 2011. **7**(7): p. 2797-2803.
200. Wang, F.S., et al., *Modulation of Dickkopf-1 Attenuates Glucocorticoid Induction of Osteoblast Apoptosis, Adipocytic Differentiation, and Bone Mass Loss.* Endocrinology, 2008. **149**(4): p. 1793-1801.
201. Bank, P.A.D., et al., *Accelerated formation of multicellular 3-D structures by cell-to-cell cross-linking.* Biotechnology and Bioengineering, 2007. **97**(6): p. 1617-1625.
202. Kurosawa, H., *Methods for inducing embryoid body formation: in vitro differentiation system of embryonic stem cells.* Journal of Bioscience and Bioengineering, 2007. **103**(5): p. 389-398.
203. O'Brien, J., et al., *Investigation of the Alamar Blue (resazurin) fluorescent dye for the assessment of mammalian cell cytotoxicity.* European Journal of Biochemistry, 2000. **267**(17): p. 5421-5426.
204. Park, J., et al., *Microfabrication-based modulation of embryonic stem cell differentiation.* Lab on a Chip, 2007. **7**(8): p. 1018-1028.
205. Gigout, A., et al., *Chondrocyte Aggregation in Suspension Culture Is GFOGER-GPP- and 1 Integrin-dependent.* Journal of Biological Chemistry, 2008. **283**(46): p. 31522-31530.
206. Tsao, Y.-S., et al., *Biomass and Aggregation Analysis of Human Embryonic Kidney 293 Suspension Cell Cultures by Particle Size Measurement.* Biotechnology Progress, 2000. **16**(5): p. 809-814.
207. Ryu, J.H., et al., *The enhancement of recombinant protein production by polymer nanospheres in cell suspension culture.* Biomaterials, 2005. **26**(14): p. 2173-2181.
208. Dang, S.M., et al., *Efficiency of embryoid body formation and hematopoietic development from embryonic stem cells in different culture systems.* Biotechnology and Bioengineering, 2002. **78**(4): p. 442-453.
209. Gothard, D., et al., *Controlled embryoid body formation via surface modification and avidin–biotin cross-linking.* Cytotechnology, 2009. **61**(3): p. 135-144.
210. Dang, S.M., et al., *Controlled, Scalable Embryonic Stem Cell Differentiation Culture.* Stem Cells, 2004. **22**(3): p. 275-282.
211. Klymkowsky, M., et al., *Abrogation of E-Cadherin-Mediated Cellular Aggregation Allows Proliferation of Pluripotent Mouse Embryonic Stem Cells in Shake Flask Bioreactors.* PLoS ONE, 2010. **5**(9): p. e12921.

212. Overstreet, M., et al., *Induction of osteoblast aggregation, detachment, and altered integrin expression by bear serum.* In Vitro Cellular & Developmental Biology - Animal, 2004. **40**(1): p. 4-7.
213. Ng, K.W., D.T.W. Leong, and D.W. Hutmacher, *The Challenge to Measure Cell Proliferation in Two and Three Dimensions.* Tissue Engineering, 2005. **11**(1-2): p. 182-191.
214. Rampersad, S.N., *Multiple Applications of Alamar Blue as an Indicator of Metabolic Function and Cellular Health in Cell Viability Bioassays.* Sensors, 2012. **12**(9): p. 12347-12360.
215. McGuigan, A.P., et al., *Cell Encapsulation in Sub-mm Sized Gel Modules Using Replica Molding.* PLoS ONE, 2008. **3**(5): p. e2258.
216. Cui, Z.F., et al., *Application of multiple parallel perfused microbioreactors and three-dimensional stem cell culture for toxicity testing.* Toxicology in Vitro, 2007. **21**(7): p. 1318-1324.
217. Al-Nasiry, S., et al., *The use of Alamar Blue assay for quantitative analysis of viability, migration and invasion of choriocarcinoma cells.* Human Reproduction, 2007. **22**(5): p. 1304-1309.
218. Woo, K.M., V.J. Chen, and P.X. Ma, *Nano-fibrous scaffolding architecture selectively enhances protein adsorption contributing to cell attachment.* Journal of Biomedical Materials Research Part A, 2003. **67A**(2): p. 531-537.
219. Junker, J.L. and U.I. Heine, *Effect of Adhesion Factors Fibronectin, Laminin, and Type IV Collagen on Spreading and Growth of Transformed and Control Rat Liver Epithelial Cells.* Cancer Research, 1987. **47**(14): p. 3802-3807.
220. Kusunoki, T., et al., *Type IV Collagen, Type IV Collagenase Activity and Ability of Cell Proliferation in Human Thyroid Tumours.* Asian Journal of Surgery, 2002. **25**(4): p. 304-308.
221. LeBleu, V.S., B. MacDonald, and R. Kalluri, *Structure and Function of Basement Membranes.* Experimental Biology and Medicine, 2007. **232**(9): p. 1121-1129.
222. Olivero, D.K. and L.T. Furcht, *Type IV collagen, laminin, and fibronectin promote the adhesion and migration of rabbit lens epithelial cells in vitro.* Investigative Ophthalmology & Visual Science, 1993. **34**(10): p. 2825-34.
223. Anbalagan, M. and A.J. Rao, *Collagen IV-mediated signalling is involved in progenitor Leydig cell proliferation.* Reproductive BioMedicine Online, 2004. **9**(4): p. 391-403.
224. Bible, E., et al., *Attachment of stem cells to scaffold particles for intra-cerebral transplantation.* Nature Protocols, 2009. **4**(10): p. 1440-1453.
225. Kupcsik, L., et al., *Statin-induced calcification in human mesenchymal stem cells is cell death related.* Journal of Cellular and Molecular Medicine, 2009. **13**(11-12): p. 4465-4473.
226. Neumann, H. and A. Lustig, *The Activation of Alkaline Phosphatase by Effector Molecules.* European Journal of Biochemistry, 1980. **109**(2): p. 475-480.
227. Fosset, M., D. Chappelet-Tordo, and M. Lazdunski, *Intestinal alkaline phosphatase. Physical properties and quaternary structure.* Biochemistry, 1974. **13**(9): p. 1783-1788.

228. Pera, M.F., B. Reubinoff, and A. Trounson, *Human embryonic stem cells.* Journal of Cell Science, 2000. **113**(1): p. 5-10.
229. Hwang, R., et al., *Calcyclin, a Ca2+ Ion-binding Protein, Contributes to the Anabolic Effects of Simvastatin on Bone.* Journal of Biological Chemistry, 2004. **279**(20): p. 21239-21247.
230. Lee, M.-H., Y.S. Cho, and Y.-M. Han, *Simvastatin Suppresses Self-Renewal of Mouse Embryonic Stem Cells by Inhibiting RhoA Geranylgeranylation.* Stem Cells, 2007. **25**(7): p. 1654-1663.
231. Song, C., et al., *Simvastatin induces estrogen receptor-alpha (ER-α) in murine bone marrow stromal cells.* Journal of Bone and Mineral Metabolism, 2008. **26**(3): p. 213-217.
232. Arpornmaeklong, P., et al., *Phenotypic Characterization, Osteoblastic Differentiation, and Bone Regeneration Capacity of Human Embryonic Stem Cell–Derived Mesenchymal Stem Cells.* Stem Cells and Development, 2009. **18**(7): p. 955-968.
233. Shafiee, A., et al., *A comparison between osteogenic differentiation of human unrestricted somatic stem cells and mesenchymal stem cells from bone marrow and adipose tissue.* Biotechnology Letters, 2011. **33**(6): p. 1257-1264.
234. zur Nieden, N.I., G. Kempka, and H.J. Ahr, *In vitro differentiation of embryonic stem cells into mineralized osteoblasts.* Differentiation, 2003. **71**(1): p. 18-27.
235. Born, A.-K., S. Lischer, and K. Maniura-Weber, *Watching osteogenesis: Life monitoring of osteogenic differentiation using an osteocalcin reporter.* Journal of Cellular Biochemistry, 2012. **113**(1): p. 313-321.
236. Mishra, S., P. Webster, and M.E. Davis, *PEGylation significantly affects cellular uptake and intracellular trafficking of non-viral gene delivery particles.* European Journal of Cell Biology, 2004. **83**(3): p. 97-111.
237. Golub, E.E. and K. Boesze-Battaglia, *The role of alkaline phosphatase in mineralization.* Current Opinion in Orthopaedics, 2007. **18**(5): p. 444-448 10.1097/BCO.0b013e3282630851.
238. Aubin, J., *Regulation of Osteoblast Formation and Function.* Reviews in Endocrine and Metabolic Disorders, 2001. **2**(1): p. 81-94.
239. Li, C.Y., S.C. Ziesmer, and O. Lazcano-Villareal, *Use of azide and hydrogen peroxide as an inhibitor for endogenous peroxidase in the immunoperoxidase method.* Journal of Histochemistry & Cytochemistry, 1987. **35**(12): p. 1457-60.
240. Ramos-Vara, J.A., *Technical Aspects of Immunohistochemistry.* Veterinary Pathology Online, 2005. **42**(4): p. 405-426.
241. Daneshtalab, N., J.J.E. Doré, and J.S. Smeda, *Troubleshooting tissue specificity and antibody selection: Procedures in immunohistochemical studies.* Journal of Pharmacological and Toxicological Methods, 2010. **61**(2): p. 127-135.
242. Burry, R.W., *Controls for Immunocytochemistry: An Update.* Journal of Histochemistry & Cytochemistry, 2011. **59**(1): p. 6-12.
243. Bonewald, L.F., et al., *Von Kossa Staining Alone Is Not Sufficient to Confirm that Mineralization In Vitro Represents Bone Formation.* Calcified Tissue International, 2003. **72**(5): p. 537-547.

244. Tran, V.-T., J.-P. Benoît, and M.-C. Venier-Julienne, *Why and how to prepare biodegradable, monodispersed, polymeric microparticles in the field of pharmacy?* International Journal of Pharmaceutics, 2011. **407**(1-2): p. 1-11.
245. Xu, Q., et al., *Preparation of Monodisperse Biodegradable Polymer Microparticles Using a Microfluidic Flow-Focusing Device for Controlled Drug Delivery.* Small, 2009. **5**(13): p. 1575-1581.
246. Duncanson, W.J., et al., *Microfluidic synthesis of monodisperse porous microspheres with size-tunable pores.* Soft Matter, 2012. **8**(41): p. 10636.
247. Oliveira, M.B. and J.F. Mano, *Polymer-based microparticles in tissue engineering and regenerative medicine.* Biotechnology Progress, 2011. **27**(4): p. 897-912.
248. Rungarunlert, S., *Embryoid body formation from embryonic and induced pluripotent stem cells: Benefits of bioreactors.* World Journal of Stem Cells, 2009. **1**(1): p. 11.
249. Huang, C.-C., et al., *Injectable PLGA porous beads cellularized by hAFSCs for cellular cardiomyoplasty.* Biomaterials, 2012. **33**(16): p. 4069-4077.
250. Lee, T.-J., et al., *Spinner-flask culture induces redifferentiation of de-differentiated chondrocytes.* Biotechnology Letters, 2010. **33**(4): p. 829-836.

APPENDIX

Appendix 1.

Metabolic activity of mES cell aggregate evaluated using Alamar Blue Assay

Fluorescence intensity was measured at $\lambda_{excitation}$ 560 nm and $\lambda_{emission}$ 590 nm.

Day 7

Day 7 5 minutes

	Fluorescence Intensity				
	Blank	**Control**	**40%C_{18}-PGA MP**	**40%C_{18}-PGA-PEG-MIHA MP**	**40%C_{18}-PGA-PEG-MIHA MP+ collagen**
	70	54	85	67	89
	80	68	75	76	104
	73	69	89	73	103
Mean	74.3	63.7	83.0	72.0	98.7
SD	3.6	5.9	3.2	5.1	5.9

Day 7 10 minutes

	Fluorescence Intensity				
	Blank	**Control**	**40%C_{18}-PGA MP**	**40%C_{18}-PGA-PEG-MIHA MP**	**40%C_{18}-PGA-PEG-MIHA MP+ collagen**
	72	130	202	168	223
	81	170	198	187	260
	76	173	232	183	258
Mean	76.3	157.7	210.7	179.3	247.0
SD	3.2	17.0	7.1	13.1	14.7

Day 7 15 minutes

	Fluorescence Intensity				
	Blank	**Control**	**40%C_{18}-PGA MP**	**40%C_{18}-PGA-PEG-MIHA MP**	**40%C_{18}-PGA-PEG-MIHA MP+ collagen**
	95	187	390	337	411
	102	209	383	357	382
	90	237	399	318	383
Mean	95.7	211.0	390.7	337.3	397.0
SD	4.3	17.7	8.0	19.5	14.0

Day 7 30 minutes

	Fluorescence Intensity				
	Blank	**Control**	**40%C_{18}-PGA MP**	**40%C_{18}-PGA-PEG-MIHA MP**	**40%C_{18}-PGA-PEG-MIHA MP+ collagen**
	98	18632	38220	32350	42130
	105	21150	38060	35890	38458
	92	22748	39890	31976	38560
Mean	98.3	20843.3	38723.3	33405.3	39716.0
SD	4.6	1467.3	716.7	1527.3	1478.7

Day 7 60 minutes

	Fluorescence Intensity				
	Blank	**Control**	**40%C_{18}-PGA MP**	**40%C_{18}-PGA-PEG-MIHA MP**	**40%C_{18}-PGA-PEG-MIHA MP+ collagen**
	105	34372	32959	37881	41960
	115	34538	39779	36770	42015
	98	29147	37893	33164	39150
Mean	106.0	32685.7	36877.0	35938.3	41041.7
SD	6.0	2167.8	2490.2	1743.7	1158.6

Day 14

Day 14 5 minutes

	Fluorescence Intensity				
	Blank	**Control**	**40%C_{18}-PGA MP**	**40%C_{18}-PGA-PEG-MIHA MP**	**40%C_{18}-PGA-PEG-MIHA MP+ collagen**
	68	398	338	376	485
	70	413	411	346	510
	68	390	339	366	463
Mean	68.7	400.3	375.0	356.0	474.0
SD	0.8	8.3	36.0	10.0	11.0

Day 14 10 minutes

	Fluorescence Intensity				
	Blank	**Control**	**40%C_{18}-PGA MP**	**40%C_{18}-PGA-PEG-MIHA MP**	**40%C_{18}-PGA-PEG-MIHA MP+ collagen**
	72	955	845	940	1212
	70	1032.5	927	865	1270
	71	975	846	915	1197
Mean	71.0	987.5	886.5	890.0	1204.5
SD	0.7	28.4	40.5	25.0	7.5

Day 14 15 minutes

	Fluorescence Intensity				
	Blank	**Control**	**40%C_{18}-PGA MP**	**40%C_{18}-PGA-PEG-MIHA MP**	**40%C_{18}-PGA-PEG-MIHA MP+ collagen**
	74	1999	1690	1867	2409
	80	2074	1564	1730	2572
	69	1975	1701	1844	2317
Mean	74.3	2024.5	1695.5	1798.5	2444.5
SD	3.9	49.5	5.5	68.5	127.5

Day 14 30 minutes

	Fluorescence Intensity				
	Blank	**Control**	**40%C_{18}-PGA MP**	**40%C_{18}-PGA-PEG-MIHA MP**	**40%C_{18}-PGA-PEG-MIHA MP+ collagen**
	102	37158	OVER	41567	71503
	115	32450	63315	43262	76096
	98	33540	65509	51650	OVER
Mean	105.0	34382.7	64412.0	45493.0	76096.0
SD	6.3	1742.7	1097.0	3817.7	2296.5

Day 14 60 minutes

	Fluorescence Intensity				
	Blank	**Control**	**40%C_{18}-PGA MP**	**40%C_{18}-PGA-PEG-MIHA MP**	**40%C_{18}-PGA-PEG-MIHA MP+ collagen**
	110	OVER	OVER	OVER	OVER
	128	OVER	OVER	OVER	OVER
	104	OVER	OVER	OVER	OVER
Mean	114.0				
SD	8.8				

*) Over indicated the high fluorescence intensity and not be able to detect using plate reader.